

**BINDING SERVICES**  
Tel +44 (0)29 2087 4949  
Fax +44 (0)29 20371921  
e-mail [bindery@cardiff.ac.uk](mailto:bindery@cardiff.ac.uk)



**Dmeso17A :A Novel Inhibitor of *Drosophila* Muscle**

**Differentiation**

**David LIOTTA**  
**PhD Thesis**

**School of Biosciences**  
**Cardiff University**

UMI Number: U584767

All rights reserved

INFORMATION TO ALL USERS

The quality of this reproduction is dependent upon the quality of the copy submitted.

In the unlikely event that the author did not send a complete manuscript and there are missing pages, these will be noted. Also, if material had to be removed, a note will indicate the deletion.



UMI U584767

Published by ProQuest LLC 2013. Copyright in the Dissertation held by the Author.  
Microform Edition © ProQuest LLC.

All rights reserved. This work is protected against  
unauthorized copying under Title 17, United States Code.

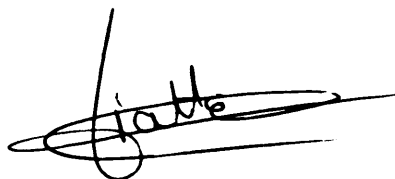


ProQuest LLC  
789 East Eisenhower Parkway  
P.O. Box 1346  
Ann Arbor, MI 48106-1346

*For Violaine*

## Declaration

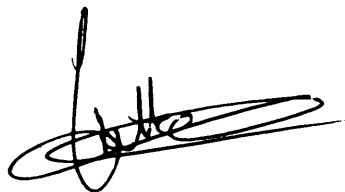
The work described in this dissertation was carried out in the department of Biosciences, Cardiff University between October 2001 and September 2005. This work has not previously been accepted in substance for any degree and is not being concurrently submitted in candidature for any degree.

A handwritten signature in black ink, appearing to be 'J. J. J.', written over a horizontal line.

30/09/05

## Statement 1

This thesis is the result of my own work, except where otherwise stated in Chapter 6, section 6.4. This dissertation contains approximately 40,000 words excluding references.

A handwritten signature in black ink, appearing to be 'J. J. J.', written over a horizontal line.

30/09/05

## Statement 2

I hereby give consent for my thesis, if accepted, to be available for photocopying and for inter-library loan, and for the title and summary to be made available to outside organisations.

A handwritten signature in black ink, appearing to be 'J. J. J.', written over a horizontal line.

30/09/05

## Acknowledgements

First, I would like to thank my supervisor, Mike Taylor. Thank you Mike for giving me the opportunity to work in your lab. It has been a privilege. Thank you for your guidance, your support and your trust. Thank you also for your help when Violaine and I first arrived in this country. Those four years have been a fantastic experience for me and you have played a big part in this.

I would also like to thank Jun, Stuart, Karen and Dan. Thank you guys for all those good moments. Thank you Jun for your help and your kindness. Stuart, thank you for your advices and for all our discussions. I will miss our cigarette breaks. Karen, sorry for all my stupid jokes, but thank you for letting me enjoy them. Dan, thank you for your fun and all the music you brought into the lab.

I would now like to thank my family and friends, but I am afraid this will have to be in French!

Avant tout je tiens à remercier mes parents. Papa, maman, merci pour tout. Merci pour votre soutien, vos encouragements et merci pour avoir cru en moi. C'est grâce à vous si j'en suis là aujourd'hui.

Je voudrais aussi remercier tous les membres de ma famille, mes sœurs, mes beaux-frères, mes neveux et nièces. La liste est trop longue pour vous remercier un par un mais merci à tous pour votre soutien. Merci également à mes beaux-parents qui m'ont encouragé tout au long de ces quatre années d'exil.

Je tiens également à remercier mes amis pour tous les bons moments qu'on a pu passer ensemble. En particulier, je veux dire simplement merci à Eric, Céline, Christel et Titou.

Enfin et surtout, je veux te remercier toi, mon ange, sans qui rien de tout cela n'aurait été possible. C'est à toi que je dédie ce travail. Merci pour tout.

# Contents

<b>Declaration and Statements</b>	<b>i</b>
<b>Acknowledgements</b>	<b>ii</b>
<b>Contents</b>	<b>iii</b>
<b>Summary</b>	<b>x</b>
<b>CHAPTER 1: Introduction</b>	
1.1 History: how and why <i>Drosophila</i> entered the laboratories	
1.1.1 How the <i>Drosophila</i> era started	<b>1</b>
1.1.2 <i>Drosophila</i> : a super model organism	<b>2</b>
1.2 Muscle as a model system	<b>3</b>
1.3 Muscle development in <i>Drosophila</i>	
1.3.1 Mesoderm specification and subdivision	
1.3.1.1 Mesoderm specification	<b>7</b>
1.3.1.2 Mesoderm subdivision	<b>9</b>
1.4 Differentiation of mesodermal derivatives	
1.4.1 The larval body wall musculature	<b>11</b>
1.4.2 The visceral musculature	<b>16</b>
1.4.3 The heart	<b>18</b>
1.4.4 The adult musculature	<b>20</b>
1.5 Genes important for somatic muscle differentiation	
1.5.1 <i>Twist</i>	<b>22</b>
1.5.2 <i>Dmef2</i>	<b>24</b>
1.6 Novel genes in muscle development	<b>27</b>



## **CHAPTER 2: Materials and Methods**

### **2.1 Molecular Biology**

2.1.1	Agarose gel electrophoresis	<b>30</b>
2.1.2	DNA extraction from agarose gels	<b>30</b>
2.1.3	Bacterial cultures and plates	<b>30</b>
2.1.4	Transformation of competent cells	<b>31</b>
2.1.5	Plasmid DNA preparation	<b>31</b>
2.1.6	DNA precipitation with ethanol	<b>32</b>
2.1.7	Restriction enzyme digest	<b>32</b>
2.1.8	Ligation of DNA fragments into plasmids	<b>33</b>
2.1.9	Polymerase chain reaction (PCR)	<b>34</b>
2.1.10	preparation of Digoxigenin-labelled RNA probe	<b>35</b>
2.1.11	Generation of <i>UAS-Dmeso17A-RNAi</i> construct	<b>36</b>
2.1.12	Total RNA extraction from <i>Drosophila</i> embryos	<b>37</b>
2.1.13	Semi-quantitative Reverse Transcription-PCR (RT-PCR)	<b>38</b>
2.1.14	Generation of the <i>Dmeso17A-GAL4</i>	<b>39</b>
2.1.15	Generation of <i>GST-Dmeso17A</i> and <i>GST-Dmeso17A-ΔWRPW</i> fusion proteins	<b>40</b>

### **2.2 Protein work**

2.2.1	Acrylamide gel electrophoresis	<b>42</b>
2.2.2	Expression of proteins in bacteria	<b>42</b>
2.2.3	Expression of radiolabelled protein <i>in-vitro</i>	<b>44</b>
2.2.4	Pull-down assay	<b>44</b>
2.2.5	Western blotting and detection of the Dmeso17A protein	
2.2.5.1	Protein extraction from drosophila embryos	<b>45</b>

2.2.5.2	Western blot	46
2.3	<i>Drosophila</i> Strains and crosses	
2.3.1	Maintenance of fly stocks	47
2.3.2	Mutant stocks used	47
2.3.3	The GAL4-UAS Expression System	48
2.3.4	GAL4 and UAS lines used	49
2.3.5	Generation of new UAS and GAL4 lines	49
2.3.6	Generation of double UAS stocks	51
2.3.7	Insertion of <i>UAS-Dmeso17A</i> , <i>UAS-Dmeso17A-RNAi</i> , <i>Twist-GAL4</i> and <i>Dmeso17A-GAL4</i> into either a <i>Dmef2<sup>65</sup></i> or a <i>gro</i> mutant backgrounds.	51
2.3.8	Embryo collection and fixation	52
2.4	Cell Biology	
2.4.1	<i>RNA In Situ Hybridisation</i>	53
2.4.2	Immunohistochemistry	54
2.4.3	Double antibody staining	54
2.4.4	Visualisation of the Him:GFP reporter	55
2.4.5	Cell death assay by Acridine Orange staining	56
2.4.6	Imaginal Wing Discs dissection and staining	56
2.4.7	Cuticle preparation	57
2.4.8	Adult thoraces dissection and observation	57
2.4.9	Larval muscle scoring and analysis	58
2.4.10	Embryo selection and larval Hatching and Survival Assay	58
2.4.11	Muscle polarised Light Assay	59
2.4.12	Buffers	60

## **CHAPTER 3: *Dmeso17A* Expression and Sequence**

<b>3.1 Introduction</b>	<b>61</b>
<b>3.2 The expression pattern of <i>Dmeso17A</i></b>	
3.2.1 <i>Dmeso17A</i> expression declines as muscle differentiation starts	62
3.2.2 <i>Dmeso17A</i> protein expression follows that of its transcript	64
<b>3.3 <i>Dmeso17A</i> sequence</b>	
3.3.1 <i>Dmeso17A</i> DNA sequence	66
3.3.2 <i>Dmeso17A</i> protein sequence	67
<b>3.4 Discussion</b>	
3.4.1 <i>Dmeso17A</i> : inhibitor or promoter of muscle differentiation?	68
3.4.2 <i>Dmeso17A</i> is a putative inhibitor of transcription	70
3.4.3 Conclusion: <i>Dmeso17A</i> , a novel inhibitor of myogenesis?	72

## **CHAPTER 4: *Dmeso17A* Gain-of-Function**

<b>4.1 Introduction</b>	<b>73</b>
<b>4.2 <i>Dmeso17A</i>: a novel inhibitor of myogenesis</b>	
4.2.1 The over-expression phenotype: <i>Dmeso17A</i> over-expression disrupt somatic myogenesis	74
4.2.2 Quantitation of the phenotype: Hatching/ Survival and polarised light assays	77
4.2.3 GAL4 drivers used	78
4.2.4 <i>Dmeso17A</i> over-expression disrupts myogenesis during the differentiation phase	80

4.2.5	Effect of <i>Dmeso17A</i> over-expression on other mesodermal derivatives	
4.2.5.1	Over-expression of <i>Dmeso17A</i> disrupts heart development	84
4.2.5.2	Investigation of the effect of <i>Dmeso17A</i> over-expression on AMPs	88
4.2.5.3	<i>Dmeso17A</i> over-expression affects adult muscle development	90
4.2.5.4	Expression of <i>Dmeso17A</i> in the visceral mesoderm impairs visceral muscle development	91
4.2.6	The effect of <i>Dmeso17A</i> over-expression is limited to the mesoderm	92
4.3	Discussion	
4.3.1	<i>Dmeso17A</i> over-expression inhibits somatic muscle differentiation	93
4.3.2	<i>Dmeso17A</i> over-expression can affect the development of other mesodermal derivatives	96
4.3.3	Conclusion	99
<b>CHAPTER 5: <i>Dmeso17A</i> Loss-of-Function</b>		
5.1	Introduction	101
5.2	<i>Dmeso17A</i> loss-of-function results in aberrant muscle differentiation	
5.2.1	The RNAi approach	
5.2.1.1	The <i>Dmeso17A</i> -RNAi phenotype	102
5.2.1.2	The effect of <i>Dmeso17A</i> -RNAi occurs during muscle differentiation	105
5.2.1.3	The effect of <i>Dmeso17A</i> -RNAi expression on other mesodermal	

derivatives	106
5.2.2 The dominant-negative approach: <i>Dmeso17A-ΔWRPW</i>	
5.2.2.1 The <i>Dmeso17A-ΔWRPW</i> phenotype	108
5.2.2.2 The effect of <i>Dmeso17A-ΔWRPW</i> effects are during muscle differentiation	110
5.2.2.3 The effect of <i>Dmeso17A-ΔWRPW</i> expression on other mesodermal derivatives	111
5.2.3 <i>Dmeso17A-RNAi</i> vs <i>Dmeso17A-ΔWRPW</i> : different mechanisms of action but same effect	112
5.3 Discussion	
5.3.1 <i>Dmeso17A</i> loss-of-function results in aberrant somatic muscle Differentiation	113
5.3.2 Conclusion	114
<b>CHAPTER 6: Genetic Interactions</b>	
6.1 Introduction	116
6.2 <i>Dmeso17A</i> and <i>Dmef2</i>	116
6.2.1 <i>Dmeso17A</i> over-expression phenocopies <i>Dmef2</i> hypomorphic alleles.	117
6.2.2 <i>Dmeso17A</i> genetically interacts with <i>Dmef2</i>	119
6.2.3 <i>Dmeso17A</i> down-regulates <i>DMef2</i> activity	121
6.3 <i>Dmeso17A</i> and <i>groucho</i>	122
6.3.1 <i>Dmeso17A</i> physically interacts with Gro	123
6.3.2 <i>Dmeso17A</i> genetically interacts with <i>groucho</i>	124
6.3.3 The loss of <i>gro</i> function affects muscle development	126

6.4	<i>Dmeso17A</i> and <i>HDAC</i>	127
6.4.1	The <i>HDAC</i> over-expression phenotype resembles that of <i>Dmeso17A</i>	129
6.4.2	<i>Dmeso17A</i> genetically interacts with <i>HDAC</i>	131
6.5	Discussion	
6.5.1	<i>Dmeso17A</i> inhibits muscle differentiation by down-regulating DMef2 activity	135
6.5.2	<i>Dmeso17A</i> requires <i>groucho</i> to inhibit muscle differentiation	137
6.5.3	<i>Dmeso17A</i> genetically interacts with <i>HDACs</i>	139
	<b>CHAPTER7: Conclusions</b>	<b>142</b>
	<b>References</b>	<b>147</b>
	<b>Appendix 1</b>	<b>168</b>

## Summary

Muscle differentiation is a complex process finely tuned by the interplay of positive and negative factors. Although key positive regulators have been identified, there is rather little evidence of restraining molecules that can control the time and place of muscle differentiation. Identification of such molecules and analysis of their function during muscle differentiation is therefore necessary to gain new insight into the molecular events that regulate this process. My work centred on a gene, *Dmeso17A* that was identified in the Taylor laboratory in a screen to isolate novel genes specifically expressed in muscle progenitors in *Drosophila* (Taylor, 2000). Its pattern of expression suggested it could be an inhibitor of muscle development. My aim was to analyse both the role and mechanism of action of *Dmeso17A*.

*Dmeso17A* expression rapidly declines as muscle differentiation starts, but persists in the adult muscle precursors that remain undifferentiated at this stage. Using the GAL4/UAS system (Brand and Perrimon, 1993) to both mis-express and over-express either full-length or modified proteins, I show that *Dmeso17A* is a novel co-repressor that inhibits muscle progenitor differentiation. *Dmef2*, the key promoter of muscle differentiation, can suppress *Dmeso17A* inhibitory effect on muscle development. This was quantitated by a hatching and survival assay. Moreover, I show that *Dmeso17A* can down-regulate *DMef2* activity. *Dmeso17A* protein contains a WRPW motif. I show that this motif is functionally important and is required for the interaction of *Dmeso17A* with the co-repressor Groucho. Finally, I show that *Dmeso17A* genetically interacts with *Histone Deacetylases* (HDACs), which are known to bind and down-regulate *Mef2* in vertebrates.

My model is that *Dmeso17A* down-regulates *DMef2* activity through interactions with Groucho and HDACs, and therefore is a component of an inhibitory complex that holds muscle precursors in an undifferentiated state until cues trigger their differentiation.

# Chapter 1: Introduction

## 1.1 History: how and why *Drosophila* entered the laboratories

### 1.1.1 How the *Drosophila* era started

The fruit fly, *Drosophila melanogaster*, entered laboratories about a 100 years ago. A major breakthrough was about to appear when, in 1907, Thomas Hunt Morgan (1866-1945) started breeding flies in “The Fly Room”. His intention was to generate an individual phenotypically different from the rest. “He hoped to find an occasional fly that had undergone a mutation, a sudden change in body form” (a phenomenon that had been previously described in plants by Hugo de Vries).

“Morgan had turned from Mendel's plants to the study of animals, but soon found that the rats and mice he was using reproduced too slowly and so, were impractical for studying heredity. His search for a more suitable organism led him to *Drosophila melanogaster*, known as the fruit fly because it feeds on decaying fruit.” He chose *Drosophila* for five reasons: (1) it is “easy to raise in the laboratory” (2) it is “fertile all year long and very prolific, producing a new generation every twelve days”; (3) “male and female offspring are easy to distinguish”; (4) “embryonic development occurs outside the body”, simplifying the study of the effects of mutations on development; (5) it “has only four pairs of chromosomes.”

In 1910, in one of his culture bottles filled with thousands of flies (simply reared on mashed bananas!), he observed a discrete variation. One male fly had white rather than the normal bright red eyes. He realised the implications of this immediately. “The birth of this single spontaneous mutant allowed him to begin addressing some key questions in heredity: How did this white eye colour originate? What determines eye colour?”



Aroused by curiosity, he bred “The Fly” with wild-type (red-eyed) females. All of the offspring (F<sub>1</sub>) were red-eyed. Morgan then crossed F<sub>1</sub> flies together and in the second generation (F<sub>2</sub>), he noticed that only some flies had white eyes, all of which were males. To explain this curious phenomenon, he postulated that the white eye colour is linked to sex. From this he developed the hypothesis of sex-linked characters, which he postulated were on the X-chromosome of females. This finding constituted the basis of Morgan's most important idea: *the chromosomal theory of heredity*. In 1915, together with his students, Sturtevant and Bridges, he summarised their work in *The Mechanism of Mendelian Heredity* (Morgan, T. H. et al., 1915), a book of historic importance (this short history of Thomas Hunt Morgan and his work is summarised from <http://www.columbia.edu/cu/alumni/Magazine/Morgan/morgan.html>).

### **1.1.2 *Drosophila*: a super model organism**

The white eye mutant discovery marked the beginning of the reign of *Drosophila*. Ever since Morgan's discovery, the fruit fly has become one of the major model systems for a wide variety of biological fields: Genetics, Developmental Biology, Biomechanics, Evolutionary Biology, Pharmacology, Neurogenetics, Ecology and many more. During one hundred years of research a wealth of knowledge in the understanding of different biological processes has been accumulated.

Today, *Drosophila* represents a great tool for biologists:

- Its genome has been completely sequenced (Adams et al., 2000). A large part of it is annotated and it is available on the *Drosophila* genome project web site (<http://www.fruitfly.org>).
- Genetic and molecular tools are available to the community. For example, mutants or particular flies can be easily obtained from the stock centres.
- A whole range of experimental techniques is easily accessible.

- Its Biology is very similar to that of humans. 60% of *Drosophila* genes have human counterparts (Rubin, G.M., 2001) and 77% of human disease genes have orthologs in *Drosophila* (Reiter et al., 2001).

In recent years, *Drosophila* researchers have developed powerful genetic techniques that allow rapid identification and characterization of genes with similar functions in higher organisms. The high level of gene conservation, the similarity of cellular processes and the functional conservation of important factors between *Drosophila* and mammals, make *Drosophila* an exceptional model to dissect the molecular mechanisms regulating the formation of complex organisms. Moreover, findings in *Drosophila* could have an important impact on the treatments of human diseases.

## 1.2 Muscle as a model system

Over the last two decades, a thorough understanding of many aspects of developmental biology has been gained through investigations of the fruit fly. Much is now known about both the establishment of the basic body plan (antero-posterior (A/P) and dorso-ventral (D/V) axes) and the specification of the three germ layers of the *Drosophila* embryo (ectoderm, mesoderm and endoderm). Some of the patterning mechanisms that subsequently subdivide the germ layers into subpopulations of progenitors for different cell-types are also quite well understood. In contrast, there is a major gap in our knowledge of how these general patterning mechanisms are interpreted to produce the range of specific cell-types and then how gene expression, cell migration and differentiation is coordinated to form functional tissue.

Muscle differentiation is a model of choice for studying this issue as over the last decade it has become a paradigm for cell differentiation. Many aspects of muscle specification and differentiation (formation, structure, molecular mechanism) have been

preserved throughout evolution between *Drosophila* and higher organisms. Like in vertebrate embryos, *Drosophila* muscle determination is influenced by signals such as Wnt, TGF $\beta$  and Hedgehog family members (Baylies et al., 1998). Genes crucial for muscle differentiation, like *twist* (Baylies and Bate, 1996; Castanon and Baylies, 2002) or *mef2* (Bour et al., 1995; Lilly et al., 1995; Ranganayakulu et al., 1995) have also been remarkably conserved. Nevertheless, a lot remain to be uncovered about the mechanisms underlying muscle differentiation. Although key positive regulators such as DMef2 have been characterised, little is known about how their expression and activity are modulated. *Dmef2* is expressed very early in the mesoderm (Taylor et al., 1995). Yet, characterised target genes are activated later during muscle differentiation (Lin et al., 1996; Damm et al., 1998). This suggests that there are inhibitory mechanisms regulating DMef2 activity before the onset of muscle differentiation.

During normal development, it is apparent that restraining mechanisms control cell differentiation, both spatially and temporally. For example, during muscle development in *Drosophila*, the precursors of the adult muscles appear early in embryogenesis and are committed to the muscle fate, but they remain undifferentiated while other myoblasts around them differentiate (Bate, 1991; Bate, 1993). Another example, from vertebrate muscle development, are the satellites cells, which also are quiescent, undifferentiated cells that are able to proliferate and differentiate to mediate post-natal growth or regeneration of muscles (Seale and Rudnicki, 2000; Morgan and Partridge, 2003). Vertebrate limb bud muscle development also provides an example of delayed differentiation of committed cells. While differentiation starts in the somite, some myoblasts migrate towards the limb bud and remain undifferentiated until they reach their final destination (Christ et al., 1995; Buckingham et al., 2003).

Restraining mechanisms are therefore required during normal development and muscle differentiation should be considered as a balance of promoting and restraining influences. A better understanding of the regulation of muscle differentiation requires the identification and characterisation of negative regulators.

In mammalian cell culture, some candidate negative regulators have been identified, but in general rather little is known of their *in vivo* roles in development (for review see Olson, 1992; Taylor, 2005). Examples include:

- Mouse Twist, which in cell culture can inhibit the function of two key regulators of myogenesis, MyoD and Mef2 (Molkentin et al., 1995; Weintraub et al., 1991; reviewed in Black and Olson, 1998; Taylor, 2005), and therefore inhibits muscle differentiation (Hebrok et al., 1994; Spicer et al., 1996). However, although mice lacking *twist* function have somite defects (Chen et al., 1995), its *in vivo* role in muscle development is not understood.
- The histone deacetylases (HDACs), which can bind to Mef2 and down-regulate its activity in cell culture, but have not been directly implicated in muscle differentiation *in vivo* (see Chapter 6, section 6.4).
- Id proteins, which are helix-loop-helix (HLH) proteins that lack a DNA binding domain. *In vitro* and cell culture experiments have shown that Id binds to E proteins, the MyoD heterodimerisation partner, and so inhibits MyoD function (Benezra et al., 1990; Jen et al., 1992). However, the role of Id during vertebrate skeletal muscle development is not established.
- HES1, a member of the HES (mammalian homologs of *Drosophila* Hairy and E(spl)) family, which in cell culture inhibits the activity of MyoD, and therefore might inhibit muscle differentiation (Sasai et al., 1992). However, over-expression of HES1 does not prevent myoblast differentiation (Shawber et al., 1996). Mice lacking HES1

display severe defects in neurogenesis, but there no report of defects in muscle differentiation (Ishibashi et al., 1995).

- MSX1, a member of the Msx homoprotein family, which with histone H1b binds to MyoD and inhibits its activity in cell culture (Lee et al., 2004). No *in vivo* role in muscle development has been described for MSX1.

Some examples of inhibitors of muscle development have also been described in *Drosophila* and include:

- *twist*, which can inhibit the development of adult indirect flight muscles (IFMs) (Anant et al., 1998; This Chapter, see section 1.5.1). This role as an inhibitor contrasts with its function in the embryo as a promoter of muscle development and as activator of *Dmef2* expression (Taylor et al., 1995, Baylies and Bate, 1996; Cripps and Olson, 1998, This Chapter, see section 1.5.1).
- *Zfh-1*, a zinc finger homeodomain transcriptional repressor, which may down-regulate *Dmef2* expression and therefore inhibit myogenesis (Fortini et al., 1991; Postigo et al, 1997; Postigo et al., 1999).
- Notch, which in the adult can inhibit IFM development, possibly through Twist, which inhibits muscle development at this stage (Anant et al., 1998). Notch also inhibits muscle differentiation during embryogenesis by down regulating *twist*, which at this stage promotes muscle development (Baylies and Bate, 1996; Tapanes-Castillo and Baylies, 2004; This Chapter, see section 1.5.2; Chapter 3, see section 3.4.2).
- Extra macrochaete (*Emc*), an HLH protein related to vertebrate Id proteins. Mutants for *emc* display extreme disruption of the somatic musculature, although the mechanism of this effect is not known (Cubas et al., 1994).

In summary, it is evident that negative regulation is a crucial aspect of muscle development and much is to be learned from the analysis of inhibitors of differentiation.

Some negative regulators have been identified, but their mechanisms of action are still to be defined *in vivo*. Finally, identification and analysis of new regulators is required to have a clearer picture of how muscle differentiation is regulated *in vivo*. For all the reasons mentioned in the previous section, *Drosophila* represents an excellent model to address these issues.

### **1.3 Muscle development in *Drosophila***

During early *Drosophila* development, like in vertebrate embryos, muscles form from the mesoderm. This process can be divided into three stages: the specification of the mesoderm, its subsequent subdivision with the formation of muscle progenitors and the expression of muscle specific genes, and lastly the differentiation of these progenitors into individual muscles. This section will present briefly the specification of the mesodermal germ layer and its subdivision leading to muscle formation.

#### **1.3.1 Mesoderm specification and subdivision**

##### **1.3.1.1 Mesoderm specification**

In *Drosophila*, the mesoderm is formed by the most ventral cells of the blastoderm-stage embryo. During the establishment of the D/V axis, a high concentration of the maternal transcription factor Dorsal, in the ventral part of the embryo, activates the expression of two zygotic genes, *snail (sna)* and *twist (twi)* (Ip et al., 1992; Jiang et al., 1991; Pan et al., 1991; Thisse et al., 1991), which are both required for mesoderm specification. Embryos mutant for either gene fail to gastrulate normally and form no mesoderm derivatives (Leptin, 1991). During gastrulation, *twi*- and *sna*-expressing mesodermal cells invaginate along the ventral furrow, divide twice and spread dorsally

to form a monolayer in close contact with the overlying ectoderm (Leptin and Grunewald, 1990).

*sna* encodes a zinc-finger transcription factor (Boulay et al., 1987), and is required for the repression of mesectodermal and neurectodermal genes (reviewed in Ip and Gridley, 2002). During gastrulation, it is also required for the initial phase of mesoderm invagination (Ip et al., 1994; reviewed in Ip and Gridley, 2002). After gastrulation, during the first stages of germ band elongation, *sna* expression disappears from the mesoderm and its transcript now accumulates in the developing central and peripheral nervous systems (Alberga et al., 1991).

*twi* encodes a bHLH transcription factor. It is expressed in all mesodermal cells (Thisse et al., 1988), and is required for the activation of muscle-specific differentiation genes. These genes include the homeobox gene *tinman* (*tin*) and the MADS domain transcription factor *Dmef2* (*Drosophila* myocyte enhancer factor 2) (Taylor et al., 1995; Yin et al., 1997; Cripps and Olson, 1998). After gastrulation, *twist* remains expressed in all mesodermal cells (Thisse et al., 1988), but at the end of germ band elongation its expression is modulated into domains of high and low levels of expression. During and after germ band retraction, its expression declines, only persisting in the adult muscle precursors (AMPs) (Bate et al., 1991).

Thus, after gastrulation, as the germ band begins to extend, the early-specified mesoderm is rather uniform with all cells expressing uniform levels of *twi*, and of its targets *tin* and *Dmef2*. Differences between mesodermal cells become evident slightly later, by the end of germ band extension. At this stage, the mesoderm enters a period of substantial reorganisation.

### 1.3.1.2 Mesoderm subdivision

Towards the end of germ band elongation, the mesoderm is segmented, along the antero-posterior (A/P) axis, into a series of units from which the progenitors of different mesodermal tissues will be formed (Dunin Borkowski et al., 1995; Azpiazu et al., 1996; Riechmann et al., 1997). The mesoderm then segregates into two layers. The external layer remains in contact with the ectoderm and will give rise to most of the somatic muscles and the heart. The internal one loses its contact with the ectoderm and will give rise to the visceral mesoderm, fat body, gonadal mesoderm, mesodermal glial cells and some dorsal somatic muscles (Dunin Borkowski et al., 1995; Riechmann et al., 1997).

This subdivision of the mesoderm is revealed by the expression pattern of Twist. At the end of germ band elongation, Twist expression is modulated in each mesodermal segment into domains of high and low levels of expression. High levels of Twist are found in the cells that form the external mesodermal layer in contact with the ectoderm. Cells in the domain of low Twist expression lose contact with the ectoderm and form the inner mesodermal layer (Bate and Rushton, 1993; Dunin Borkowski et al., 1995). This segmentally repeated modulation of Twist expression is a crucial element to the subdivision of the mesoderm. High levels of Twist are necessary for switching cells into somatic myogenesis, whereas low levels allow the development of other mesodermal derivatives (Baylies and Bate, 1996; Castanon et al., 2001; see section 1.5.1).

This subdivision of the mesoderm along the A/P, but also the D/V axis, is induced by intrinsic transcription factors together with signals coming from surrounding tissues. Most of these factors and signals, coming from different regions of the overlying ectoderm, are used in many developmental processes and include the signals *wingless* (*wg*), *hedgehog* (*hh*) and *decapentaplegic* (*dpp*), a member of the BMP superfamily (for review see Baylies et al., 1998).



Along the A/P axis, the mesoderm is partitioned by the pair-rule genes *even-skipped* (*eve*) and *sloppy-paired* (*slp*). *Eve* domains will give rise to visceral muscles and the fat body, whereas somatic muscle and the heart will form from *Slp* domains (Azpiazu et al., 1996; Riechmann et al., 1997). In *eve* mutants the primordia of the fat body and of the visceral mesoderm fail to develop (Azpiazu et al., 1996; Riechmann et al., 1997), and no heart or somatic muscle is formed in the absence of *slp* (Riechmann et al., 1997).

*Eve* and *Slp* are expressed in the mesoderm as well as in the ectoderm and their effects on mesodermal patterning are both direct and indirect. They act directly, within the mesoderm, inducing or repressing genes. For example, *Eve* induces *bagpipe* (*bap*), which is important for visceral muscle differentiation (Azpiazu and Frasch, 1993). Their indirect action is through the activation of downstream targets within the ectoderm, like *wg* (for *Slp*) or *hedgehog* (for *Eve*) (Riechmann et al., 1997). *Wg*, by maintaining *twi* expression (Bate and Rushton, 1993), allocates cells of the *Slp* domain to the somatic differentiation pathway.

Along the dorso-ventral (D/V) axis, the mesoderm is divided by *dpp*. *Dpp* is expressed dorsally in the ectoderm and, as the mesodermal cells migrate dorsally, they come under its influence. *Dpp* acts on the mesoderm by maintaining *tin* expression, which is required for the differentiation of dorsal mesodermal derivatives (Azpiazu and Frasch, 1993; Frasch, 1995). At the same time, *Dpp* represses ventrally expressed genes (Staebling-Hampton et al., 1994).

Thus, at the end of germ band extension, each mesodermal segment is subdivided along both the A/P and the D/V axes. In the posterior part of each segment, in the *Slp* domain, dorsal cells under the influence of *Dpp* and *Wg* give rise to the heart and some dorsal somatic muscles. Ventral cells that receive only *Wg* from the ectoderm, give rise to most of the somatic muscles. In the anterior part of the segments, within the *Eve*

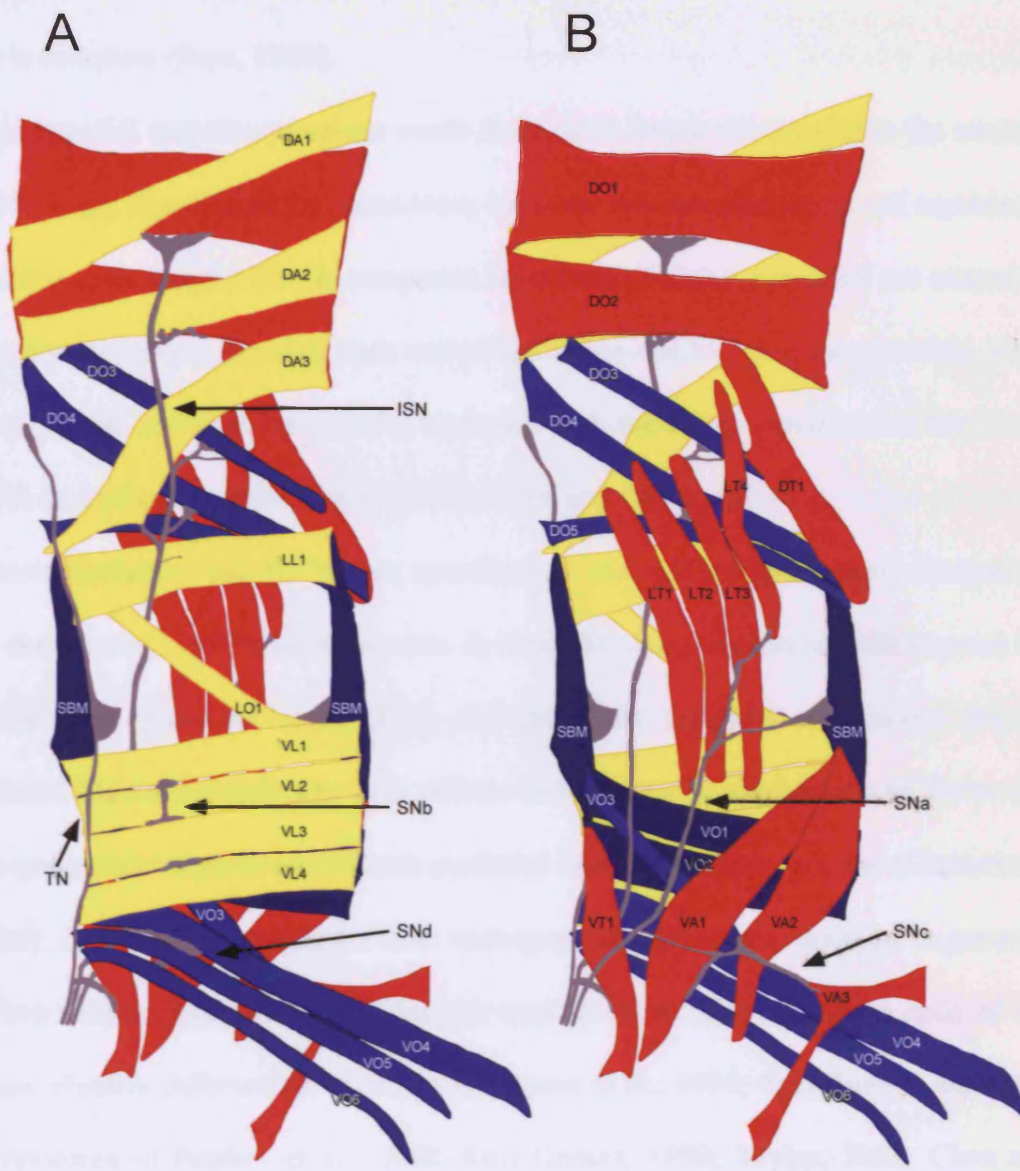
domain, dorsal cells that are under the influence of Dpp and Hh give rise to the visceral musculature, whereas ventral cells are committed to generate the fat body and other derivatives (for review see Baylies et al., 1998).

## **1.4 Differentiation of mesodermal derivatives**

### **1.4.1 The larval body wall musculature**

At the end of embryogenesis, the larval somatic muscles of *Drosophila* form an intricate pattern of syncytial and striated muscles on the inner surface of the ectoderm (Bate, 1990; Bate, 1993). Each muscle is formed by the fusion of myoblasts and inserts into the epidermis. They are individual units distinguishable from their neighbours by size, shape, orientation, epidermal attachment, innervation and position (Bate, 1990). Each of the abdominal segments A2-A7 has a very stereotyped set of thirty muscles (Figure 1.1) with a modified pattern in A1 (where only 29 muscles are present). There also are unique patterns in A8, the thorax and the more terminal segments. This intersegmental diversity is determined by autonomous function of homeotic genes in mesodermal cells (Michelson, 1994). In all my experiments, I have only considered abdominal segments A2-A7.

The morphogenesis of the larval somatic muscle has been well characterised (Bate 1990). The first sign of muscle development occurs at the onset of germ band shortening with the appearance of fused doublets or triplets of cells in the most ventral part of the mesoderm. These small syncytia are the precursors of some of the ventral somatic muscles. During germ band shortening, new syncytia form ventrally, but also dorsally and laterally. By the end of germ band shortening, the location of these precursors containing two to three nuclei prefigures the future muscle pattern. Each precursor then enlarges by fusion with neighbouring myoblasts, expresses structural



**Figure 1.1: Wild-type somatic muscle pattern in *Drosophila*.**

A flattened view of an A2-7 abdominal hemisegment. (A) Internal view. (B) External view. Abbreviations: DA: dorsal acute; DO; dorsal oblique; DT; dorsal transverse; LL: lateral longitudinal; LO: lateral oblique; LT: lateral transverse; VA: ventral acute; VL: ventral longitudinal; VO: ventral oblique; VT: ventral transverse; ISN: intersegmental nerve; SN: segmental nerve; TN: transverse nerve. This figure is from Bate (1993).

genes and projects processes towards their final attachment sites on the ectoderm. By 13 hours after egg laying (end of stage 15 (all stages according to Campos-Ortega, 1997)), characteristic insertion points on the ectoderm have been established and the muscle pattern is complete (Bate, 1990).

The syncytial muscle precursors result from early fusion events within the somatic muscle-forming domains of the mesoderm, between two specific classes of myoblasts: the founder cells and the fusion competent myoblasts (FCMs). Founders are central to somatic muscle development as each one of them give rise to a particular muscle. They act as attractants and seed the muscles by fusion with the FCMs (reviewed in Baylies et al., 1998; Ruiz-Gomez, 1998; Taylor, 2002; Chen and Olson, 2004).

Muscle founders and FCMs are specified, at the end of germ band elongation, within domains of high Twist expression. In these domains, clusters of cells express the proneural gene lethal of scute (*l'sc*) and have the potential to become muscle progenitors. However, only one cell within each cluster is singled out to become a muscle progenitor. This is by a Notch-mediated lateral inhibition process (Carmena et al., 1995). Each muscle progenitor then undergoes an asymmetric division to generate either two muscle founders or one founder and an AMP. The remaining cells of the myogenic clusters differentiate as FCMs (Carmena et al., 1998; Ruiz-Gomez and Bate, 1997; reviewed in Baylies et al., 1998; Ruiz-Gomez, 1998; Taylor, 2002; Chen and Olson, 2004).

Each muscle progenitor expresses a particular combination of genes that determine its identity. These so-called "identity genes" include *S59* (Dohrman et al., 1990), *Krüppel (Kr)* (Gaul et al., 1987), *vestigial (vg)* (Williams et al., 1991), *connectin (con)* (Nose et al., 1992), *apterous (ap)* (Bourgouin et al., 1992) and *even-skipped (eve)* (Frasch et al., 1987). When the progenitors divide, the pattern of identity genes is not

necessarily conserved in the two sibling founders. In some cases, the pattern of gene expression initiated in the progenitor is maintained in both founders. This is the case for progenitors expressing connectin (Nose et al, 1992). In some other cases, expression of one or more identity genes changes in at least one of the founders. One such example is the progenitor of the VA1 and VA2 muscles, which expresses the identity genes *S59* and *Kr*. As it divides, *S59* expression is maintained in both founders, whereas *Kr* is lost from the founder of the VA1 muscle (Ruiz-Gomez et al., 1997).

Thus, shortly before the onset of germ band shortening, founders arise from the division of muscle progenitors and each one of them expresses a combination of identity genes. These genes are characteristic of individual muscles and determine specific muscle differentiation (Ruiz-Gomez et al., 1997; Baylies et al., 1998; Taylor, 2002; Chen and Olson, 2004). During the fusion process, FCMs are recruited to the characteristic pattern of identity genes of the founder they fuse with. Therefore, the syncytial muscle precursors and, later, the muscles themselves can be identified by their pattern of identity gene expression.

Although differential expression of identity genes specifies each founder, the general process of fusion with FCMs is common. This process can be divided into cell attraction, adhesion, alignment and finally the fusion itself (Doberstein et al., 1997). Several genes encoding products involved in fusion have been identified (reviewed in Taylor, 2002; Taylor, 2003; Chen and Olson, 2004).

Some of these genes are expressed in both founders and FCMs. These include *myoblast city (mbc)* (Rushton et al., 1995; Erikson et al., 1997), *Dmef2* (Bour et al., 1995; Lilly et al., 1995), *blown fuse (blow)* (Doberstein et al., 1997), and *Dtitin* (Zhang et al., 2000). Mutations in any of these result in disruption of myoblast fusion. Another gene, *roughest (rst)*, encodes an immunoglobulin (Ig)-domain containing cell adhesion

molecule (Strünkelnberg et al., 2001) and is expressed at the surface of both types of myoblast. The lack of *rst* however has very little effect on muscle development (Strünkelnberg et al., 2001). Other genes are specific to either founders or FCMs.

In muscle founders, three have been described. (1) *dumbfounded (duf)*, which, like *rst*, encodes an Ig-domain cell adhesion molecule (Ruiz-Gomez et al. 2000). Duf and Rst act redundantly, at the surface of founders, as attractants of FCMs. Deletion of both genes causes a complete block of fusion (Ruiz-Gomez et al., 2000; Strünkelnberg et al., 2001); (2) *antisocial [(ants)*, also called *rolling pebbles (rols)*]. Ants is an adaptor protein that binds Duf on the inner surface of the membrane, and Mbc, which is a cytoplasmic protein implicated in mediating changes in the cytoskeleton (Chen and Olson, 2001; Erikson et al., 1997). (3) *loner*, which encodes a regulator of the ADP-ribosylation factor (ARF)6 small GTPase (Chen et al., 2003).

In FCMs, two genes encoding transmembrane molecules have been described. Sticks and stones (*Sns*) and Hibris (*Hbs*), which are both Ig-domain cell adhesion molecules (Bour et al., 2000; Dworak et al., 2001). The loss of *sns* results in lack of fusion (Bour et al., 2000). *Hbs* on the other hand, is not essential for myoblast fusion, but it could inhibit *Sns* function. The over-expression of *hbs* blocks myoblast fusion, whereas the absence of *hbs* causes only minor defects (Dworak et al., 2001; Artero et al., 2001).

The description of all these molecules has allowed a model for myoblast fusion to emerge (see Taylor, 2002; Taylor, 2003; Chen and Olson, 2004). First, founders attract FCMs. Then after the initial recognition, the cells adhere maybe thanks to the binding of Duf to *Sns*. In the founder cell cytoplasm, Duf binds *Rols/Ants*, which in turn binds *Mbc*. *Mbc* then activates the small GTPase *Drac*, which regulates actin-cytoskeleton rearrangements. Duf can also recruit *Loner*, which activates *ARF6*. *ARF6* is required

for the proper subcellular localisation of Drac. Downstream effectors of Drac might include the structural protein Dtitin. Relatively little is known about the signalling components in the fusion competent cells. Moreover, although cytoskeleton rearrangement is a prerequisite for fusion, little is known about the actual fusion of the membranes (for review, see Taylor, 2002; Chen and Olson, 2004).

By the end of germ band retraction, each muscle precursor is specified expressing a particular combination of identity genes. They then start differentiating into functional multinucleated muscles by further fusion, activation of structural genes and by finding their final attachment sites on the ectoderm.

A key gene involved in the differentiation process is *Dmef2*. As mentioned earlier, *Dmef2* is a direct target of Twist in the somatic mesoderm (Taylor et al., 1995; Cripps and Olson, 1998). In *Dmef2* mutants, genes such as *eve*, *S59* or *ap* are expressed in the somatic mesoderm indicating that founders form and are specified (Lilly et al., 1995; Bour et al., 1995, Ranganayakulu et al., 1995). However, later stages of muscle differentiation are impaired. There is an almost complete lack of myosin expressing cells within the somatic mesoderm and multinucleated fibres fail to form (Bour et al., 1995; Lilly et al., 1995; Ranganayakulu et al., 1995; Gunthorpe et al., 1999). Moreover, it has been shown that different levels of DMef2 can affect different aspects of muscle differentiation (Gunthorpe et al., 1999). *Dmef2* is therefore required both for fusion and for the activation of genes necessary for the general process of differentiation.

Only few direct targets for DMef2 have been identified. These include Tropomyosin and  $\beta$ 3-tubulin, which are both characteristic components of differentiated muscles (Lin et al., 1996; Damm et al., 1998), and Actin57B, which is the major myofibrillar actin expressed in muscle during embryogenesis (Kelly et al. 2002). However, there is evidence suggesting that *Dmef2* regulates other genes that play a role in somatic muscle

differentiation. These include, the muscle LIM proteins Mlp60A and Mlp84B, which are components of the muscle contractile apparatus (Stronach et al., 1999), muscle Myosin and Paramyosin (Lilly et al., 1995, Bour et al, 1995; Gunthorpe et al, 1999; Arredondo et al., 2001), and Muscleblind, whose function is required for the formation of Z-bands and tendon cells at muscle attachment sites (Artero et al., 1998).

As they are differentiating, myotubes begin to search for their future attachment sites. During this phase, myotubes form filopodia that presumably sense the environment for guidance cues. They finally attach to specific tendon-like cells on the inner surface of the ectoderm (Bate, 1990). The earliest known marker for tendon cell precursors is the zinc-finger transcription factor *Stripe* (Volk and VijayRaghavan, 1994). The crucial influence of tendon cell precursors on muscle migration and attachment has come from the analysis of *stripe* mutants (Frommer et al., 1996). In these mutants, myotubes migrate to aberrant positions and fail to attach to the epidermis. This demonstrates an instructive role of the tendon cell precursors for myotube pathfinding. Moreover, the analysis of these mutants also suggests a role of the tendon cells in sending signals to the myotubes that have reached their destination to stop their search for attachment sites. Indeed, in *stripe* mutants, some myotubes continue to migrate at a time when they would have normally stopped and attached (Frommer et al., 1996; Schnorrer and Dickinson, 2004).

### **1.4.2 The visceral musculature**

Two types of visceral muscle surround the larval midgut and provide the force for the peristaltic movements of digestion: inner circular and outer longitudinal muscles (Bate, 1993; Campos-Ortega, 1997). In contrast, only one type envelops the foregut and the hindgut.



Progenitors of the midgut circular visceral muscles arise from segmentally repeated subsets of cells, within the Eve domains, expressing a low level of Twist. These cells express the homeodomain transcription factor Bap (Azpiazu et al., 1996). The expression of *bap* in these cells is induced by Tin, whose expression is restricted to the dorsal mesoderm. Mutations in both *tin* and *bap* disrupt the formation of the visceral mesoderm (Azpiazu and Frasch, 1993; Bodmer, 1993). During midgut development, the *bap*-expressing cells move internally and spread along the A/P axis to give rise to the circular midgut visceral mesoderm (Azpiazu and Frasch, 1993). As the midgut forms, it goes through a series of morphogenetic movements leading to the formation of three constrictions. The correct differentiation of the visceral musculature is essential for the proper formation of these constrictions (Reuter and Scott, 1990).

Although *bap* is required for correct visceral mesoderm development, it is not maintained during visceral muscle development (Azpiazu and Frasch, 1993). Differentiation of these muscles therefore occurs through downstream genes. These include *vimar* (Lo et al., 1998),  *$\beta$ 3-tubulin* (Zaffran and Frasch, 2002) and *bin* (Zaffran et al., 2001). *bin* is a particularly important downstream target for Bap as in its absence differentiation of visceral muscle fails (Zaffran et al., 2001).

Tin also induces the expression of *Dmef2* and  *$\beta$ 3-tubulin* in the developing visceral mesoderm (Cripps et al., 1999; Kremser et al., 1999). As in the somatic musculature, *Dmef2* is a central component of visceral muscle differentiation. In *Dmef2* mutants, the visceral midgut mesoderm forms, as *tin* and *bap* are normally expressed (Lilly et al., 1995), but fails to constrict and there is almost no myosin expression in the visceral midgut musculature (Bour et al., 1995). Interestingly, unlike in the somatic musculature,  *$\beta$ 3-tubulin* is not a target of DMef2 in the visceral musculature (Damm et al., 1998). Evidence suggests that in the visceral mesoderm DMef2 can regulate the expression of

*αPS2 integrin* (Ranganayakulu et al., 1995; Lin et al, 1997) and myosin (Lilly et al., 1995, Bour et al, 1995; Gunthorpe et al, 1999).

Visceral muscles, like the somatic muscles, are syncytial units resulting from the fusion of founders and FCMs (San Martin et al., 2001; Klapper et al., 2001). Two different classes of founder myoblasts have been described for the circular and the longitudinal muscles, but there appears to be one common pool of FCMs (Martin et al., 2001; Klapper et al., 2002). The specification of visceral muscle founders requires the function of *jelly-belly (jeb)* which encodes an LDL receptor repeat-containing protein. In *jeb* mutants, founder cells do not develop and all the visceral muscle progenitors become FCMs and are incorporated into the somatic musculature (Weiss et al., 2001; Lee et al., 2003; Englund et al., 2003; Stute et al., 2004).

There are other similarities with somatic muscles. For example, like in the somatic mesoderm, *Duf* and *Sns* are expressed in founders and FCMs respectively (San Martin et al., 2001; Klapper, 2002). Moreover, identity genes such as *connectin* are also found in the developing visceral musculature (San Martin et al., 2001).

All these similarities provide evidence that the same general process of myoblast fusion applies to both somatic and visceral muscles. Founder cells are specified by distinct patterns of gene expression and then fuse with FCMs to form muscle progenitors that enlarge by further fusion (San Martin et al., 2001; Klapper et al., 2002).

### **1.4.3 The heart**

The *Drosophila* heart is a dorsomedial muscular tube also termed the dorsal vessel that pumps haemolymph throughout the body cavity. It is composed of two cell types: the cardioblasts and the pericardial cells (for reviews see Cripps and Olson, 2002; Zaffran and Frasch, 2002). Cardioblasts are arranged in two rows at the dorsal midline

of the embryo and are surrounded by four rows of pericardial cells (Ward and Skeath, 2000). Whereas the cardioblasts express muscle proteins and form the contractile heart tube, the role of the pericardial cells is poorly understood. They do not express muscle proteins and have been called the pericardial nephrocytes and described as excretory cells (Han and Olson, 2005).

The different cell types of the heart derive from segmentally repeated clusters of dorsal mesodermal cells within the domain of high *Twist* expression. As cells from low *twist*-expressing domains move interiorly to form visceral muscles, the heart progenitors rearrange and, as the germ band retracts, form a continuous line on both sides of the embryos. During embryogenesis, heart precursors migrate from each side of the embryo to the dorsal midline where they converge to form the dorsal vessel.

The early activation of *tin* by *Dpp* in the dorsal part of the embryo is central in the control of heart development. *Tin* is required for the specification of all heart cells (Bodmer, 1993; Azpiazu and Frasch, 1993). For example, together with *Twist*, *Tin* maintains the expression of *eve* which is required for the determination of some pericardial cells (Su et al., 1999; Halfon et al., 2000; Knirr and Frasch, 2001). *Tin* also directly activates *Dmef2*, which is required for the differentiation of the cardioblasts, and  *$\beta$ 3-tubulin*, which is characteristic of differentiated cardioblasts (Cripps et al., 1999; Kremser et al., 1999). It is interesting to note that like in the visceral musculature and unlike in the somatic musculature, *Dmef2* does not regulate expression  *$\beta$ 3-tubulin* in the cardioblasts (Damm et al., 1998). Although *Tin* is required for heart development, it is not sufficient to promote cardiogenesis. Another factor is required, *pannier*, which encodes a GATA family transcription factor. *Pannier* and *Tin* function synergistically to promote cardiogenesis (Klinedinst et al., 2003; Gajewski et al., 1999).

During the migration of heart precursors to the dorsal midline, the different populations of cells are specified by the activation of a complex network of genes (reviewed in Cripps and Olson, 2002; Zaffran and Frasch, 2002). As they arrive at the dorsal midline, differential gene expression allows the identification of the cardioblasts and different subsets of the pericardial cells. For example, cardioblasts express DMef2 (Lilly et al., 1994; Taylor et al., 1995), Myosin,  $\beta$ 3-tubulin (Damm et al. 1998) and Tin (Bodmer, 1993; Azpiazu and Frasch, 1993). Pericardial cells express, amongst others, ZfhI (Lai et al., 1991), Eve (Frasch et al., 1987) and Odd (Ward and Coulter, 2000; Ward and Skeath, 2000).

#### **1.4.4 The adult musculature**

In *Drosophila*, adult muscles form during pupal metamorphosis and replace the larval somatic muscles. During this period almost all larval somatic muscles degenerate by histolysis (Bate, 1993). The adult muscles develop in characteristic positions and differ from the larval muscle by their size and the fact that they can be constituted of multiple fibers (Miller, 1950). This latter characteristic makes *Drosophila* adult muscles more like vertebrate skeletal muscle than the larval somatic muscles. In this section I will describe the development of the adult thoracic and abdominal muscles.

Although they only develop during metamorphosis, adult muscles originate in the embryonic mesoderm (Lawrence, 1982, Bate et al., 1991, Bate, 1993). All through embryogenesis and part of the larval life, these Twist-expressing muscle precursors remain in an undifferentiated state. They are only triggered to proliferate and differentiate later in larval life and during the early pupal stages (Bate et al., 1991; Bate, 1993). In this respect, *Drosophila* AMPs resemble vertebrate satellite cells, which, as mentioned earlier, are also quiescent, undifferentiated cells that proliferate and

differentiate to mediate muscle growth and regeneration (reviewed in Seale and Rudnicki, 2000; Morgan and Partridge, 2003).

The adult thoracic muscles develop from the adepithelial cells associated with the wing imaginal disc (Bate, 1993). These muscles are subdivided in two groups: the direct flight muscles (DFMs) and the indirect flight muscles (IFMs). The latter comprises two subclasses of muscles: the Dorso-Ventral Muscles (DVMs) and the Dorso-Lateral Muscles (DLMs) (Bate, 1993; Roy and VijayRaghavan; 1999; Taylor, 2005). At the onset of metamorphosis, larval muscles begin to hystolyse. An exception is three oblique muscles, which will serve as templates for the formation of the DLMs. By twelve hours after pupae formation (APF), the histolysis is complete and the precursors associated with the wing discs migrate to the muscle-forming regions near the epidermis (Fernandes et al., 1991; reviewed in Roy and VijayRaghavan; 1999; Taylor, 2005). This migration of precursors can be compared to that of vertebrate progenitors, which migrate to form the limb muscle for example. Thirteen hours APF, the larval template muscles split and the DLMs start assembling. DLMs are formed by 16-17 hours APF. At the same time, the DVMs form by *de novo* fusion of muscle precursors. By 24 hours APF, DLMs and DVMs are complete (Fernandes et al., 1991; Bate, 1993; Farrell et al., 1996; reviewed in Roy and VijayRaghavan; 1999; Taylor, 2005).

In the abdomen, muscle formation occurs later than in the thorax and gives rise to a well-defined set of fibres, which form dorsally, laterally and ventrally in each segment (Currie and Bate, 1991). During the early pupal stages (0-24 hours APF), the AMPs proliferate and migrate along the nerves to the muscle forming-regions. By 28-30 hours APF, these precursors begin to fuse. By 50 hours APF, the pattern of the abdominal muscles is complete (Bate, 1993, Roy and VijayRaghavan; 1999; Taylor, 2005).

As in the embryo, the formation of adult muscles could be initiated by founder cells. A recent study (Dutta et al., 2004) has shown that the pattern of adult muscles is prefigured by a pattern of precursors expressing *Duf*, which is a founder specific gene in the embryo (Ruiz-Gomez et al. 2000). Analysis of the DVMs showed that the number of *Duf*-expressing cells corresponds to the number of fibers in an adult muscle. Moreover, they showed that, when fusion is compromised, these cells develop as myosin-expressing cells (Dutta et al., 2004). In the embryo, this a key feature of founder myoblasts (Rushton et al., 1995). Nevertheless, unlike in the embryo, the adult founders do not seem to be segregated by Notch-mediated lateral inhibition (Dutta et al., 2004). A recent study suggests a key role for FGF signaling in this process (Dutta et al., 2005).

## **1.5 Genes important for somatic muscle differentiation**

In *Drosophila*, the main pathway of somatic muscle differentiation is centered on two key regulators: Twist and its direct target, DMef2 (Taylor et al., 1995; Baylies and Bate, 1996; Cripps and Olson, 1998; reviewed in Black and Olson, 1998; Taylor, 2005). Earlier in this Chapter, I presented an overview of their roles during the development of the different muscle types. I will now focus on what is known about their function during somatic muscle differentiation.

### **1.5.1 *Twist***

*Drosophila* Twist is the founding member of a conserved family of bHLH transcriptional regulators found in human, mouse, nematodes, zebrafish and chicken (for review see Castanon and Baylies, 2002). Genetic analysis of *twist* function in *Drosophila* showed that it can promote somatic muscle differentiation (Baylies and Bate, 1996). In this study, Baylies and Bate investigated *twist* function using gain-of and loss-

of-function approaches. Gain-of-function was achieved using the GAL4/UAS system (Brand and Perrimon, 1993) and loss-of-function was obtained with a temperature-sensitive combination of two *twist* alleles [*twist*<sup>v50</sup>/*twist*<sup>ry50</sup>; Simpson, 1983; Thisse et al, 1987]. Because in the absence of *twist* no mesoderm is formed (Simpson, 1983; Leptin, 1991), the use of this heteroallelic combination was necessary to knock-out *twist* function after the formation of the mesoderm. They showed that high levels of *twist* are necessary for switching cells into somatic myogenesis, whereas low levels allow the development of other mesodermal derivatives (Baylies and Bate, 1996).

This function of promoter of muscle differentiation for Twist in *Drosophila* contrasts with that of mouse Twist (MTwist). In cell culture, MTwist can inhibit the function of MyoD and Mef2 proteins and therefore can inhibit myogenesis (Hebrok et al., 1994; Spicer et al., 1996). However, further analysis of *twist* function in *Drosophila* showed that, even though it promotes somatic myogenesis in the embryo, it can also play a role as an inhibitor of IFM differentiation (Anant et al., 1998). As mentioned earlier, *twist* expression persists in the precursors of the adult muscles during embryogenesis (Bate et al. 1991). As these precursors start their differentiation, *twist* declines (Currie and Bate, 1991; Fernandes et al., 1991). Anant et al. have shown that this decrease of *twist* expression is required for IFM differentiation. Persistent *twist* expression in the precursors of the adult muscles results in a reduction of myosin expression and degeneration of the IFMs (Anant et al., 1998).

Although this inhibitory function is consistent with the role of MTwist, it contrasts with *twist* function in the embryo. An explanation for this duality of *twist* function is provided by Castanon et al. who have further defined the role of *twist* and the importance of Twist levels in the differentiation of mesodermal derivatives in *Drosophila*. They showed that the activity of Twist as a promoter or an inhibitor of

somatic muscle differentiation depends on its dimerisation partner. In domains of high Twist expression, Twist homodimerises and promotes somatic myogenesis. In domains of low Twist expression, Twist predominantly dimerises with Daughterless (Da), which is the homologue of vertebrate E protein and is required for mesoderm development (Castanon et al., 2001). Twist/Da heterodimers can repress somatic myogenesis (Castanon et al., 2001).

### 1.5.2 *Dmef2*

The Myocyte enhancer factor 2 (Mef2) was first identified in mammalian cell culture as a protein binding an A/T rich sequence in an enhancer of the *muscle creatine kinase (mck)* gene (Gosset et al., 1989). The Mef2-binding site was subsequently identified in nearly all known skeletal muscle genes (reviewed in Black and Olson, 1998). Mef2 proteins belong to the MADS box family of transcription factors and are essential for the activation of muscle gene expression (for review see Black and Olson, 1998; Taylor, 2005). However, although numerous mammalian cell culture studies indicate that Mef2 proteins are essential for skeletal muscle differentiation, their role in the process *in vivo* is still unclear.

Four vertebrate *mef2* genes [*mef2a*, *-b*, *-c* and *-d*; (Pollock and Treisman, 1991; Chambers et al., 1992; Yu et al., 1992; Breitbart et al., 1993; Leifer et al., 1993; Martin et al., 1993; McDermott et al., 1993; Ticho et al. 1996; Morisaki et al., 1997)] have been identified. These genes regulate myogenesis, at least in part, through interaction with other transcription factors. The best studied examples of such interactions involve the Myogenic Regulatory Factor (MRF) family (reviewed in Black and Olson, 1998; Taylor, 2005). Members of this family are bHLH transcription factors and include MyoD, Myf5, Myogenin and MRF4 (Weintraub et al., 1991). MyoD, the founding member of



this family, can convert any cell type into myoblasts. These myoblasts can then differentiate into muscles (Weintraub et al., 1991). In cultured cells, Mef2 proteins can interact with members of the MRF family to synergistically activate muscle gene expression (Kaushal et al., 1994; Molkenin et al., 1995). In addition to the bHLH factors, other transcription factors interact with Mef2 to promote myogenesis. For example, the Ets domain transcription factor, polyoma virus enhancer activator 3 (PEA3), can promote the differentiation of satellite cells following degeneration and this action is potentiated by interaction with Mef2 (Taylor et al., 1997).

Interactions of Mef2 with other transcription factors can also inhibit its activity. As mentioned in the previous section, MTwist can interact with Mef2 and inhibit its activity (Spicer et al., 1996). This inhibition of Mef2 activity by MTwist is dependent on binding of MTwist to the C-terminal transcriptional activation domain of Mef2 (Spicer et al., 1996). This activity of MTwist contrasts with that of *Drosophila twist*, which has been shown to positively regulate *Dmef2* expression (Taylor et al., 1995; Cripps and Olson, 1998). Other transcriptional regulators such as HDACs have also been shown to bind to Mef2 and repress its activity in cell culture (see Chapter 6, section 6.4).

Because of the overlapping pattern of expression and possibly function of the four Mef2 genes (reviewed in Black and Olson, 1998), analysis of Knock-out mice is rather complicated. Analysis of mice lacking *mef2-c*, which is the earliest of the four genes to be expressed in developing skeletal muscles (Edmondson et al., 1994), indicates that Mef2-C could be required for the activation of the skeletal muscle differentiation program (Lin et al., 1998). This analysis is limited to the observation of some muscle defects through the expression of a muscle specific reporter transgene.

In contrast to vertebrates, *Drosophila* possesses a single *mef2* gene (*Dmef2*) (Lilly et al., 1994) and its *in vivo* role during somatic muscle differentiation is clearly established. In *Dmef2* mutant embryos, there is an almost complete loss of Myosin-expressing cells within the somatic mesoderm and multinucleated fibres fail to form (Bour et al., 1995; Lilly et al., 1995; Ranganayakulu et al., 1995; Gunthorpe et al., 1999). These effects occur quite late in the muscle differentiation process. Muscle founders are specified normally, as revealed by the expression of markers such as *eve* or *S59*, but they fail to fuse (Lilly et al., 1995; Bour et al., 1995, Ranganayakulu et al., 1995). These unfused founders do not differentiate into mononucleated fibres (Prokop et al., 1996). *Dmef2* is therefore required for the fusion of founder cells with FCMs and for the subsequent differentiation of the somatic muscle precursors. Loss of *Dmef2* also affects the differentiation of visceral and cardiac muscle (see sections 1.4.2 and 1.4.3). This mutant phenotype demonstrates that, in *Drosophila*, *Dmef2* is central to the differentiation of all muscle types.

However, as mentioned in section 1.4.1, only a few targets have been identified for *Dmef2*. These include Tropomyosin and  $\beta$ 3-tubulin, which are both characteristic components of differentiated muscles (Lin et al., 1996; Damm et al., 1998), and Actin57B, which is the major myofibrillar actin expressed in muscle during embryogenesis (Kelly et al. 2002). Moreover, the analysis of *Dmef2* has mainly focused on its function during differentiation. Yet, *Dmef2* is expressed in the mesoderm long before the onset of muscle differentiation (Taylor et al., 1995), and therefore could affect gene expression earlier than generally supposed. Two examples of early *Dmef2* targets have been described supporting this idea: *Dmeso18E*, whose expression is dependent upon *Dmef2* function at stage 11-12 (Taylor, 2000) and Actin57B, whose

expression is reduced from stage 10 in *Dmef2* mutant embryos (Kelly et al., 2002). This facet of *Dmef2* function remains to be fully explored.

Like vertebrate Mef2 proteins, Dmef2 has been shown to directly interact with other transcription factors to regulate muscle differentiation. For example, its interaction with the *Drosophila* PAR domain-bZIP transcription factor PDP1 is necessary for regulating somatic muscle differentiation and the activation of the *tropomyosinI* gene (Lin et al., 1997). Moreover, the regulation of Actin57B by DMef2 might require a co-factor (Kelly et al., 2002).

In conclusion, although Mef2 proteins play key roles in muscle differentiation in both vertebrates and *Drosophila*, a lot remains to be uncovered about their mechanism of action and the regulation of their activity *in vivo*.

## **1.6 Novel genes in muscle development**

Progress in a molecular understanding of muscle development requires both the identification and analysis of genes that operate downstream of the molecules that pattern the mesoderm and also an understanding of the events that subsequently occur in muscle differentiation.

In order to investigate this issue, Dr Taylor undertook a screen to identify genes that are specifically expressed in the progenitors of the developing muscle. The analysis of these genes has two aims. The first is to analyse the control of their expression to determine how the general signals and transcription factors that pattern the mesoderm initiate cell-type specific gene expression. This forges an initial link from the early patterning events to the production of functional tissue. The second is to analyse what these genes do and how do they do it. The aim here is to understand the molecular

events of muscle differentiation. It is this second aspect that is the focus of my PhD project.

Dr Taylor's screen used the technique of subtractive hybridisation linked to cDNA library construction (Taylor, 2000). He made a subtracted cDNA library enriched more than 100-fold for mesodermal cDNAs. Essentially, the approach was to take cDNA from wild type embryos and to subtract that from *twist* mutant embryos, which develop with no mesoderm. cDNAs from the subtracted library were then screened by *in situ* hybridisation to identify genes with specific expression patterns early in muscle differentiation. DNA sequencing determined whether clones with temporally and spatially significant expression patterns were previously undescribed. These novel genes are a rich source for current and future research. This innovative screen was the first to use zygotic mutations coupled to subtractive hybridisation to isolate genes specifically associated with a particular developmental event. The philosophy of this approach is to first identify differentially expressed genes, and then use reverse genetics to determine functions of the gene. This is greatly facilitated by resources provided by The *Drosophila* Genome Project.

The screen led to the isolation of novel genes specifically expressed in precursor cells of the different muscle types. My project centres on one of these genes: *Dmeso17A*.

Preliminary work in the laboratory has centred on a basic description of the gene, making/isolating essential gene-specific reagents, and initiating studies of what the gene does. The general approach was:

- Isolation of full-length cDNA and genomic DNA
- Analysis of the expression pattern of the gene to obtain clues on its function
- Making antibodies to detect protein expression and to compare with RNA expression

- Computer-based analysis of the gene sequence to look for protein motifs and similar genes in other species
- Making transgenic lines to manipulate gene expression

My work on this gene is divided into two parts: the first aim is to analyse the role of the gene in the development of the different muscle types. The second aim, after investigating what the gene does, is to determine how does it do it. What is the gene function? Is it a transcription factor? Does it modulate signalling? Which proteins does it interact with?

My general approach was to manipulate the gene's expression in order to determine what its role is and what is the mechanism by which it acts. Using the GAL4/UAS system to both miss-express and over-express full length or modified proteins, I have been able to test genetic interactions between *Dmeso17A* and putative interactor(s) or target(s).

## **Materials and Methods**

### **2.1 Molecular Biology**

#### **2.1.1 Agarose gel electrophoresis**

Electrophoresis was used to separate DNA fragments. 1% agarose (w/v) / 1X TBE (90mM Tris-Borate, 2mM EDTA, pH 8.3) gels were used. 5-10  $\mu$ l of a 10mg/ml ethidium bromide solution was added to the gels and the fragments were visualised using an UV transilluminator to detect the fluorescence of the ethidium bromide that had intercalated within the DNA. A 1Kb ladder (Fermentas) or Lambda HindIII were used as molecular weight markers.

#### **2.1.2 DNA extraction from agarose gels**

DNA fragments were extracted from agarose gels using the QIAquick gel extraction kit (Qiagen) following the manufacturer's instructions

#### **2.1.3 Bacterial cultures and plates**

Bacteria were grown either in liquid culture in Luria-Bertani (LB) medium (per Litre: 10g Bacto-tryptone, 5g yeast extract, 5g NaCl, pH 7.0) at 37°C with continuous shaking at 300rpm, or on LB-agar (LB plus 15g/L Bacto-Agar) plates at 37°C.

Ampicillin, at a final concentration of 100 $\mu$ g/ml, or Kanamycin, at a final concentration of 50 $\mu$ g/ml, were used as selectors.

#### 2.1.4 Transformation of competent cells

The *E.coli* DH5 $\alpha$  bacterial strain was used for transformation. 50 $\mu$ l of competent cells were incubated with 1-5 $\mu$ l (20 to 100ng) of DNA for 20 minutes on ice, heat-shocked at 42°C for 45 seconds and replaced on ice for at least 1 minute. 450 $\mu$ l of SOC medium (2% Tryptone, 0.5% Yeast Extract, 10mM NaCl, 10mM KCl, 10mM MgCl<sub>2</sub>, 10mM MgSO<sub>4</sub>, 20mM Glucose) was added and the transformed cells incubated at 37°C for 30 minutes to allow them to recover and to express the antibiotic resistance gene. 50 $\mu$ l and 250 $\mu$ l of sample were plated onto LB-agar/ antibiotic plates and incubated overnight at 37°C.

#### 2.1.5 Plasmid DNA preparation

Small scale DNA preparations (minipreparations) were undertaken either by a rapid boiling lysis method (boiling miniprep), or by using the QIAprep Spin Miniprep Kit (Qiagen). In both methods, 1.5ml of a 3ml overnight *E.coli* DH5 $\alpha$  culture was collected by centrifugation at 13 000rpm in a microfuge for 5 minutes.

When the QIAprep Spin Minirep Kit was used, the manufacturer's instructions were followed.

For the boiling miniprep method, the bacterial pellets were resuspended in 150 $\mu$ l STET buffer (0.1M NaCl, 10mM Tris-HCl pH 8.0, 1mM EDTA pH 8.0, 5% Triton X-100) supplemented with 15  $\mu$ l fresh lysozyme (Sigma, 10mg/ml). Cells were then lysed in a boiling water bath for 45 seconds. After centrifugation (13 000rpm in a microfuge for 10 minutes), the supernatant was transferred into a fresh 1.5ml microcentrifuge tube and the DNA was precipitated with an equal volume of isopropanol. The DNA was pelleted by centrifugation (13 000rpm in a microfuge for 10 minutes), washed with 70% ethanol and resuspended in 30 $\mu$ l TE containing RNase A (Sigma, 5 $\mu$ g/ml).

Larger scale DNA preparations (midpreparations) were undertaken using the QIAfilter Plasmid Midi Kit (Qiagen) according to the manufacturer's instructions.

### **2.1.6 DNA precipitation with ethanol**

DNA was precipitated by the addition of 2 volumes of ice cold ethanol after the salt concentration was adjusted with 1/10 volume of 3M sodium acetate. The mixture was incubated for 20-30 minutes at -80°C and the DNA was recovered by centrifugation at 13,000 rpm in a microfuge for 15 minutes. The pellet was washed with 70% ethanol, air dried and resuspended in a suitable volume of double distilled H<sub>2</sub>O.

### **2.1.7 Restriction enzyme digest**

Reactions were carried out in 50 µl containing the DNA to be digested, the restriction endonuclease(s) (NEB or Promega) and the appropriate reaction buffer (NEB or Promega). An excess of enzyme (typically 3-fold) per µg of DNA was used (without exceeding 10% of the reaction volume). Reactions were incubated at 37°C for 2 hours and stopped by heat killing the enzyme for 20 minutes at the temperature indicated by the manufacturer. For double digests, reactions were performed either simultaneously or sequentially. In the first case, the buffer providing optimum reaction conditions for both restriction endonucleases was selected. If no single buffer was found, the reaction was carried out with the first enzyme alone, then the DNA was precipitated with ethanol and finally digested with the second enzyme.

When 5' overhang filling was required to generate blunt ends, the DNA was digested with the first enzyme and the reaction was stopped by heat killing the enzyme. 1 µl of T4 DNA polymerase (3U/µl; NEB) and 0.5 µl of 10mM dNTPs (Promega) were



then added. The reaction was incubated for 30 minutes at 37°C. After completion, the DNA was precipitated with ethanol and digested with the second enzyme.

For the preparation of plasmid DNA for ligations, 5µl of 1µg/µl vectors were digested as described above, precipitated with ethanol and the DNA pellet was resuspended in 26µl H<sub>2</sub>O. Linearised vectors were then dephosphorylated by the addition of 3µl of 10x buffer 3 (NEB) and 1µl of alkaline phosphatase calf intestinal (CIP) (NEB). Reaction were incubated at 37°C for 30 minutes and stopped by the addition of 0.5µl of 0.5M EDTA and then by heat killing the CIP for 5 minutes at 65°C.

In all cases, restriction fragments and linearised vectors were purified by gel extraction prior to ligation.

### **2.1.8 Ligation of DNA fragments into plasmids**

Ligation of cohesive or blunt end DNA fragment was carried out in a 10µl volume containing 1µl of 10X ligation buffer (NEB), 1µl of T4 DNA ligase (NEB), 1µl of linearised plasmid DNA (50ng/µl) and a 3x molar excess of DNA fragment to be ligated. Reactions were incubated overnight at 16°C or at 12°C if EcoRI was used for the digests. 3-5µl of ligation reactions were used for transformation.

### 2.1.9 Polymerase Chain Reaction (PCR)

Standard PCR reactions were carried out for the generation of the various constructs (see sections 2.1.11; 2.1.14; 2.1.15). Unless otherwise stated, the DyNAzyme EXT high fidelity DNA Polymerase (Finnzymes) was used. Typically, reactions were carried out in a 50 $\mu$ l volume, containing 5 $\mu$ l of optimised DyNAzyme EXT buffer (containing 1.5mM MgCl<sub>2</sub>), 1 $\mu$ l of 10mM dNTPs (Promega), 1 $\mu$ l of 10 $\mu$ M forward oligonucleotide primer (MWG), 1 $\mu$ l of 10 $\mu$ M reverse oligonucleotide primer (MWG), 1 $\mu$ l of 100ng/ $\mu$ l template DNA (plasmid or genomic) and 1 $\mu$ l of DNA polymerase. The volume was then adjusted with double distilled H<sub>2</sub>O. The DNA templates were amplified using 20-25 cycles in a Peltier thermal cycler (MJ Research) equipped with a heated lid.

The following program was used:

- Initial denaturation: 95°C, 5 minutes
- Denaturation: 95°C, 1 minute
- Annealing: 55-65°C, 1 minute
- Extension: 72°C, 1 minute/Kb of template sequence
- Final extension: 72°C, 5-10 minutes

At the end of the program, 5 $\mu$ l of the PCR reaction was used to analyse the products on a 1% agarose gel and 2 $\mu$ l were used to measure the concentration of the products using a spectrophotometer. The PCR products were then ligated by TA cloning into the PGEM-T cloning vector (Promega) according to the manufacturer's instructions. The TA cloning was possible because the DyNAzyme EXT DNA Polymerase adds a non-templated adenine residue at the 3' end of a DNA fragments.

### 2.1.10 Preparation of Digoxigenin-labelled RNA probe

The DNA template for the *Dmeso17A* RNA probe was a 579bp cDNA fragment in pBluescript II KS (-) isolated from a subtracted library (Taylor, 2000). The 2.6kb  $\beta$  *tubulin* cDNA fragment (from construct PC60-1L, a gift from Detlev Buttgereit) was subcloned into pBluescript II KS (+). The *Dmef2* cDNA (an approximately 3kb fragment) was in pBluescript II KS (-) (Taylor et al., 1995).

Prior to transcription, DNA templates were linearised as described in section 2.1.7. The *Dmeso17A* cDNA was digested with HindIII (NEB), the  $\beta$  *tubulin* cDNA with XhoI (NEB) and the *Dmef2* cDNA with HindIII (NEB). Linearised DNAs were then purified by gel extraction.

Transcription reactions were carried out in 50 $\mu$ l containing approximately 500ng of linearised template DNA, 1 $\mu$ l of 10X transcription buffer (Roche), 1 $\mu$ l of DIGNTP mix (Roche), 0.5 $\mu$ l of RNase inhibitor (Roche) and 1 $\mu$ l of T7 RNA polymerase (Roche). The volume was then adjusted to 10 $\mu$ l with double distilled H<sub>2</sub>O. Reactions were incubated at 37°C for 2 hours. After transcription, the DNA template was removed by the addition of 1 $\mu$ l of DNaseI buffer, 6 $\mu$ l of H<sub>2</sub>O and 3 $\mu$ l of DNaseI RNase free (10U/ $\mu$ l; Roche). This was incubated at 37°C for 15 minutes. The RNA probes were then fragmented with 80 $\mu$ l of 125mM sodium carbonate (pH 10.2) at 60°C for 15minutes. The alkaline hydrolysis of the probes was stopped by adding of 50 $\mu$ l 7.5M ammonium acetate. RNA was precipitated with isopropanol, washed with 70% ethanol, air dried and resuspended in TE:formamide (1:1).

The yield of DIG-labelled RNA was estimated in a spot test using a DIG-labelled control (Roche). The test was performed following the manufacturer's instructions. Briefly, dilutions of both the control and the probes (all in RNase free double distilled H<sub>2</sub>O) to be tested were spotted and cross-linked to a positively-charged nylon

membrane (Roche). The spots were then colorimetrically detected and the comparison of the intensities of the spot allowed an estimation of labelling yield. Probes were diluted with TE:formamide (1:1) to 25ng/μl and 5μl was used for *in situ* hybridisation.

### 2.1.11 Generation of the *UAS-Dmeso17A-RNAi* construct

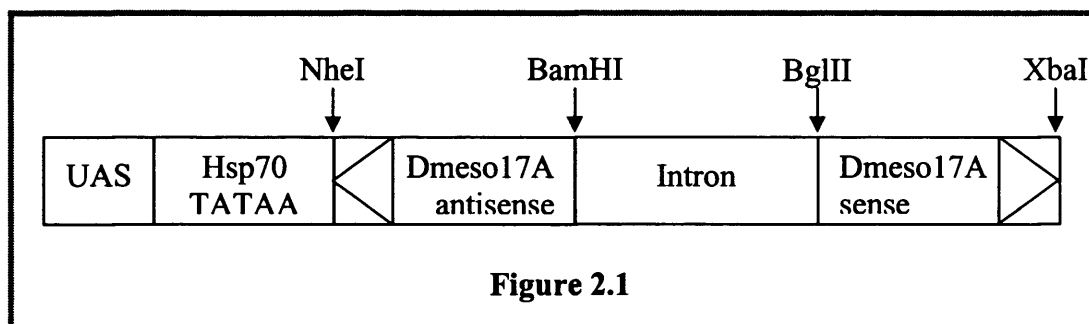
Knock-down of *Dmeso17A* was achieved *via* dsRNA interference (RNAi) using a splice-activated UAS hairpin vector (pJM1084; Reichhart et al, 2002). The entire coding region of *Dmeso17A* was used and convenient restriction sites were inserted by PCR at the 5' and 3' ends of *Dmeso17A* cDNA. The following primers were used:

- 5' **GGAGCTAGCATGGGCGTCATCTACAAG** 3' (Tm 68.0°C; bold: NheI site)
- 5' **GGAGGATCCCTACCAAGGTCGCCACAC** 3' (Tm 71.0°C; bold: BamHI site)

The Tms indicated in brackets were calculated according to the formula given on the MWG web site for primers longer than 15bp (<http://www.mwg-biotech.com>).

The PCR fragment was ligated into pGEM-T (Promega), grown and sequenced. It was then digested, using the BamHI and NheI restriction endonucleases, and gel purified. The purified product was ligated into pJM1084 on both sides of the intronic spacer, in between the BamHI and NheI sites (Antisense, 5' of the intron) or the compatible BglII and XbaI sites (Sense, 3' of the intron) (Figure 2.1).

The construct was then prepared and injected as described in section 2.3.5 and the GAL4/UAS system (Brand and Perrimon, 1993) was used to express the dsRNA construct.



### 2.1.12 Total RNA extraction from *Dmeso17A-RNAi*-expressing embryos

To test whether *Dmeso17A-RNAi* is inducing a knock-down of *Dmeso17A*, RNA was extracted from embryos expressing *Dmeso17A-RNAi* in order to perform semi-quantitative RT-PCR. Females homozygous for a *UAS-Dmeso17A-RNAi* construct were crossed with males homozygous for *Dmeso17A-GAL4*. Wild-Type flies were used as a control. Crosses were set up in cages where flies were allowed to lay eggs on apple juice-agar plates supplemented with fresh yeast at 25°C for 40 minutes. The plates were then further incubated at 25°C until the embryos reached stage 12 (7 hours).

30 minutes before they reached the desired stage, the embryos were transferred into a mesh basket and rinsed thoroughly with water to eliminate the yeast. They were then arranged in one layer on a new plate to facilitate sorting. The stage of development of the embryos was checked by looking at the yolk autofluorescence using a green filter. The yolk shape changes during development allowing precise staging of the embryos. A minimum of 150 embryos were selected for RNA extractions. Unfertilized embryos were discarded.

Selected embryos were transferred to a 1.5ml microcentrifuge tube and rinsed 3 times with double distilled H<sub>2</sub>O. After the last rinse, the embryos were spun down for a

few seconds at maximum speed and all the water carefully removed. Embryos were frozen in liquid nitrogen and stored at -70°C prior to RNA extraction

RNA was extracted using the RNeasy Protect Mini Kit (Qiagen) according to manufacturer's instructions. The concentration of RNA was determined by spectrophotometry.

### 2.1.13 Semi-quantitative Reverse Transcription-PCR (RT-PCR)

Reverse transcription was performed using the SuperScript III First-Strand Synthesis System for RT-PCR (Invitrogen) following the manufacturer's instructions. 500ng of total RNA from *Dmeso17A-RNAi* over-expressing or wild type embryos was used for first strand cDNA synthesis. The following gene-specific primers were used to reverse transcribe both *Dmeso17A* and a control, *rp49* (Tamate et al., 1990; Borie et al., 1999):

- For *Dmeso17A*: 5' TACCAAGGTCGCCACACCAC 3' (T<sub>m</sub> 61.4°C)
- For *rp49*: 5' TGTGTATTCCGACCACGTTACAAG 3' (T<sub>m</sub> 61.0°C)

2.5µl of cDNA products were used for amplification with 1µl of BIOTAQ DNA polymerase (5U/µl; Bioline), in the buffer provided by the manufacturer and in the presence of the specific primers for both *Dmeso17A* and *rp49*, which was used as an internal control. Reactions were carried out in a Peltier thermal cycler (Mj Research) using the following program:

- Initial denaturation: 95°C, 3 minutes
- Denaturation: 95°C, 1 minute
- Annealing: 60°C, 1 minute
- Extension: 72°C, 1 minute
- Final extension: 72°C, 5 minutes

A total of 25 cycles was used. This number was chosen so that the amplification products were clearly visible on an agarose gel and can be quantified, but also that the reaction was in the exponential phase and had not reached a plateau of amplification. The two sets of primers were also tested to make sure that they did not compete when used in the same PCR reaction.

Images of the RT-PCR agarose gels were acquired with a lcd camera and quantification of the bands was performed using the Gene tool software (Syngene) .

#### **2.1.14 Generation of the *Dmeso17A-GAL4***

*Dmeso17A-GAL4* was generated using a 2.8Kb restriction fragment (EcoRI/ XhoI) from the *Dmeso17A* enhancer region. This fragment has previously been tested in the laboratory in a reporter construct. LacZ expression driven by this enhancer is very similar to that of *Dmeso17A*.

The 2.8Kb were cloned into the pPTGAL vector (Sharma et al., 2002) which contains the *GAL4* coding sequence and allows insertion of enhancer fragments and immediate injection for the generation of transgenic lines.

Because there is no XhoI restriction site in the pPTGAL polylinker, the 2.8Kb fragment and the vector were first digested with XhoI and BamHI respectively and blunt ends were generated by 5' overhang filling. DNAs were then digested with EcoRI, gel purified and ligated.

The construct was then prepared and injected as described in section 2.3.5.

### 2.1.15 Generation of *GST-Dmeso17A* and *GST-Dmeso17A-ΔWRPW* fusion proteins

To allow expression in either rabbit reticulocyte lysate or prokaryotic system, the constructs were generated using the pET-3a vector (Novagen) in which the T7-Tag was removed and replaced by GST (GST-pET-3a). The following primers, containing NdeI or BamHI restriction sites, were used to amplify the GST DNA from the pGEX-2TK vector (Amersham Bioscience):

- 5' **GCATATG**TCCCCTATACTAGGTTATTGG 3' (T<sub>m</sub> 63.6°C; bold: NdeI restriction site)
- 5' **GGATCC**ATCCGATTTTGGAGGATGGTTCG 3' (T<sub>m</sub> 68°C; bold: BamHI restriction site)

The PCR fragment was ligated into pGEM-T (Promega), grown and its sequence verified. It was then digested, using NdeI and BamHI, and gel purified. The pET-3a vector was also digested with NdeI and BamHI, to remove the T7-Tag, dephosphorylated and gel purified.

Fragment and vector were ligated as described in section 2.1.8 (Figure 2.2). The new GST-pET-3a vector was then prepared by digestion with BamHI, dephosphorylation and gel purification.

*Dmeso17A* and *Dmeso17A-ΔWRPW* DNA fragments, containing BamHI restriction sites at both ends, were generated by PCR from *Dmeso17A* cDNA in pBluescript II KS (-) (Taylor, 2000). The following primers were used:

- For *Dmeso17A* full length:
  - 5' **GGAGGATCC**ATGGGCGTCATCTACAAG 3' (T<sub>m</sub> 68°C; bold: BamHI restriction site)



- 5' CTCGGATCCCTACCAAGGTCGCCAC 3' (T<sub>m</sub> 69.5°C; bold: BamHI restriction site)

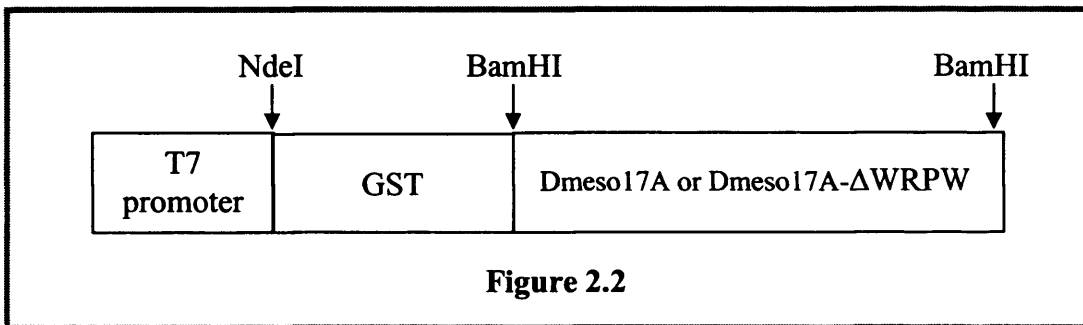
▪ For *Dmeso17A-ΔWRPW*:

- 5' GGAGGATCCATGGGCGTCATCTACAAG 3' (T<sub>m</sub> 68°C; bold: BamHI restriction site)

- 5' CTCGGATCCCTACACCACCATTGCTG 3' (T<sub>m</sub> 69.5°C; bold: BamHI restriction site)

The PCR fragments were ligated into pGEM-T (Promega), grown and sequenced. They were then digested, using BamHI, and gel purified. Full length and truncated *Dmeso17A* were ligated into GST-pET-3a (Figure 2.2).

Constructs were then prepared and injected as described in section 2.3.5.



## 2.2 Protein work

### 2.2.1 Acrylamide gel electrophoresis

Acrylamide gel electrophoresis was used to separate protein samples. Gels and samples were prepared following the method described in Sambrook and Russell (Molecular Cloning, third edition, 2001) A 12% acrylamide/SDS resolving gel (12% acrylamide/bis-acrylamide, 375mM Tris-HCl pH 8.8, 0.1% SDS) and a 4% acrylamide/SDS stacking gel (4% acrylamide/bis-acrylamide, 125mM Tris-HCl pH 6.8, 0.1% SDS) were used. Samples were run, in a mini proteanIII electrophoresis cell (Biorad), at 70 volts through the stacking gel and at 100 volts through the resolving gel in Tris-glycine running buffer (25mM Tris, 250mM glycine, 0.1% SDS, pH8.3). The SeeBlue Plus2 protein standard (Invitrogen) was used as a molecular weight marker.

Gels were either fixed in 50% methanol/10% glacial acetic acid and dried before exposure to X-ray film for autoradiography, or stained for 30 minutes in a Coomassie Brilliant Blue solution (1g/L Coomassie Brilliant Blue (Sigma), 10% methanol; 10% glacial acetic acid). Stained gels were submerged overnight in destain solution (10% methanol; 10% glacial acetic acid) to remove excess Coomassie Brilliant Blue.

### 2.2.2 Expression of proteins in bacteria

GST-fusion protein constructs were expressed using the *E.coli* BL21 strain (Stratagene). Prior to purification, miniprotein preparations were performed to assess the expression of each construct. To do so, 500 $\mu$ l of an overnight culture of a selected colony grown in LB ampicillin was used to inoculate 4.5ml of LB ampicillin (1:10 dilution). The culture was grown for 1.5 hours at 30°C with shaking at 250rpm. Before induction with freshly made IPTG (isopropyl- $\beta$ -D-thiogalactopyranoside, 0.6mg/ml, Sigma), a 2ml sample was removed for SDS PAGE analysis. The induced culture was

grown for a further 3 hours at 30°C and bacteria were harvested by centrifugation for 1 minute at 13 000rpm in a microfuge in a 2ml tube. The cells were resuspended in 100µl SDS sample buffer and boiled for 3 minutes. 20µl were loaded onto an SDS polyacrylamide gel.

In order to purify the GST-fusion proteins, selected clones expressing the constructs were grown in larger cultures. A 10ml culture was grown at 30°C with shaking at 250rpm until the OD<sub>550</sub> reached 2.0-2.5 (usually about 14-16 hours growth). About 5ml of this culture was then diluted into 100ml of LB amp and incubated at 30°C with shaking at 250rpm until the OD<sub>550</sub> reached 0.5 (usually 1-1.5 hours growth). Expression of the fusion protein was induced with 60mg/100ml IPTG and the cultures were further incubated for 3 hours at 30°C. Cells were then harvested by centrifugation at 4000rpm at 4°C in a Sorvall SS-34 rotor for 10 minutes. Bacterial pellets were resuspended in 10ml MTPBS (150mM NaCl, 16mM Na<sub>2</sub>HPO<sub>4</sub>, 4mM NaH<sub>2</sub>PO<sub>4</sub>, pH 7.3) supplemented with protease inhibitors (Roche mini-complete EDTA free tablets) and 0.1% β-mercaptoethanol (Sigma). A 1ml sample was removed at this point to check the level of induction prior to purification. The resuspended bacteria were transferred into a 50ml tube on ice and sonicated using a Soniprep150 sonicator for 1 minute at 12-14 microns amplitude. The samples were cooled and then sonicated for a further 30 seconds. The probe was also allowed to cool during the interval. 1ml of 10% Triton was added and insoluble material was removed by centrifugation at 13 000rpm in a Sorvall SS-34 rotor at 4°C for 10 minutes. The supernatant (SN) was transferred to a 15ml Falcon tube and a 1ml sample was removed for SDS PAGE analysis. The rest of the SN was mixed with 2ml of glutathione-sepharose beads (Qiagen)/MTPBS (1:1 slurry). The beads were prepared by pre-swelling and washing in MTPBS with 0.1% β-mercaptoethanol at 4°C 3hours before use. The SN and beads were rolled at 4°C for 30

minutes before pouring into a plastic column (Pierce). The columns were washed with 3 times 10ml MTPBS supplemented with protease inhibitors. 0.1% Triton was added for the first 2 washes. The beads were recovered from the column and stored at 4°C as a 50:50 slurry with MTPBS supplemented with protease inhibitors. A sample was taken to check the purification and estimate the amount of fusion protein recovered on SDS PAGE.

### **2.2.3 Expression of radiolabelled Groucho protein *in-vitro***

*In-vitro* translated Groucho (Gro) was produced using the TNT rabbit reticulocyte lysate system (Promega) which couples transcription and translation. Manufacturer's instructions were followed and T7 RNA polymerase (Promega) was used. Template was full length groucho, cloned in pET-3A (pET-gro, a gift from M.Wainwright). Reactions were performed with 1µg of DNA template and Redivue [<sup>35</sup>S]-Methionine (Amersham Biosciences) was used to radiolabel the translation products. [<sup>35</sup>S]-Gro was analysed and visualised by SDS PAGE and autoradiography (see section 2.2.1).

### **2.2.4 Pull-down assay**

In each protein-protein interaction assay, the amounts of fusion protein used, estimated by Coomassie staining of SDS PAGE gels, were normalised to 30µl of beads of the least concentrated one. Blank glutathione beads, blocked with normal goat serum, were used to bring the volume in all tubes to 30µl. Then, 180µl of binding buffer (20mM Hepes-KOH pH 7.9, 50mM KCl, 2.5mM MgCl<sub>2</sub>, 10% glycerol, 1mM DTT, 0.2% NP40, 3µl/180µl normal goat serum, 3µl/180µl 100mM PMSF (17.42 mg/ml in isopropanol)) was added to each tube and the slurry was rolled at 4°C for one hour. Approximately 25µl of programmed reticulocyte lysate containing radiolabelled Gro

was then added and the tubes rolled overnight at 4°C. The beads were then washed four times with 1ml RIPA buffer (10mM Tris-HCl pH 7.5, 150mM NaCl, 1mM EDTA, 0.2% NP40). After each wash, tubes were briefly spun at 1000rpm in a microfuge and the supernatant carefully removed. 100µl of SDS loading buffer (0.1M Tris-HCl, pH 6.8, 20% glycerol, 10% β-mercaptoethanol, 4% SDS, 0.2% bromophenol blue) was then added to the beads. Before loading on the gel, samples were boiled to release bound proteins, centrifuged for 2 minutes at 13000rpm in a microfuge to pellet the beads and the supernatant containing the released proteins was transferred to a fresh 1.5ml microcentrifuge tube. Equal amounts of each sample were loaded onto an SDS PAGE and radiolabelled Gro was visualised by autoradiography (see section 2.2.1).

## **2.2.5 Western blotting and detection of the Dmeso17A protein**

### **2.2.5.1 Protein extraction from *Drosophila* embryos**

Flies were allowed to lay eggs on an apple juice-agar plate for 20 minutes at 25°C. Embryos were further incubated at 25°C until the desired stage of development was reached and they were then staged and selected under a dissecting microscope. Protein samples were prepared from 50 stage 12 embryos.

Embryos were dechorionated and then homogenised in 12.5µl of lysis buffer (10mM Hepes pH 7.4, 5mM EGTA, 5mM EDTA, 0.44% benzamide, 5% SDS, protease inhibitors (Roche mini complete EDTA free tablets)). They were then boiled for 4 minutes before addition of 12.5µl of 2X SDS loading buffer. Samples were boiled for a further 4 minutes and stored at -70°C until required.

### 2.2.5.2 Western blot

Western blot was performed using a Mini-Trans Blot electrophoretic transfer cell (Biorad). The gel was blotted onto Immobilon P PVDF membrane (Amersham Biosciences) in transfer buffer (192mM glycine, 25mM Tris). After the transfer, the membrane was blocked overnight at 4°C in TBST (10mM Tris-HCl pH 7.5, 150mM NaCl, 0.05% Tween) containing 5% non-fat dried milk (Marvel). The blot was then cut in half at the level of the 36Kd marker. The upper half was incubated with a 1:1000 dilution of the anti- $\beta$ -tubulin antibody (E7 Ab; Developmental Studies Hybridoma Bank, Iowa). The lower half was incubated with the anti-Dmeso17A antibody diluted 1:1000. Both antibodies were diluted in TBST+5% milk and incubations were for 1 hour at room temperature. Both halves were then washed 2x 15 minutes with TBST and blocked for 1 hour at room temperature with TBST+5% milk. The lower half was incubated with a 1:10000 dilution of peroxidase-tagged anti-guinea pig secondary antibody (Jackson) and the upper half with a 1:10000 dilution of peroxidase-tagged anti-mouse secondary antibody (Vector laboratories). Dilutions and incubations were performed as described above. Membranes were then washed 2x 15 minutes with TBST. Proteins were detected using the Super Signal Chemiluminescence kit (Pierce) following the manufacturer's instructions.

## 2.3 *Drosophila* stocks and crosses

### 2.3.1 Maintenance of fly stocks

Fly stocks were maintained on a medium containing 6.77% cornmeal, 7.26% dextrose, 1.45% yeast, 0.68% agar and 2.26% nipagin. The majority of the stocks were kept at 18°C and changed every four weeks. When making stocks, crosses were kept at 25°C.

When collecting flies for UAS/GAL4 experiments, the stocks were amplified and kept at 25°C during the day and 18°C during the night to optimise virgin females collection. The laying cages were kept at either 18°C or 25°C according to the severity of the phenotype desired.

New stocks received from the *Drosophila* stock centre (Bloomington) or other groups were kept in quarantine for at least three generations and inspected for mite infection before being brought into the laboratory's fly room.

In all my experiments, *Oregon R* flies (OR) were used as wild-type.

### 2.3.2 Mutant stocks used

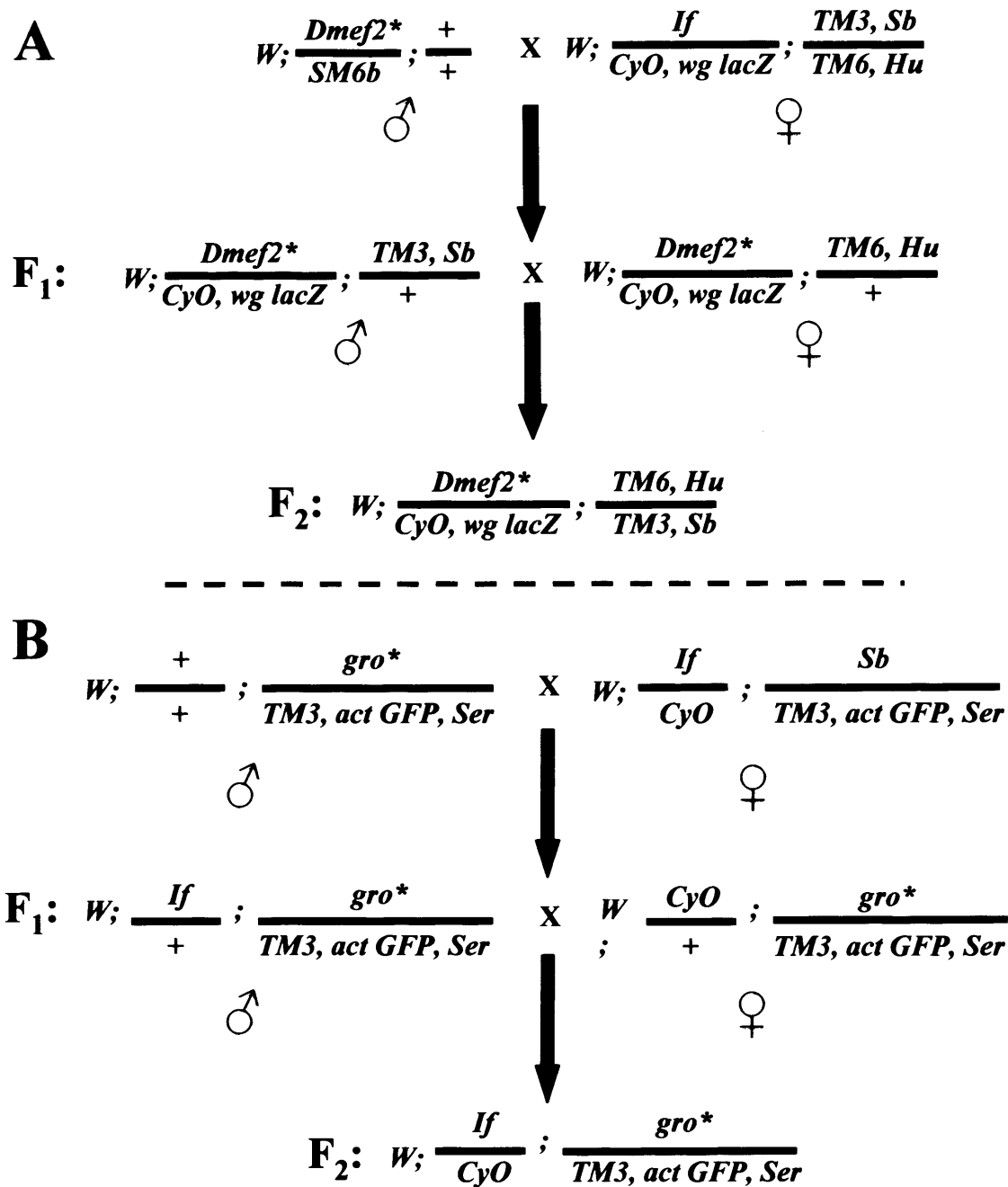
Table 1 lists the mutant stocks used.

In order to identify homozygous mutant embryos, *Dmef2*<sup>65</sup> and *gro* mutant alleles were placed over a blue or a green balancer chromosome (Figure 2.3). The balancer chromosomes carry a P-element insertion driving the expression of either  $\beta$ -galactosidase, for the so-called blue balancer, or *Green Fluorescent Protein* (*GFP*) for the green balancer. Both  $\beta$ -galactosidase and *GFP* are under the control of specific promoters/ enhancers. Antibody staining was used to assess  $\beta$ -galactosidase or *GFP* expression.

**Table 1: List of mutant stocks used**

Stock	Comments	Origin	References
<i>Dmef2</i> <sup>113</sup> / <i>SM6b</i>	EMS induced strong hypomorphic allele	Robert Schulz	Ranganayakulu et al. (1995)
<i>Dmef2</i> <sup>424</sup> / <i>SM6b</i>	EMS induced moderate hypomorphic allele	Robert Schulz	Ranganayakulu et al. (1995)
<i>Dmef2</i> <sup>65</sup> / <i>SM6b</i>	EMS induced weak hypomorphic allele	Robert Schulz	Ranganayakulu et al. (1995)
<i>gro</i> <sup>E48</sup> / <i>TM3,Sb</i>	EMS induced point mutation	Amy Bejsovec	Preiss et al. (1988)
<i>gro</i> <sup>BX22</sup> / <i>TM3,Sb</i>	Deficiency that removes several genes from the Enhancer of split ( <i>E(spl)</i> ) complex	Amy Bejsovec	Preiss et al. (1988)





**Figure 2.3: Generation of *Dmef2* or *gro* mutant balanced stocks.**

(A) Males carrying a *Dmef2* mutant allele were crossed with virgin females carrying dominant markers and a blue balancer on the second chromosome. F1 males carrying *CyO, wg lacZ; TM3, Sb* and females carrying *CyO, wg lacZ; TM6, Hu* were selected and crossed together. F2 flies carrying *CyO, wg lacZ; TM3, Sb/TM6, Hu* were kept and expanded into a stock. (B) Males carrying a *gro* mutant allele were crossed with virgin females carrying dominant markers and a green balancer on the third chromosome. F1 males carrying *If; TM3, actGFP, Ser* and females carrying *CyO; TM3, actGFP, Ser* were selected and crossed together. F2 flies carrying *If/CyO; TM3, actGFP, Ser* were kept and expanded into a stock.

For making the *Dmef2*-mutant balanced stocks (Figure 2.3A), the *CyO*, *wg lacZ* blue balancer was used. Females *w; If/CyO, wg lacZ; TM3, Sb/TM6, Hu* were crossed with *Dmef2\** males. F<sub>1</sub> males carrying *CyO, wg lacZ* and *TM3, Sb*, but not *If*, were crossed with F<sub>1</sub> virgin females carrying *CyO, wg lacZ* and *TM6, Hu* but not *If*. Males and virgin females of the F<sub>2</sub> carrying *CyO, TM3* and *TM6* were selected to make the following stock: *w; Dmef2\*/CyO, wg lacZ; TM3, Sb/TM6, Hu*.

For the *gro* mutant alleles (Figure 2.3B), the *TM3, actin GFP, ser* green balancer was used. Females *w; If/CyO; TM3, act GFP, Ser/Sb* were crossed with males *w; +/+; gro\*/TM3, Sb*. F<sub>1</sub> males carrying *If* and *TM3, act GFP, Ser*, but not *Sb* were crossed with F<sub>1</sub> virgin females carrying *CyO* and *TM3, act GFP, Ser*, but not *Sb*. Males and virgin females of the F<sub>2</sub> carrying *If, CyO* and *TM3, act GFP, Ser* were selected to make the following stock: *w; If/CyO; gro\*/TM3, act GFP, Ser*.

### 2.3.3 The GAL4-UAS Expression System

The GAL4/UAS system was used to mis-express particular genes in specific cells or tissues within the embryo (Brand et al., 1994; Brand and Perrimon, 1993). There are two components to this system: the driver stock that expresses the yeast transcriptional activator protein, GAL4, under the regulation of a tissue/cell specific promoter/enhancer, and the UAS stock that carries a transgene whose expression is regulated by the GAL4 upstream activation sequence (UAS). When GAL4 and UAS stocks are crossed, the transgene is expressed in the same pattern as the GAL4 protein. Thus, ectopic expression of the transgene depends on the promoter that regulates GAL4 expression.

The activity of the GAL4 protein is temperature dependent in *Drosophila* such that more severe phenotypes are observed at higher temperatures (Brand et al., 1994). In

my over-expression experiments, the crosses were kept at 18<sup>0</sup>C, 21<sup>0</sup>C or 25<sup>0</sup>C (see text in results sections) to generate different strengths of phenotype.

### **2.3.4 GAL4 and UAS lines used**

Tables 2 and 3 list the GAL4 and UAS lines used together with comments, origin and relevant references. To make sure that the phenotypes observed in the different over-expression experiments are not due to the insertion of the transgenes, at least three UAS lines were tested in each case. Appendix 1 lists all the UAS lines tested together with informations on the phenotype.

### **2.3.5 Generation of new UAS and GAL4 lines**

*UAS-Dmeso17A-RNAi* and *Dmeso17A-GAL4* lines were generated by injection of the constructs described in section 2.1.11 and 2.1.14 into one hour old embryos.

For each construct, midpreparations of DNA were made using the QIAfilter Plasmid Midi Kit (Qiagen). Generally, 20 $\mu$ g of DNA were then precipitated with ethanol and resuspended in 10 $\mu$ l of double distilled H<sub>2</sub>O in order to obtain a concentration of 2 $\mu$ g/ $\mu$ l. The injection mix was then prepared in 1X Spradling buffer (1mM Sodium Phosphate buffer pH6.8, 0.5mM KCl) with the DNA to be injected at a final concentration of 1 $\mu$ g/ $\mu$ l and the helper DNA (which is a source of transposase that will promote the mobilisation of the constructs from the plasmid into the genome) at a final concentration of 0.25 $\mu$ g/ $\mu$ l. The mix was spun for 10 minutes at full speed and 0.5-1 $\mu$ l was loaded into the injection needles prepared by pulling capillaries (1.0mm x 0.78mm, Harvard Apparatus) with a needle puller (KOPF Instruments).

Embryos for injection were obtained from young *yellow-white* females. Flies were grown as described in section 2.3.1 and the stock was expanded to obtain as many young flies as possible. A minimum of 150 young females and approximately 50 males were placed into laying cages and allowed to lay eggs onto apple juice-agar plates for

**Table 2: List of GAL4 lines used**

Stock	Comments	Origin	References
<i>w, twist-GAL4; twist-GAL4</i> ( <i>twist/twist-GAL4</i> )	Two copies of <i>twist-GAL4</i> , on the X and 2 <sup>nd</sup> chromosome. GAL4 expression is driven by a <i>twi</i> enhancer and promoter included within a 1.4kb HindIII-ClaI fragment that includes the elements necessary for proper <i>twi</i> expression.	Mary Baylies	Baylies and Bate (1996)
<i>Bap-GAL4</i>	Gal4 line driving expression in the visceral mesoderm from stage 10	Ruth Palmer	Zaffran et al. (2001)
<i>24B-GAL4</i>	GAL4 line driving expression in the mesoderm from stage 10.	Mar Ruiz Gomez	Brand and Perrimon (1993)
<i>69B-GAL4</i>	GAL4 line driving expression in the ectoderm from stage 9	Andrea Brand	Brand and Perrimon (1993)
<i>Dmef2-GAL4</i>	GAL4 line that drives expression in the mesoderm from stage 7	G.Ranganayakulu	Ranganayakulu <i>et al</i> (1996)
<i>Dmeso17A-GAL4</i>	GAL4 line that drives expression in the somatic mesoderm from stage 10 to 12 and in the pericardial cells from stage 11 until the end of embryogenesis	David Liotta	unpublished
<i>w;twist-GAL4; TM3/TM6</i>	GAL4 line that drives expression in the mesoderm from gastrulation	Alan Michelson	unpublished
<i>1151-GAL4</i>	Gal4 line that drives expression in the ad epithelial cells associated with the wing and leg imaginal discs. Expression continues in the pupa and the adult muscles.	Uppendra Nongthomba	Roy and VijayRaghavan (1998)

**Table 3: List of UAS lines used**

Stock	Comments	Origin
<i>UAS-Dmeso17A (J7)</i>	Full length <i>Dmeso17A</i> coding sequence under the control of UAS regulatory sequences. The stock is homozygous on the 2 <sup>nd</sup> chromosome.	Mike Taylor, Clare Garvey
<i>UAS-Dmeso17A (J13)</i>	Full length <i>Dmeso17A</i> coding sequence under the control of UAS regulatory sequences. The stock is homozygous on the 3 <sup>rd</sup> chromosome.	Mike Taylor, Clare Garvey
<i>UAS-Dmeso17A- ΔWRPW (1a)</i>	<i>Dmeso17A</i> coding sequence lacking the last 9 base pairs under the control of UAS regulatory sequences. The stock is homozygous on the 2 <sup>nd</sup> chromosome	Mike Taylor, Clare Garvey
<i>UAS-Dmeso17A- ΔWRPW (1b)</i>	<i>Dmeso17A</i> coding sequence lacking the last 9 base pairs under the control of UAS regulatory sequences. The stock is homozygous on the 3 <sup>rd</sup> chromosome	Clare Garvey
<i>UAS-Dmeso17A-RNAi (L1.4.2)</i>	Full length <i>Dmeso17A</i> coding sequence cloned sense and antisense under the control of UAS regulatory sequences. The stock is homozygous on the 3 <sup>rd</sup> chromosome	David Liotta

Stock	Comments	Origin
<i>UAS-Dmeso17A-RNAi</i> (L4.2)	Full length <i>Dmeso17A</i> coding sequence cloned sense and antisense under the control of UAS regulatory sequences. The stock is homozygous on the 2 <sup>nd</sup> chromosome	David Liotta
UAS- <i>Dmef2</i>	Entire <i>Dmef2</i> coding sequence under the control of UAS regulatory sequences. The stock is homozygous on the 3 <sup>rd</sup> chromosome	Kathryn Beatty
<i>UAS-human HDAC5-SA</i>	Constitutively active form of human HDAC5. A serine changed to alanine prevents the exportation out of the nucleus. The stock is homozygous on the 3 <sup>rd</sup> chromosome.	E.N. Olson
<i>UAS-flag-Drosophila HDAC4-ΔC</i>	Constitutively active form of fly HDAC4 where the nuclear export signal has been deleted. The stock is homozygous on the 2 <sup>nd</sup> chromosome	E.N. Olson

few days until they reached their “laying peak” (usually 3-4 days). On the day of injection, plates were changed 3-4 times before the injection and then every 30 minutes during injection. Embryos from the 30 minutes lays were collected into a mesh basket and dechorionated in 50% sodium hypochlorite (Sigma). They were then aligned onto a coverslip, covered with glue (prepared by placing double side Scotch TM tape in 50-100ml of heptane), posterior end at the edge. Aligned embryos were dessicated for approximately 10 minutes, by placing them in a pot containing Silica-gel 6-16 mesh self-indicating (Fisher), and then covered with halocarbon oil (Votalef, H10S). They were injected using a micromanipulator connected to a pump (Narishige) and a Nikon microscope.

Coverslips with injected embryos were placed into a humidified chamber (apple juice-agar plate supplemented with fresh yeast and fixed with damp Whatman paper) at 18°C. Embryos were allowed 48 to 50 hours to recover and hatch. Newly hatched first instar larvae were then collected and transferred into a vial containing fly medium described in section 2.3.1. Vials were placed at 25°C until F<sub>0</sub> adults emerged.

F<sub>0</sub> males were individually mated with three virgin females carrying balancer chromosomes and dominant markers in a *white* background (*w; If/CyO; TM3, Sb/TM6, Hu*). F<sub>1</sub> generation was then screened for transformants by looking at the eye colour.

F<sub>1</sub> virgins carrying *CyO* and *TM3, Sb* were crossed with F<sub>1</sub> males carrying *If* and *TM6, Hu*. This cross produces homozygous flies and allows chromosome mapping of the insertion. I assumed that all F<sub>1</sub> flies have the same insertion. Coloured-eyed F<sub>2</sub> flies carrying two markers on the same chromosome were crossed together to make a stock.

When the insertion was on the X chromosome, males transformants were individually crossed with flies carrying a balancer chromosome and dominant markers on the X chromosome (*y,ct/ FM7, ftz lacZ*).

New stocks were maintained and expanded as described in section 2.3.1.

### 2.3.6 Generation of double UAS stocks

Table 4 lists the double UAS stocks generated.

To test genetic interactions, stocks homozygous for two different UAS constructs were made. Lines were generated as follow (Figure 2.4): stocks homozygous for each UAS construct were crossed together. Progeny flies carrying two markers (*CyO* and *TM3* females and males) were selected and crossed again together. F2 males and females without any markers were kept as a stable stock. For all UAS flies, markers were first put on the chromosome that does not carries the insert. To do so, UAS flies were crossed with a balancer stock (*w; If/CyO; TM3, Sb/TM6, Hu*) and the progeny carrying three markers selected and crossed together.

### 2.3.7 Insertion of *UAS-Dmeso17A*, *UAS-Dmeso17A-RNAi*, *Twist-GAL4* and *Dmeso17A-GAL4* into either a *Dmef2*<sup>65</sup> or a *gro* mutant backgrounds.

Table 5 lists the UAS lines put into mutant backgrounds.

In order to analyse the effect of *Dmeso17A* gain-of or loss-of-function when either *gro* or *Dmef2* function is reduced, UAS and GAL4 flies were recombined in *gro* or *Dmef2* mutant backgrounds (Figure 2.5).

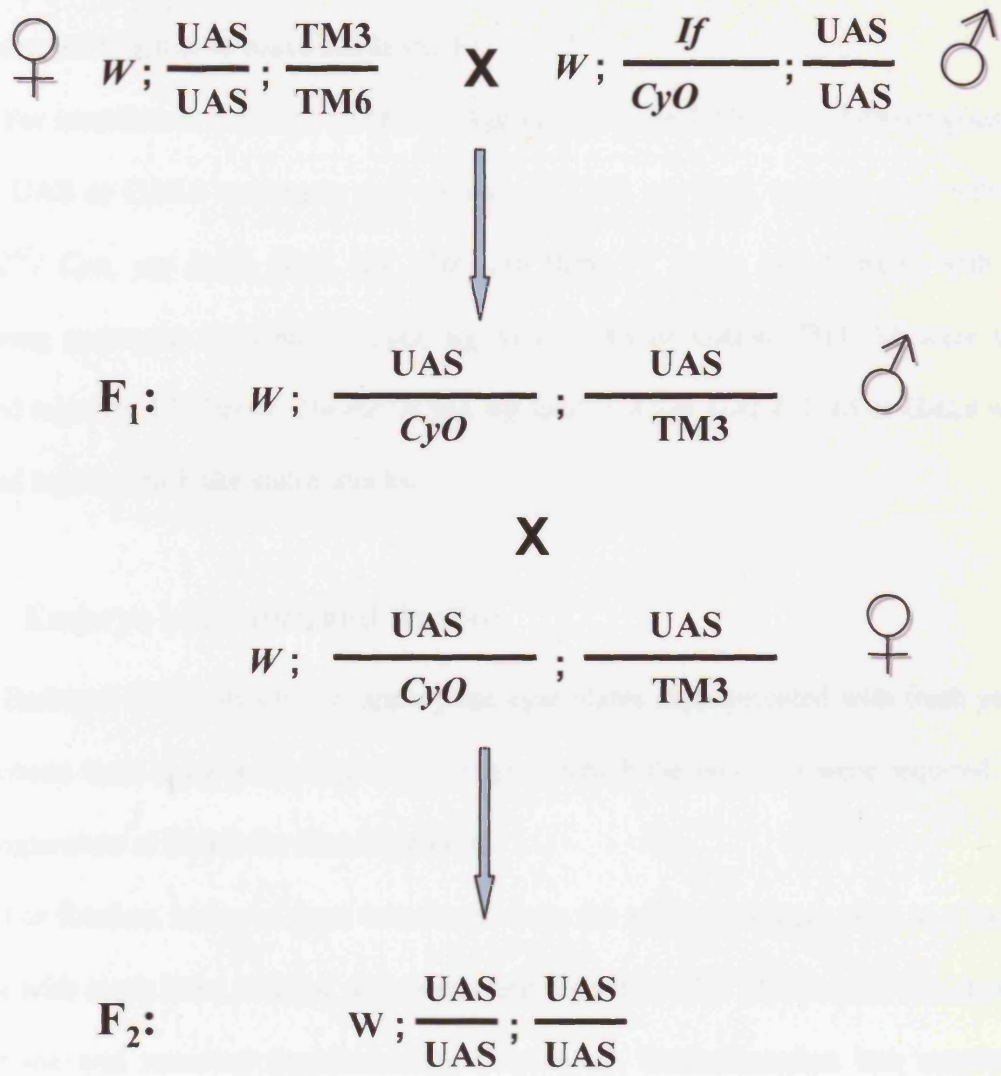
All UAS and GAL4 flies were first crossed with either blue or green balancer flies in order to facilitate subsequent crosses and to allow the identification of homozygous mutant embryos.

For insertion in a *gro* mutant background (Figure 2.5A), flies homozygous for either UAS or GAL4 constructs and carrying *TM6, Hu/ TM3, act GFP, Ser*, were



**Table 4: List of the double UAS stocks generated**

<b>Genotype</b>
<i>w; UAS-Dmeso17A; UAS-Dmeso17A-RNAi</i>
<i>w; UAS-Dmeso17A; UAS-ΔWRPW</i>
<i>w; UAS-Dmeso17A; UAS-Dmef2</i>
<i>w; UAS-Dmeso17A; UAS-hHDAC5-SA</i>
<i>w; UAS-flag-DHDAC4-ΔC; UAS-Dmeso17A</i>
<i>w; UAS-Dmeso17A-RNAi; UAS-hHDAC5-SA</i>
<i>w; UAS-flag-DHDAC4-ΔC; UAS-Dmeso17A-RNAi</i>
<i>w; UAS-Dmeso17A-ΔWRPW; UAS-hHDAC5-SA</i>
<i>w; UAS-flag-DHDAC4-ΔC; UAS-Dmeso17A-ΔWRPW</i>
<i>w; UAS-flag-DHDAC4-ΔC; UAS-Dmef2</i>



**Figure 2.4: Generation of double UAS stocks.**

Males and virgin females carrying dominant markers and homozygous for different UAS constructs were crossed together. F1 males and females with 2 markers were selected. These were crossed and F2 flies, which did not have any markers, were kept and expanded into a stock.

crossed with *w; If/ CyO; gro\*/ TM3, act GFP, Ser* flies. F1 males and females with the following genotype: *w; UAS or GAL4/ CyO; gro\*/ TM3, act GFP, Ser* were then crossed together. F2 flies *w; UAS or GAL4/ UAS or GAL4; gro\*/ TM3, act GFP, Ser* were crossed together to make stable stocks.

For insertion in a *Dmef2* mutant background (Figure 2.5B), flies homozygous for either UAS or GAL4 constructs and carrying *If/ CyO, wg lacZ*, were crossed with *w; Dmef2<sup>65</sup>/ CyO, wg lacZ; TM3, Sb/ TM6, Hu* flies. F1 males and females with the following genotype: *w; Dmef2<sup>65</sup>/CyO, wg lacZ; UAS or GAL4/ TM3, Sb* were then crossed together. F2 flies *w; Dmef2<sup>65</sup>/CyO, wg lacZ; UAS or GAL4/ UAS or GAL4* were crossed together to make stable stocks.

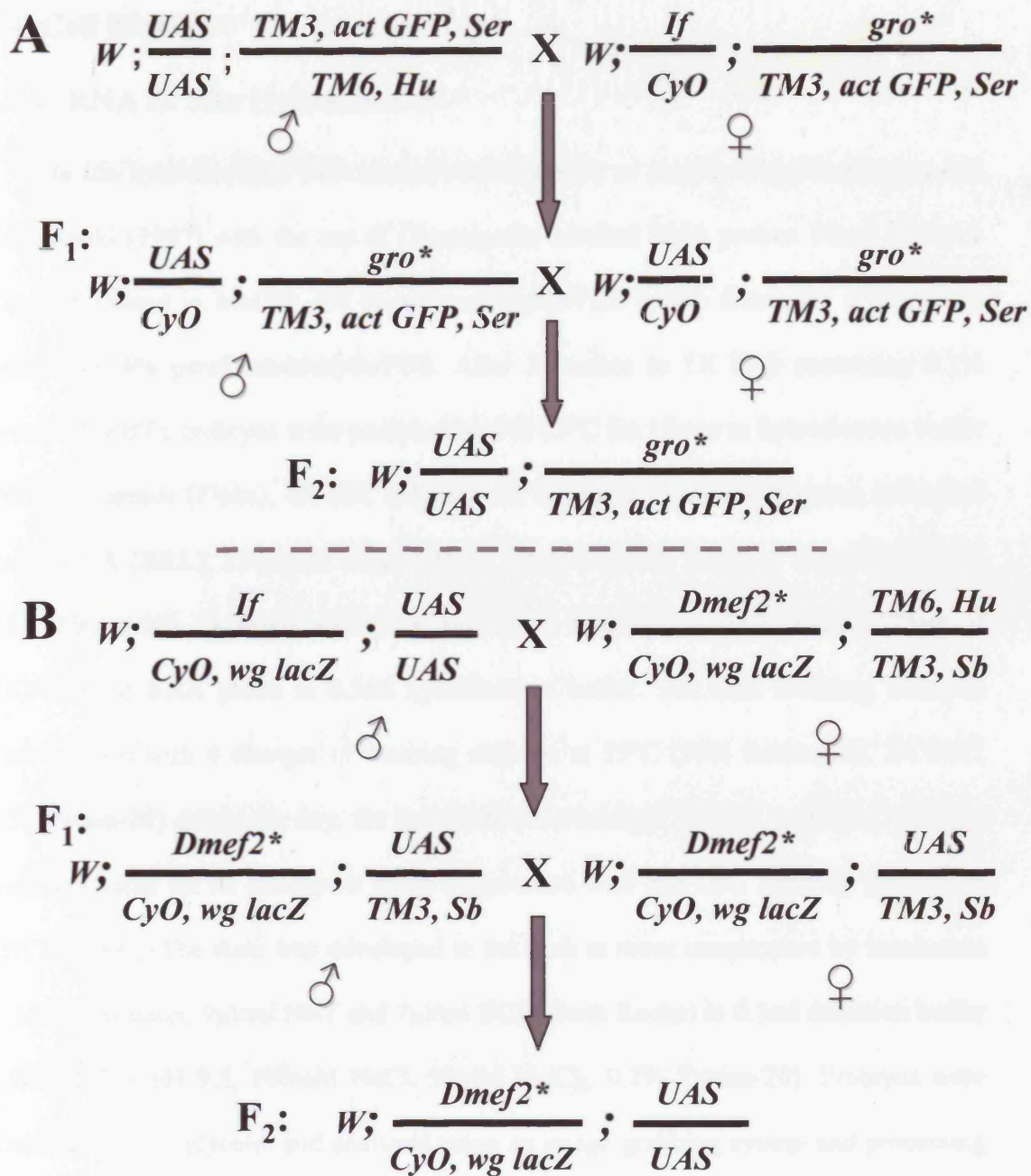
### 2.3.8 Embryo collection and fixation

Embryos were collected on apple juice-agar plates supplemented with fresh yeast. Collections were made according to the stage at which the embryos were required and the temperature at which the flies were kept.

For fixation, embryos were transferred from the apple juice-agar plate to a basket with a wire mesh base, washed with water and placed in 50% bleach until the chorion membrane was removed (approximately 2 minutes). Dechoriation was monitored under a dissecting microscope. Dechorionated embryos were rinsed, dried and transferred into a 2ml tube containing heptane. They were then fixed for 20 minutes in heptane: 4% paraformaldehyde/PBS (1:1), and the vitelline membrane removed by vortexing in a mix of heptane and methanol (1/1). The embryos were then washed and stored in methanol at -20°C until required.

**Table 5: List of the UAS and GAL4 lines inserted into mutant backgrounds**

<b>Genotype</b>
<i>w; UAS-Dmeso17A; gro<sup>BX22</sup>/TM3, act GFP, Ser</i>
<i>w; twist-GAL4; gro<sup>E48</sup>/TM3, act GFP, Ser</i>
<i>w; Dmef2<sup>65</sup>/CyO, wg lacZ; UAS-Dmeso17A-RNAi</i>
<i>w; Dmef2<sup>65</sup>/CyO, wg lacZ; Dmeso17A-GAL4</i>



**Figure 2.5: Insertion of UAS or GAL4 transgenes into either *gro* or *Dmef2* mutant background.**

(A) Males homozygous for a UAS construct and carrying dominant markers and a green balancer on the third chromosome were crossed with virgin females carrying a *gro* mutant allele over a green balancer and dominant markers on the second chromosome. F1 males and females carrying *Cyo;TM3,actGFP,Ser* were selected. These were crossed and F2 flies carrying only *TM3,actGFP,Ser* were kept and expanded into a stock. (B) Males homozygous for a UAS construct and carrying dominant markers and a blue balancer on the second chromosome were crossed with virgin females carrying a *Dmef2* mutant allele over a blue balancer and dominant markers on the third chromosome. F1 males and females carrying *Cyo,wglacZ;TM3,Sb* were selected and crossed together. F2 flies carrying only *Cyo,wglacZ* were kept and expanded into a stock. The same method was used to insert the different GAL4 transgenes into the mutant backgrounds.

## 2.4 Cell Biology

### 2.4.1 RNA *In Situ* Hybridisation

*In situ* hybridisations were carried out essentially as described by Noordermer and Kopczynski (1997) with the use of Digoxigenin-labelled RNA probes. Fixed embryos were rehydrated in MeOH: 4% paraformaldehyde/PBS before fixing for a further 10 minutes in 4% paraformaldehyde/PBS. After 3 washes in 1X PBS containing 0.1% tween-20 (PBT), embryos were prehybridised at 55°C for 1 hour in hybridisation buffer (50% formamide (Fluka), 4X SSC (Sigma), 1X Denhardt's solution (Sigma), 250µg/ml yeast tRNA (BRL), 250µg/ml salmon testis DNA (Sigma), 50µg/ml heparin (Sigma), 0.1% Tween-20). Embryos were then hybridised overnight at 55°C with 0.125µg of DIG-labelled RNA probe in 0.5ml hybridisation buffer. The next morning, embryos were washed with 4 changes of washing solution at 55°C (50% formamide, 2X SSC, 0.1% tween-20) during the day, the last wash was overnight. For the detection, embryos were incubated for 90 minutes at room temperature with anti-DIG antibody (Roche) in PBT (1:2000). The stain was developed in the dark at room temperature by incubation in colour solution: 9µl/ml NBT and 7µl/ml BCIP (both Roche) in 0.3ml detection buffer (100mM Tris pH 9.5, 100mM NaCl, 50mM MgCl<sub>2</sub>, 0.1% Tween-20). Embryos were mounted in 80% glycerol and analysed using an image grabbing system and processing set up (Axiocam digital camera + *Axiovision* software) linked to a *Zeiss Axioskop* microscope.

### **2.4.2 Immunohistochemistry**

Single antibody staining was performed essentially as in Rushton et al. (1995). Fixed embryos were washed in 1X PBS containing 0.3% Triton X-100 (PBS-TX) and then blocked in PBS-TX + 0.5% bovine serum albumin (BSA) (Sigma) for 30 minutes at room temperature. They were then incubated overnight at 4°C with primary antibodies diluted in PBS-TX (see table 6 for the list of antibodies used and the working dilutions). All the primary antibodies were preabsorbed against very young fixed OR embryos. Embryos were then washed with PBS-TX and incubated with a 1:200 dilution of biotinylated secondary antibodies (anti-mouse, anti-rabbit or anti-guinea pig, all from Vector Laboratories) for one hour at room temperature. The signal was amplified using the Vectastain Elite ABC kit (Vector Laboratories) and, for Dmeso17A, Twist, Zfh1 stainings, the Tyramide Signal Amplification (TSA) kit (PerkinElmer) following the manufacturer's instructions. The stain was then developed with 0.5mg/ml diaminobenzadine (DAB) (Sigma) and 0.02% hydrogen peroxide. Embryos were mounted either in an acetone: araldite mixture (1 :1 ratio), or in 80% glycerol. OR embryos were stained in each case and used as controls. Embryos were viewed on a *Zeiss Axioskop* microscope in bright field and photographed using the *axiovision* software connected to a digital camera.

### **2.4.3 Double antibody staining**

Double antibody stainings were performed essentially as described in the previous section with the following modifications:

When primary antibodies were raised in different species, both were added at the same time and developed sequentially. After the overnight incubation, embryos were washed, the first secondary antibody was added and the stain developed using nickel

**Table 6: Primary antibodies used**

Antibody	Animal raised in	Working dilution	Origin
Anti- $\beta$ 3-tubulin	Rabbit	1:1500	R. Renkawitz-Pohl
Anti- $\beta$ galactosidase	Mouse	1:5000	Promega
Anti-Dmeso17A	Guinea pig	1:1500	Mike Taylor Huw Williams
Anti-Even-skipped	Rabbit	1:3000	Manfred Frasch
Anti-Fasciclin III	Mouse	1:100	Cory Goodman
Anti-Krüppel	Guinea pig	1:1000	Dave Kosman
Anti-DMef2	Rabbit	1:1000	Bruce Patterson
Anti-Muscle Myosin	Rabbit	1:500	Daniel Kiehart
Anti-Odd	Rabbit	1:500	James Skeath
Anti-Twist	Rabbit	1:5000	Siegfried Roth
Anti-Zfh-1	Mouse	1:100	Zhe-Chun Lai



salts (which gives a black colour). Embryos were then washed and blocked with 0.5% BSA and incubated for one hour at room temperature with the second secondary antibody. This was developed without nickel salts to give a light brown precipitate.

When primary antibodies were raised in the same animal, embryos were incubated overnight at 4°C with the first antibody and developed using nickel salts. Embryos were then washed, blocked with 0.5% BSA and incubated overnight at 4°C with the second primary antibody. This was developed the next day without nickel salts.

Embryos were visualised and analysed as previously described.

For fluorescent double stainings, secondary antibodies conjugated with fluorescent dyes were used (Vector laboratories). In all cases, primary antibodies were raised in different animals. Embryos were incubated in the dark with the secondary antibodies at room temperature for 2 hours and, after washing, they were mounted in vectashield (Vector laboratories) fluorescent mounting media. Embryos were viewed on a *Zeiss Axioskop* microscope using appropriate filters. They were photographed using the *axiovision* software connected to a digital camera.

#### **2.4.4 Visualisation of the Him:GFP reporter**

Flies homozygous for a 4.0 Kb Him:GFP reporter construct (Rebeiz et al., 2002) were allowed to lay overnight. Embryos were collected into a mesh basket, dechorionated and rinsed thoroughly with water. They were then transferred onto a microscope slide, covered with halocarbon oil (Votalef, H10S) and overlaid with a coverslip. They were analysed using an appropriate filter on a Zeiss *Axioskop* microscope.

For the observation of larvae, embryos were incubated at 25°C until hatching and the larvae aged up to the desired stage. GFP expressing larvae were then simply rinsed before being transferred onto a microscope slide and then treated as the embryos.

#### **2.4.5 Cell death assay by Acridine Orange staining**

Acridine orange staining was performed essentially as described in Sullivan, Ashburner and Hawley (*Drosophila* Protocols, 2000). Embryos from overnight lays were collected into mesh baskets, dechorionated in 50% bleach and rinsed thoroughly with water. They were then transferred into 1.5ml microcentrifuge tubes and shaken vigorously for 5 minutes in 750µl of heptane plus 750µl of freshly made acridine orange (5 µg/ml in sodium phosphate buffer pH 7.2) in 0.1M sodium phosphate buffer (pH 7.2). After all the liquid was carefully removed, the embryos were rinsed 2X with heptane and transferred onto microscope slides with a paint brush. They were then covered with halocarbon oil and overlaid with a coverslip. Stained embryos were visualised and analysed using an appropriate filter on a *Zeiss Axioskop* microscope. Photographs were taken using the grabbing system described previously.

#### **2.4.6 Imaginal Wing Disc dissection and staining**

Wandering third instar larvae were dissected as described in Sullivan, Ashburner and Hawley (*Drosophila* Protocols, 2000) in cold 1X PBS. Discs were fixed for 30 minutes at room temperature in 4% paraformaldehyde/PBS with gentle shaking, dehydrated in an Ethanol series (30, 50, 70, 90 and 100%) and stored in 100% Ethanol at -20°C until required.

In situ hybridisation on the dissected discs was carried out essentially as described for the embryos in section 2.4.1 with the exception that Ethanol, instead of Methanol, was used for the rehydration of the discs.

For the observation of GFP, dissected discs were placed on a slide in a drop of halocarbon oil and overlaid with a coverslip. They were then observed as described for the embryos and the larvae in section 2.4.4.

### **2.4.7 Cuticle preparation**

Males homozygous for a *UAS-Dmeso17A* construct were crossed with females homozygous for *69B-GAL4*. OR flies were used as a control. Flies were allowed to lay eggs for 4h on apple-juice agar plate supplemented with fresh yeast. Embryos were then incubated until hatching and the larvae were aged up to the desired stage at 25°C. Larvae were then transferred into a Petri dish containing 70% glycerol and they were pricked with a fine tungsten needle. They were then transferred into a 1.5ml microcentrifuge tube containing fixative (glycerol: acetic acid [4:1]) and incubated overnight at 60°C. Larvae were mounted in lactic acid:H<sub>2</sub>O [3:1] and incubated overnight at 60°C. The edges of the coverslip were sealed with nail varnish. Larval cuticles were observed on a Zeiss Axioskop microscope using phase contrast and photographed with the grabbing system described previously.

### **2.4.8 Adult thorax dissection and observation**

For analysis of the indirect flight muscles (IFMs) in adult flies, hemithoraces were prepared following a method adapted from the procedure described in Nongthomba and Ramachandra, 1999. Whole flies were anesthetised in ether, frozen in liquid nitrogen and immediately bisected longitudinally with a razor blade. Sectioned flies were then dehydrated through an alcohol series (50, 70, 80, 90 and 100% ethanol; 2 hours minimum for each step) and cleared in methyl salicylate (BDH). Heads, wings, halteres and abdomens were then removed and clean thoraces were mounted in DPX (BDH).

The sections were observed and photographed with a *Zeiss Axioskop* microscope using polarised light optics and the grabbing system described previously.

#### **2.4.9 Larval muscle scoring and analysis**

Qualitative analysis of the effect on somatic musculature in the different experiments was performed by precise examination of the muscle pattern. Each of the 30 muscle was analysed systematically in three abdominal hemisegments (A2 to A4) following specific criteria: presence/absence; shape; size; number; nuclei organisation. Defects in any of these characteristic for individual muscles were noted. The wild-type muscle pattern was used as a reference for comparison.

For each muscle and each criterion the percentage of hemisegments affected was calculated.

Due to the variability of phenotype observed from segment to segment and from embryo to embryo, a minimum of 50 embryos were analysed in each experiment.

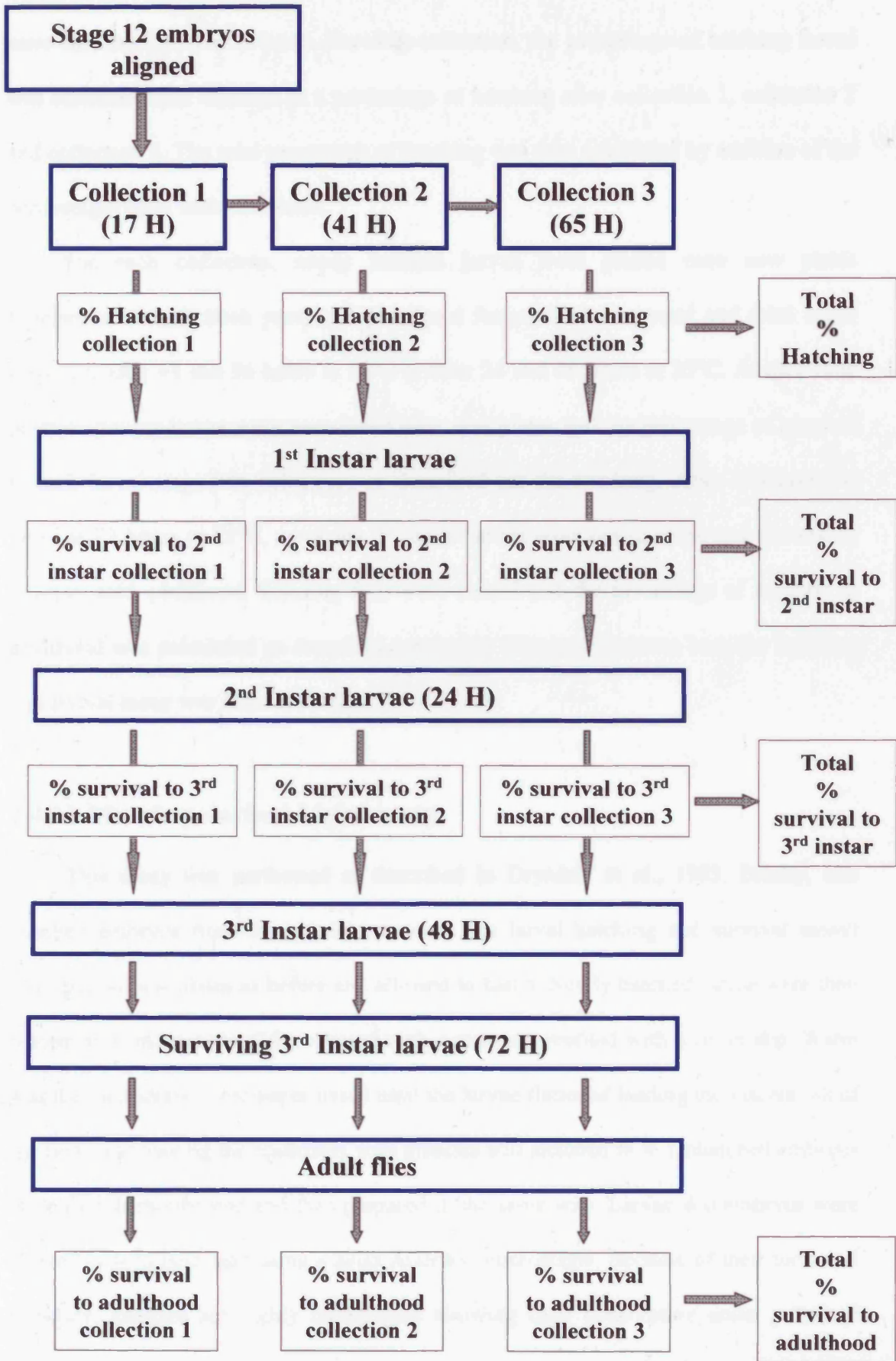
#### **2.4.10 Embryo selection and Larval Hatching and Survival Assay**

Females homozygous for different GAL4 drivers were crossed with males homozygous for each UAS construct. Crosses were set up in cages where flies were allowed to lay eggs on apple juice-agar plates at 18°C for 4 hours or at 25°C for 2 hours. The plates were then further incubated at 18°C for 14 hours or at 25°C for 7 hours to allow the embryos to reach stage 12. Developing embryos were selected and staged by looking at the yolk autofluorescence using a filter. Unfertilised embryos were discarded.

Three hundred developing embryos from each cross were collected, aligned on new plates covered with a very thin layer of fresh yeast paste and incubated at 18°C or at 25°C. Newly hatched larvae (first instar larvae) were scored after 34, 82 and 130

**Figure 2.6: Larval hatching and survival assay at 18°C.**

Stage 12 embryos were aligned on apple juice-agar plate supplemented with fresh yeast. Hatching larvae were collected and transferred on new plates after 17, 41 and 65 hours. The percentages of hatching from each collection were combined to obtain a total percentage of hatching. Larvae were then monitored for survival to 3<sup>rd</sup> instar. At each stage the surviving larvae were transferred on new plates. The percentage of survival to each larval stage was calculated. Surviving 3<sup>rd</sup> instar larvae were then transferred into tubes. The percentage of survival to adulthood was calculated. Wild-type embryos were always used as a control.



hours at 18°C or after 17, 41 and 65 hours at 25°C to ensure that even the weak ones have had enough time to hatch. For each collection, the percentage of hatching larvae was calculated and reported as a percentage of hatching after collection 1, collection 2 and collection 3. The total percentage of hatching was then calculated by addition of the percentages from each collection.

For each collection, newly hatched larvae were placed onto new plates supplemented with fresh yeast and monitored for survival to second and third instar stage, i.e. after 48 and 96 hours at 18°C or after 24 and 48 hours at 25°C. At each time point, surviving larvae were transferred onto new plates and the percentage of survival to each larval stage was calculated as described for the hatching. After 144 hours at 18°C or 72 hours at 25°C, surviving 3<sup>rd</sup> instar larvae were put in tubes and allowed to develop until adulthood. Eclosing flies were scored and the percentage of survival to adulthood was calculated as described previously (Figure 2.6 shows how the hatching and survival assay was done at 18°C).

#### **2.4.11 Muscle polarised Light Assay**

This assay was performed as described in Drysdale et al., 1993. Briefly, one hundred embryos from the previous crosses (see larval hatching and survival assay) were put on new plates as before and allowed to hatch. Newly hatched larvae were then placed on a microscope slide, covered with water and overlaid with a cover slip. Water was then withdrawn with paper tissue until the larvae flattened leading the viscera out of the body and leaving the epidermis with muscles still attached to it. Unhatched embryos were first dechorionated and then prepared in the same way. Larvae and embryos were viewed in polarised light using a *Zeiss Axioskop* microscope. Because of their form and structure, muscles are highly birefringent allowing their observation under polarised

light. By rotating the larvae or embryos with respect to the plane of polarisation, all muscles can be observed. Photographs were taken using the *axiovision* software linked to a digital camera.

#### **2.4.12 Buffers**

**Sodium phosphate buffer pH 7.2:** 68.4mM Na<sub>2</sub>HPO<sub>4</sub>, 31.6mM NaH<sub>2</sub>PO<sub>4</sub>

**PBS 20X:** 2.7M NaCl, 53.6mM KCl, 0.2M Na<sub>2</sub>HPO<sub>4</sub>, 1mM KH<sub>2</sub>PO<sub>4</sub>



## CHAPTER 3: *Dmeso17A* Expression and Sequence

### 3.1 Introduction

Much can be learned from the expression pattern of a gene. A simple, yet detailed analysis of its expression can provide information on the possible roles of a gene during a developmental process. Of course, one has to be careful extrapolating from pattern to function, but this information can nevertheless guide the strategy to adopt for the study of a gene. Thus, the first step in the analysis of *Dmeso17A* was to analyse its pattern of expression.

The second step in the investigation of the role of *Dmeso17A* was to analyse both its DNA and protein sequence. This type of analysis, complementing the information given by the expression pattern, can provide crucial elements to refine the strategy to adopt. For example, it can help finding orthologs in other species and/or known domains of functional importance like DNA binding domains or protein/protein interaction motifs. The *Drosophila* Genome Project (BDGP) and all the bioinformatic tools available on line greatly facilitate this analysis. Furthermore, the available genomic sequences of other species and their annotations, now allow phylogenetic footprinting analysis of orthologous gene sequences. This approach compares sequences between species to identify functional regions by their evolutionary conservation and therefore highlights regions in genes likely to mediate biological function.

In the following sections, I will present the results I obtained for the initial analysis of *Dmeso17A*. First, its expression pattern was examined using RNA *in situ* hybridisation and immunohistochemistry, and then its DNA and protein sequences were analysed using various bioinformatic tools.

## 3.2 The expression pattern of *Dmeso17A*

### 3.2.1 *Dmeso17A* expression declines as muscle differentiation starts

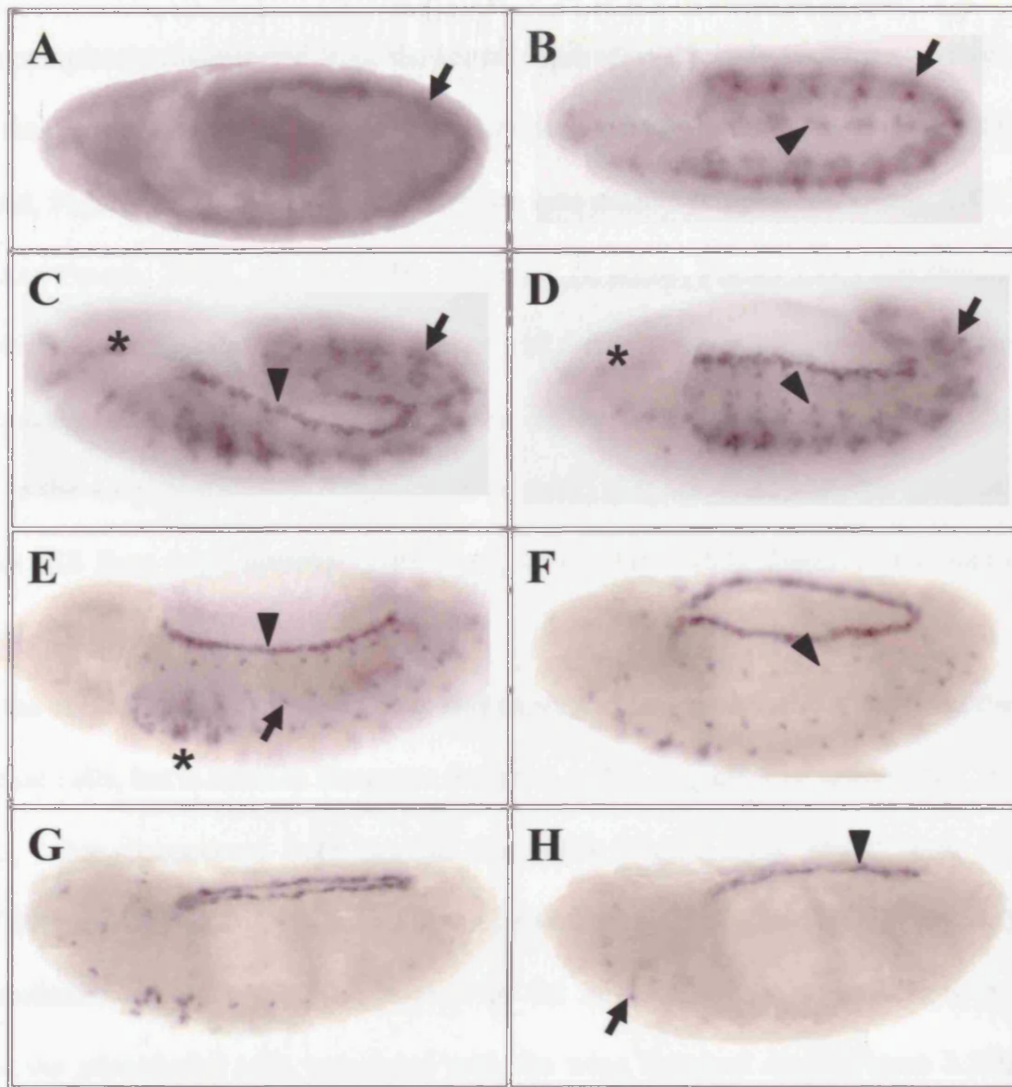
*In situ* hybridisation revealed a very specific pattern of expression for *Dmeso17A*. It is transiently expressed in the developing mesoderm and, as muscle differentiation starts, it declines and only persists in the adult muscle precursors (AMPs) and the pericardial cells of the heart.

*Dmeso17A* transcripts appear at stage 9 in the developing mesoderm (Figure 3.1A arrow). From stage 11, as the mesoderm becomes subdivided along the A/P and D/V axes (for review see Baylies et al., 1998), *Dmeso17A* expression appears segmentally repeated in the somatic mesoderm compartments (figure 3.1B arrow) and, dorsally, it is found in the precursors of the heart (Figure 3.1B arrowhead).

During germ band retraction (stage 12) (Figure 3.1 C and D), *Dmeso17A* expression is clearly restricted to the somatic mesoderm (figure 3.1C and D arrow, figure 3.2A) and dorsally, to the precursors of the heart (figure 3.1C arrowhead), which are now forming a continuous line of cells on both sides of the embryo (for reviews see Cripps and Olson, 2002; Zaffran and Frasch, 2002). *Dmeso17A* is also found in the precursors of the pharyngeal muscles (Figure 3.1C asterisk).

By the end of stage 12, as the appearance of ventral muscle precursors signals the onset of muscle differentiation (Bate, 1990), *Dmeso17A* expression begins to decrease in the somatic mesoderm and dorsally is restricted to the heart pericardial cells. AMPs expressing *Dmeso17A* becomes visible in the dorsal and lateral part of the somatic mesoderm (figure 3.1D arrowhead).

By stage 13, more muscle precursors are identifiable (Bate, 1990) and muscle differentiation markers such as Myosin Heavy Chain can be clearly detected. *Dmeso17A*



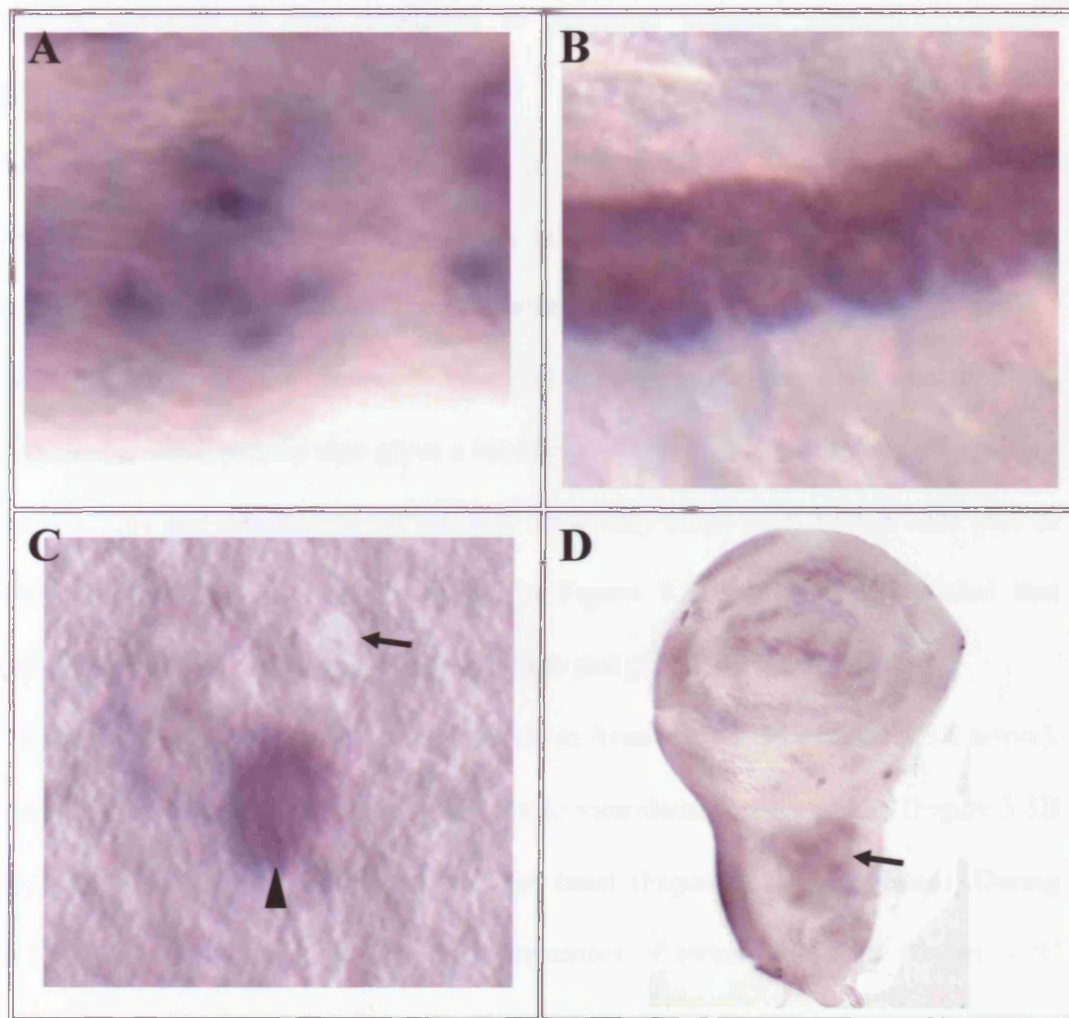
**Figure 3.1: *Dmeso17A* expression rapidly declines as muscle differentiation starts.**

Whole mount *in situ* hybridisation of stage 10-17 wild-type embryos with a *Dmeso17A* RNA probe. In this and all subsequent figures, embryos are shown as a lateral view with anterior to the left and dorsal uppermost unless stated otherwise. (A) Stage 10 embryo showing *Dmeso17A* expression in the mesoderm (arrow). (B) Stage 11. *Dmeso17A* expression becomes restricted to the somatic mesoderm (arrow) and the precursors of the heart (arrowhead). (C) Stage 12. *Dmeso17A* expression is restricted to the somatic mesoderm (arrow), and the pericardial cells (PCs) (arrowhead). Expression is also detected in the precursors of the pharyngeal muscles (asterisk). (D) At the end of stage 12, *Dmeso17A* is still expressed in the somatic mesoderm (arrow), but begins to decrease dorsally and become restricted to the adult muscle precursors (AMPs) (arrowhead). (E) Stage 13. *Dmeso17A* has disappeared from the differentiating somatic mesoderm, but remains in the AMPs (arrow), the PCs (arrowhead) and the ad epithelial cells (asterisk). (F) Stage 15. *Dmeso17A* expression persists in the PCs but starts to decrease in the AMPs (arrowhead). (G) Stage 16. *Dmeso17A* has almost completely disappeared from the AMPs, but remains expressed in the PCs and the ad epithelial cells. (H) Stage 17. Persistent expression of *Dmeso17A* in the PCs (arrowhead). Expression in the ad epithelial cells begins to fade (arrow).

has then completely disappeared from the somatic mesoderm. It only remains expressed in cells that are set aside from muscle differentiation: the pericardial cells (Figure 3.1E arrowhead, Figure 3.2B) that do not differentiate into muscle (Cripps and Olson, 2002; Zaffran and Frasch, 2002), and the AMPs (Figure 3.1E arrow, Figure 3.2C) that remain in an undifferentiated state and only proliferate and differentiate in the larva to form the adult muscles (Bate et al., 1991; Bate, 1993). In the thoracic segments, *Dmeso17A* persists in the adepithelial cells (Figure 3.1E asterisk) that associate with the imaginal discs and will form adult muscles (Bate et al., 1991; Bate 1993). *Dmeso17A* remains expressed in these cells until stage 15.

By the end of stage 15, *Dmeso17A* is still expressed in the pericardial cells and the adepithelial cells, but it starts to disappear from the AMPs (Figure 3.1F arrowhead). By stage 16, it has disappeared from most of the AMPs (Figure 3.1G) and at stage 17, *Dmeso17A* transcripts are only detected in the pericardial cells (Figure 3.1H arrowhead) and adepithelial cells (Figure 3.1H arrow). In the larvae, *Dmeso17A* transcripts are found in the adepithelial cells associated with the wing imaginal discs (Figure 3.2D) (Rebeiz et al., 2002; Butler et al., 2003).

Thus, like *twist* (see Chapter 1 section 1.5.1), the disappearance of *Dmeso17A* correlates with the onset of muscle differentiation and it persists in the precursors of the adult myoblasts. This striking pattern of expression suggests that *Dmeso17A* plays a role in somatic muscle and pericardial cell development. It might function, like *twist* (see Chapter 1 section 1.5.1), to switch cells towards a myogenic fate or alternatively as an inhibitor of muscle development. Its rapid disappearance and its expression in the pericardial cells, which do not differentiate into muscle, suggest that a role of inhibitor of muscle development for *Dmeso17A* is more probable.



**Figure 3.2: *Dmeso17A* expression.**

Whole mount *in situ* hybridisation of wild-type embryos with a *Dmeso17A* RNA probe. **(A)** Stage 12. High magnification of *Dmeso17A* expression in the somatic mesoderm at stage 12. **(B and C)** Stage 13. Two rows of PCs expressing *Dmeso17A* are clearly visible **(B)**, but *Dmeso17A* is not expressed in the somatic mesoderm anymore (arrow in C) and is restricted to the AMPs (arrowhead in C). **(D)** During larval life, *Dmeso17A* persists in the ad epithelial cells (arrow) associated with the wing imaginal discs.

### 3.2.2 *Dmeso17A* protein expression follows that of its transcript

As described above, *Dmeso17A* RNA disappears very rapidly at the onset of muscle differentiation. Since this characteristic feature of its expression might be related to *Dmeso17A* function, it was important to establish whether *Dmeso17A* protein disappears at the same time.

In order to determine if *Dmeso17A* protein followed the same dynamic of expression as that observed for the transcript, I used an antibody made in the laboratory. Laboratory members have made several attempts to produce an antibody against *Dmeso17A* but, to date, I have only obtained a specific staining with one of them. Unfortunately, this antibody also gives a lot of non-specific background staining. Using higher dilutions and developing the staining for a very short time, I have been able to minimise the background and, as shown in Figure 3.3, the staining revealed that *Dmeso17A* protein accumulates at the same time and place as the transcript.

*Dmeso17A* protein is found in the mesoderm from stage 9-10 (Figure 3.3A arrow). By stage 11, it becomes restricted to the somatic mesoderm compartments (Figure 3.3B arrow) and dorsally, in the precursors of the heart (Figure 3.3B arrowhead). During stage 12, *Dmeso17A* is restricted to the progenitors of somatic muscles (Figure 3.3C and D arrow) and in the pericardial cells (Figure 3.3C and D arrowhead).

At stage 13, it has disappeared from differentiating somatic mesoderm and only remains expressed in the AMPs (Figure 3.3E arrow), the pericardial cells (Figure 3.3E arrowhead) and the adepithelial cells (Figure 3.3E asterisk). Like its transcript, *Dmeso17A* remains in those cells until stage 15 when it starts to disappear from dorsal AMPs (Figure 3.3F arrowhead).

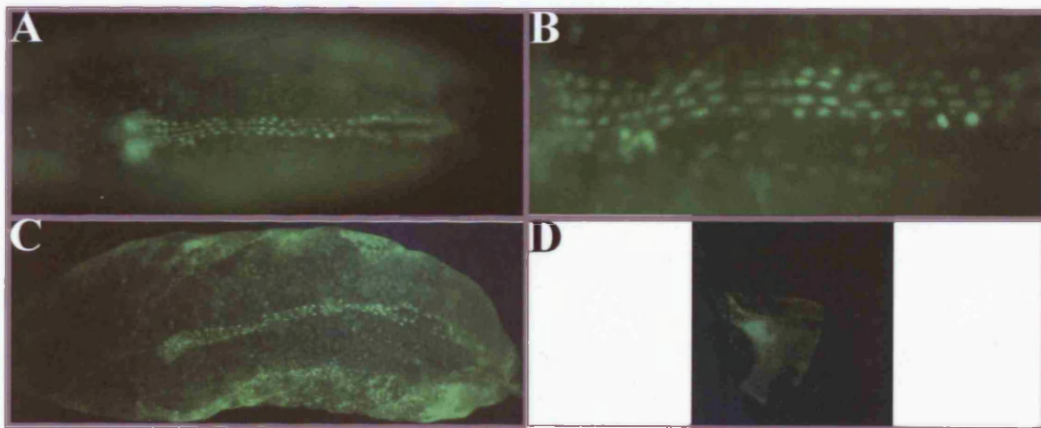
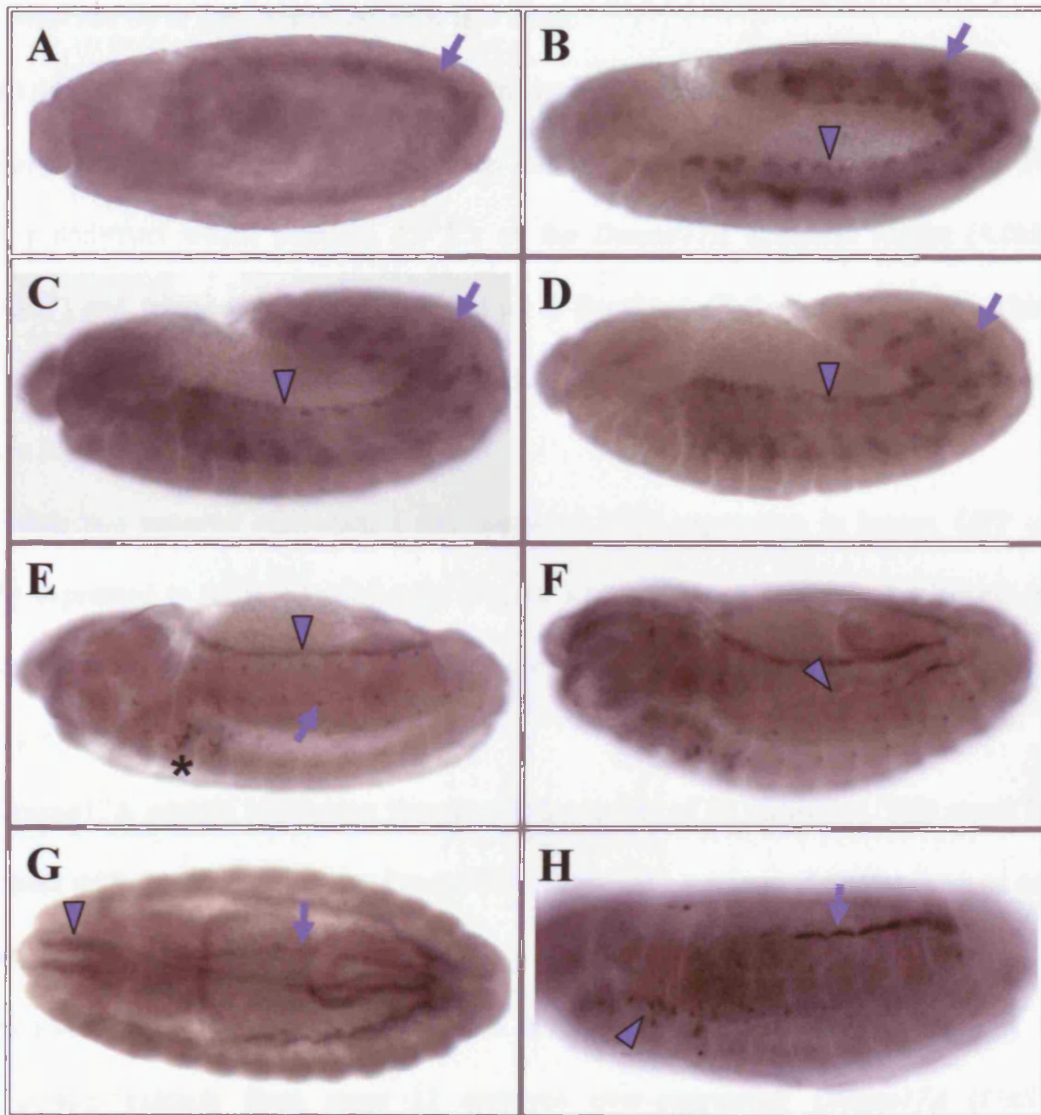
By stage 16, *Dmeso17A* is only found in the pericardial cells (Figure 3.3G and H arrows) and in the adepithelial cells (Figure 3.3H arrowhead). At this stage, staining of

**Figure 3.3: Dmeso17A protein expression follows that of its transcript.**

Wild-type embryos were stained with a guinea pig anti-Dmeso17A antibody. **(A)** Stage 10. Dmeso17A is expressed in the mesoderm (arrow). **(B)** Stage 11. Dmeso17A expression becomes restricted to the somatic mesoderm (arrow) and the precursors of the heart (arrowhead). **(C and D)** Stage 12. Dmeso17A expression is restricted to the somatic mesoderm (arrows), and PCs (arrowheads). **(E)** Stage 13. Dmeso17A has disappeared from the differentiating somatic mesoderm, but remains in the AMPs (arrow), the PCs (arrowhead) and the adepithelial cells (asterisk). **(F)** Stage 15. Dmeso17A expression persists in the PCs but starts to decrease in the AMPs (arrowhead). **(G and H)** Stage 16. Dmeso17A remains expressed in the PCs (arrow in G), and is also found in the pharyngeal muscles (arrowhead in G). Dmeso17A also remains expressed in the adepithelial cells (arrowhead in H).

**Figure 3.4: Expression of a Dmeso17A-GFP reporter construct.**

**(A and B)** Stage 17. GFP expression is detected in the PCs. **(C)** During the first instar larval stage, GFP expression persists in the PCs. **(D)** In a third instar larva, GFP is found in the adepithelial cells associated with the wing imaginal discs.





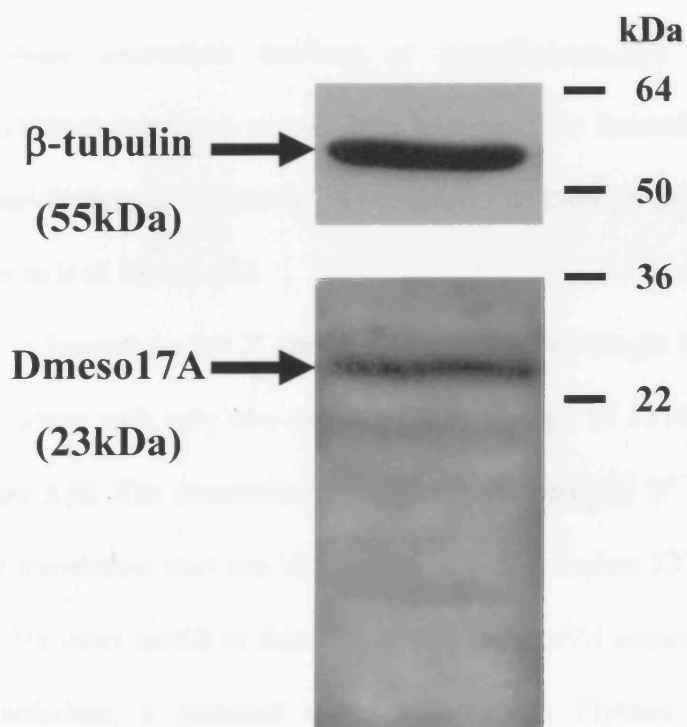
the pharyngeal muscles can also be observed (Figure 3.3G arrowhead). This has never been observed by *in situ* hybridisation at this stage.

At stage 17, even with a very short developing time, the background masks any specific staining. Nonetheless, I have been able to assess the expression of a GFP-reporter construct which contains 4.0 Kb of the *Dmeso17A* enhancer region (4.0kb Him:GFP) and which was kindly provided by J. Posakony (Rebeiz et al., 2002). This construct shows GFP expression in the pericardial cells of a late stage 17 embryo (Figure 3.4 A and B).

Using this reporter construct, I also assessed GFP expression in larvae. GFP is clearly expressed in the pericardial cells (Figure 3.4C) and, as also shown by Rebeiz et al. (Rebeiz et al., 2002), in the ad epithelial cells associated with the wing imaginal discs (Figure 3.4D).

*Dmeso17A* protein expression therefore follows that of its transcript. This result is consistent with the hypothesis that *Dmeso17A* might play a role in the mesoderm as an inhibitor of differentiation

In addition, I tested the anti-*Dmeso17A* antibody on Western blot (Figure 3.5). I used protein extracts from stage 12 embryos over-expressing *Dmeso17A* (*UAS-Dmeso17A* will be described in Chapter 4). The antibody reveals one major band (Figure 3.5, arrow) which has a molecular weight corresponding to that of *Dmeso17A* (23 KDa). This, together with *Dmeso17A* RNA expression, suggests that the expression pattern described above is that of *Dmeso17A*.



**Figure 3.5: The anti-Dmeso17A antibody detects a 23kDa protein.**

Western blot showing that the anti-Dmeso17A antibody reveals a major band at 23kDa which is the size of Dmeso17A. Extracts were from 50 stage 12 embryos.  $\beta$ -tubulin was assayed as a control

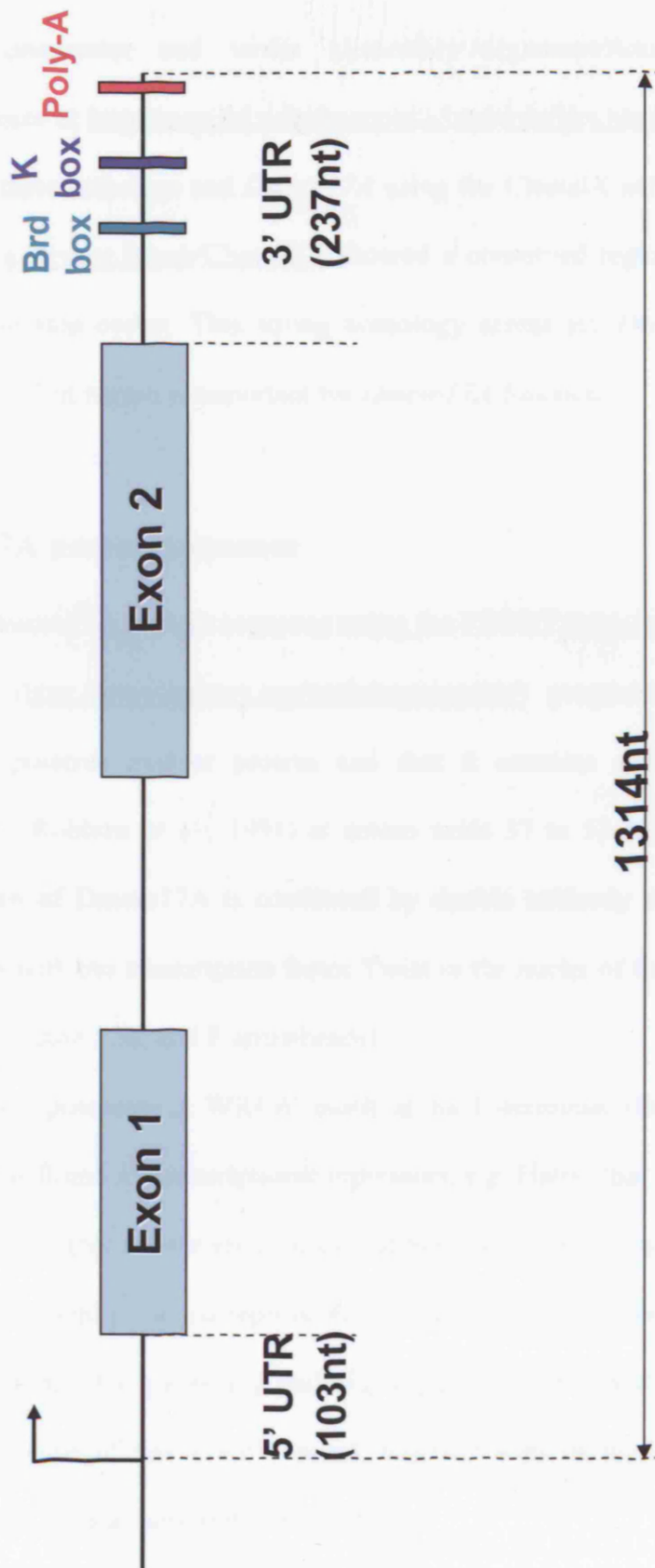
### 3.3 *Dmeso17A* sequence

#### 3.3.1 *Dmeso17A* DNA sequence

As mentioned in the Introduction, *Dmeso17A* cDNA has been isolated in a subtractive hybridisation-based screen (Taylor, 2000). Using this cDNA sequence to perform a blast search against the *Drosophila* genome (NCBI BLAST at <http://flybase.net/blast>), I have accessed the Flybase report concerning the gene *Dmeso17A* (flybase annotation database at <http://flybase.net>). In the database, *Dmeso17A* (CG15064) has been named *Him* because it is located next to the HES-related gene, *Her* (Rebeiz et al., 2002). Nevertheless, all through this dissertation I will continue to refer to it as *Dmeso17A*.

*Dmeso17A* is located on the X chromosome and its cytologic location is 17A2. It has a simple structure with only two exons and has a length of 1314 nt on the genomic sequence (Figure 3.6). The annotation predicts that *Dmeso17A* 5' UTR spans 103 nt upstream of the translation start site and that its 3' UTR reaches 237 nt downstream of the stop codon. No other motifs or domains within *Dmeso17A* sequence is shown in the database. Nevertheless, a personal communication to Flybase (Posakony, 2002) mentions that the *Dmeso17A* 3' UTR contains a Bearded (Brd) box (AGCTTTA) (Lai and Posakony, 1997) and a K box (TGTGAT) (Lai et al., 1998). These two motifs, when present in the 3' UTR of genes, have been shown to confer instability to transcripts (Lai and Posakony, 1997; Lai et al., 1998). This mode of regulation of mRNA stability is consistent with the dynamic expression observed for *Dmeso17A* transcript. I have also found a polyadenylation signal (Wickens and Stephenson, 1984) 217 nt downstream of the stop codon.

Comparison of the *Dmeso17A* DNA sequence with other *Drosophila* species genomes revealed the presence of putative orthologs in *Drosophila yakuba*, *mojavensis*,



**Figure 3.6: The *Dmeso17A* genomic locus.**

*Dmeso17A* has two exons and including its 5' and 3' UTRs has a length of 1314nt. Its 5' UTR spans 103nt and its 3' UTR 237nt. The 3' UTR contains a Brd box (light blue) and a K box (dark blue), which are both implicated in RNA stability (see text), together with a polyadenylation signal (red).

*pseudoobscura*, *ananassae* and *virilis* (Assembly/Alignment/Annotation of 12 *Drosophila* Genomes at <http://rana.lbl.gov/drosophila/multipleflies.html>). Alignment of the sequences of these orthologs and *Dmeso17A* using the ClustalX software (available at <ftp://ftp-igbmc.u-strasbg.fr/pub/ClustalX/>) showed a conserved region spanning 117 nt upstream of the stop codon. This strong homology across six *Drosophila* species suggests that this 117 nt region is important for *Dmeso17A* function.

### 3.3.2 *Dmeso17A* protein sequence

Analysis of *Dmeso17A* protein sequence using the PSORT (<http://psort.nibb.ac.jp/>) and ScanProsite (<http://www.expasy.org/tools/scanprosite/>) programs revealed that *Dmeso17A* is a putative nuclear protein and that it contains a bipartite nuclear localisation signal (Robbins et al., 1991) at amino acids 37 to 53 (Figure 3.7). The nuclear localisation of *Dmeso17A* is confirmed by double antibody staining showing that it co-localises with the transcription factor Twist in the nuclei of the AMPs and the adepithelial cells (Figure 3.8E and F arrowheads).

*Dmeso17A* also possesses a WRPW motif at its C-terminus (Figure 3.7). This tetrapeptide motif is found in transcriptional repressors, e.g. Hairy, that interact with the Groucho protein (Gro) (for review see Courey and Songtao, 2001). *Drosophila* Gro is a key member of a family of co-repressors that have roles in many aspects of development including D/V patterning and *Wg* signalling (Chen and Courey, 2000). Therefore, the presence of this WRPW motif, together with its nuclear localisation, suggest that *Dmeso17A* is a transcriptional inhibitor.

BLAST search against the genomes of other *Drosophila* species revealed proteins similar to *Dmeso17A* in the five *Drosophila* species mentioned above (Assembly/Alignment/Annotation of 12 *Drosophila* Genomes at

.....|.....|.....|.....|.....|.....|.....|.....|.....|  
 10                      20                      30                      40  
**MGVIYKILKQQRSMDSLSSATRCKVQAAIKQRQQRRLE**

.....|.....|.....|.....|.....|.....|.....|.....|.....|  
 50                      60                      70                      80  
**DHMVEERDRDRERDQQPDQDQNVQNHIDKDKEELAEQQL**

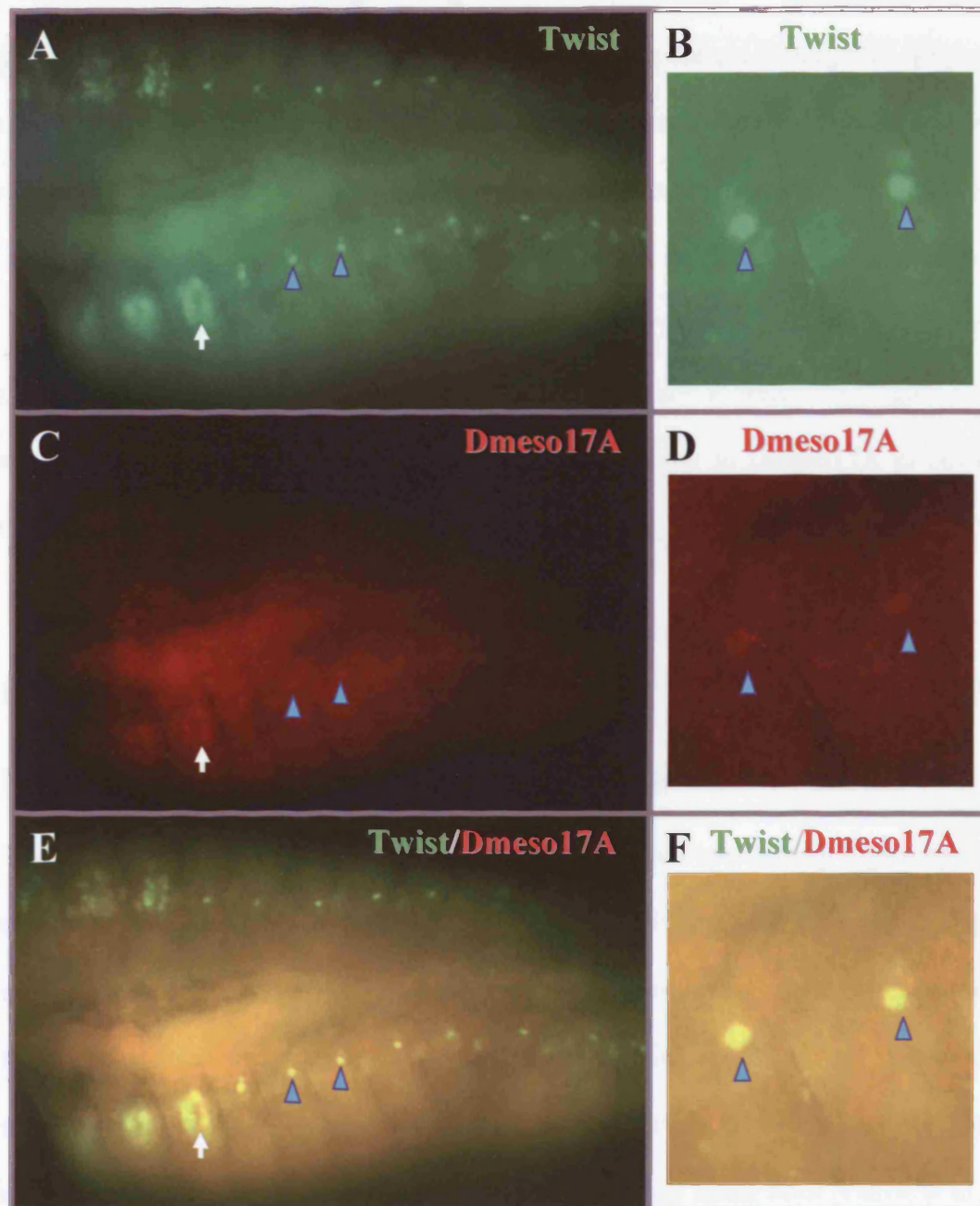
.....|.....|.....|.....|.....|.....|.....|.....|.....|  
 90                      100                      110                      120  
**QQLCRFLAENAARKKRQRFKLQYQCNLAIDQDNDQEQMPE**

.....|.....|.....|.....|.....|.....|.....|.....|.....|  
 130                      140                      150                      160  
**KEHFAAPPHEMDLEFIEQLQQSSPAKSHGATGQAPRDSIL**

.....|.....|.....|.....|.....|.....|.....|.....|.....|  
 170                      180                      190  
**LKIRHQIFERKRQRQLAELVQORMVVRPW**

**Figure 3.7: *Dmeso17A* protein sequence.**

The predicted *Dmeso17A* protein sequence is 192 amino acids in length and contains a bipartite nuclear localisation signal (NLS) at amino acids 37-53 (blue) and a WRPW motif at its C-terminus (red). This tetrapeptide is found in transcriptional repressors that interact with the co-repressor Gro.



**Figure 3.8: *Dmeso17A* co-localises with Twist in both the thoracic and abdominal adult muscle precursors.**

Stage 13 wild-type embryos were double stained with anti-Twist and anti-*Dmeso17A* antibodies. (A-B) Twist is expressed in the nuclei of the abdominal AMPs (blue arrowheads) and the thoracic ad epithelial cells (white arrows). (C-D) *Dmeso17A* is expressed in the same cells. (E-F) Merged image showing that *Dmeso17A* and Twist co-localise in the nuclei of the AMPs (blue arrowheads) and the ad epithelial cells (white arrows).

<http://rana.lbl.gov/drosophila/multipleflies.html>). As for its DNA sequence, alignment of *Dmeso17A* with its orthologs using ClustalX (available at <ftp://ftp-igbmc.u-strasbg.fr/pub/ClustalX/>) showed a conserved region across the six *Drosophila* species (boxed in Figure 3.9). This portion of almost perfect homology at the protein level is located at amino acids 154 to 192. This high degree of conservation strongly suggests that this segment of *Dmeso17A* sequence is essential for its function in the somatic mesoderm. It contains the WRPW motif and the MotifScan program (<http://scansite.mit.edu>) predicts a putative phosphorylation site at serine158 (Figure 3.9 arrowhead). However, I have not found any sequence similar to *Dmeso17A* in other organisms.

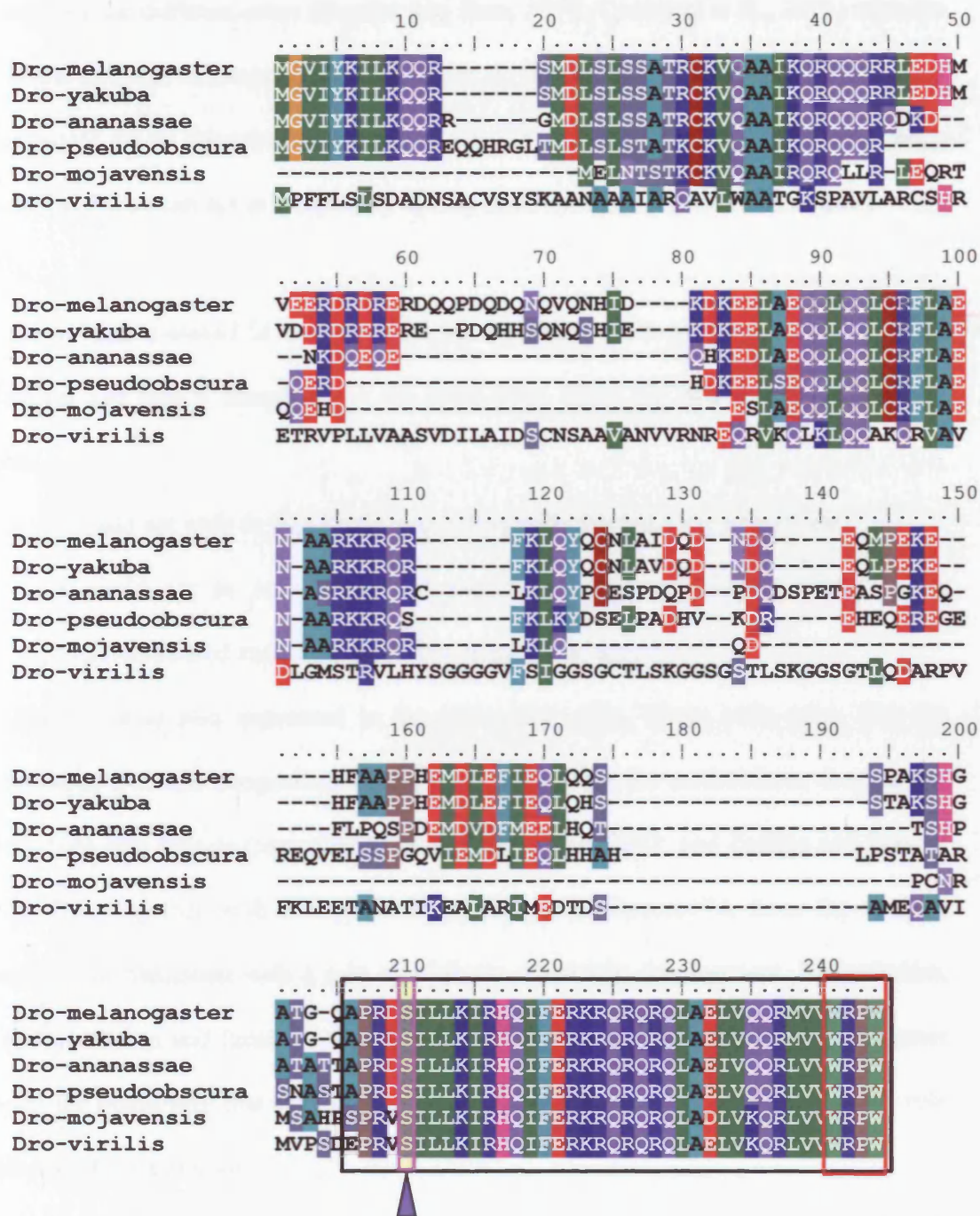
### 3.4 Discussion

#### 3.4.1 *Dmeso17A*: inhibitor or promoter of muscle differentiation?

The aim of Dr. Taylor's screen was to isolate novel genes specifically expressed in the mesoderm before and during the early steps of muscle differentiation (Taylor, 2000). *Dmeso17A* fulfils this aim. It is expressed early in the developing somatic mesoderm and it disappears from it as muscle differentiation starts. However, it remains expressed in the progenitors of the adult muscles and also in the pericardial cells. This specific pattern of expression is very similar to that of the transcription factor *twist* (Currie et al., 1991; Bate and Rushton, 1993; Dunin Borkowski et al., 1995), with the exception of the pericardial cells, and therefore is consistent with an important role for *Dmeso17A* in somatic myogenesis.

*twist* is expressed very early and specifies the mesoderm (Thisse et al., 1988; Leptin 1991), but it disappears as muscle differentiation starts and only persists in the AMPs





**Figure 3.9: Dmeso17A sequence alignment with its orthologs in different *Drosophila* species.**

Alignment of Dmeso17A orthologs from five *Drosophila* species with *Drosophila melanogaster* Dmeso17A. Similar or conserved residues are coloured. A region of almost perfect homology is found at amino acids 154-192 (black box). This region contains the WRPW motif (red box) and a putative phosphorylation site at serine158 (arrowhead).

(Currie et al., 1991). Studies have shown that high levels of Twist are necessary for somatic muscle differentiation (Baylies and Bate, 1996; Castanon et al., 2001) whereas low levels of Twist can repress it (Castanon et al., 2001). This differential Twist activity is dependent on its dimerisation partner (Castanon et al., 2001). Moreover, it has been shown that Twist can act as a repressor during adult muscle differentiation (Anant et al., 1998).

Given that *Dmeso17A* is expressed in the same cells as *twist* in the somatic mesoderm and that it disappears at the same time, there are two possibilities for its action:

- It could act with or like Twist, propelling cells toward a myogenic fate.
- It could act as an inhibitor of muscle development, keeping cells in an undifferentiated state, maybe by blocking Twist action.

*Dmeso17A* is also expressed in the pericardial cells. These cells arise, like the cardioblasts, from the progenitors of the heart but, unlike the cardioblasts, they do not differentiate into muscle (reviewed in Cripps and Olson, 2002; and Zaffran and Frasch, 2002). This, together with the quick disappearance of *Dmeso17A* from the somatic mesoderm, is consistent with a role of inhibitor of muscle development. Nevertheless, the differentiation and function of pericardial cells is poorly understood and one cannot rule out the possibility that the role of *Dmeso17A* in these cells is different than its role in the somatic mesoderm.

In addition to the information given by the *Dmeso17A* pattern of expression, it is important to note that the antibody against *Dmeso17A* obtained in the laboratory as well as the GFP reporter construct provided by the Posakony laboratory (Rebeiz et al., 2002) are very useful tools. Indeed, they can be used for studying both the AMPs and the pericardial cells for which there are very few markers available.

### 3.4.2 *Dmeso17A* is a putative inhibitor of transcription

Sequence analysis of *Dmeso17A* revealed that it is a nuclear protein and, because of the presence of a WRPW motif, that it is a putative Groucho interactor.

Gro is the key member of a family of transcriptional co-repressors. It is a non-DNA binding protein and it is recruited to the DNA via protein-protein interactions with transcriptional repressors that possess a WRPW motif (reviewed in Gasperowicz and Otto, 2005). For example, Gro is recruited by Hairy to regulate neurogenesis and segmentation (Rushlow et al., 1989; Paroush et al., 1994). The WRPW motif present at the C-terminus of the Hairy protein is necessary and sufficient for the interaction with Gro (Paroush et al., 1994; Fisher et al., 1996).

*Dmeso17A* is a nuclear protein and possesses a WRPW motif at its C-terminus. It is therefore possible that, even though it does not possess a DNA-binding domain, *Dmeso17A* interacts with Gro maybe acting as an adaptor protein. *Dmeso17A* might function as a link between Gro and DNA-binding repressors.

In addition to this, a study, based on a computational approach on the whole *Drosophila* genome, led to the identification of *Dmeso17A* as a target of the Notch-regulated transcription factor *Suppressor of Hairless (Su(H))* (Rebeiz et al., 2002). They showed that the expression of *Dmeso17A* in the wing imaginal discs is dependent on Su(H) activity. Su(H) is a DNA-binding protein and is a key component of the Notch pathway, which is known to be crucial for cell fate decisions. Moreover, there is evidence indicating that Notch/Su(H) regulates *twist* both directly and indirectly. In the embryo, Notch/Su(H) directly represses *twist* expression and its indirect action is through the activation of proteins that repress Twist (Tapanes-Castillo and Baylies, 2004). Some of these Notch/Su(H)-regulated proteins could be encoded by the genes of

the *enhancer of split (E(spl))* complex, which includes *gro* (Tapanes-Castillo and Baylies, 2004). Tapanes-Castillo and Baylies also showed that individual genes from the *E(spl)* complex are not sufficient to repress Twist and suggest that they might work with another factor. Thus, these results correlate with my analysis and reinforce the idea that *Dmeso17A* plays an important role in the mesoderm and that it might function with Gro to keep cells in an undifferentiated state.

*Dmeso1A* sequence analysis also revealed the presence of a Brd box (Lai and Posakony, 1997) and a K box (Lai et al., 1998) in its 3' UTR (Posakony, 2002, personal communication to Flybase). These motifs could provide another level of regulation for *Dmeso17A* controlling the accumulation of its transcript. The presence of these motifs is not only consistent with *Dmeso17A* dynamic pattern of expression, but it also suggests that there is a need for a precise regulation of *Dmeso17A* transcript accumulation.

Finally, phylogenetic analysis of *Dmeso17A* sequence showed a strong conservation in five *Drosophila* species of a region spanning 38 amino acids including the WRPW motif and a putative phosphorylation site. Even though this high degree of conservation suggests a functional importance for this region, there are no significant similarities in other organisms. Nevertheless, my subsequent results (described in Chapter 5) indicate that *Dmeso17A* is involved in a complex formed by highly conserved proteins, e.g. Gro and HDAC. This suggests that even if there is no significant conservation in higher organisms, *Dmeso17A* function in muscle development could be conserved. Moreover, motifs such as the WRPW tetrapeptide, even if well characterised, are too short to give significant values in alignments. It is therefore possible that, even using BLAST search for short nearly exact matches (<http://www.ncbi.nlm.nih.gov/BLAST>), I have missed short motifs that are conserved.

### 3.4.3 Conclusion: *Dmeso17A*, a novel inhibitor of myogenesis?

Taken together, the results I obtained with the analysis of *Dmeso17A* expression pattern and sequence suggests that it might be a novel inhibitor of muscle development. The presence of a WRPW motif in its sequence links *Dmeso17A* with the co-repressor Gro suggesting that *Dmeso17A* inhibits transcription during somatic myogenesis. Moreover, in the wing imaginal discs, *Dmeso17A* is positively regulated by Notch/Su(H) (Rebeiz et al., 2002), which, in the embryo, might activate *gro* to down-regulate Twist (Tapanes-Castillo and Baylies, 2004). This is consistent with the hypothesis that *Dmeso17A* function with Gro and that together they can inhibit muscle development. If Twist promotes myogenesis by regulating *mef2* expression, *Dmeso17A* could prevent cells from differentiating. Analysis of *Dmeso17A* function could therefore be highly informative and might provide new insights in the understanding of the mechanisms underlying muscle development.

The strategy I have adopted to study *Dmeso17A* during my PhD is based on these hypotheses. As described in the next chapters, my approach to test these hypotheses has been to utilise both gain-of-function and loss-of-function using the GAL4/UAS system. I first analysed the phenotype of *Dmeso17A* gain-of and loss-of-function and then I investigate the link between *Dmeso17A* and Gro. I also tested genetic interactions between *Dmeso17A* and known regulators of muscle development, *Dmef2* and *histone deacetylases (HDACs)*.

## CHAPTER 4: *Dmeso17A* Gain-of-Function

### 4.1 Introduction

The GAL4/UAS system (Brand and Perrimon, 1993; Brand et al., 1994; see Chapter 2 section 2.3.3) is a powerful tool for studying gene function giving researchers the ability to mis-express any given target gene in a spatially and temporally-controlled way. Over the last decade, it has become a crucial element for many studies and the list of applications for this system has rapidly grown (for review see Duffy, 2002). For instance, it provides an excellent alternative when mutant phenotypes are too severe or if there is no mutant available and there are many examples in the literature of genes whose function has been determined, at least in part, using the GAL4/UAS system. For example, it has been used for studying *twist* function in somatic myogenesis (Bate and Baylies, 1996). In *twist* mutants, no mesoderm is formed (Simpson, 1983; Leptin, 1991), making studies of subsequent mesodermal differentiation very hard to achieve. Although in this case temperature sensitive *twist* alleles were available and proved useful, the GAL4/UAS system provided an excellent complement to unravel *twist* function. Another example is *Dmef2* whose regulation of expression and function have also been studied using this system (Taylor et al., 1995; Cripps et al., 1998, Gunthorpe et al., 1999).

Because there was no mutant or P-element insertion available for *Dmeso17A*, I decided to use the GAL4/UAS system to study *Dmeso17A* function and test whether it can inhibit muscle differentiation. My approach was to first analyse the effect of full-length *Dmeso17A* over-expression. I then achieved *Dmeso17A* loss-of-function using RNAi and dominant negative approaches (these will be described in the next Chapter).

Using a range of specific GAL4 drivers, I promoted *Dmeso17A* expression in the mesoderm before and during differentiation of the mesodermal derivatives. The effects of *Dmeso17A* mis-expression on each mesodermal derivative were then analysed. I also induced ectopic expression of *Dmeso17A* in the ectoderm to determine whether it can affect the development of non-mesodermal tissues. The GAL4 drivers used and the results of my analysis are described in the following sections.

## **4.2 *Dmeso17A*: a novel inhibitor of myogenesis**

### **4.2.1 The over-expression phenotype: *Dmeso17A* over-expression disrupt somatic myogenesis**

To over-express *Dmeso17A*, flies homozygous for a UAS-*Dmeso17A* construct were crossed to stocks homozygous for specific GAL4 drivers (All the UAS-*Dmeso17A* lines tested are listed in Appendix1). In order to test the effect of *Dmeso17A* over-expression on the different mesodermal derivatives and, as presented in Chapter 6, to test genetic interactions, I used several GAL4 drivers. Each one of them drives *Dmeso17A* expression in different times and places (these drivers are described in section 4.2.3). As a consequence, different degrees of severity of phenotype can be obtained for each driver used. The severity can be further modulated by changing the temperature at which the crosses are kept. More severe effects can be obtained at higher temperature (see below and section 4.2.3). Here I present two examples of the effect of *Dmeso17A* over-expression on somatic muscle development using two different GAL4 drivers: *Dmef2-GAL4* and *twist/twist-GAL4*. The temperature used is stated for each experiment.

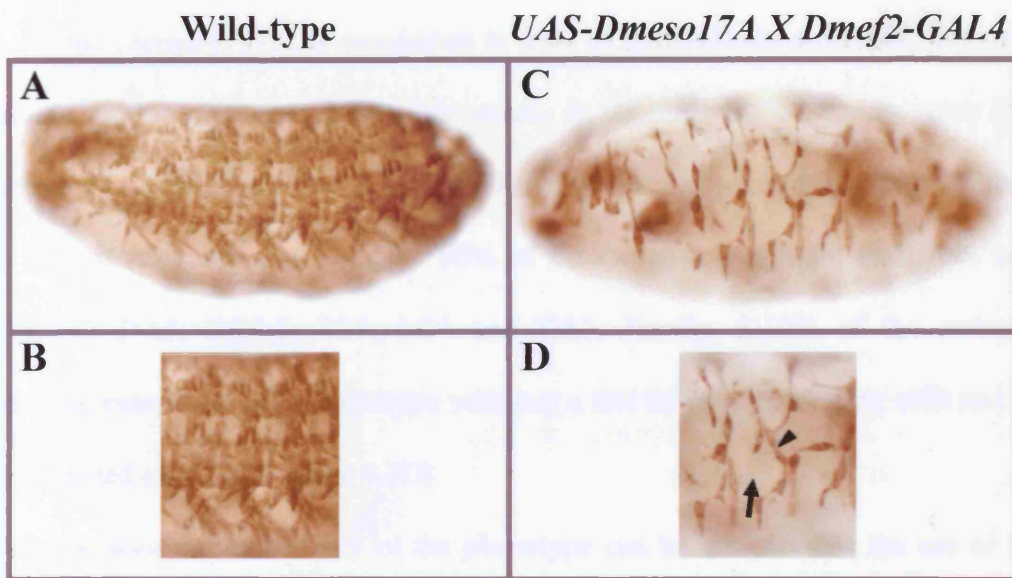
As revealed by muscle myosin expression, over-expression of *Dmeso17A* driven by *Dmef2-GAL4* at 25°C leads to disruption of the somatic musculature, with considerable

reduction of the number of myosin-expressing cells. Fusion of the remaining myoblasts occurs, but muscle formation and differentiation is dramatically impaired. Only a few incorrectly shaped muscles are able to form (Figure 4.1; compare A-B with C-D). In these embryos, the midgut also fails to constrict and has a swollen appearance. As visceral musculature is essential for the formation of these constrictions (Reuter and Scott, 1990), this suggests that the differentiation of the visceral muscles is impaired. Cardioblast differentiation is also affected in these embryos (the effect of *Dmeso17A* over-expression on heart and visceral muscles development is described in sections 4.2.5.1 and 4.2.5.4 respectively). This result, consistent with its pattern of expression, shows that *Dmeso17A* can inhibit muscle development.

Using *twist/twist-GAL4*, the effect of *Dmeso17A* over-expression at 18°C is less severe with relatively high number of myosin-expressing cells (Figure 4.2). In contrast to the phenotype induced when using *Dmef2-GAL4*, the visceral musculature is not affected as the midgut constricts normally. This difference could be explained by the fact that *twist/twist-GAL4* does not drive strong expression in the visceral mesoderm after stage 11 (Baylies and Bate, 1996), whereas *Dmef2-GAL4* drives expression in all muscle lineages from stage 7 until the end of embryogenesis (Ranganayakulu and Olson, 1996). In these embryos, two rows of cardioblasts expressing myosin were always present. This is probably due to the fact that *twist/twist-GAL4* does not drive strong expression in the heart.

In order to precisely analyse the effect of *Dmeso17A* over-expression driven by *twist/twist-GAL4* on somatic musculature, the muscle pattern was examined. Each of the 30 muscles was analysed systematically in three abdominal hemisegments (A2 to A4). Variation from embryo to embryo was observed with a range of severity. Segment to segment variation within the same embryos was also frequently noticed. Nevertheless,





**Figure 4.1: *Dmeso17A* over-expression disrupts myogenesis.**

A *UAS-Dmeso17A* line was crossed with *Dmef2-GAL4* at 25° C to over-express *Dmeso17A* in the mesoderm. Stage 17 embryos were stained with an antibody against muscle Myosin. **(A-B)** Wild-type embryo showing the normal muscle pattern. **(C-D)** *Dmeso17A* over-expressing embryo. Muscle differentiation is profoundly affected with missing (arrow) or misshapen (arrowhead) muscles.





some muscles, such as DT1 or VA3 for example, are affected in more than 70% of the embryos analysed (see Figure 4.2 right column).

Figure 4.2 shows the different severity of phenotype obtained. In 25 to 30% of the embryos, the phenotype is weak and the muscle pattern is almost complete, but never were all muscles wild-type in appearance, (Figure 4.2A). For example, DT1 and the ventral muscles are misshapen in 40% of these embryos. A moderate phenotype is observed in 15-20% of the embryos with more muscles missing or misshapen (Figure 4.2B). In this category, DT1 is misshapen in 80% of the embryos and DO3, DO5 and LL1 are missing in more than 30% of the cases. In the most represented category (50-55% of the embryos), the effect on muscle differentiation is much more severe (Figure 4.2C). DT1 is misshapen in more the 90% of the embryos and more than 70% lack muscles like DA3, DO3-5, LL1, LO1 and VA3. Finally, 5-10% of the embryos presented an extreme muscle phenotype with just a few myosin-expressing cells and no muscles formed correctly (Figure 4.2D).

This variation in the severity of the phenotype can be attributed to the use of the GAL4/UAS system (Brand et al., 1994; see section 4.2.3), but it also suggests that muscle differentiation is very sensitive to the *Dmeso17A* level.

When the over-expression of *Dmeso17A* using *twist/twist-GAL4* is performed at 25<sup>o</sup>C instead of 18<sup>o</sup>C, similar variations are observed, but the proportion of the different categories of phenotype has changed (Figure 4.3). Embryos like those in Figure 4.2A and 4.2B represent only 5-10% and 10-15% respectively (Figure 4.3 A and B), whereas those from the third category, in Figure 4.2C, now represent 70 to 75% of the embryos (Figure 4.3C). A very dramatic effect is still observed in 5-10% of the embryos (Figure 4.3D). The severity of the phenotype has therefore increased. Together, these results

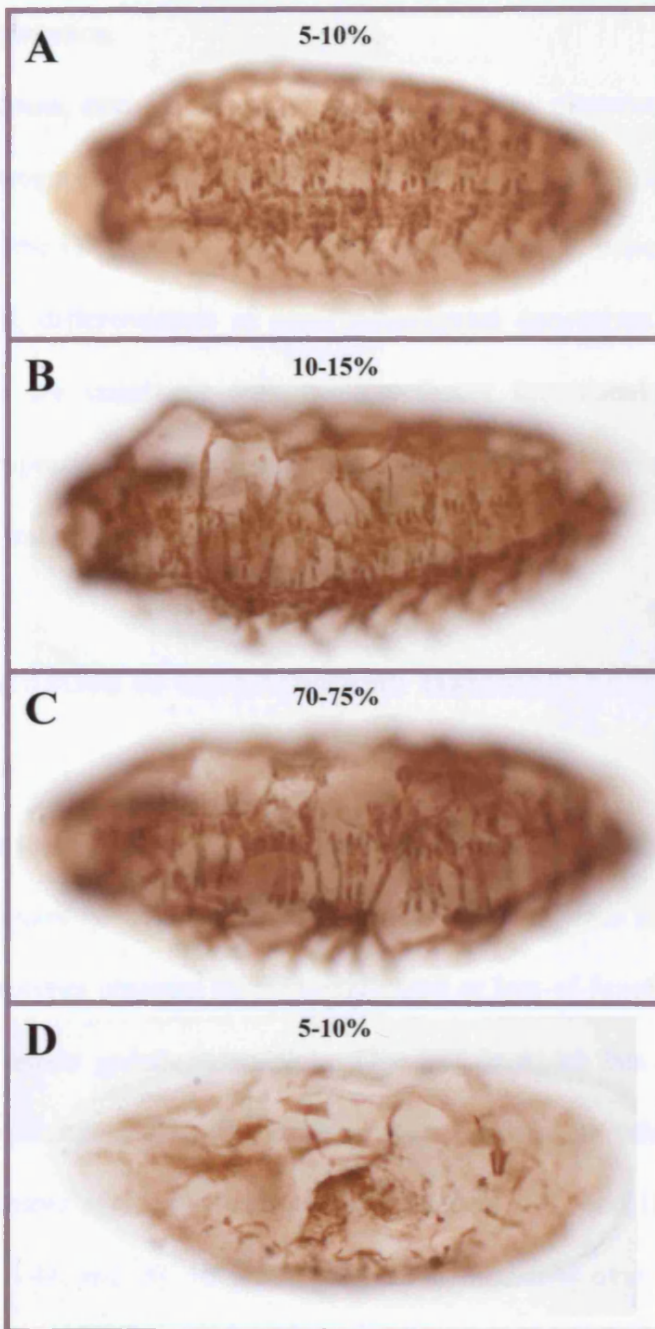
***UAS-Dmeso17A X***  
***twist/twist-GAL4 18°C***

<p><b>A</b> 25-30%</p> 	<p>DT1 misshapen in 40% of the embryos. DO5 missing in &gt;30%.</p> <p>1 or 2 VO muscles often missing.</p>
<p><b>B</b> 15-20%</p> 	<p>DT1 misshapen in 80% of the embryos. DO3, DO5 and LL1 missing in &gt;30%. VA3 missing in 40% of the embryos.</p>
<p><b>C</b> 50-55%</p> 	<p>DT1 and ventral muscles misshapen in 90% of the embryos. DA3, DO3-5, LL1, LO1 and VA3 missing in &gt;70%. 8-10 ventral muscles present but often misshapen.</p>
<p><b>D</b> 5-10%</p> 	<p>No muscle formed correctly</p>

**Figure 4.2: Muscle phenotype variations in *Dmeso17A* over-expressing embryos.**

*Dmeso17A* was over-expressed using *twist/twist-GAL4* at 18°C. Stage 17 embryos were stained with an antibody against muscle Myosin. A range of phenotypes is observed: **(A)** Weak. The muscle pattern is almost complete. **(B)** Moderate. More muscles are missing or misshapen. **(C)** Severe. The muscle pattern is considerably affected. **(D)** Extreme. No muscle formed correctly. The proportion of each category is given, together with details of the muscle pattern defects.

*UAS-Dmeso17A X twist/twist-GAL4 25°C*



**Figure 4.3: The severity of the *Dmeso17A* over-expression phenotype increases with the temperature.**

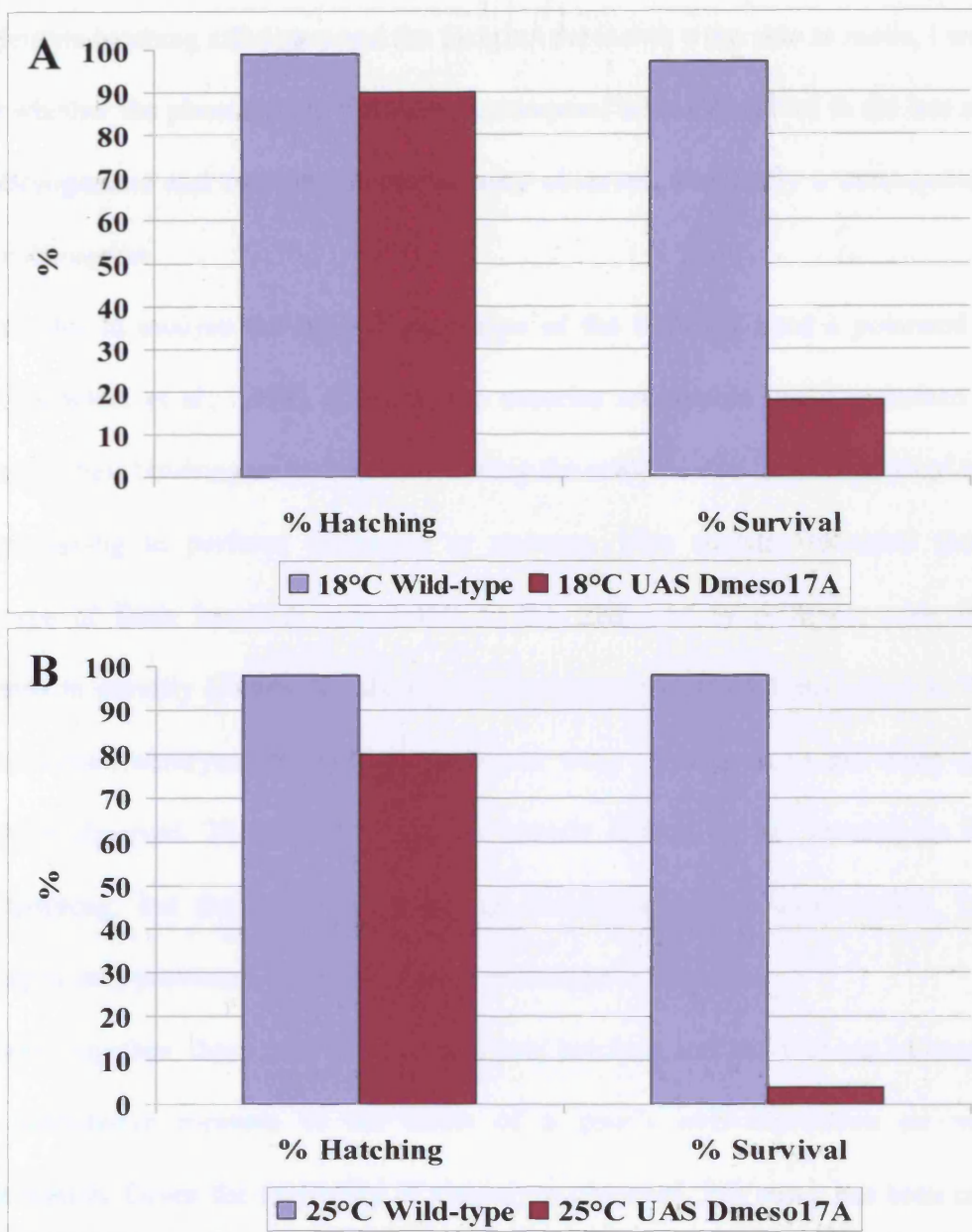
The muscle phenotype of embryos over-expressing *Dmeso17A* using *twist/twist-GAL4* was analysed at 25° C. Stage 17 embryos were stained with an antibody against muscle Myosin. At this temperature, the range of phenotypes obtained is similar to that described at 18° C (see Figure 4.2): weak (A), moderate (B), severe (C) and extreme (D). However, the proportion of embryos in each category has changed with a considerable increase in the proportion of severely affected embryos (C; compare with Figure 4.2C).

clearly indicate that an increase of *Dmeso17A* level can have a substantial effect on muscle differentiation.

In conclusion, over-expression of *Dmeso17A* in the mesoderm results in disruption of somatic myogenesis and the severity of the phenotype obtained can be influenced by the choice of the GAL4 driver used and the temperature at which the crosses are kept. As mentioned, differentiation of other mesodermal derivatives can also be affected. These results are consistent with the hypotheses formulated after the analysis of *Dmeso17A* expression, and suggest that *Dmeso17A* is a novel inhibitor of muscle development in *Drosophila*.

#### **4.2.2 Quantitation of the phenotype: Hatching/ Survival and polarised light assays**

Although it was now clear that *Dmeso17A* can inhibit muscle differentiation, it was necessary to quantify the effect of its over-expression in order to be able to compare it with the phenotypes obtained by over-expression or loss-of-function of other genes, and ultimately to assess genetic interactions. One way in which this can be achieved, is by assessing the hatching efficiency, as muscles are essential for this to happen. I therefore scored the number of embryos able to hatch, both at 25<sup>0</sup>C and 18<sup>0</sup>C, compared to wild type (Figure 4.4A and B). 90% and 80% of the embryos over-expressing *Dmeso17A* using *twist/twist-GAL4* were able to hatch at 18<sup>0</sup>C and 25<sup>0</sup>C respectively. However, most of these larvae were smaller, slower and very translucent compared to wild type. I also observed that most of them were not able to survive until adulthood, 18% gave adult flies at 18<sup>0</sup>C and only 4% did at 25<sup>0</sup>C. Thus, although the remaining muscles in embryos over-expressing *Dmeso17A* are sufficient to produce hatching movements, the defects lead to a substantial lethality of the larvae. Nevertheless, because of the



**Figure 4.4: Larval Hatching and Survival.**

Embryos over-expressing *Dmeso17A* were aligned on plates and the frequency of hatched and surviving larvae was scored at 18°C (**A**) and 25°C (**B**) (see Chapter 2 section 2.4.10). At both temperatures, hatching is not substantially affected, but the percentage of survival to adulthood is considerably reduced compared to wild-type. This assay was used as a quantitative measure of the effect of *Dmeso17A* over-expression on muscle differentiation.

In this experiment and the following hatching and survival assays, three groups of one hundred embryos were aligned for each genotype at either 18°C or 25°C. Standard deviations (S.D) were calculated in each case. Results are indicated as mean percentages  $\pm$  S.D.

Here, mean percentages  $\pm$  S.D are: (**A**) Wild-type, hatching= $99\% \pm 0.081$ , Survival= $97\% \pm 0.16$ ; *Dmeso17A*, Hatching= $90\% \pm 0.24$ , Survival= $18\% \pm 0.31$ . (**B**) Wild-type, hatching= $98\% \pm 0.081$ , Survival= $98\% \pm 0.082$ ; *Dmeso17A*, Hatching= $80\% \pm 0.2$ , Survival= $4\% \pm 0.9$ .

considerable hatching efficiency and the fact that the larvae were able to move, I wanted to test whether the phenotype of the larvae correspond to that observed in the late stages of embryogenesis and therefore if the lethality observed was really a consequence of muscle disruption.

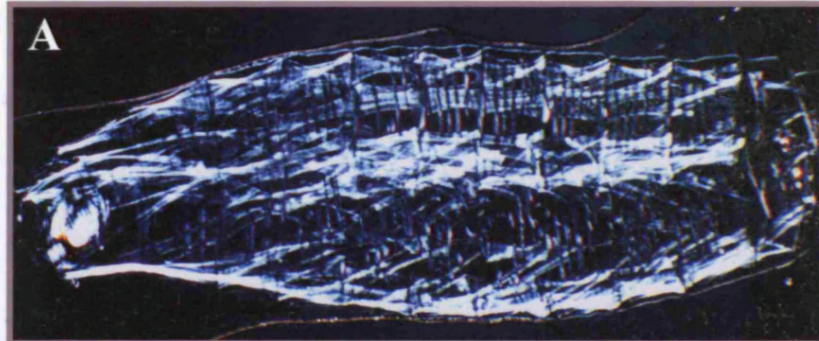
In order to analyse the muscle phenotype of the larvae, I used a polarised light assay (Drysdale et al., 1993). The somatic muscles are visible under polarised light because of their birefringent properties allowing the analysis of a large number of larvae without having to perform dissection or staining. This analysis revealed that the phenotype of these larvae is comparable to that observed in embryos, with similar variations in severity (Figure 4.5 shows the phenotype of one of these larvae at 18<sup>0</sup>C). The unhatched embryos, analysed in the same way, correspond to the more severe phenotype observed. This confirms that the muscle defects do not prevent the larvae from hatching, but they result in a strong diminution of the survivability. Larval hatching is only prevented when the muscle phenotype is dramatic.

Taken together, these results show that larval hatching and survival can be used as a clear quantitative measure of the effect of a gene's over-expression on muscle differentiation. Given the variability of phenotype observed, this assay has been crucial in my analysis of *Dmeso17A*, in particular to assess genetic interactions.

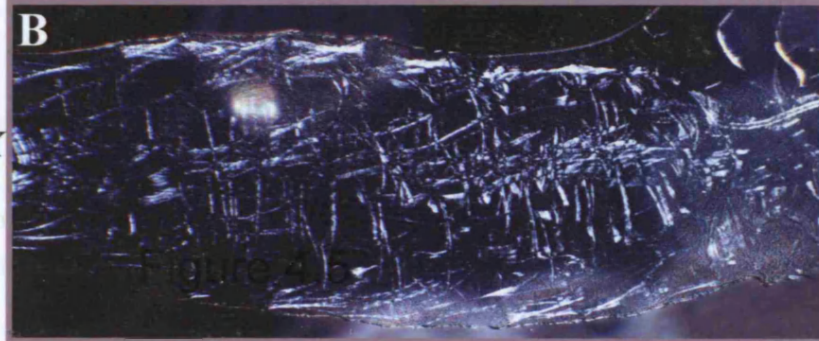
### 4.2.3 GAL4 drivers used

As mentioned previously, I used several specific GAL4 drivers to induce *Dmeso17A* expression in different times and places. This was to test the effect of *Dmeso17A* over-expression on the different mesodermal derivatives and to test genetic interactions. Each GAL4 driver was chosen for where and when it drives expression (see Chapter 2, Table 2), and also for the strength of phenotype induced. The GAL4

Wild-type



*UAS-Dmeso17A X  
twist/twist-GAL4*



**Figure 4.5: Severe muscle defects do not prevent hatching.**

The muscle pattern of *Dmeso17A* over-expressing larvae was analysed under polarised light. (A) Wild-type first instar larva showing the normal pattern of muscles. (B) *Dmeso17A* over-expressing larva. The muscle pattern is severely affected, as in Figure 4.2C, but this larva was still able to hatch. The orientation is the same as in wild-type.

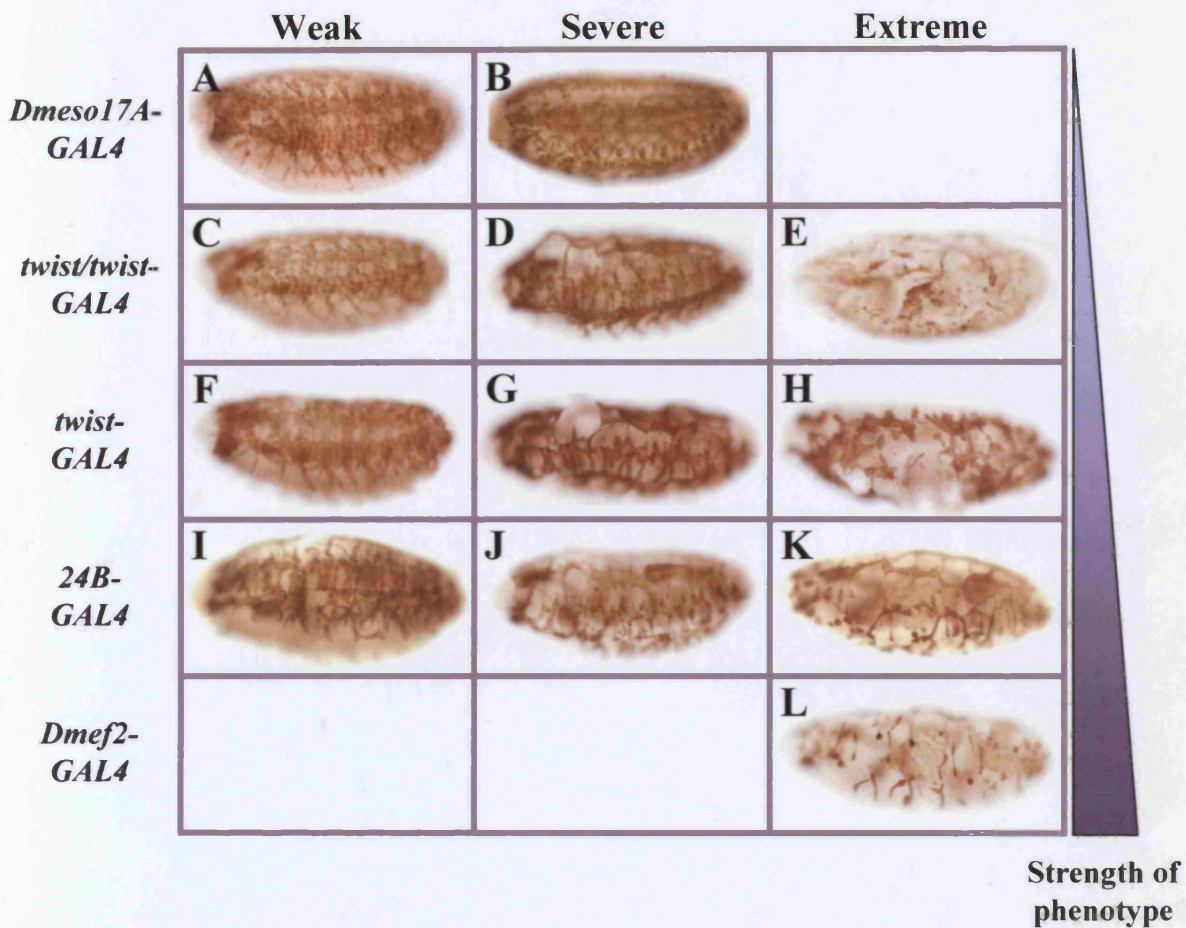


drivers used will be stated for each of my subsequent experiments. Here I present the effect of *Dmeso17A* over-expression, induced at 18°C by the different Gal4 drivers that I used, on somatic muscle development (All *UAS-Dmeso17A* lines tested gave similar results, see Appendix1).

Figure 4.6 shows stage 17 embryos over-expressing *Dmeso17A* using *Dmeso17A-GAL4* (Figure 4.6A-B), *twist/twist-GAL4* (Baylies and Bate, 1996) (Figure 4.6C to E), *twist-GAL4* (Figure 4.6F to H), *24B-GAL4* (Brand and Perrimon, 1993) (Figure 4.6I to K) or *Dmef2-GAL4* (Ranganayakulu *et al.*, 1996) (Figure 4.6L). All the embryos are stained with an antibody against muscle myosin.

Comparison of the phenotypes shows that, as described in section 4.2.1 for *Dmef2-GAL4* and *twist/twist-GAL4*, these drivers induce different strength of phenotype. For example, expression of *Dmeso17A* driven by *Dmef2-GAL4* (Figure 4.6L) has a much stronger effect on somatic myogenesis than when *twist-GAL4* is used (Figure 4.6F). These differential effects can be attributed to the fact that *Dmeso17A* expression is driven in different times and places, but also that each of these drivers induces different levels of *Dmeso17A*.

Moreover, for each driver used I obtained a range of severity of phenotype. This variation can be due to the use of the GAL4/UAS system which is known to give variable effects (Brand *et al.*, 1994). Variation has also been reported in studies analysing muscle pattern defects in mutant embryos (for examples see Drysdale *et al.*, 1993; Lai *et al.*, 1993). Three categories (weak to very severe) are presented in Figure 4.6, but for some drivers there could be more or less variation. For instance, embryos over-expressing *Dmeso17A* using *Dmeso17A-GAL4* can only be classified into two categories of phenotype (Figure 4.6 A-B), and only one category of phenotype is obtained when *Dmef2-GAL4* is used (Figure 4.6L). In contrast, as described in section



**Figure 4.6: Different GAL4 drivers induce different strength of phenotype.**

Several GAL4 drivers were used to promote *Dmeso17A* expression in different times and places at 18°C. For each driver used, stage 17 embryos were stained with an anti-muscle Myosin antibody to assess the muscle phenotype. Each driver produces a range of phenotype. Three phenotypic categories are shown: weak (left column), severe (central column) and extreme (right column). The different drivers induce different strength of phenotype (graded blue arrowhead). **(A-B)** *Dmeso17A-GAL4*. **(C-E)** *twist/twist-GAL4*. **(F-H)** *twist-GAL4*. **(G-K)** *24B-GAL4*. **(M)** *Dmef2-GAL4*.

4.2.1, the use of *twist/twist-GAL4* results in four categories of phenotype (Figure 4.2 and 4.3). The different categories have been established on the basis of muscle scoring (described in Chapter 2, section 4.9). As a general rule, in the “very severe phenotype” category (Figure 4.6 right column) there are very few muscle formed and in the “severe phenotype” category (Figure 4.6 central column) more muscles are present and in a better shape. In the “weak phenotype” category (Figure 4.6 left column), muscle pattern is close to wild-type.

In addition to this variation, it is possible to modulate the severity of the phenotype induced by each driver simply by increasing or decreasing the temperature. As described in section 4.2.1, more severe effects are observed at higher temperature. I used this property of the GAL4/UAS system (Brand et al., 1994) in some of my experiments in order to obtain different strength of phenotype for a given GAL4 driver.

#### **4.2.4 *Dmeso17A* over-expression disrupts myogenesis during the differentiation phase**

In the somatic muscle forming domains of the mesoderm, the formation of each muscle is initiated by the specification of a distinctive class of myoblast: the founder cell. Founders arise from the asymmetric division of muscle progenitors and express genes characteristic of an individual muscle or a subset of muscles, the “identity genes” (reviewed in Baylies et al., 1998; Ruiz-Gomez, 1998). Neighbouring myoblasts, the fusion competent myoblasts (FCMs), are recruited to this pattern of expression during the fusion process (reviewed in Baylies et al., 1998; Taylor, 2002; Taylor, 2003). Fusion of founders with FCMs gives rise to small syncytia that will enlarge by further fusion and differentiate to form a fully functional muscle.

In embryos over-expressing *Dmeso17A* using the *twist/twist-GAL4* driver, myogenesis is disrupted with missing or misshapen muscles. This could be the

consequence of the disruption of founder specification, the fusion process or the differentiation phase. It was therefore necessary to establish which step of the muscle formation is affected in order to define the role of *Dmeso17A* and to identify putative interactor(s) and/or target(s).

One way in which one can follow the first steps of myogenesis– specification of founders and fusion– is to examine the expression of founder cell markers, the “identity genes”. The sequence of events, i.e. order of appearance, position within a segment and increase in number during fusion, for each founder is very stereotyped and easy to follow. To analyse the *Dmeso17A* over-expression phenotype, I used the markers Even-Skipped (*Eve*) and Krüppel (*Kr*) (Figure 4.7 and 4.8). These two genes have a very specific pattern of expression and are required for the acquisition of identity of the founders in which they are expressed (Ruiz-Gomez et al., 1997; Su et al., 1999).

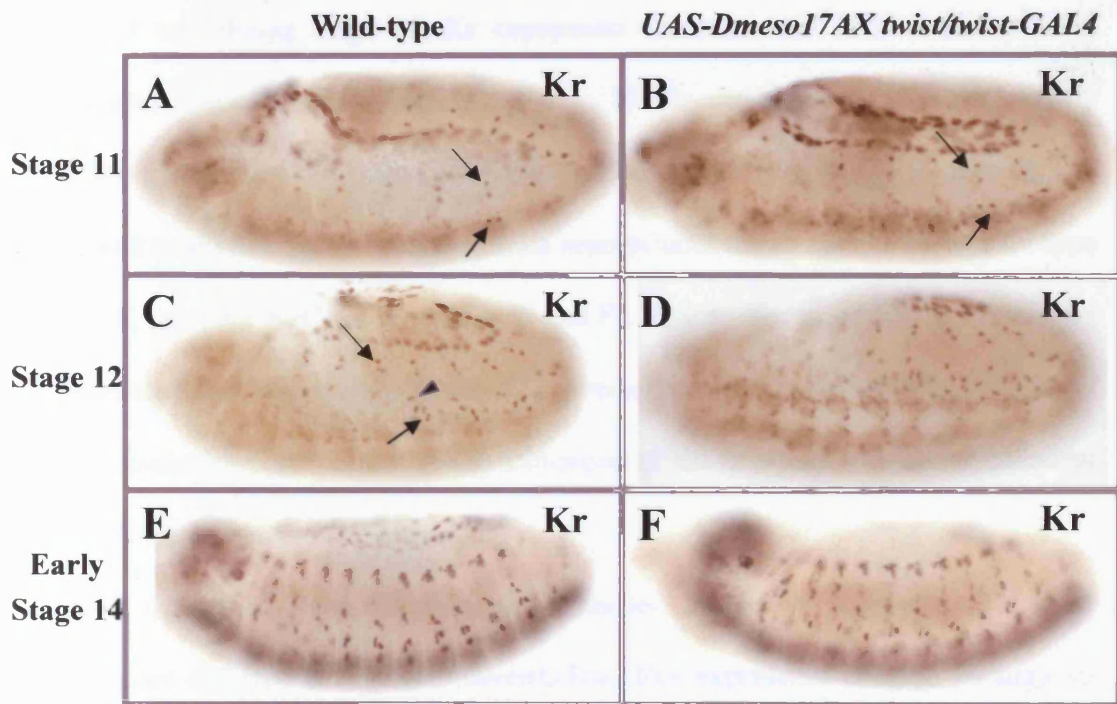
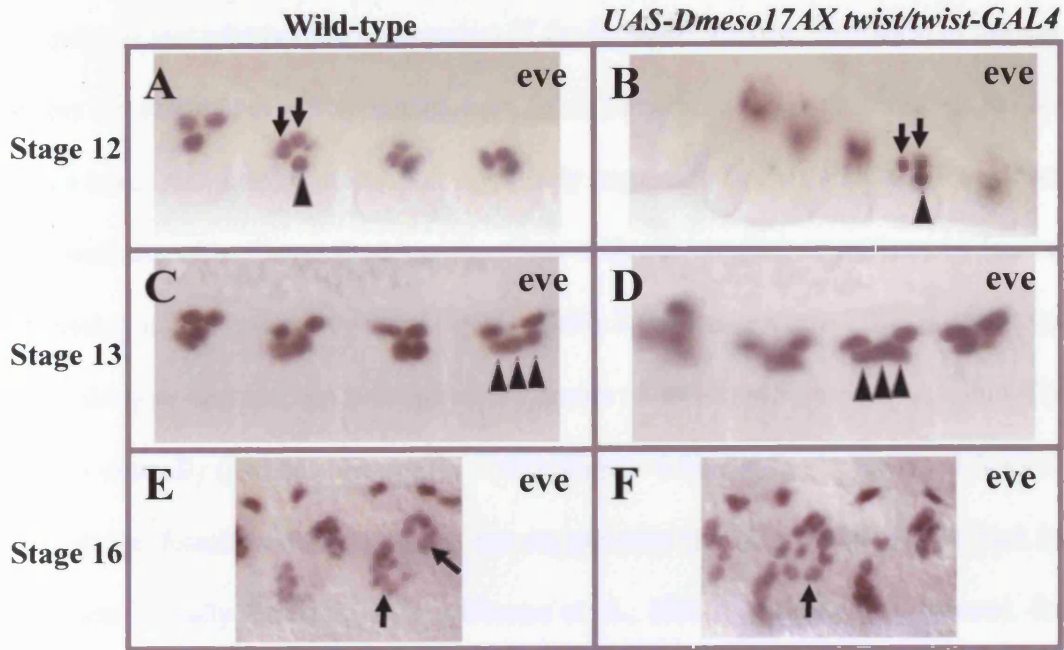
At stage 12, in a wild type embryo, *Eve* is expressed in the founder of the dorsal muscle DA1 (Figure 4.7A, arrowhead) and in the founders of two pericardial cells (Figure 4.7A, arrows) (Frasch et al., 1987; Carmena et al., 1998; Su et al., 1999). At stage 13, the DA1 founder has started fusing with neighbouring myoblasts. There are now two or three nuclei expressing *Eve* in the precursor of DA1 (Figure 4.7C, arrowheads). At stage 16, *eve*-expressing nuclei are organised in two “arches” facing each other at both extremities of DA1 (Figure 4.7E, arrows). When *Dmeso17A* is over-expressed using the *twist/twist-GAL4* driver at 25°C, the pattern of *Eve*-expressing cells at stages 12 and 13 is identical to that of the wild type (Figure 4.7B and D, arrowheads). This suggests that the precursors expressing *Eve* segregate normally and that the first fusions of the founders with FCMs are not affected. Nevertheless, at stage 16, the organisation of *Eve*-expressing nuclei is deranged (Figure 4.7F, arrows) suggesting that

**Figure 4.7: *Dmeso17A* over-expression affects DA1 in the late stages of differentiation.**

Embryos were stained with an anti-Eve antibody. (A, C, E) wild-type. (B, D, F) Embryos over-expressing *Dmeso17A* using the *twist/twist-Gal4* driver at 25°C. (A-B) Stage 12. Wild-type Eve expression pattern (A) in the DA1 founder (arrowheads) and in two PCs founders (arrows) is unchanged in embryos over-expressing *Dmeso17A* (B). (C-D) Stage 13. Wild-type Eve expression (C) in the two or three nuclei of the DA1 muscle precursor (arrowheads) is unaffected by *Dmeso17A* over-expression (D). (E-F) Stage 16. Whereas DA1 nuclei expressing Eve are well organised in the wild-type (arrows in E), they are deranged in embryos over-expressing *Dmeso17A* (arrow in F).

**Figure 4.8: *Dmeso17A* over-expression does not affect the early steps of development of Kr expressing muscles.**

Wild-type (A, C, E) and embryos over-expressing *Dmeso17A* using *twist/twist-GAL4* at 25°C (B, D, F) were stained with an anti-Krüppel antibody. (A-B) Stage 11. The wild-type Kr expression pattern (A) in four muscle progenitors (arrows) is unaffected when *Dmeso17A* is over-expressed (B). (C-D) Stage 12. In the wild type (C), Kr is expressed in the founders resulting from the division of the progenitors in which it was initially expressed (arrows) and also in additional founders (arrowhead). In embryos over-expressing *Dmeso17A* (D), this Kr pattern is unchanged. (E-F) Stage 14. The number and position of Kr expressing cells is identical in the wild-type (E) and in embryos over-expressing *Dmeso17A* (F).



the effect of *Dmeso17A* over-expression is taking place later in the myogenic program, probably during the differentiation phase.

In order to test whether the segregation of the founders and the formation of muscle precursors are affected in muscles other than DA1, I examined the expression of Kr. *Kr* encodes a transcriptional regulator that is initially expressed in the founders of a subset of body wall muscles. These founders then fuse with surrounding myoblasts to form a Kr-expressing muscle precursor (Gaul et al., 1987; Ruiz-Gomez et al., 1997). At stage 11, in a wild type embryo, Kr is found in the nuclei of two muscle progenitors dorsally and in two ventrally (Ruiz-Gomez et al., 1997) (Figure 4.8A, arrows). At stage 12, Kr is detected in the founders resulting from the asymmetric division of the progenitors in which it was initially expressed (Ruiz-Gomez et al., 1997) (Figure 4.8C, arrows). Its expression is also initiated in other founders (Figure 4.8C arrowhead). At the beginning of stage 14, Kr-expressing muscles (DA1, DO1, LL1, LT2-4, VL3, VA2, and VO2-4) can be identified by their position (Ruiz-Gomez et al., 1997) (Figure 4.8E). At the end of stage 14 and during stage 15, Kr expression decreases and later is absent from differentiated muscles (Ruiz-Gomez et al., 1997). In embryos over-expressing *Dmeso17A* using the *twist/twist-GAL4* driver at 25°C (Figure 4.8B, D and F), the number and position of Kr expressing cells remain unchanged compared to wild-type (Figure 4.8, compare A, C and E with B, D and F). This confirms the result obtained by the analysis of *Eve* expression: *Dmeso17A* over-expression does not affect the early steps of muscle development, i.e. the specification of the founders and their subsequent fusion with the FCMs.

As Kr disappears from differentiating muscles, late effects of *Dmeso17A* over-expression are difficult to monitor. Nevertheless, *Eve* expression at stage 16 suggests that the effects of *Dmeso17A* over-expression occur during the differentiation phase. In

order to test this, I assessed the expression of DMef2 in embryos over-expressing *Dmeso17A* using the *twist/twist-GAL4* driver at 25°C (Figure 4.9). DMef2 is expressed in all myogenic cells of the somatic mesoderm at the onset of muscle development and it persists in the differentiating muscles until the end of embryogenesis (Lilly et al., 1994; Bour et al., 1995; Taylor et al., 1995). Therefore, if only the differentiation phase of myogenesis is affected, one might expect to see a normal DMef2 expression before then and alteration of DMef2 expression as muscles differentiate. Indeed, in embryos over-expressing *Dmeso17A*, DMef2 expression is normal at stage 13 (Figure 4.9, compare A with B), but during stage 14, alterations of DMef2 expression are observed in places (Figure 4.9 arrows, compare C and D). By stage 16, DMef2 expression is clearly disrupted (Figure 4.9, compare E and F). This result confirms that in embryos over-expressing *Dmeso17A*, the muscle development program is disrupted during the differentiation phase.

Finally, because there are fewer muscles formed in embryos over-expressing *Dmeso17A*, I wanted to test what is happening to the cells that do not differentiate into muscle and in particular, I wanted to assess whether they are dying. To assess cell death, I used acridine orange (AO) staining (Figure 4.10). At stage 13, embryos over-expressing *Dmeso17A* do not show more cell death than the wild type (Figure 4.10, compare A with B). At stage 14, whereas in the wild type most apoptotic cells are concentrated in the dorsal part of the head and the ventral midline (Figure 4.10C) (Abrams et al., 1993), in embryos over-expressing *Dmeso17A* using the *twist/twist-GAL4* driver at 25°C there are numerous additional AO-positive cells (Figure 4.10D). By stage 16, the number of AO positive cells in embryos over-expressing *Dmeso17A* increases and is substantially more than in the wild type (Figure 4.10, compare E with F). This result is consistent with an effect of *Dmeso17A* over-expression during

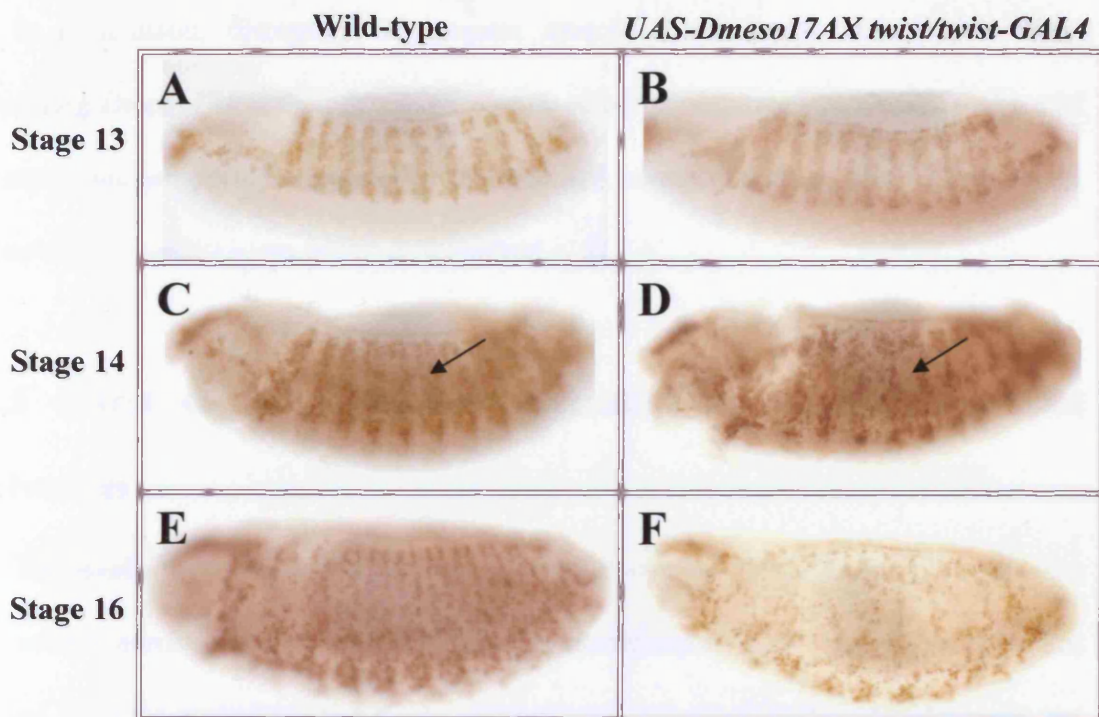


**Figure 4.9: *Dmeso17A* over-expression disrupts myogenesis during the differentiation phase.**

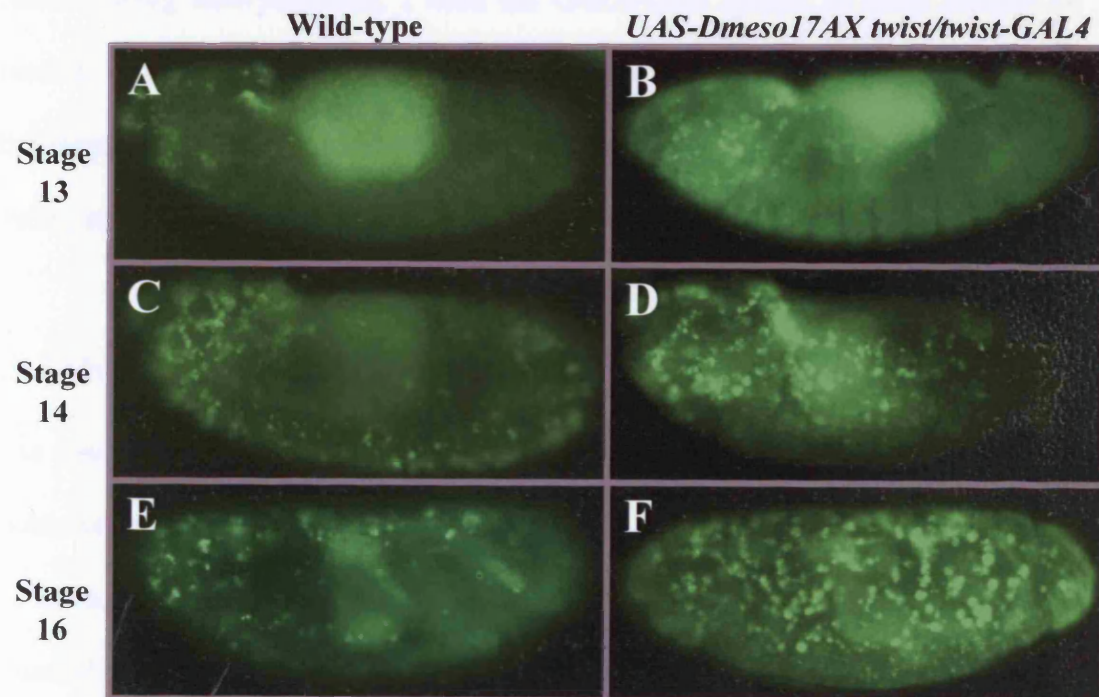
Wild-type (A, C, E) and embryos over-expressing *Dmeso17A* using *twist/twist-GAL4* at 25°C (B, D, F) were stained with an anti-DMef2 antibody. (A-B) Stage 13. DMef2 expression is identical in the wild-type (A) and in embryos over-expressing *Dmeso17A* (B). (C-D) Stage 14. As muscles differentiate, the wild-type expression pattern of DMef2 (C) is altered in places when *Dmeso17A* is over-expressed (D; arrows). (E-F) Stage 16. Compared to wild-type (E), DMef2 expression is substantially disrupted in embryos over-expressing *Dmeso17A* (F).

**Figure 4.10: *Dmeso17A* over-expression increases cell death during muscle differentiation.**

Acridine orange (AO) staining was carried out on wild-type (A, C, E) and embryos over-expressing *Dmeso17A* using *twist/twist-GAL4* at 25°C (B, D, F). (A-B) Stage 13. Only a few AO positive cells are detected in both wild-type (A) and embryos over-expressing *Dmeso17A* (B). (C-D) Stage 14. As muscles differentiate, cell death in the wild type (C) is largely in the dorsal part of the head and in the ventral midline. In contrast, in embryos over-expressing *Dmeso17A* (D), additional apoptotic cells are detected laterally. (E-F) Stage 16. Whereas in the wild-type (E) there are only a few AO positive cells, many more are detected when *Dmeso17A* is over-expressed (F).



*UAS-Dmeso17AX twist/twist-GAL4* overexpression. This is necessary to induce the expression of *UAS-Dmeso17AX twist/twist-GAL4* in the mesoderm. The *UAS-Dmeso17AX twist/twist-GAL4* is necessary for the expression of *UAS-Dmeso17AX twist/twist-GAL4* in the mesoderm.



differentiation and suggests that the cells that do not differentiate into muscle undergo apoptosis.

In conclusion, disruption of somatic muscle development in embryos over-expressing *Dmeso17A* is the consequence of an effect during the differentiation phase of the myogenic program. Founder cells are specified normally and the first fusions occur, but newly formed syncytia fail to differentiate.

#### **4.2.5 Effect of *Dmeso17A* over-expression on other mesodermal derivatives**

The results presented in the previous sections show that *Dmeso17A* over-expression can inhibit somatic muscle differentiation. Nevertheless, other tissues or cells are derived from the mesoderm and it was interesting to test whether their development can be affected by *Dmeso17A* over-expression. This is especially important for the pericardial cells, the AMPs and the ad epithelial cells in which *Dmeso17A* is normally expressed during embryogenesis. I used the GAL4/UAS system to drive *Dmeso17A* expression in these cells. I also tested the effect of *Dmeso17A* over-expression on cardioblasts and visceral mesoderm differentiation. These results are detailed in the following sections.

##### **4.2.5.1 Over-expression of *Dmeso17A* disrupts heart development**

As described in Chapter 1, the *Drosophila* heart is composed of two cell types: the cardioblasts and the pericardial cells (for reviews see Cripps and Olson, 2002; Zaffran and Frasch, 2002). At the end of embryogenesis, two rows of cardioblasts are surrounded by four rows of pericardial cells at the dorsal midline of the embryo (Figure

4.11, drawn after Ward and Skeath, 2000). The cardioblasts are contractile and express muscle proteins, but the role of the pericardial cells is poorly understood.

In the heart, *Dmeso17A* is only expressed in the pericardial cells and it was necessary to know if its over-expression could affect their differentiation. As very little is known about the differentiation of these cells, this could be informative. I also wanted to test the effect of *Dmeso17A* over-expression on the cardioblasts. Over-expression in the pericardial cells was achieved by using the *Dmeso17A-GAL4* driver and expression in the cardioblasts by using the *Dmef2-GAL4* driver both at 25°C (Ranganayakulu et al., 1996). I then used markers specific for each cell type to assess their development.

When over-expressed in the pericardial cells, *Dmeso17A* disrupts aspects of their development (Figures 4.12D-F; 4.14B; 4.15B and D). Pericardial cells were visualised using anti-*Zfh-1*, anti-*Odd* or anti-*Eve* antibodies. Each of these markers is specific for subsets of pericardial cells. *Zfh-1* is expressed in most pericardial cells (Lai et al., 1991); *Odd* identifies four cells per hemisegment (Ward and Coulter, 2000; Ward and Skeath, 2000) and *Eve* marks two pericardial cells per hemisegment (Frasch et al., 1987).

As revealed by *Zfh-1* staining, the general organisation of the *Zfh-1*-expressing pericardial cells when *Dmeso17A* is over-expressed is deranged. Arrowheads in Figure 4.12 point at examples of regions where the organisation of *Zfh-1*-expressing cells is different in the wild type and embryos over-expressing *Dmeso17A* (compare A-C with D-F). Yet, as pericardial cells are loosely attached to the heart and the effect of *Dmeso17A* over-expression is not very strong, the analysis of the organisation of the pericardial cells is problematic. Therefore, in order to confirm my observations, I concentrated on the number of cells and counted the number of *Zfh-1*-expressing cells in both wild type and embryos over-expressing *Dmeso17A* at stage 17. Figure 4.13 shows a graphic representation of the numbers obtained. There are on average 10 more

**Figure 4.11: Structure of the *Drosophila* heart.**

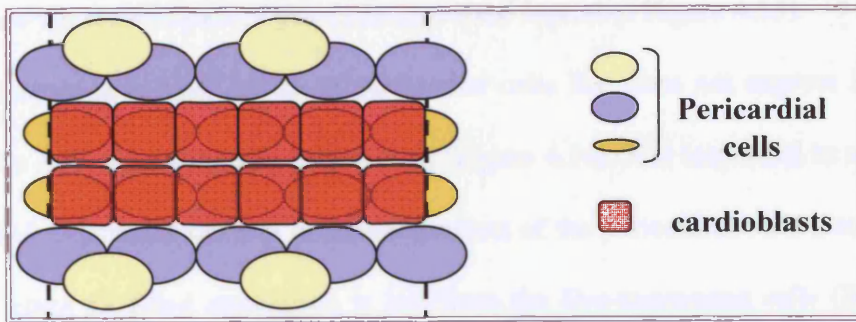
Schematic representation of a dorsal view of a mature wild-type embryonic heart showing the two rows of the cardioblasts (red squares) surrounded by four rows of pericardial cells (PCs) (blue, yellow and orange ovals). Only one segment is represented. This figure was inspired by Ward and Skeath, 2000.

**Figure 4.12: *Dmeso17A* over-expression disrupts the organisation of *Zfh-1*-expressing pericardial cells.**

Stage 17 embryos, were stained with an anti-*Zfh-1* antibody. (A-C) In the wild-type, *Zfh-1* is expressed in a large number of PCs. (D-F) In embryos over-expressing *Dmeso17A* using *Dmeso17A-GAL4* at 25°C, the general organisation of these cells is deranged. Arrowheads point at regions of the heart where the organisation of *Zfh-1*-expressing PCs is different in the wild-type and in embryos over-expressing *Dmeso17A*.

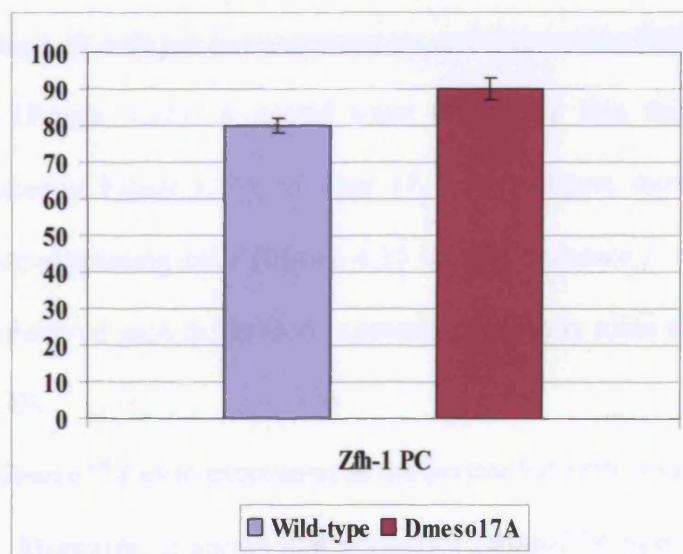
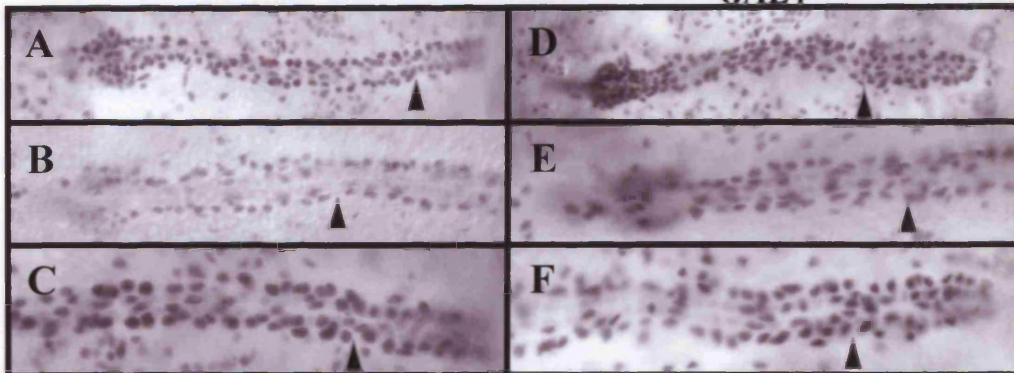
**Figure 4.13: *Dmeso17A* over-expression increases the number of *Zfh-1*-expressing pericardial cells.**

The number of *Zfh-1*-expressing cells was scored in both wild type and embryos over-expressing *Dmeso17A* using *Dmeso17A-GAL4* at stage 17. Twenty embryos were analysed in each case. 80 cells on average were found in the wild-type whereas, in embryos over-expressing *Dmeso17A*, there were 90. A paired t-test was carried out to test the significance of this difference. The p value obtained ( $p= 1.12 \times 10^{-15}$ ) with a 95% confidence interval shows a significant difference in *Zfh-1*-expressing PCs number between the wild-type and in embryos over-expressing *Dmeso17A*. Error bars indicate standard deviation.



Wild-type

*UAS-Dmeso17A X Dmeso17A-GAL4*



Zfh-1-expressing cells in the heart of embryos over-expressing *Dmeso17A*. A paired t-test confirmed the significance of this difference (see legend of Figure 4.13).

I then looked at another subset of pericardial cells that does not express Zfh-1 at this stage: the Eve-expressing pericardial cells (Figure 4.14). It is important to note that Eve and Zfh-1 expression overlap in the progenitors of the pericardial cells (early stage 11), but by stage 17 Zfh-1 expression is lost from the Eve-expressing cells (Su et al., 1999). In stage 17 embryos over-expressing *Dmeso17A*, there are defects in the arrangement of the Eve-expressing cells compared to the wild type (Figure 4.14 arrowheads in A and B). However, the number of Eve-expressing cells remains unchanged. One possible explanation for these results taken together is that, under the influence of persistent *Dmeso17A* over-expression, some Eve cells have retained Zfh-1 expression during their differentiation.

Finally, I assessed the expression of Odd in embryos over-expressing *Dmeso17A* (Figure 4.15). By stage 14 in the wild type, four pericardial cells per hemisegment express Odd. These Odd-expressing cells also express Zfh-1, but not Eve (Ward and Skeath, 2000). At this stage, in embryos over-expressing *Dmeso17A*, although the general aspect of the Odd staining looks normal (Figure 4.15 compare A with B), cell counting reveals that 4.49 cells per hemisegment are now expressing Odd when 4.18 are in the wild type (Figure 4.16). A paired t-test confirmed that this difference is significant (see legend of Figure 4.16). At stage 17, these embryos show defects in the organisation of Odd-expressing cells (Figure 4.15 arrows, compare C and D). At this stage, I have also observed gaps in the Odd expression pattern in some embryos (Figure 4.15 arrowhead in D).

In summary, *Dmeso17A* over-expression in the pericardial cells results in defects in their organisation. Moreover, it seems that persistent *Dmeso17A* over-expression can

**Figure 4.14: *Dmeso17A* over-expression affects the organisation of Eve-expressing pericardial cells.**

Stage 17 embryos were stained with an anti-Eve antibody. In the wild-type (A) two Eve PCs are found in every hemisegment. When *Dmeso17A* is over-expressed using *Dmeso17A-GAL4* at 25°C (B), this organisation can be deranged (arrowheads).

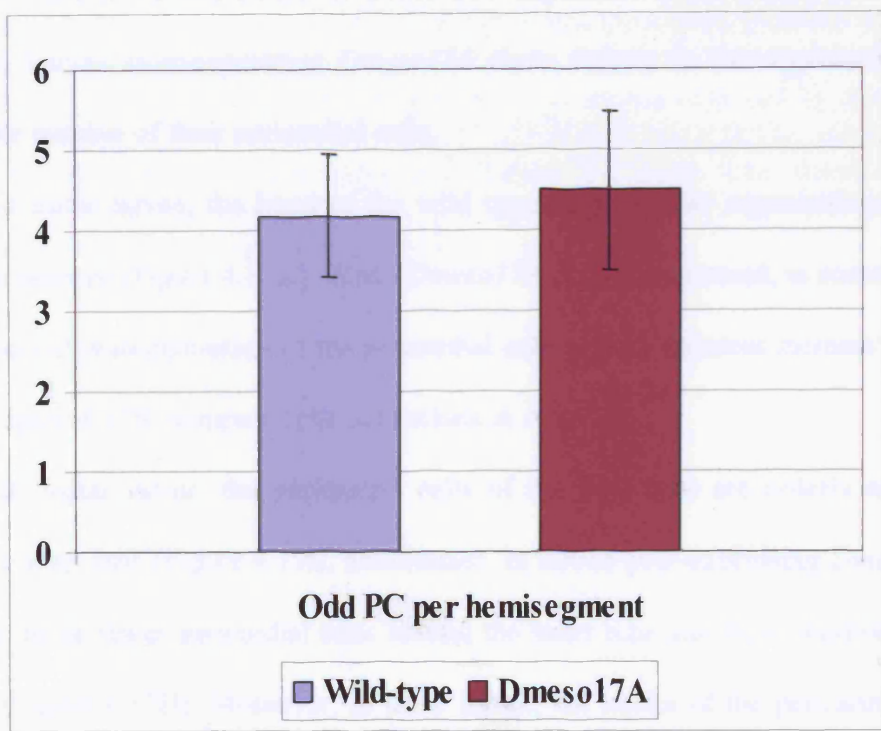
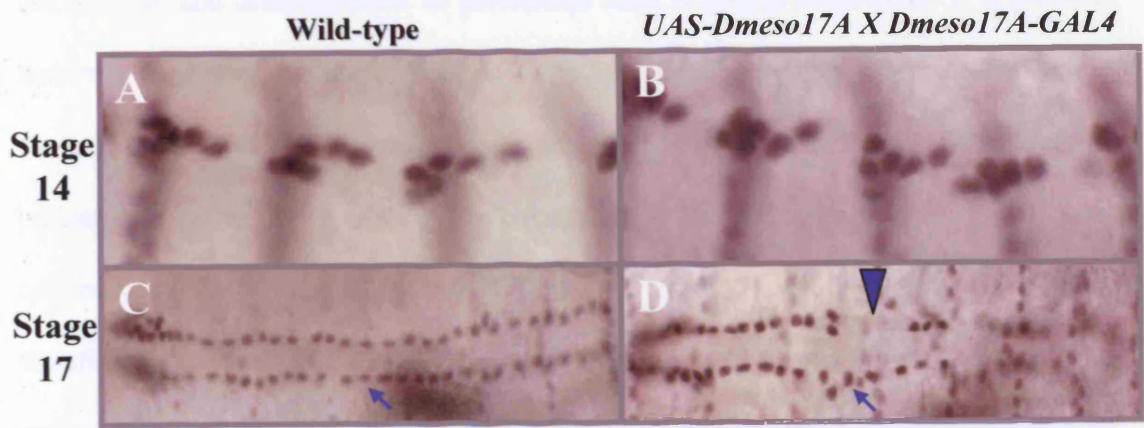
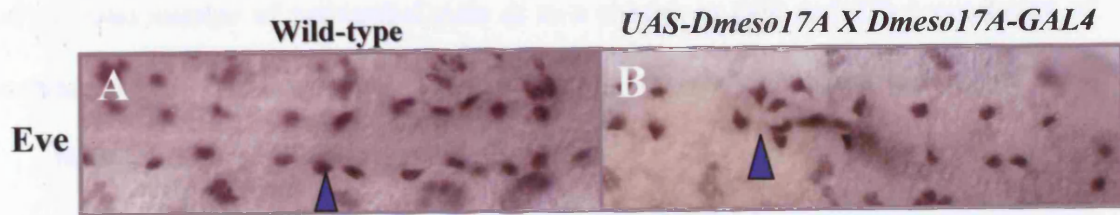
**Figure 4.15: *Dmeso17A* over-expression affects the development of Odd-expressing pericardial cells.**

Wild type (A, C) and embryos over-expressing *Dmeso17A* using *Dmeso17A-GAL4* at 25°C (B, D) were stained with an anti-Odd antibody. (A-B) Stage 14. The organisation of Odd PCs appear identical in the wild-type (A) and in embryos over-expressing *Dmeso17A* (B). (C-D) Stage 16. Whereas in the wild-type (C) Odd PCs are well organised in two rows, in embryos over-expressing *Dmeso17A* (D) there are gaps (arrowhead) and defects in their organisation (arrow).

**Figure 4.16: *Dmeso17A* over-expression increases the number of Odd-expressing pericardial cells.**

The number of Odd-expressing cells per hemisegment was scored in both wild type and embryos over-expressing *Dmeso17A* using *Dmeso17A-GAL4* at stage 14. 144 hemisegments were analysed in each case. There was an average of 4.18 cells per hemisegment in the wild-type whereas, in embryos over-expressing *Dmeso17A*, there were 4.49 cells. A paired t-test showed that this difference is significant. The p value = 0.006 with a 95% confidence interval. Error bars indicate standard deviation.



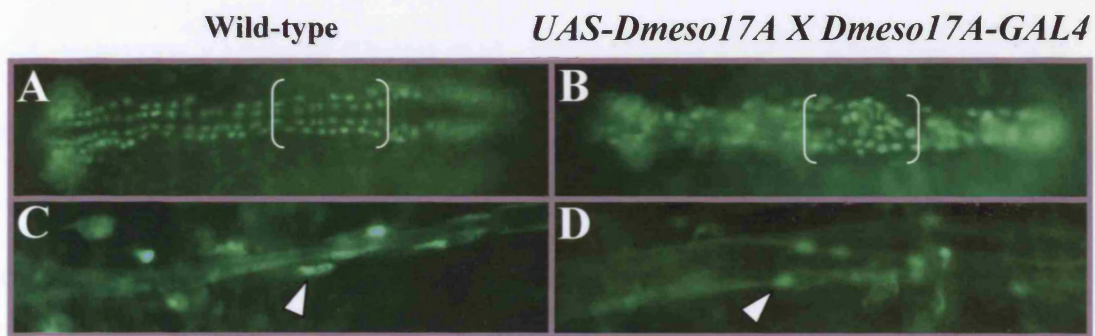


increase the number of *Zfh-1* and *Odd*-expressing cells. This could be due to an increase of the total number of pericardial cells or to a change in *Odd* and *Zfh-1* regulation of expression. For example, it is possible that *Zfh-1* expression persists in the *Eve* cells.

Nevertheless, although these results show that *Dmeso17A* over-expression can affect the development of the pericardial cells, further investigation is needed to understand these effects and to determine *Dmeso17A* function in these cells. Moreover, the function and differentiation of pericardial cells is poorly understood. It is possible that their differentiation is not finished at the end of embryogenesis, but that it is rather starting. Indeed, changes in shape, size and organisation have been reported for the pericardial cells during larval and pupal life (Curtis et al., 1999; personal communication from A. Paululat). Persistent *Dmeso17A* over-expression could therefore have more effect during larval life than it does during embryogenesis. As a preliminary experiment, I have over-expressed *Dmeso17A*, using *Dmeso17A-GAL4*, in the 4.0 Kb *Him:GFP* background (Figure 4.17). As mentioned in the previous Chapter (section 3.2.2), this reporter construct drives GFP expression in the pericardial cells of the larvae. Larvae over-expressing *Dmeso17A* show defects in the organisation and possibly the number of their pericardial cells.

In first instar larvae, the heart of the wild type has a similar organisation as that seen in the embryo (Figure 4.17A). When *Dmeso17A* is over-expressed, in some larvae, I have observed disorganisation of the pericardial cells and an apparent increase in their number (Figure 4.17B, compare cells in brackets in A and B).

In third instar larvae, the pericardial cells of the wild type are orderly arranged around the heart tube (Figure 4.17C, arrowhead). In larvae over-expressing *Dmeso17A*, there seem to be fewer pericardial cells around the heart tube and their organisation is deranged (Figure 4.17D). Moreover, in these larvae, the nuclei of the pericardial cells



**Figure 4.17: *Dmeso17A* over-expression affects the organisation of pericardial cells in the larva.**

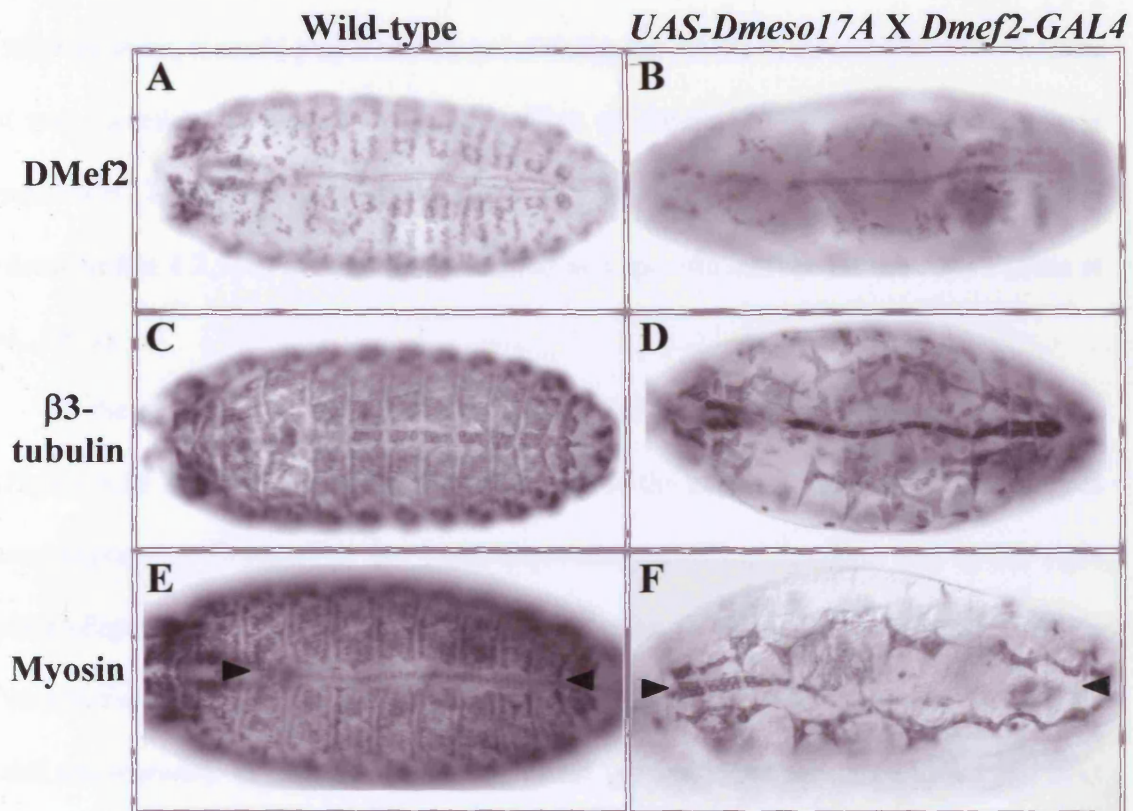
*Dmeso17A* was over-expressed using *Dmeso17A-GAL4* at 25°C in a *Him-GFP* background. The expression of GFP in the PCs was monitored in larvae (**B, D**) and compared to wild-type (**A, C**). (**A-B**) In first instar larvae, the wild-type heart (**A**) has a similar organisation to that in the embryo. This organisation can be disrupted by *Dmeso17A* over-expression (**B**; brackets). (**C-D**) In third instar larvae, whereas in the wild-type (**C**) PCs are well organised around the heart tube (arrowhead), in *Dmeso17A* over-expressing embryos (**D**) they appear randomly positioned and smaller (arrowhead). Their number also seems to be reduced.

look smaller than in the wild type (Figure 4.17, arrowheads). These results come from simple observations, but they at least show that the effect of *Dmeso17A* over-expression on the pericardial cells should not be only considered in the embryo, but need to be investigated in the larvae and maybe later during pupal development.

When expressed in the cardioblasts, *Dmeso17A* disrupts their differentiation (Figure 4.18). At stage 17, in the wild type, there are six pairs of cardioblasts per segment forming the dorsal vessel (Ward and Skeath, 2000). They all express DMef2 (Lilly et al., 1994; Taylor et al., 1995) (Figure 4.18A) and myosin (Figure 4.18E), but only four pairs out of six express  $\beta$ 3-tubulin (Damm et al., 1998) (Figure 4.18C). When *Dmeso17A* is expressed in the cardioblasts (Figure 4.18B, D and F), DMef2 and  $\beta$ 3-tubulin expression in these cells, at stage 17, is not affected (Figure 4.18B and D). This suggests that cardioblasts are specified correctly and that at least some aspects of their differentiation are not affected. However, myosin expression in the cardioblasts of these embryos is severely impaired (Figure 4.18F). This resembles the *Dmef2* mutant phenotype (Ranganayakulu et al., 1995; Damm et al., 1998) and suggests that, even though the cardioblasts can form and develop to a certain extent, the presence of *Dmeso17A* disrupts their differentiation. Moreover, this result is consistent with that obtained for *Dmeso17A* over-expression in the somatic mesoderm, i.e. *Dmeso17A* over-expression can inhibit differentiation, but not specification of myoblasts.

#### **4.2.5.2 Investigation of the effect of *Dmeso17A* over-expression on AMPs**

After mesoderm subdivision, progenitors of the somatic muscles divide asymmetrically to give rise to either two founder myoblasts or a founder and an AMP (reviewed in Baylies et al., 1998 and Taylor, 2005). Whereas the founders fuse with



**Figure 4.18: *Dmeso17A* over-expression disrupts cardioblast differentiation.**

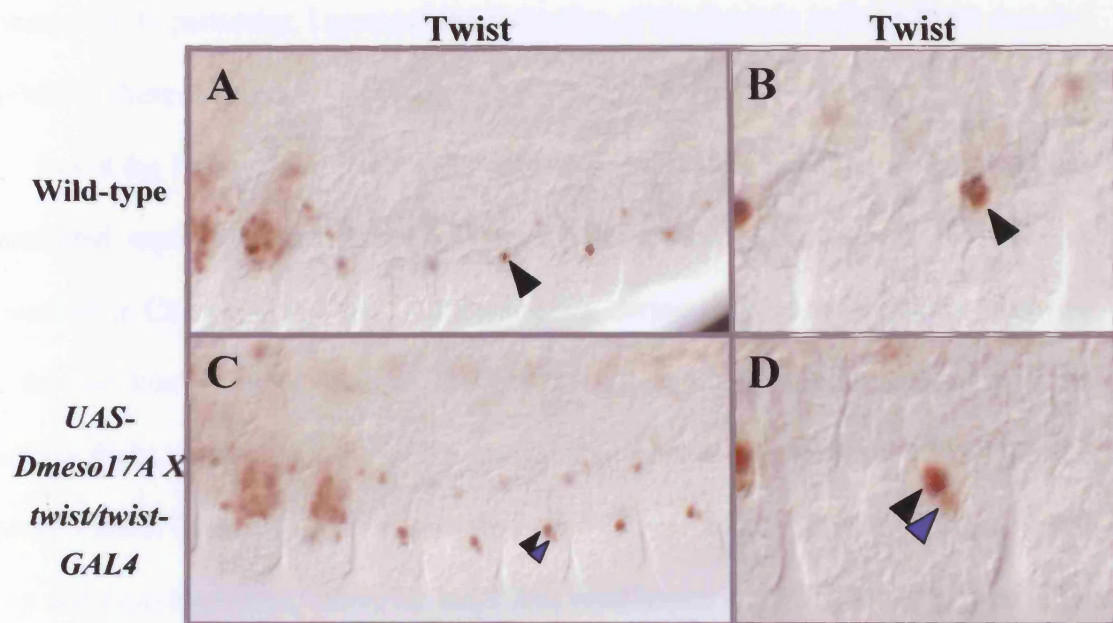
Stage 17 embryos were stained with anti-DMef2 (A-B), anti- $\beta$ 3-tubulin (C-D) or anti-Myosin (E-F) antibodies. *Dmeso17A* was over-expressed using *Dmef2-GAL4* at 25°C. (A-B) DMef2 expression in embryos over-expressing *Dmeso17A* (B) is identical to wild-type (A). (C-D)  $\beta$ 3-tubulin expression in embryos over-expressing *Dmeso17A* (D) is comparable in wild-type (C). (E-F) Myosin expression is severely affected by *Dmeso17A* over-expression (F) when compared to wild-type (E) (arrowheads).

FCMs and subsequently differentiate, the AMPs are set aside and remain undifferentiated throughout embryogenesis. Their proliferation and subsequent differentiation is triggered later in development (during larval life) to make adult muscle (Bate, 1993; reviewed in Taylor 2005).

*Dmeso17A* is specifically expressed in the AMPs and, as a putative inhibitor of differentiation, it could play a role in maintaining the AMPs in an undifferentiated state. It was therefore interesting to test the effect of *Dmeso17A* over-expression in these precursors. *Dmeso17A* over-expression was achieved by using the *twist-GAL4* driver (described in 4.2.1) at 25°C. Twist was used as a specific marker for the AMPs (Bate et al., 1991).

In the wild type, AMPs are clearly identifiable as single Twist-expressing cells (Figure 4.19 A and B, arrowheads point at one of the most ventral AMPs). In embryos over-expressing *Dmeso17A*, the Twist-expressing AMPs are present and in the right place (Figure 4.19 C and D, black arrowheads point at one of the most ventral AMP). Nevertheless, other Twist-expressing cells can also be detected (Figure 4.19C and D, blue arrowheads). In embryos where this effect is seen, these cells are located just next to each of the normal most ventral AMPs and seem to be slightly more internal. In some embryos, I have also observed these cells next to the lateral or dorsal AMPs.

This result shows that *Dmeso17A* over-expression can increase the number of persistent Twist-expressing cells. The origin of these extra Twist-expressing cells remains to be determined. Nevertheless, one can speculate that they could be the result of the division of the AMPs or they could be founder cells that have retained Twist expression and remain undifferentiated.



**Figure 4.19: *Dmeso17A* can increase the number of persistent Twist-expressing cells.**

Stage 14 embryos were stained with an anti-Twist antibody. (A-B) In the wild-type, Twist-expressing AMPs appear as single cells (arrowhead). (C-D) In embryos over-expressing *Dmeso17A* using *twist/twist-GAL4* at 25°C, the normal Twist-expressing AMPs are present (black arrowheads point at one of them), but extra Twist-expressing cells can also be detected (blue arrowheads).

### 4.2.5.3 *Dmeso17A* over-expression affects adult muscle development

In addition to the pericardial cells and the abdominal AMPs, *Dmeso17A* is also expressed in the adepithelial cells. These cells associate with imaginal discs and form the adult thoracic and leg muscles (Bate et al., 1991; Broadie and Bate, 1991). Therefore, to test the effect of *Dmeso17A* over-expression on adepithelial cell differentiation, I examined the formation of adult muscles in embryos over-expressing *Dmeso17A*. In particular, I assessed the formation of the thoracic indirect flight muscles (IFMs) in these embryos.

I used the 1151-GAL4 driver at 25°C to drive expression in the wing imaginal disc-associated myoblasts (the adepithelial cells) (Roy and VijayRaghavan, 1998). As described in Chapter 1, section 1.4.4, these cells, during pupal metamorphosis, give rise to the two kind of adult thoracic muscles: the direct flight muscles (DFMs) and the indirect flight muscles (IFMs). IFMs are subdivided in two subclasses of muscles: the Dorso-Ventral Muscles (DVMs) and the Dorso-Lateral Muscles (DLMs) (Bate, 1993; Roy and VijayRaghavan; 1999; Taylor, 2005; see Chapter 1 section 1.4.4) (Figure 4.20). I analysed the effect of *Dmeso17A* over-expression on both DVMs and DLMs (Figure 4.21).

In the wild type, the DLMs comprises six muscles (Figure 4.21A, muscles are marked with red asterisks) and the DVMs consist of three groups of muscles (Figure 4.21C, red brackets). Each of these DVM groups is composed of two or three muscles. When *Dmeso17A* is over-expressed, the development of the IFMs is impaired. The number of muscles present in both DLMs and DVMs is reduced with only two to three DLMs and two DVM groups present (Figure 4.21B and D). Moreover, the remaining DLMs appear bigger than in the wild-type (Figure 4.21B).

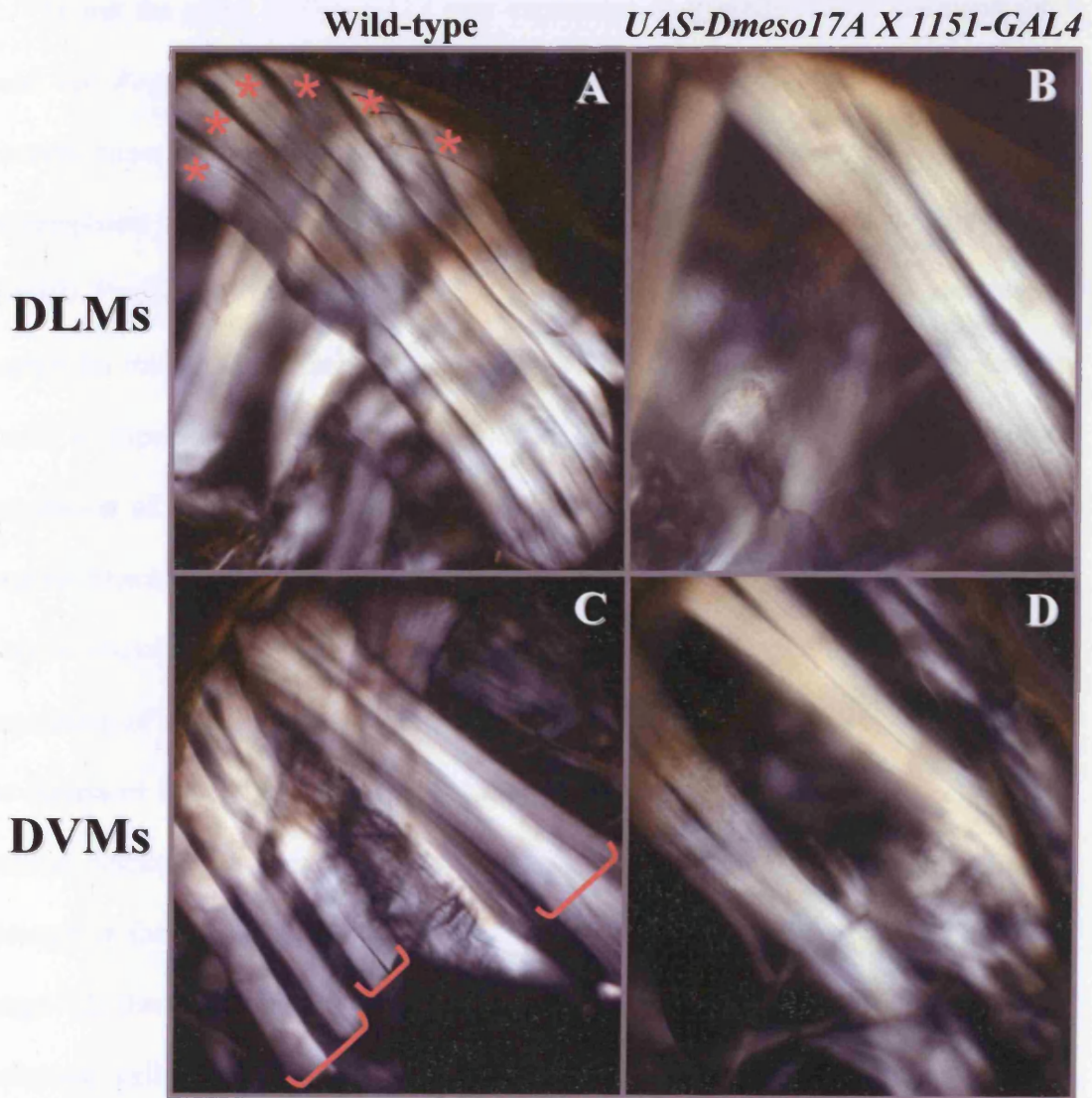
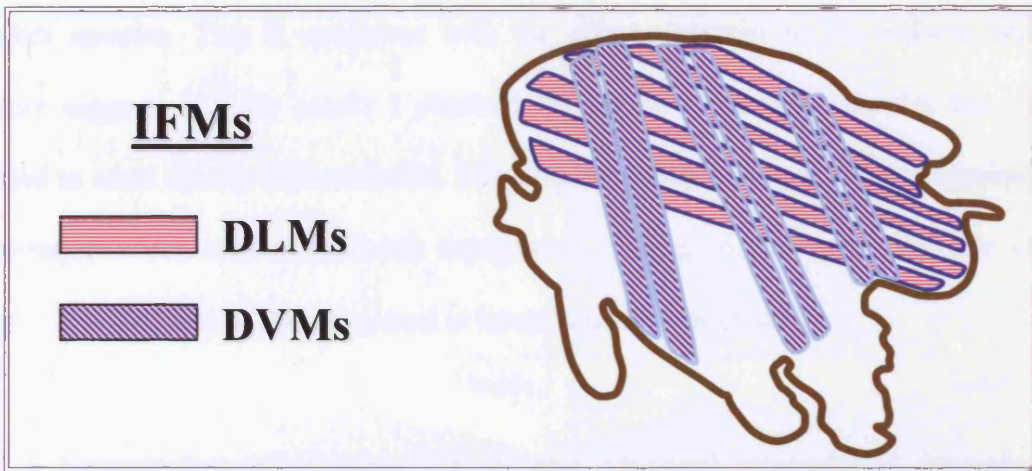


**Figure 4.20: The indirect flight muscles.**

Schematic representation of an adult *Drosophila* hemithorax showing the number and relative position of the indirect flight muscles (IFMs). Dorso-lateral muscles (DLMs) are in blue and dorso-ventral muscles (DVMs) in red.

**Figure 4.21: *Dmeso17A* over-expression affects IFM development.**

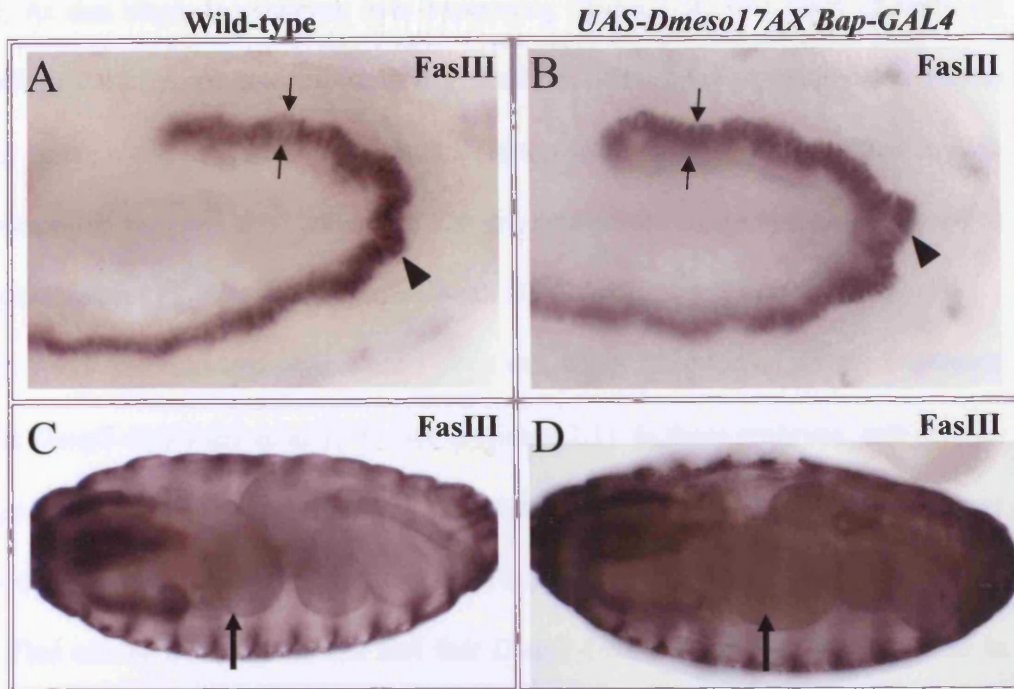
IFMs were visualised under polarised light (see chapter 2, section 2.4.8). (A) In the wild-type, DLMs are constituted of six muscles (red asterisks). (B) Flies over-expressing *Dmeso17A* driven by the *1151-GAL4* driver at 25°C (B) have only two or three DLMs. These remaining DLMs appear bigger than in the wild-type. (C) Wild-type DVMs consist of three groups of two muscles (red brackets). (D) *Dmeso17A* over-expression results in the loss of one or two of these groups.



This result shows that *Dmeso17A* over-expression can disrupt the development of the adult muscles. This is consistent with the effect observed in the embryo and therefore suggests that the results I obtained for the larval somatic muscles can be extended to adult muscle differentiation. Nevertheless, further investigation is required to determine which step of the adult myogenesis is affected and see if the role of *Dmeso17A* is the same as that suggested in larval somatic myogenesis.

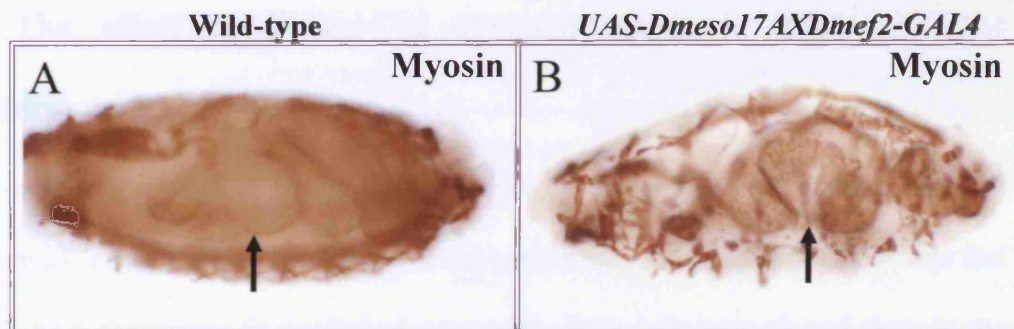
#### **4.2.5.4 Expression of *Dmeso17A* in the visceral mesoderm impairs visceral muscle development**

To test the effect of *Dmeso17A* over-expression on visceral muscle development, I used the *Bagpipe-GAL4* (*Bap-GAL4*) driver which drives expression in the trunk visceral mesoderm from stage 10 (Zaffran et al., 2001). Crosses were kept at 25°C. Development of visceral muscles was monitored using an antibody against Fasciclin III (FasIII). FasIII is an Ig-domain adhesion molecule and represents an early and specific marker for midgut musculature (Patel et al., 1987). At stage 11, in the wild type embryo, FasIII is expressed in two populations of cells in the developing midgut. The first population of cells are the progenitors of the circular visceral muscles, which also express Dumbfounded (Duf). These cells can be compared to the founder cells of the somatic muscles (Bate, 1993; San Martin et al., 2001; Klapper et al., 2002). The second population of cells in which FasIII is expressed is adjacent to these progenitors and can be compared to the fusion competent myoblasts of the somatic mesoderm. These cells express Sticks and stones (Sns) (San Martin et al., 2001). FasIII expression is much stronger in the progenitors of the circular visceral muscles (San Martin et al., 2001). At stage 12, these progenitors have divided and are orderly arranged in two rows of columnar cells (San Martin et al., 2001) (Figure 4.22A arrows). At this stage, in



**Figure 4.22: *Dmeso17A* over-expression impairs visceral mesoderm development.**

Wild-type (A, C) and embryos over-expressing *Dmeso17A* using the *bap-GAL4* driver at 25°C (B, D), were stained with an anti-FasIII antibody. (A-B) Stage 12. In wild-type embryos, the progenitors of the circular visceral muscles are arranged in two rows of columnar cells (arrows). In embryos over-expressing *Dmeso17A*, two rows of progenitors are also present (arrows), but their organisation is disturbed in the posterior part of the visceral mesoderm (arrowheads). (C-D) Stage 16. Compared to wild-type (C), *Dmeso17A* over-expression affects midgut constrictions (D; arrows).



**Figure 4.23: *Dmeso17A* over-expression disrupts visceral muscle development.**

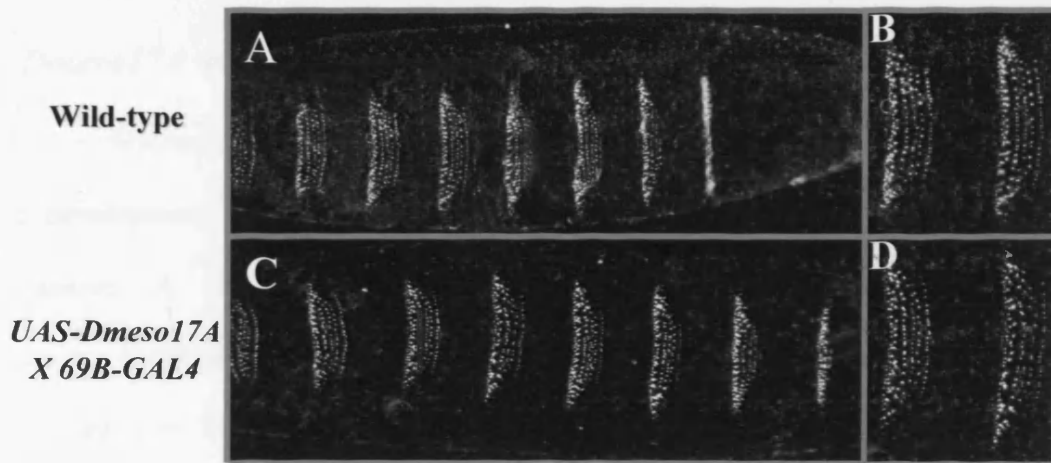
Stage 17 embryos were stained with an anti-Myosin antibody. (A) Wild-type embryo showing normal midgut constrictions (arrow). (B) In embryos over-expressing *Dmeso17A* using the *Dmef2-GAL4* driver at 25°C, midgut constrictions are severely disrupted (arrow).

arrows). At this stage, in embryos over-expressing *Dmeso17A*, two rows of cells are visible (Figure 4.22B, arrows), but their organisation is deranged especially in the most posterior portion of the visceral mesoderm (Figure 4.22, arrowheads, compare A with B). By stage 16, embryos show abnormal constrictions of the midgut when compared to wild type (Figure 4.22, arrows, compare C with D).

This result is consistent with what I observed when *Dmeso17A* is over-expressed using the *Dmef2-GAL4* driver at 25°C (see section 4.2.1). In these embryos, anti myosin staining revealed that the midgut fails to constrict and has a swollen appearance (Figure 4.23, arrows, compare A with B). This effect is stronger than that observed in Figure 4.22D. This can be attributed to the fact that *Dmef2-GAL4* drives strong expression in all muscle lineages from stage 7 until the end of embryogenesis (Ranganayakulu et al., 1996), whereas *Bap-GAL4* driven expression decreases after segregation of the trunk visceral mesoderm (Zaffran et al., 2001). Nevertheless, these results show that ectopic expression of *Dmeso17A* can impair midgut constriction and, as visceral musculature is essential for the formation of the constrictions (Reuter and Scott, 1990), they also suggest that ectopic expression of *Dmeso17A* can inhibit midgut muscle development.

#### **4.2.6 The effect of *Dmeso17A* over-expression is limited to the mesoderm**

In order to test whether *Dmeso17A* over-expression can affect the differentiation of other tissues, I ectopically-expressed it in the ectoderm. I used the 69B-GAL4 line that drives GAL4 expression in epidermal precursors from late stage 9 and then in the epidermis (Brand and Perrimon, 1993). Crosses were kept at 25°C. Cuticle preparations were carried out to assess the effect of ectopic *Dmeso17A* expression on the epidermis (Figure 4.24). The final pattern of the cuticle of the *Drosophila* larvae depends on



**Figure 4.24: *Dmeso17A* over-expression does not affect epidermal differentiation.**

*Dmeso17A* was over-expressed in the ectoderm using the *69B-GAL4* driver at 25°C. Cuticle preparations did not reveal any difference between wild-type (A-B) and *Dmeso17A* over-expressing (C-D) larvae.

epidermis (for review see Payre, 2004) and is therefore a good measure of normal epidermal differentiation. Ectopic *Dmeso17A* expression in the ectoderm did not result in visible changes of the cuticular pattern of the larvae (Figure 4.24 compare A-B with C-D). This implies that, despite the presence of *Dmeso17A*, the epidermis of these larvae can still secrete a normal cuticle and therefore that epidermal differentiation is not affected. This result shows that, although *Dmeso17A* over-expression profoundly inhibits the differentiation of somatic muscles and other mesodermally-derived cell types, it does not inhibit all differentiation processes.

## 4.3 Discussion

### 4.3.1 *Dmeso17A* over-expression inhibits somatic muscle differentiation

Muscle differentiation is a finely tuned process and a central issue for correct muscle development is the balance between influences that promote and restrain differentiation. A slight perturbation of this equilibrium can have dramatic repercussions on muscle development and functionality. Key positive regulators such as Mef2 (reviewed in Taylor 2005; see Chapter 1 section 1.5.2) have been extensively studied in both *Drosophila* and vertebrates, but there is little information on the role of specific negative regulators during normal muscle development (reviewed in Taylor, 2005; see Chapter 1 section 1.2). Some candidates have been identified, largely in mammalian cell culture. For example, Histone deacetylases (HDACs), which can bind and regulate Mef2 activity (Lu et al., 2000; for review on HDAC function in muscle development see McKinsey et al., 2001; see Chapter 6, section 6.4). Identification of negative regulators and analysis of their function during muscle differentiation in *Drosophila* is therefore crucial to gain new insight into the molecular events that regulate this process. My results indicate that *Dmeso17A* could be one such molecule.

I have shown that over-expression of *Dmeso17A* can lead to a profound inhibition of somatic myogenesis. Muscle myosin expression revealed that maintenance of a high level of *Dmeso17A* dramatically impairs muscle development, suggesting that *Dmeso17A* is a novel inhibitor of myogenesis. Analysis of its function could therefore bring new information for a better understanding of the mechanisms underlying muscle differentiation.

In embryos over-expressing *Dmeso17A*, there is variability in the severity of the phenotype. This can be attributed to the fact that the level of GAL4-mediated transcription can vary from cell to cell (Brand et al., 1994). Variability has also been noted in previous studies analysing muscle pattern defects in mutant embryos (Drysdale et al., 1993; Lai et al., 1993). For example, mutants for *Zfh-1* display a variety of pattern errors and range of severity (Lai et al., 1993). Moreover, it is known that different levels of *Dmef2* can affect distinct aspects of muscle differentiation (Gunthorpe et al., 1999). Taken together, these results suggest that variations of *Dmeso17A* level can affect muscle development, but also that small variations in its level of expression can affect different muscles in different ways.

The somatic muscle phenotype of embryos over-expressing *Dmeso17A* can be characterised by specific criteria: shape; size; presence/absence; number, nuclei organisation. In my experiments, I used these criteria as a way of comparing muscle phenotypes and assessing genetic interactions. Furthermore, I have shown that the larval hatching and survival assay is a clear and quantitative measure of the effect produced by the over-expression. Together with the qualitative assessment mentioned above, this allowed me to deal with the variation of phenotype and was essential in assessing genetic interactions.



The formation of the muscle pattern is a multi-step process and can be divided into the specification of myoblasts, their fusion with FCMs and finally the differentiation of the muscle precursors (for review see Baylies et al., 1998; Ruiz-Gomez, 1998). It was therefore necessary to establish which step of muscle development is affected by the increase in *Dmeso17A* level. To do so, I examined the expression of specific markers in embryos over-expressing *Dmeso17A*. In these embryos, as revealed by Eve and Kr expression, muscle founders are specified and the first fusion events leading to the formation of muscle precursors are not affected. In the wild type, at the end of germ band shortening (stage 13), the location of these precursors containing two to three nuclei prefigures the future muscle pattern (Bate, 1990). At this stage in embryos over-expressing *Dmeso17A*, Eve and Kr-expressing precursors are in place and their relative position is identical to that seen in the wild type. Therefore, the effect of *Dmeso17A* over-expression takes place later during the myogenic program as muscle precursors increase in size by further fusions and acquire their characteristics (size, shape, point of attachment) (Bate, 1990). Indeed, analysis of later stages of embryogenesis showed that the pattern of Eve-expressing cells is then deranged. This was confirmed by defects in the DMef2 expression pattern from stage 14 onward as muscle precursors differentiate. Taken together, these data suggest that the inhibition of muscle development by *Dmeso17A* over-expression occurs during the differentiation of somatic muscle precursors.

In addition, I have shown that, in embryos over-expressing *Dmeso17A*, there is an increase in cell death from stage 14 onward. As muscle precursors are specified and properly located in these embryos, the dying cells are likely to be FCMs that do not fuse. However, I have observed that the apoptotic bodies are of different size. It is possible that this is because they contain one or more nuclei, which could mean that muscle



precursors that do not differentiate can undergo apoptosis, as well as FCMs can. Another indication that syncytial muscle precursors can die is that, at the end of embryogenesis, Kr expressing muscles such as LL1 are missing in a large proportion of the embryos even though their precursors were present earlier. Interestingly, cell death increase during the differentiation phase of muscle development has also been reported in *Dmef2* mutants (Ranganayakulu et al., 1995). In these mutants, somatic myoblast are specified normally, but they fail to differentiate (Lilly et al., 1995; Ranganayakulu et al., 1995). Taken together, these results confirm that, in embryos over-expressing *Dmeso17A*, muscle differentiation is affected, and they show that the cells that do not differentiate undergo apoptosis. This is consistent with the results of Abrams et al., who have shown that during normal development, the embryo has the ability to eliminate cells unable to complete their differentiation program (Abrams et al., 1993).

#### **4.3.2 *Dmeso17A* over-expression can affect the development of other mesodermal derivatives**

It was now clear that *Dmeso17A* can inhibit somatic muscle differentiation. However, the expression of *Dmeso17A* in the pericardial cells, the AMPs and the adepithelial cells suggests that it could play a role in these cells too. It was therefore important to test this hypothesis. It was also interesting to know what would be the effect of the expression of *Dmeso17A* on other mesodermally-derived tissues, such as the cardioblasts and the visceral muscles, in which it is not normally expressed. I therefore induced *Dmeso17A* expression using specific GAL4 drivers in each of these mesodermal derivatives. The analysis of the effect using specific markers revealed that *Dmeso17A* can affect their formation.

Pericardial cell development is disrupted by *Dmeso17A* over-expression. *Zfh-1*, *Eve* and *Odd* stainings revealed that, at stage 17, the organisation of pericardial cells is deranged suggesting that their differentiation is affected. Cell counting was used to assess this effect and it showed that in these embryos the number of *Zfh-1* and *Odd*-expressing cells increases compared to the wild type. The disruption of pericardial cells organisation can therefore be due to an increase in their number. This could be the result of extra divisions of the pericardial cells precursors or from changes in the fate of neighbouring cells (cardioblasts or dorsal muscles precursors). However, the number of *Eve*-expressing cells does not change. During wild type development, as *Eve* cells differentiate, they normally lose *Zfh-1* expression (Su et al., 1999). Thus, it is possible that in embryos over-expressing *Dmeso17A*, *Zfh-1* expression is retained in the differentiating *Eve* cells and that the increase in cell number observed is due to a change in the expression pattern of *Zfh-1* and *Odd*. It is apparent that further investigation is required to understand the effect of *Dmeso17A* over-expression and to determine its function in the pericardial cells. Moreover, there is evidence that these cells continue their differentiation during larval and pupal life (Curtis et al., 1999; personal communication from A. Paululat). It is therefore possible that it will be necessary to analyse pericardial cell differentiation during larval and pupal stages too in order to assess any effect of *Dmeso17A*. My preliminary observations are consistent with this possibility.

AMPs, at the end of germ band retraction, appear as single *Twist*-expressing cells at specific positions within each abdominal segment (Bate et al., 1991). In embryos over-expressing *Dmeso17A*, some of these *Twist*-expressing cells appear as doublets at this stage. These extra cells are located internally compared to the AMPs. As AMPs are more external than the somatic muscles (Bate et al., 1991), one might speculate that

these extra Twist-expressing cells are founders that did not differentiate and have retained Twist expression. It is also possible that they result from the division of the AMPs. The nature and origin of these extra cells remains to be determined, but one possibility is that *Dmeso17A* could act to keep cells in an undifferentiated state.

AMPs normally proliferate and differentiate during larval life to produce the abdominal adult muscles (Bate, 1991; Bate, 1993). However, little is known about the mechanism that holds them in an undifferentiated state during embryogenesis. Given my results, one can imagine that *Dmeso17A* acts to prevent the AMPs from differentiating. *Drosophila* AMPs can be compared to vertebrate satellite cells, which remain undifferentiated and can participate to muscle growth and regeneration (reviewed in Seale and Rudnicki, 2000; Taylor, 2005). Therefore, if *Dmeso17A* functions to keep AMPs undifferentiated, analysis of its mechanism of action in these cells could be of great interest.

*Dmeso17A* is also expressed in the adepithelial cells that give rise to the adult thoracic muscles. Over-expression of *Dmeso17A* in these cells leads to a reduction of the number of these muscles. This suggests that the inhibitory role of *Dmeso17A* is not limited to embryogenesis, but it is also implicated in adult muscle formation. Adult muscles in *Drosophila*, like the larval somatic muscles, are in many respects similar to vertebrate skeletal muscles. Yet, *Drosophila* adult muscles and skeletal muscles are more comparable. For example, in contrast to the larval somatic muscles, the adult muscle precursors migrate to the muscle forming region and differentiated adult muscles can be constituted of multiple fibres like in vertebrates (reviewed in Taylor, 2005; see Chapter 1 section 1.4.4). The analysis of *Dmeso17A* function and mechanism of action in adult muscle formation could therefore be relevant to skeletal muscle development.

Finally, expression of *Dmeso17A* in visceral muscle and cardioblasts disrupts their development. This is consistent with what happens in somatic muscles and suggests that a *Dmeso17A* target(s) is also present in these tissues. One common factor between the three muscle types is *Dmef2*, the key promoter of muscle differentiation (Lilly et al., 1994; Taylor et al., 1995). The effect of *Dmeso17A* over-expression in the cardioblasts resembles the phenotype observed in *Dmef2* mutant (Ranganayakulu et al., 1995; Damm et al., 1998). In these mutants, like in embryos over-expressing *Dmeso17A*, cardioblasts express  $\beta$ 3-tubulin, but Myosin expression is disrupted. This suggests that there is a relationship between *Dmeso17A* and *Dmef2*, and maybe that in the cardioblast *Dmef2* is a *Dmeso17A* target. Moreover, *Dmeso17A* over-expression can affect all three muscle types (somatic, visceral and heart), and *Dmef2* is required for the differentiation of all these muscles (Bour et al., 1995; Lilly et al., 1995; Ranganayakulu et al., 1995, Gunthorpe et al., 1999). One can therefore imagine that the relationship between *Dmeso17A* and *Dmef2* can be extended to the somatic and visceral muscles. I have explored the link between *Dmeso17A* and *Dmef2* in the somatic muscles. This will be described in Chapter 6.

### 4.3.3 Conclusion

Taken together, my results show that *Dmeso17A* is an inhibitor of muscle differentiation. As discussed above, there are indications of a relationship with the key promoter of muscle differentiation, *Dmef2*. My data also suggest that *Dmeso17A* could affect the adult muscle precursors maybe keeping them in an undifferentiated state. Consistent with this, I have shown that *Dmeso17A* over-expression can affect the development of adult muscles.

As mentioned at the beginning of this section, a detailed understanding of muscle differentiation requires the identification and *in vivo* analysis of negative regulators. My results show that *Dmeso17A* is one such molecule. Its analysis could provide new insights on how muscle cell differentiation is controlled *in vivo*.

## CHAPTER 5: *Dmeso17A* Loss-of-Function

### 5.1 Introduction

To achieve *Dmeso17A* loss-of-function, I chose to use RNA interference (RNAi) from a splice-activated UAS hairpin vector (Reichhart et al, 2002). This method has at least two advantages compared to dsRNA injection. First, the transgene is stably inherited and second, with the use of the GAL4/UAS system, it allows cell, tissue and/or stage specific knock down of the gene of interest. Injection of dsRNA interferes with gene expression only transiently and is not stably inherited (Kennerdell and Carthew, 1998; Kennerdell and Carthew, 2000; Yang et al., 2000). Moreover, it can induce mosaic effects (Kennerdell and Carthew, 1998).

In addition to the RNAi approach, I have used a UAS line previously made in the laboratory that carries a form of *Dmeso17A* lacking the WRPW motif. The reason for using this truncated form of *Dmeso17A* is based on the assumption that the WRPW motif has a functional importance for *Dmeso17A* and that *Dmeso17A* interacts with proteins other than Gro and/or with DNA. Over-expression of a transgene of this truncated form of *Dmeso17A* will then have a dominant negative effect on the endogenous protein, and therefore it will provide a mechanistically distinct way of knocking down *Dmeso17A* function.

## **5.2 *Dmeso17A* loss-of-function results in aberrant muscle differentiation**

Analysis of a loss-of-function is crucial to the analysis of gene function and was necessary for my analysis of *Dmeso17A*. I used RNAi and dominant negative approaches to knock down *Dmeso17A* function. I used similar assays for my analysis of the *Dmeso17A* loss-of-function phenotype to those adopted for the gain-of-function. I tested the specificity of the effects of *Dmeso17A-RNAi* and *Dmeso17A-ΔWRPW* by determining whether they suppressed the inhibitory effect of *Dmeso17A* gain-of-function on muscle differentiation. In the next sections, I will present the results I obtained. All *UAS-Dmeso17A-RNAi* and *UAS-Dmeso17A-DWRPW* lines tested are listed in Appendix 1.

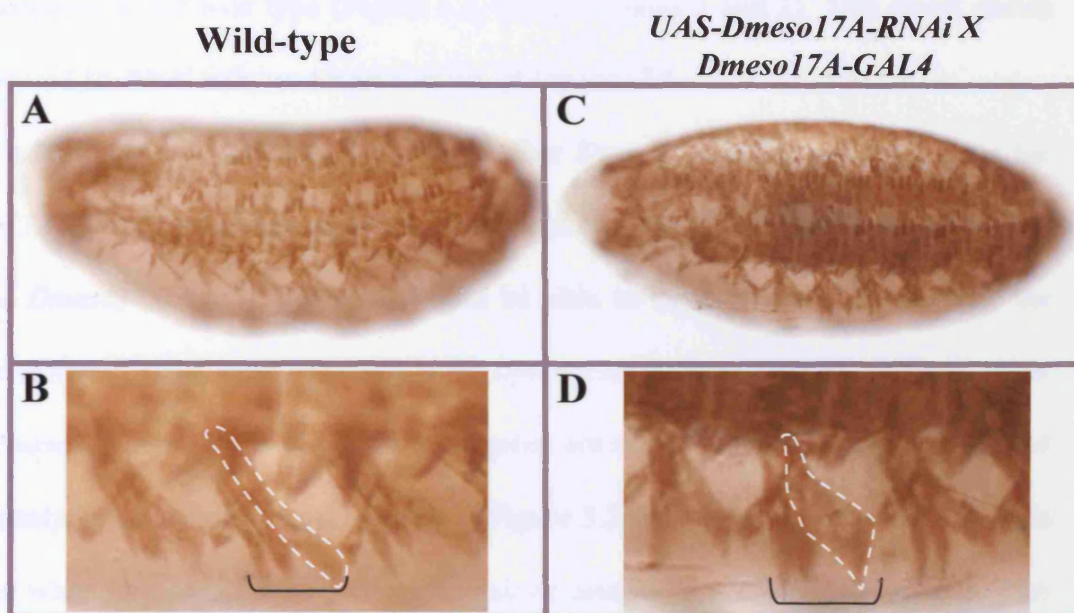
### **5.2.1 The RNAi approach**

#### **5.2.1.1 The *Dmeso17A-RNAi* phenotype**

As for gain-of-function, several GAL4 drivers were used to express *Dmeso17A-RNAi* in the somatic mesoderm. Although the phenotypes obtained with the different GAL4 drivers were comparable, stronger effects were obtained using *Dmeso17A-GAL4* at 25°C.

In embryos expressing *Dmeso17A-RNAi* using *Dmeso17A-GAL4*, the overall muscle pattern looks normal (Figure 5.1, compare A with C). However, a close observation revealed that although muscles are able to form, several of their characteristics are altered. Their morphology (shape and/or size), the organisation of their nuclei, their attachment and even their number can be affected. For example, in a large proportion of the embryos, the shape of the ventral oblique (VO) muscles is deranged (Figure 5.1, compare B with D, VO4 is outlined). This result suggests that in





**Figure 5.1: *Dmeso17A*-RNAi disrupts muscle development.**

*Dmeso17A-RNAi* was expressed using *Dmeso17A-GAL4* at 25°C. Stage 17 embryos were stained with an anti-muscle Myosin and compared to wild-type. (A-B) Wild-type embryo showing the normal muscle pattern (A) and correctly shaped VO muscles (brackets in B). (C-D) In embryos expressing *Dmeso17A-RNAi*, the overall muscle pattern is essentially normal (C). However, aspects of muscle development are affected. For example, VO muscles can be misshapen (brackets in D) compared to wild type (B).

*Dmeso17A-RNAi*-expressing embryos, muscles are specified and can develop, but the acquisition of specific characteristics of differentiated muscle is impaired.

However, before undertaking a detailed analysis of the phenotype, it was necessary to assess the efficiency of *Dmeso17A-RNAi*. I therefore tested whether its expression could induce *Dmeso17A* mRNA degradation. Semi-quantitative RT-PCR revealed that in embryos expressing *Dmeso17A-RNAi*, the level of *Dmeso17A* mRNA is reduced by half compared to the wild type (Figure 5.2, compare lanes 1 and 2). This result shows that *Dmeso17A-RNAi* induces a knock down of *Dmeso17A*.

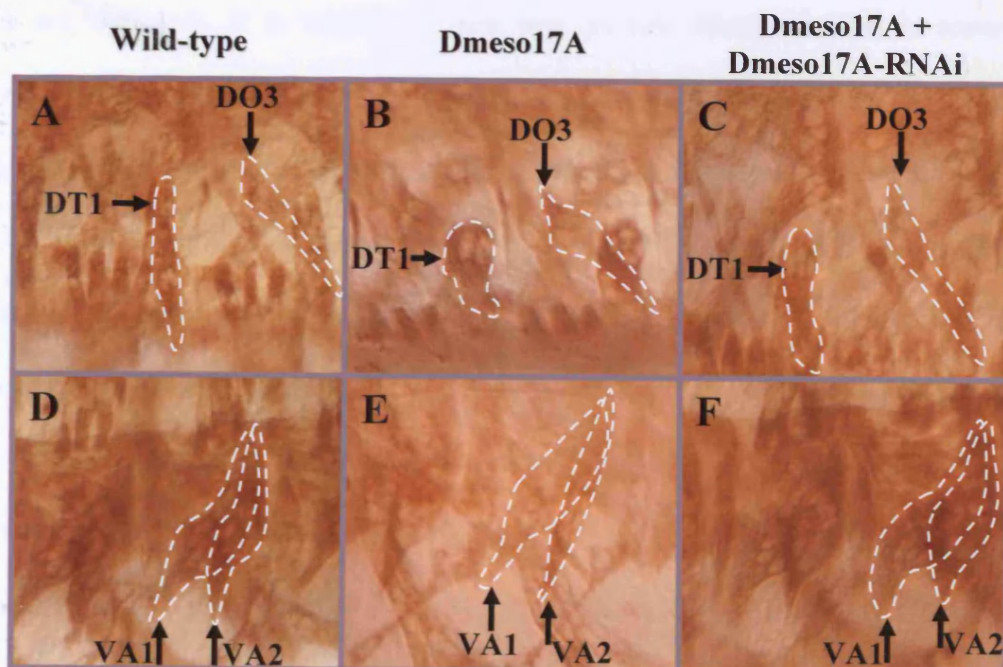
In addition to the RT-PCR, I tested whether *Dmeso17A-RNAi* could suppress the *Dmeso17A* over-expression phenotype. The prediction was that, as *Dmeso17A-RNAi* induces *Dmeso17A* knock down, it should be able to suppress, at least partially the muscle differentiation inhibitory effect of *Dmeso17A* over-expression. Indeed, when both *Dmeso17A* and *Dmeso17A-RNAi* transgenes are expressed using *Dmeso17A-GAL4*, the phenotype is rescued towards wild type. Figure 5.3 shows the rescue of four muscles affected when *Dmeso17A* is over-expressed alone using *Dmeso17A-GAL4*. In more than 50% of the embryos over-expressing *Dmeso17A*, muscles DT1 and DO3 appear misshapen compared to the wild type (Figure 5.3, arrows, compare A with B). When both transgenes are expressed, these muscles appear wild type (Figure 5.3, arrows, compare A, B and C). Other muscles are misshapen in a large (>40%) proportion of embryos over-expressing *Dmeso17A*. These include VA1 and VA2 which appear elongated (Figure 5.3, arrows, compare D with E). The expression of *Dmeso17A-RNAi* together with *Dmeso17A* rescues these muscles (Figure 5.3, arrows, compare D, E and F).

**Figure 5.2: *Dmeso17A-RNAi* reduces the level of *Dmeso17A* RNA.**

Semi-quantitative RT-PCR was carried out to assess the efficiency of *Dmeso17A-RNAi*. The level of *Dmeso17A* RNA in embryos expressing *Dmeso17A-RNAi* using *Dmeso17A-GAL4* at 25°C (Lane 2) is reduced by half compared to wild-type (Lane 1). *rp49* was used as a control. Quantification of the bands was performed using the Gene tool software (Syngene).

**Figure 5.3: *Dmeso17A-RNAi* can suppress the effects of *Dmeso17A* over-expression.**

*Dmeso17A* was over-expressed either alone or together with *Dmeso17A-RNAi* using *Dmeso17A-GAL4* at 25°C. Stage 17 embryos were stained with an anti-muscle Myosin antibody and the muscle phenotypes were analysed and compared to wild-type. The muscles described are outlined and labelled in each picture. (A-C) Rescue of muscles DT1 and DO3 by *Dmeso17A-RNAi*. (A) Wild-type DT1 and DO3. (B) In embryos over-expressing *Dmeso17A*, these two muscles are clearly misshapen. (C) Expression of *Dmeso17A-RNAi* can suppress the effect of *Dmeso17A* and rescues DT1 and DO3 towards wild-type. (D-F) Rescue of muscles VA1 and VA2. (D) In the wild-type, VA1 and VA2 have a very characteristic kinked shape. (E) Over-expression of *Dmeso17A* disrupts the shape of these muscles. They now are straighter and elongated. (F) In embryos expressing both *Dmeso17A* and *Dmeso17A-RNAi*, VA1 and VA2 are rescued towards wild-type.



Taken together, these results show that *Dmeso17A-RNAi* can induce a partial loss-of-function and that this reduction of *Dmeso17A* level of activity is sufficient to alter muscle differentiation.

As shown in Figure 5.4, in depth analysis of the *Dmeso17A-RNAi* phenotype adds some details to these observations:

- In more than 50% of the embryos, there were defects of the shape of muscles. For example, the LT muscles are frequently affected and in particular LT4 (Figure 5.4, dotted outline, compare A with B). VO muscles are also often misshapen (Figure 5.1D, VO4 is outlined). Muscles such as DA1, DA3, DO4-5 or VA1-2 are misshapen only in a few embryos.
- The same proportion of embryos (>50%) have defects in the organisation of the nuclei within muscles. This effect was observed for all the muscles, but it is most frequent in the dorsal muscles (DO1-2, DA1-3) and the ventral muscles (VO4-6, VA1-3). Figure 5.4D shows nuclear disorganisation in muscle VO4 (compare C with D, nuclei are outlined). It is worthy of note that nuclear disorganisation is sometimes observed in muscles that are normal in appearance.
- In 30% of the embryos, the size of some muscles is increased compared to the wild type. I found this for muscles such as DO4 (Figure 5.4, compare E with F, DO4 is outlined), DA3, and VO4. Occasionally, DO1-2, DA1-2 and VA1-2 also appear bigger.
- In a smaller proportion of embryos (20%), some muscles are attached incorrectly. In most of these cases, DA3 is incorrectly attached (Figure 5.4, arrowheads, compare G with H), but DA1 or DO1 can also be affected.
- Finally, about 10% of the embryos have duplications of muscles. In all the embryos I analysed, I only observed this effect for VA3 (Figure 5.4, arrowheads, compare I with J) and DO1-2.

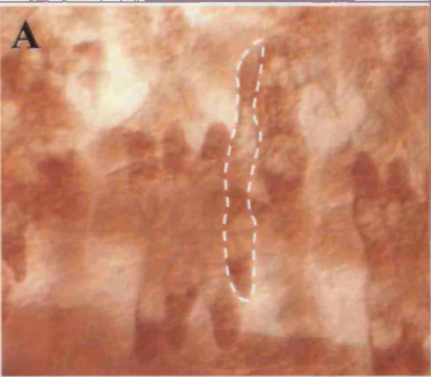
**Figure 5.4: *Dmeso17A* loss-of-function results in aberrant muscle differentiation.**

The muscle phenotype of stage 17 embryos expressing *Dmeso17A-RNAi* using *Dmeso17A-GAL4* at 25°C (**B, D, F, H, J**) was analysed in detail and compared to wild-type (**A, C, E, G, I**). Anti-Myosin staining revealed defects in muscle shape (**A-B**), in the distribution of nuclei within a muscle (**C-D**), in muscle size (**E-F**), attachment (**G-H**) and number (**I-J**). (**A-B**) In embryos expressing *Dmeso17A-RNAi* (**B**) the shape of muscles such as LT4 (dotted outlines in **A** and **B**) can be altered compared to wild-type (**A**). (**C-D**) The organisation of the nuclei within muscles such as VO4 is often deranged when *Dmeso17A-RNAi* is expressed (compare **C** and **D**; nuclei in VO4 are outlined). (**E-F**) *Dmeso17A-RNAi* expression can also result in an increase in muscle size. For example, DO4 (dotted outlines in **E** and **F**) appear bigger than in wild-type. (**G-H**) Muscles such as DA3 can be incorrectly attached in *Dmeso17A-RNAi* expressing embryos. Arrowheads show the attachment points of DA3 in the wild-type (**G**) and in *Dmeso17A-RNAi* expressing embryos (**H**). (**I-J**) In a small proportion of embryos expressing *Dmeso17A-RNAi*, there is duplication of muscles such as VA3 (arrowheads in **J** and **I**).

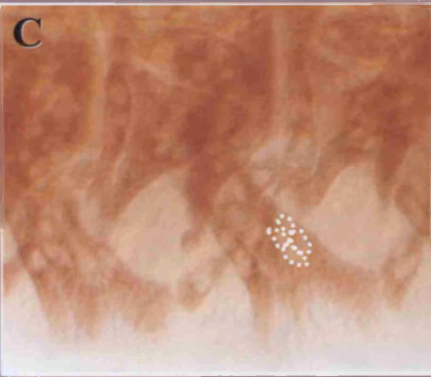
Wild-type

*UAS-Dmeso17A-RNAi X*  
*Dmeso17A-GAL4*

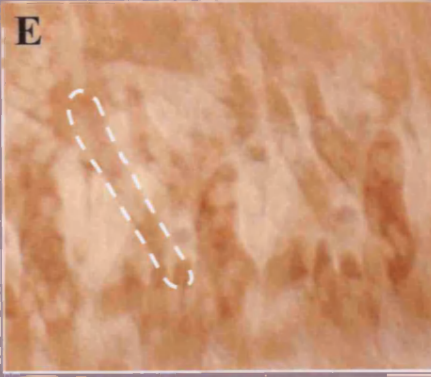
Shape



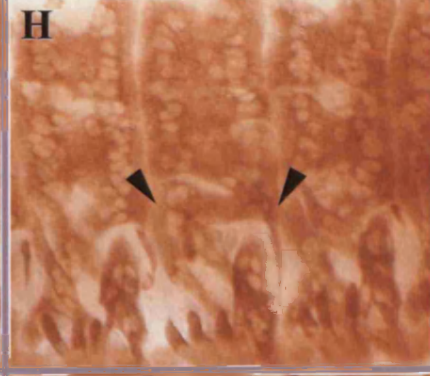
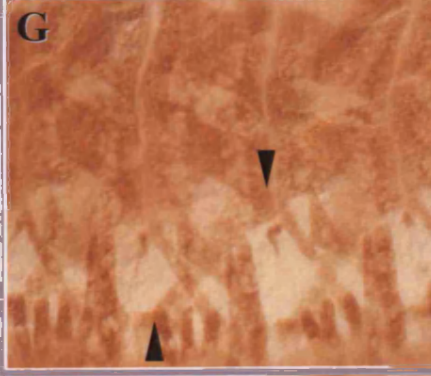
Nuclei  
organisation



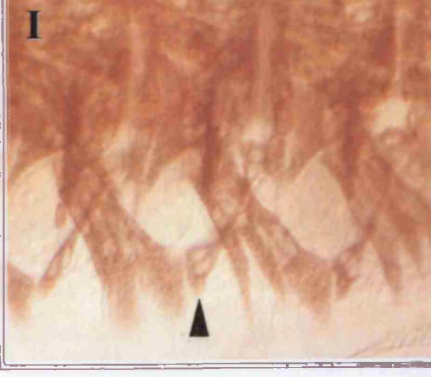
Size



Attachment



Number



Taken together, these results show that expression of *Dmeso17A-RNAi* can affect muscle differentiation. The range of effects observed suggests that *Dmeso17A* is not implicated only in one particular aspect of muscle differentiation, but rather is involved in a more general way in the regulation of the process.

### **5.2.1.2 The effect of *Dmeso17A-RNAi* occurs during muscle differentiation**

As described earlier, I have shown that *Dmeso17A* over-expression disrupts myogenesis during the differentiation phase. Given the *Dmeso17A-RNAi* phenotype and given that *Dmeso17A RNAi* induces knock down of *Dmeso17A* function, it was likely that only the differentiation phase was affected in embryos over-expressing *Dmeso17A-RNAi*. Yet, this needed to be confirmed. I therefore tested which step of myogenesis was affected using the same assays as described for *Dmeso17A* gain-of-function.

In embryos expressing *Dmeso17A-RNAi* using *Dmeso17A-GAL4*, the number and position of Kr and Eve-expressing founders is unchanged compared to wild type (Figure 5.5, compare A with B and C with D). This suggests that the first steps of the myogenic program are not affected. Moreover, in these embryos, defects in DMef2 expression are only detected during the muscle differentiation phase (Figure 5.6). At stage 13, DMef2 expression in embryos expressing *Dmeso17A-RNAi* is identical to that of the wild type (Figure 5.6, compare A with B). Later, as revealed by MHC/DMef2 double staining, defects such as disorganisation of DMef2-expressing nuclei within a muscle can be observed (Figure 5.6C-F). These results suggest that *Dmeso17A* knock down does not affect the early stages of muscle development, but rather affects muscle differentiation. This is consistent with my results on *Dmeso17A* over-expression.

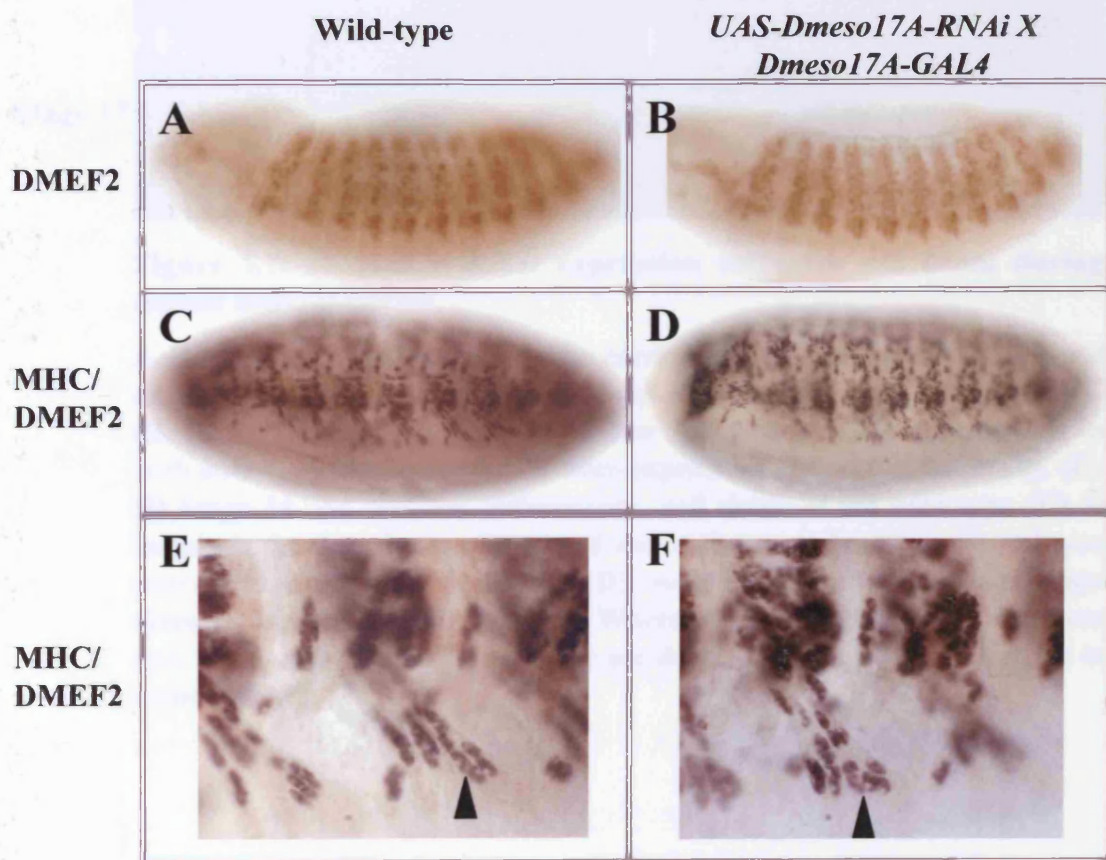
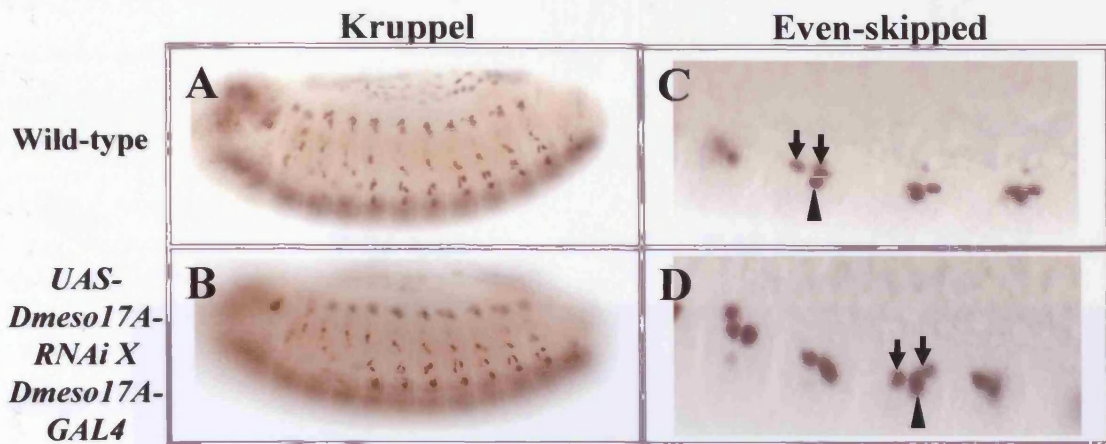


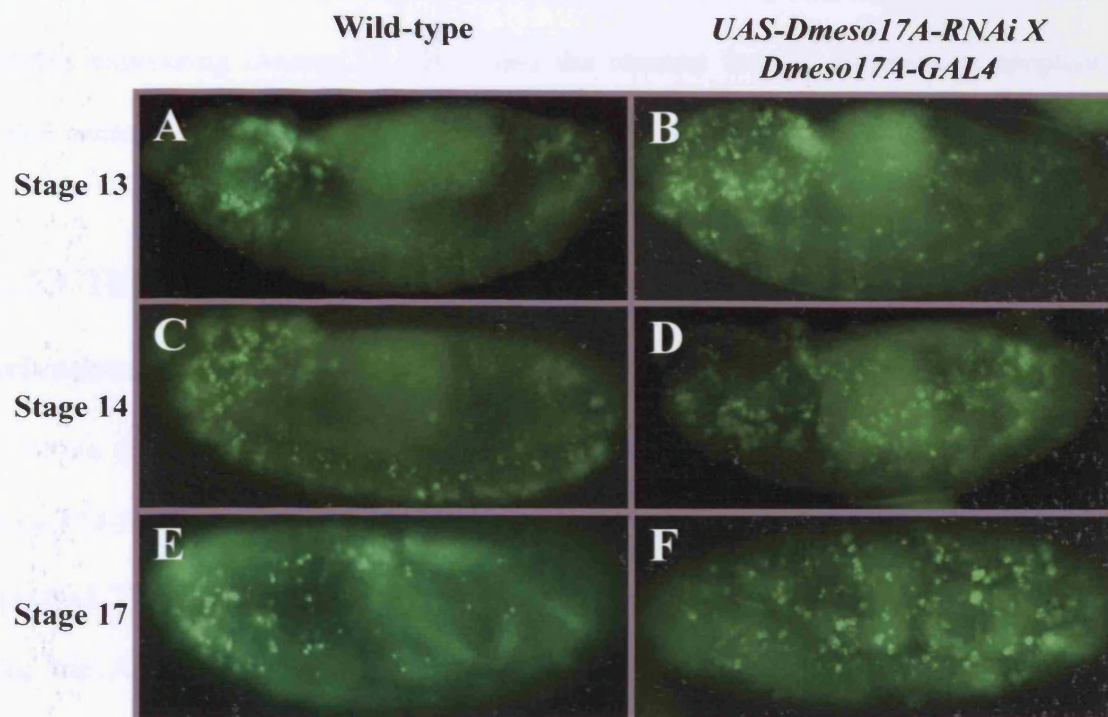
**Figure 5.5: *Dmeso17A-RNAi* expression does not affect the early steps of muscle development.**

Wild-type and embryos over-expressing *Dmeso17A-RNAi* using *Dmeso17A-GAL4* at 25°C were stained with anti-Krüppel (A-B) or anti-Eve (C-D) antibodies. (A-B) Stage 14. The number and position of Kr expressing cells is identical in the wild-type (A) and in embryos over-expressing *Dmeso17A-RNAi* (B). (C-D) Stage 12. Wild-type Eve expression pattern (C) in the DA1 founder (arrowheads) and in two PCs founders (arrows) is unchanged in embryos over-expressing *Dmeso17A-RNAi* (D).

**Figure 5.6: The effect of *Dmeso17A-RNAi* occurs during muscle differentiation.**

Wild-type and embryos over-expressing *Dmeso17A-RNAi* using *Dmeso17A-GAL4* at 25°C were either stained with an anti-DMef2 antibody (A-B) or double stained with anti-Myosin and anti-DMef2 antibodies (C-F). (A-B) Stage 13. DMef2 expression is comparable in the wild-type (A) and in embryos over-expressing *Dmeso17A-RNAi* (B). (C-F) Stage 17. The overall DMef2 expression pattern looks essentially normal in embryos expressing *Dmeso17A-RNAi* (compare C and D). However, there are defects such as the disorganisation of DMef2-expressing nuclei in the VO4 muscle (arrowheads in E and F).





**Figure 5.7: *Dmeso17A-RNAi* expression increases cell death during muscle differentiation.**

Acridine orange (AO) staining was carried out on wild-type (A, C, E) and embryos over-expressing *Dmeso17A-RNAi* using *Dmeso17A-GAL4* at 25°C (B, D, F). (A-B) Stage 13. Only a few AO positive cells are detected in both wild-type (A) and embryos over-expressing *Dmeso17A-RNAi* (B). (C-D) Stage 14. As muscles differentiate, cell death in the wild type (C) is largely in the dorsal part of the head and in the ventral midline. In embryos over-expressing *Dmeso17A-RNAi* (D), some additional apoptotic cells are detected laterally. (E-F) Stage 16. Whereas in the wild-type (E) there are only a few AO positive cells, more are detected when *Dmeso17A-RNAi* is expressed (F).

Although no muscles were missing in embryos expressing *Dmeso17A-RNAi*, acridine orange staining revealed an increase in apoptosis as muscle differentiate. Figure 5.7 shows increased cell death in these embryos at stage 14 and 16. One possibility for this result is that some FCMs do not fuse and undergo apoptosis. However, I have not found a significant reduction in the number of muscle nuclei in embryos expressing *Dmeso17A RNAi*, and the reasons for this increase in apoptosis remain unclear.

### **5.2.1.3 The effect of *Dmeso17A-RNAi* expression on other mesodermal derivatives**

Given the mechanism of RNAi (reviewed in Agrawal et al., 2003) and my results, *Dmeso17A-RNAi* can only be effective in the cells where *Dmeso17A* is normally expressed. Therefore, expressing *Dmeso17A-RNAi* might have an effect on pericardial cells, the AMPs and the adepithelial cells, but no effect on visceral muscle and cardioblasts development should be expected. I tested the effect of *Dmeso17A-RNAi* expression on the development of these tissues or cells. The strategy was identical to that adopted for the gain-of-function analysis.

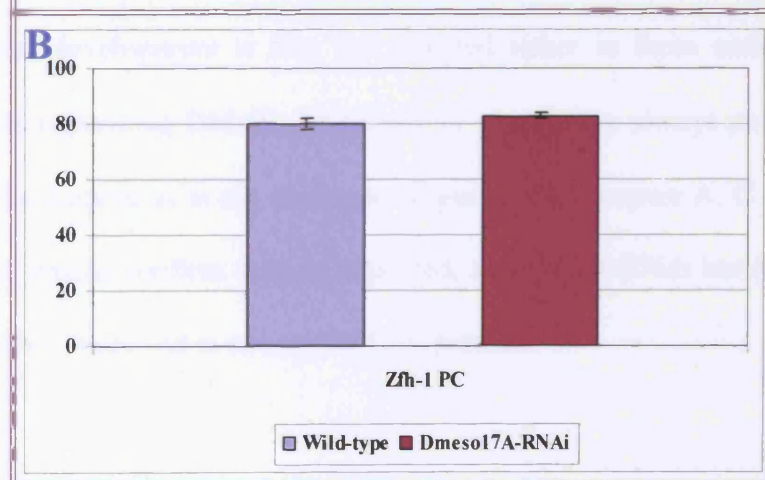
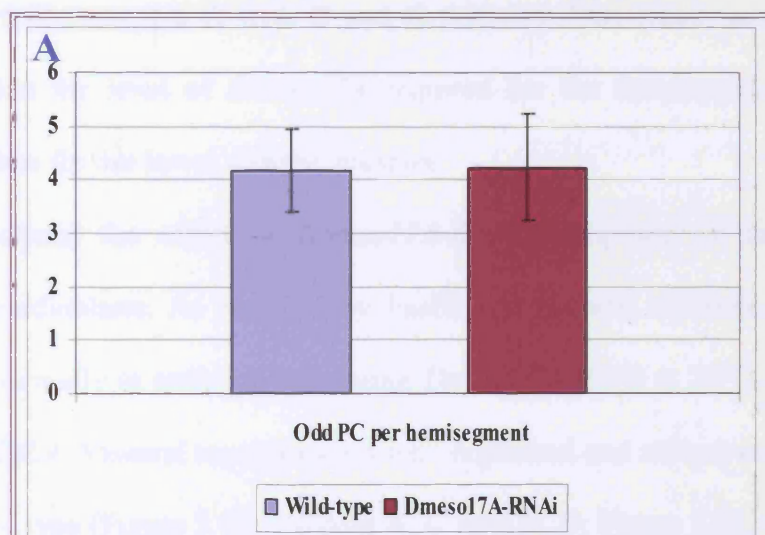
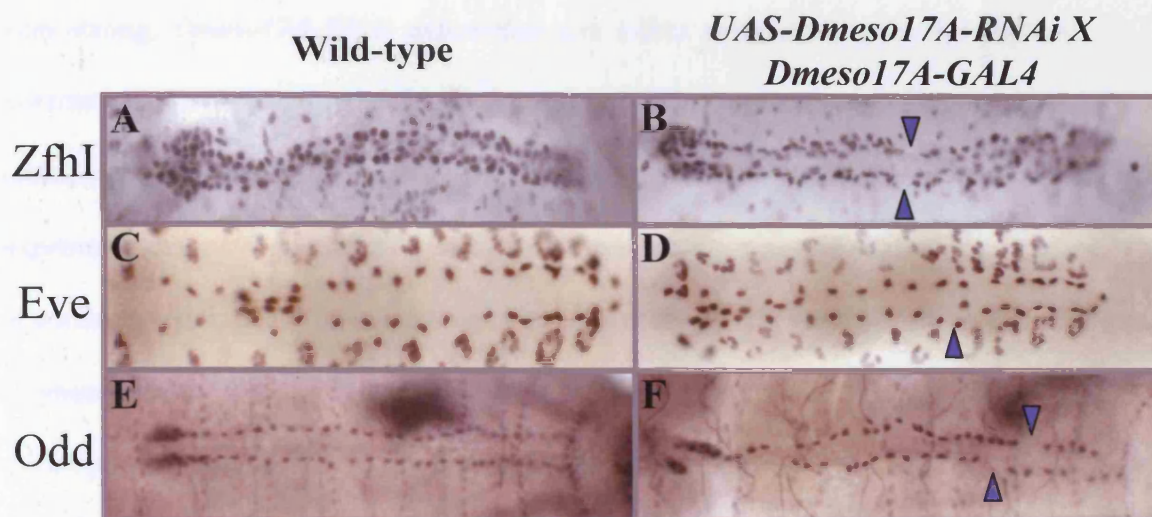
I first tested the effect of *Dmeso17A-RNAi* on the cells where *Dmeso17A* expression is detected, i.e. the pericardial cells, the AMPs and the adepithelial cells. In embryos expressing *Dmeso17A-RNAi* using *Dmeso17A-GAL4* at 25°C, cell counting did not reveal any significant difference in the number of Odd-expressing cells, at stage 14, and *Zfh-1*-expressing cells, at stage 17, when compared to the wild type (Figure 5.9A and B). This was confirmed by a paired t-test (see legend of Figure 5.9). Nevertheless, pericardial cells organisation is somewhat deranged and occasionally there are gaps in markers expression (*Zfh-1*, *Eve* and *Odd*) (Figure 5.8 arrowheads,

**Figure 5.8: *Dmeso17A-RNAi* expression affects pericardial cells development.**

Stage 17 embryos, wild-type or expressing *Dmeso17A-RNAi* using *Dmeso17A-GAL4* at 25°C, were stained with anti-Zfh-1 (A-B), anti-Eve (C-D) or anti-Odd (E-F) antibodies. (A-B) Compared to wild-type (A), the pattern of Zfh-1-expressing PCs in embryos expressing *Dmeso17A-RNAi* is disrupted (B). Gaps are occasionally observed (arrowheads). (C-D) Compared to wild-type (C), the pattern of Eve-expressing PCs can also be disrupted when *Dmeso17A-RNAi* is expressed (arrowhead in D). (E-F) whereas in the wild-type (E) Odd PCs are well organised in two rows, in embryos over-expressing *Dmeso17A-RNAi* (F) there are gaps (arrowhead) and defects in their general organisation.

**Figure 5.9: *Dmeso17A-RNAi* expression does not affect pericardial cells number.**

(A) The number of Odd-expressing cells per hemisegment was scored in both wild type and embryos over-expressing *Dmeso17A-RNAi* at stage 14. 144 hemisegments were analysed in each case. There was an average of 4.18 and 4.22 cells per hemisegment in the wild-type and in embryos over-expressing *Dmeso17A-RNAi* respectively. A paired t-test showed that there is no significant difference between these numbers. The p value = 0.37 with a 95% confidence interval. (B) The number of Zfh-1-expressing cells was also scored in both wild type and embryos over-expressing *Dmeso17A-RNAi* at stage 17. Twenty embryos were analysed in each case. 80 and 83 cells on average were found in the wild-type and in embryos over-expressing *Dmeso17A-RNAi* respectively. A paired t-test was carried out to test the significance of this difference. The p value obtained (p= 0.054) with a 95% confidence interval shows that the difference in Zfh-1-expressing PCs number between the wild-type and in embryos over-expressing *Dmeso17A* is not significant. Error bars indicate standard deviation.



compare A, C and E with B, D and F). This suggests that even though the effect is not very strong, *Dmeso17A-RNAi* expression can affect pericardial cells development. In contrast, as shown in Figure 5.10, Twist staining did not reveal any effect on the AMPs (compare A-B with C-D). These results taken together suggest that *Dmeso17A-RNAi* expression can have an effect in cells, other than somatic myoblasts, where *Dmeso17A* is normally expressed. The weakness of the effect on the pericardial cells or the absence of phenotype for the AMPs suggests that the level of *Dmeso17A* required for the proper development of these cells is lower than in somatic muscles.

I then assessed the development of IFMs in flies expressing *Dmeso17A-RNAi* using the *1151-GAL4* driver at 25°C. In these flies both the DLMs and the DVMs are formed correctly (Figure 5.11, compare A with B and C with D). This result, as mentioned above, suggests that the level of *Dmeso17A* required for the development of these muscles is lower than for the larval somatic muscles.

Finally, I analysed the effect of *Dmeso17A-RNAi* expression on the visceral muscles and the cardioblasts. As revealed by FasIII and Myosin expression, visceral muscles develop normally in embryos expressing *Dmeso17A-RNAi* at 25°C using *bap-GAL4* or *Dmef2-GAL4*. Visceral myoblasts are well organised and midgut constrictions occur as in the wild type (Figure 5.12, compare A, C with B, D; Figure 5.13, compare A with B). Cardioblast development is also not affected either in these embryos. Two rows of cardioblasts expressing DMef2,  $\beta$ 3-tubulin or myosin are always present in the dorsal midline of the embryo as in the wild type (Figure 5.14, compare A, C and E with B, D and F). These results confirm that, as expected, *Dmeso17A-RNAi* has no effect in tissues or cells where *Dmeso17A* is not normally expressed.

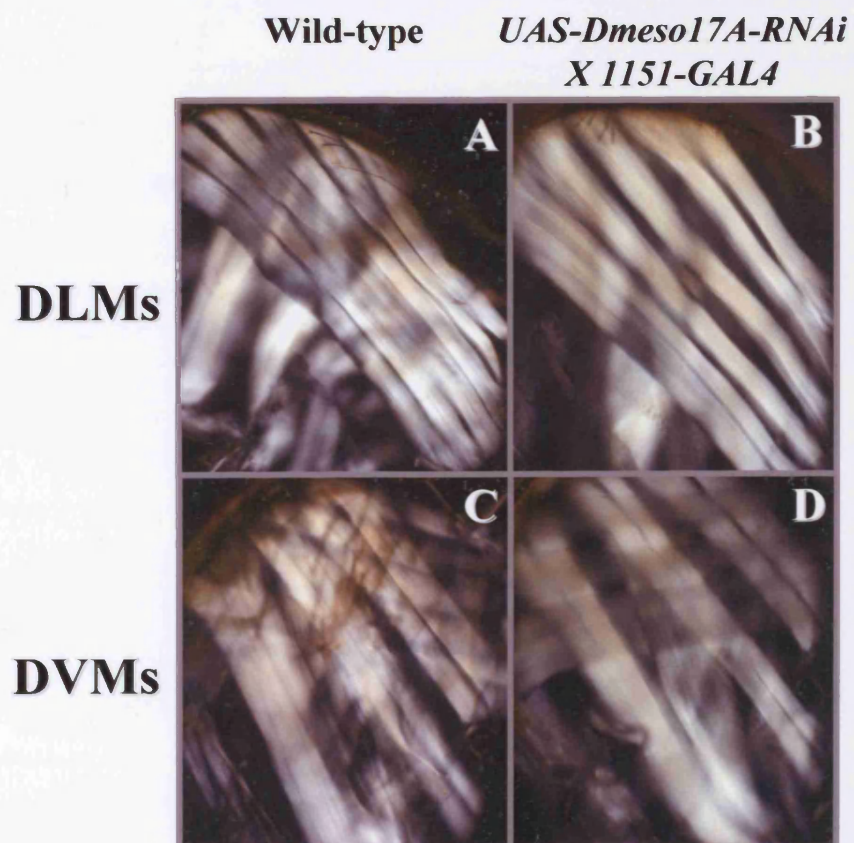
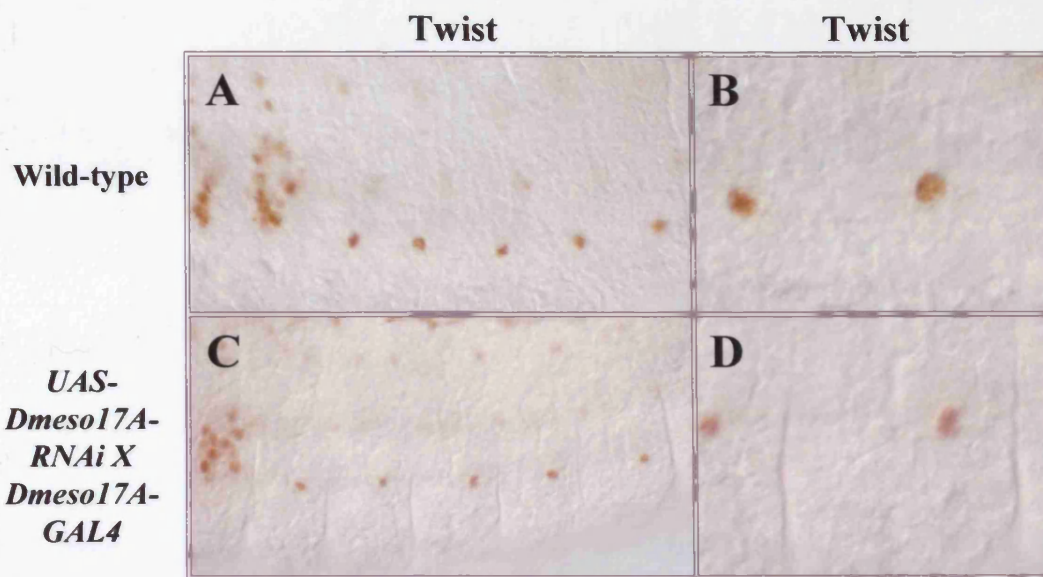
**Figure 5.10: *Dmeso17A-RNAi* expression does not affect the number of persistent Twist-expressing cells.**

Stage 14 embryos were stained with an anti-Twist antibody. Twist expression in the AMPs is identical in the wild-type (A-B) and in embryos expressing *Dmeso17A-RNAi* using *Dmeso17A-GAL4* at 25°C (C-D).

**Figure 5.11: *Dmeso17A-RNAi* expression does not affect the development of IFMs.**

IFMs were visualised under polarised light (see chapter 2, section 2.4.8). DLMs and DVMs appear identical in both the wild-type (A, C) and Embryos expressing *Dmeso17A-RNAi* using the *1151-GAL4* driver at 25°C (B, D).





**Figure 5.12: *Dmeso17A-RNAi* expression does not affect visceral mesoderm development.**

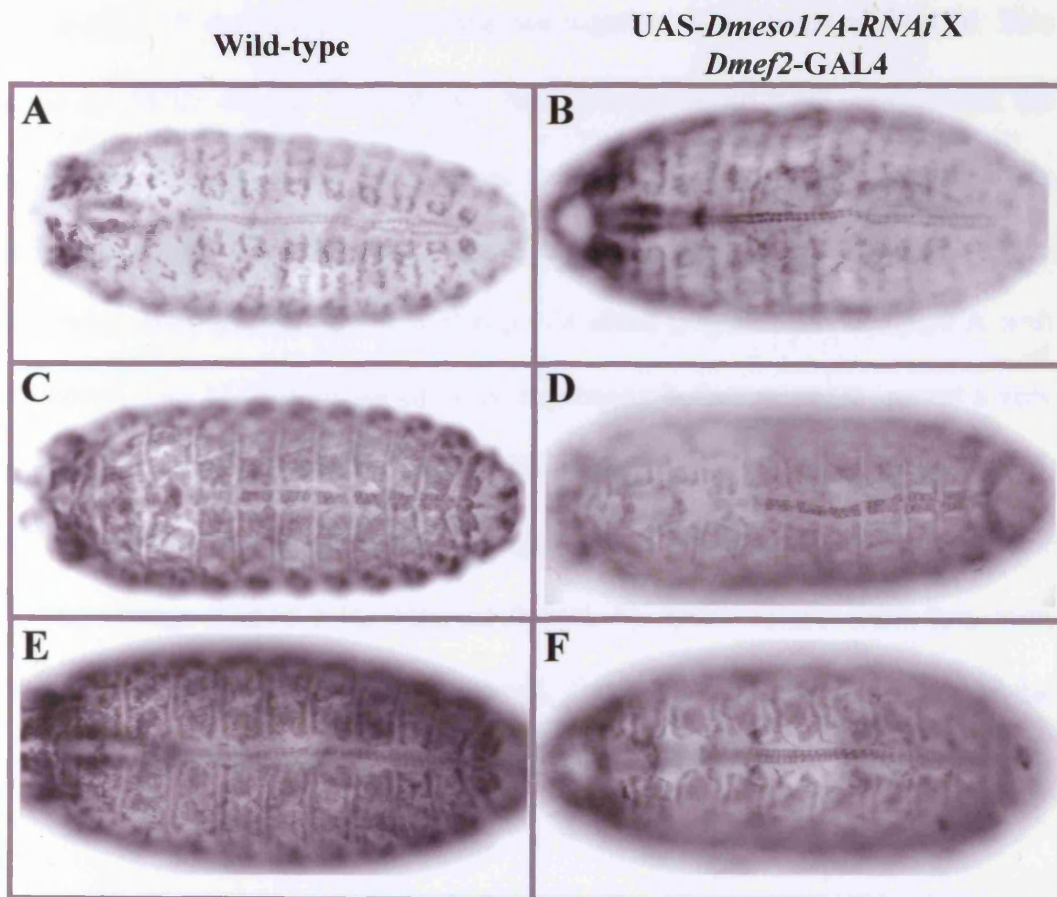
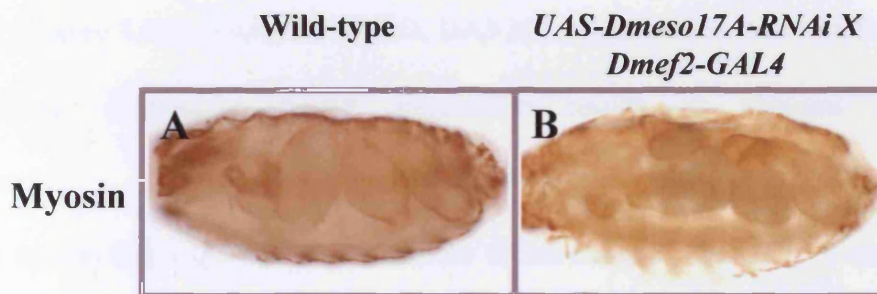
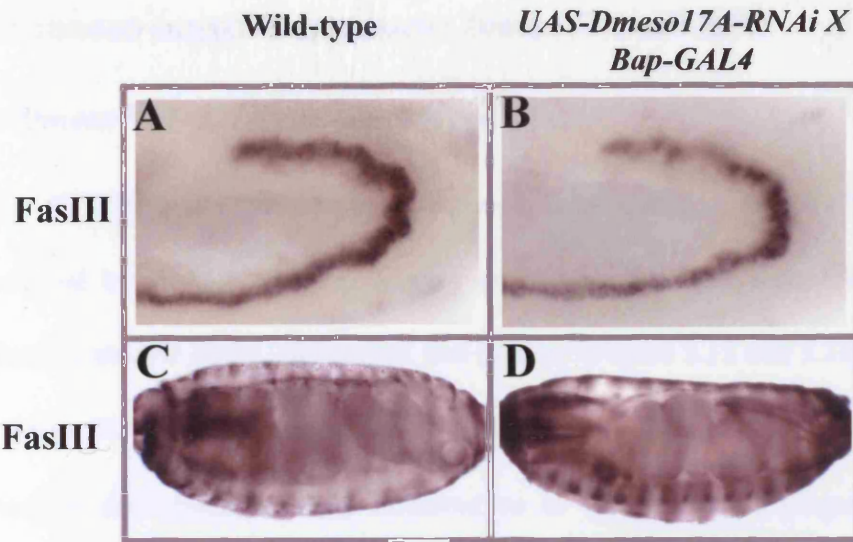
Wild-type (A, C) and embryos over-expressing *Dmeso17A-RNAi* using the *bap-GAL4* driver at 25°C (B, D), were stained with an anti-FasIII antibody. Expression of *Dmeso17A-RNAi* using *bap-GAL4* affects neither the organisation of the circular visceral muscle progenitors nor the midgut constrictions (compare A with B, and C with D).

**Figure 5.13: *Dmeso17A-RNAi* expression does not affect visceral muscle development.**

Stage 17 embryos were stained with an anti-Myosin antibody. In embryos over-expressing *Dmeso17A-RNAi* using the *Dmef2-GAL4* driver at 25°C (B), midgut constrictions occur as in the wild-type (A).

**Figure 5.14: *Dmeso17A-RNAi* expression does not affect cardioblast differentiation.**

Stage 17 embryos were stained with anti-DMef2 (A-B), anti- $\beta$ 3-tubulin (C-D) or anti-Myosin (E-F) antibodies. Expression of these three markers in the cardioblasts of embryos expressing *Dmeso17A-RNAi* using *Dmef2-GAL4* at 25°C (B, D, F) is comparable to that of the wild-type (A, C, E).



## 5.2.2 The dominant-negative approach: *Dmeso17A-ΔWRPW*

### 5.2.2.1 The *Dmeso17A-ΔWRPW* phenotype

*Dmeso17A-ΔWRPW* was expressed using the *twist/twist-GAL4* driver at 25°C. The phenotype revealed by myosin staining is very similar to that of *Dmeso17A-RNAi*. There are defects in muscle shape, attachment and number (Figure 5.15 and 5.18)

As for *Dmeso17A-RNAi*, in embryos expressing *Dmeso17A-ΔWRPW* the main features of muscle differentiation have occurred as in the wild type (Figure 5.15, compare A with C). However, close analysis reveals, for example, misshapen muscles such as DA3 (Figure 5.15, compare B with D, DA3 is outlined). This indicates that, like *Dmeso17A-RNAi*, *Dmeso17A-ΔWRPW* expression results in aberrant muscle differentiation.

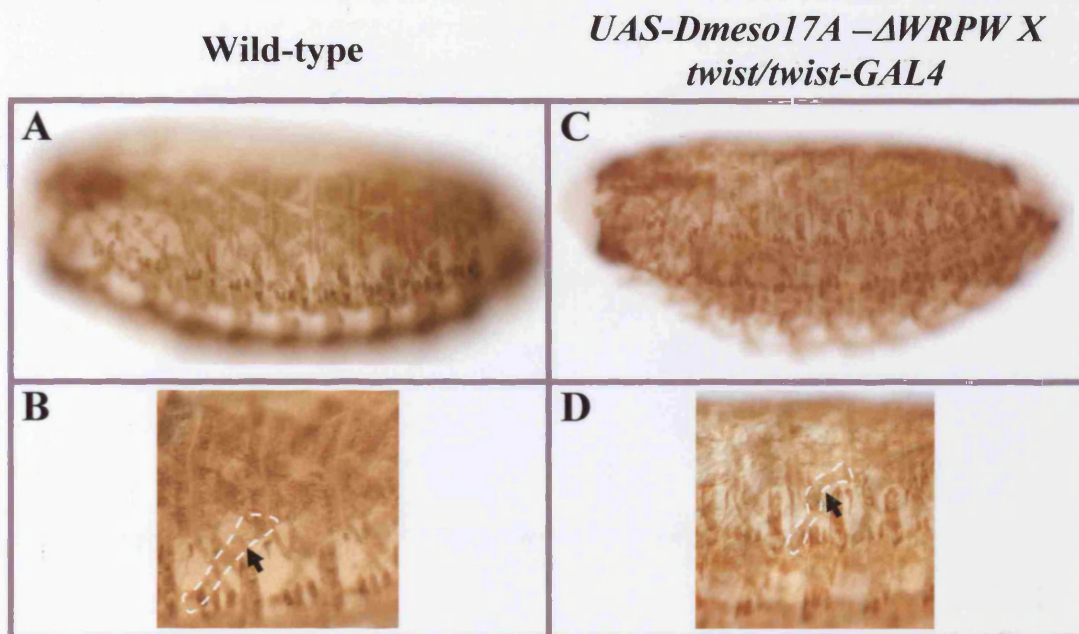
In order to test that these effects on muscle differentiation are due to a dominant negative effect and not a residual activity of *Dmeso17A*, I over expressed both *Dmeso17A-ΔWRPW* and *Dmeso17A* transgenes together using *twist/twist-GAL4*. This was done at 18°C. Figure 5.16 shows that *Dmeso17A-ΔWRPW* can rescue the phenotype towards wild type. Comparison with *Dmeso17A* over-expression using *twist/twist-GAL4* revealed that 55-60% of the embryos now have a phenotype close to wild-type when only 25-30% did with *Dmeso17A* alone (Figure 5.16, compare A with D). Moreover, only 15-20% of the embryos expressing both transgenes present a very severe phenotype when more than 50% did with *Dmeso17A* alone (Figure 5.16, compare C with F). The proportion of embryos with a moderate phenotype does not significantly change (Figure 5.16, compare B with E). These results show that, even though a variety of phenotype is still observed, *Dmeso17A-ΔWRPW* can suppress the inhibitory effect of *Dmeso17A* and therefore that it acts as a dominant negative.

**Figure 5.16: *Dmeso17A-ΔWRPW* acts as a “dominant negative”.**

*Dmeso17A* and *Dmeso17A-ΔWRPW* were over-expressed together using *twist/twist-GAL4* at 18°C. (A-C) Variation of phenotype in *Dmeso17A* over-expressing embryos (categories are the same as in Figure 4.2). (D-F) *Dmeso17A-ΔWRPW* rescues the phenotype towards wild-type. The proportion of weak (D) and moderate (E) phenotypes has substantially increased, whereas the number of severely affected embryos (F) is considerably reduced (compare with A, B and C respectively). This demonstrates a “dominant negative” effect.

**Figure 5.17: *Dmeso17A-ΔWRPW* suppresses the lethality induced by *Dmeso17A* over-expression.**

Larval hatching and survival assay was carried out as in Figure 4.4. The percentage of hatching of larvae over-expressing both *Dmeso17A* and *Dmeso17A-ΔWRPW* does not change substantially compared to that obtained with *Dmeso17A* alone. However, the survival is considerably increased. Mean percentages  $\pm$  S.D are: *Dmeso17A*, Hatching=90%  $\pm$  0.24, Survival=18%  $\pm$  0.31; *Dmeso17A+Dmeso17A-ΔWRPW*, Hatching=95%  $\pm$  0.21, Survival=66%  $\pm$  0.43.

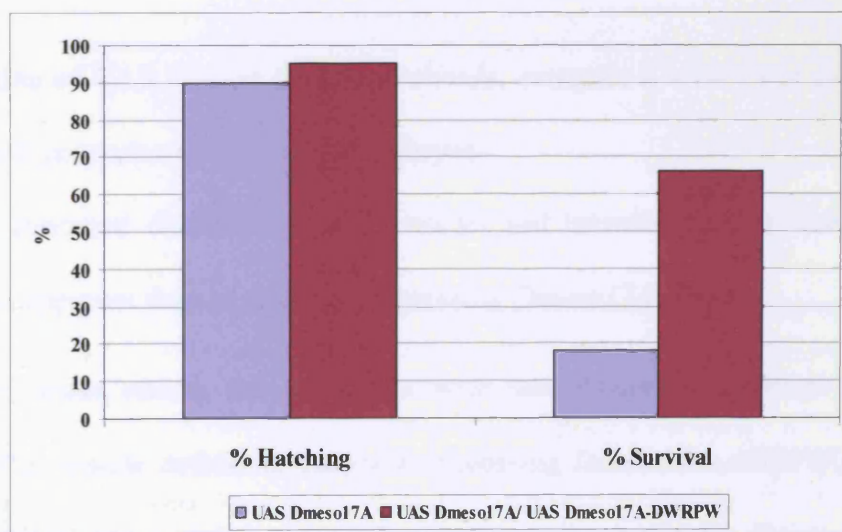
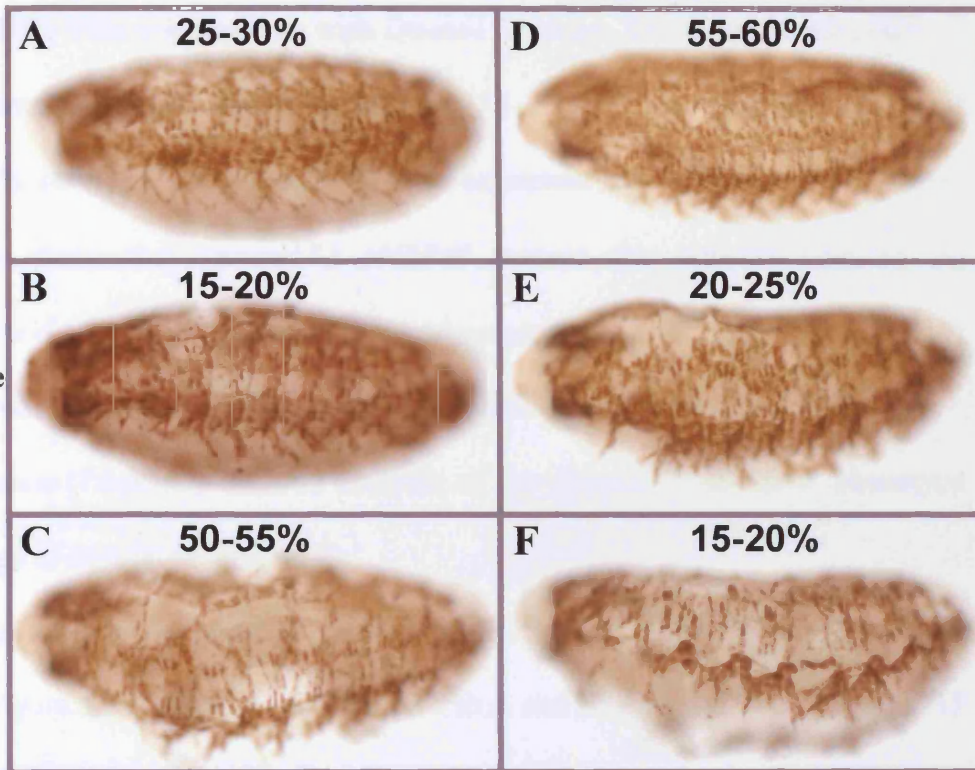


**Figure 5.15: *Dmeso17A-ΔWRPW* expression disrupts muscle development.**

*Dmeso17A-ΔWRPW* was over-expressed using *twist/twist-GAL4* at 25°C. Stage 17 embryos were stained with an anti-muscle Myosin and compared to wild-type. (A-B) Wild-type embryo showing the normal muscle pattern (A) and correctly shaped DA3 muscle (dotted outline in B). (C-D) In embryos expressing *Dmeso17A-ΔWRPW*, the overall muscle pattern is essentially normal (C). However, aspects of muscle development are affected. For example, DA3 can be misshapen (dotted outline in D) compared to wild type (B).

*UAS-Dmeso17A X twist/twist-GAL4*

*UAS-Dmeso17A/; UAS-Dmeso17A- $\Delta$ WRPW X twist/twist-Gal4*



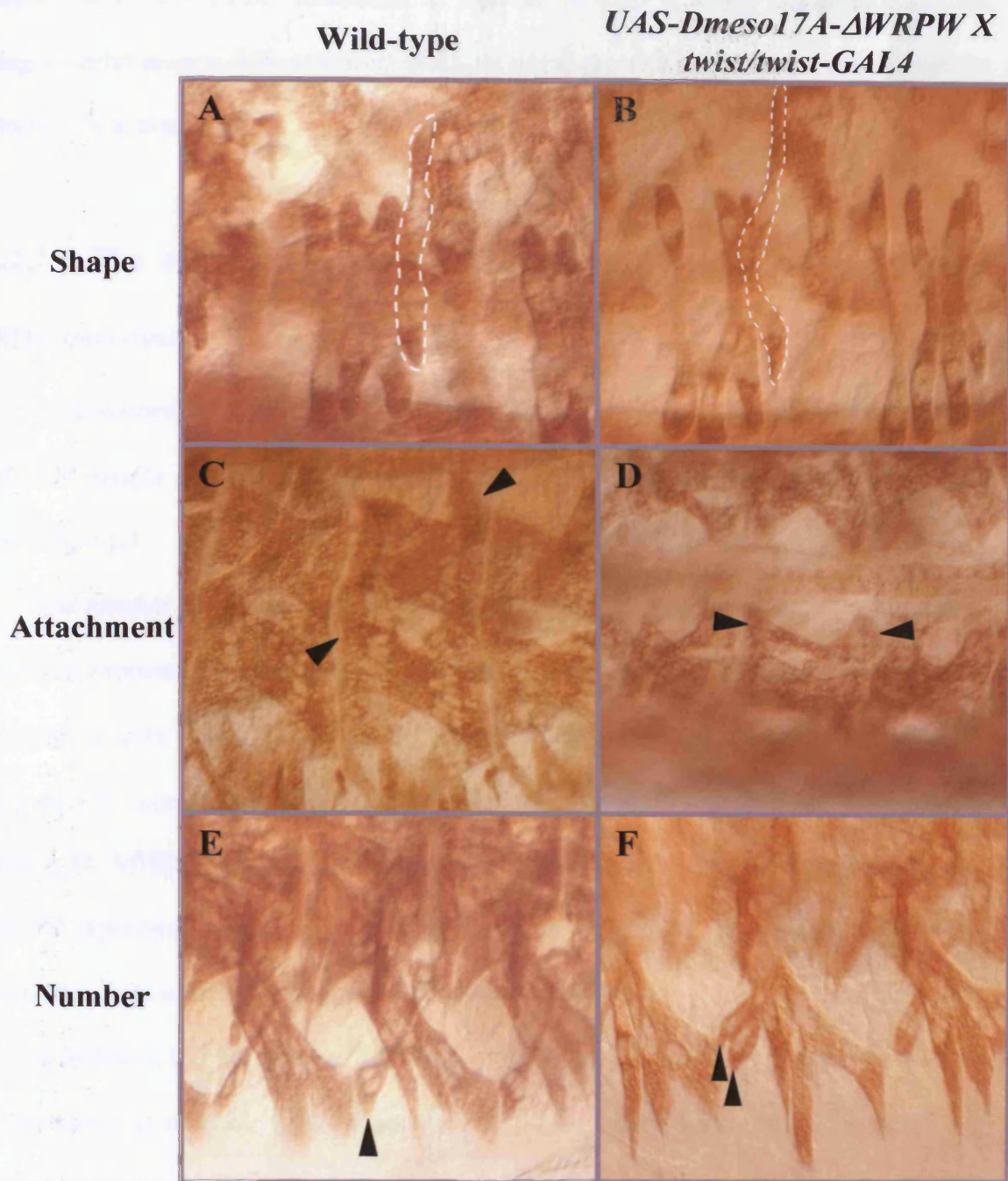
Because of this variety of phenotype, it was necessary to quantitate this rescue. I therefore used the larval hatching and survival assay (described in Chapter 4 section 4.2.2). 95% of the embryos expressing both *Dmeso17A* and *Dmeso17A-ΔWRPW* were able to hatch. 90% were able to do so with *Dmeso17A* alone. Most importantly, 66% of the larvae expressing both *Dmeso17A* and *Dmeso17A-ΔWRPW* survived until adulthood, when only 18% survived with *Dmeso17A* over-expressed alone (Figure 5.17). These results clearly show that *Dmeso17A-ΔWRPW* rescues the lethality induced by *Dmeso17A* over-expression and confirm its “dominant negative” effect. The muscle defects observed are therefore probably due to a reduction of *Dmeso17A* activity.

As for *Dmeso17A-RNAi*, detailed analysis of the *Dmeso17A-ΔWRPW* phenotype revealed a range of defects (Figure 5.18):

- In more than 40% of the embryos, some muscles are misshapen. These include the LT muscles (Figure 5.18, compare outlined LT4 in A and B), but also DA3 (Figure 5.15 compare B with D), DO3-4 or VO4-6.
- Muscle attachment is affected in 20% of the embryos. In most of these cases, DA1 is wrongly attached (Figure 5.18, arrowheads, compare C with D). This effect is also seen on DA3 and DO1.
- Finally, duplication of VA3 (Figure 5.18, arrowheads, compare E with F) or DO1-2 occurs in a very small proportion (<5%) of the embryos.
- There was also abnormal distribution of the nuclei and increase muscle size, but these effects are less apparent than in embryos expressing *Dmeso17A-RNAi*.

Taken together, these results are consistent with the phenotype obtained with *Dmeso17A-RNAi*. The muscle defects in embryos expressing *Dmeso17A-ΔWRPW*, due to a reduction of *Dmeso17A* activity, are similar to those observed with *Dmeso17A-RNAi*, where the level of *Dmeso17A* is reduced. This suggests that level and activity of





**Figure 5.18:** *Dmeso17A-ΔWRPW* expression results in aberrant muscle differentiation.

The muscle phenotype of stage 17 embryos expressing *Dmeso17A-ΔWRPW* using *twist/twist-GAL4* at 25°C was analysed in detail and compared to wild-type. Anti-Myosin staining revealed defects in muscle shape (A-B), attachment (C-D), number (E-F). (A-B) In embryos expressing *Dmeso17A-ΔWRPW* (B) the shape of muscles such as LT4 (dotted outlines in A and B) can be altered compared to wild-type (A). (C-D) Muscles such as DA1 can be incorrectly attached in *Dmeso17A-ΔWRPW*-expressing embryos. Arrowheads show the attachment points of DA1 in the wild-type (C) and in *Dmeso17A-ΔWRPW* expressing embryos (D). (E-F) In a small proportion of embryos expressing *Dmeso17A-ΔWRPW*, there is duplication of muscles such as VA3 (arrowheads in E and F).

*Dmeso17A* are correlated. Moreover, as without its WRPW motif *Dmeso17A* can no longer inhibit muscle differentiation, these results suggests that this motif is required for *Dmeso17A* action.

### 5.2.2.2 The effect of *Dmeso17A-ΔWRPW* effects are during muscle differentiation

As described for *Dmeso17A-RNAi*, I tested whether *Dmeso17A-ΔWRPW* expression affected muscle development during the differentiation phase. The results I obtained were identical.

The number and position of Kr and Eve-expressing founder cells is unchanged in embryos expressing *Dmeso17A-ΔWRPW* using *twist/twist-GAL4* at 25°C (Figure 5.19, compare A with B and C with D). Moreover, DMef2 expression is normal at stage 13 (Figure 5.20, compare A with B), but is altered at stage 17 (Figure 5.20, compare C,E with E,F). MHC/DMef2 double staining revealed defects such as disorganisation of DMef2-expressing nuclei (Figure 5.20, compare E with F). These results show are consistent with an effect during the differentiation phase.

In addition, like for *Dmeso17A-RNAi*, acridine orange staining revealed an increase in apoptosis as muscles differentiate (Figure 5.21). Again, I did not find a significant reduction in the number of muscle nuclei in embryos expressing *Dmeso17A-ΔWRPW*, the reason for this increase in cell death is unclear.

**Figure 5.19: *Dmeso17A-ΔWRPW* expression does not affect the early steps of muscle development.**

Wild-type and embryos over-expressing *Dmeso17A-ΔWRPW* using *twist/twist-GAL4* at 25°C were stained with anti-Krüppel (A-B) or anti-Eve (C-D) antibodies. (A-B) Stage 14. The number and position of Kr expressing cells is identical in the wild-type (A) and in embryos over-expressing *Dmeso17A-ΔWRPW* (B). (C-D) Stage 12. Wild-type Eve expression pattern (C) in the DA1 founder (arrowheads) and in two PCs founders (arrows) is unchanged in embryos over-expressing *Dmeso17A-ΔWRPW* (D).

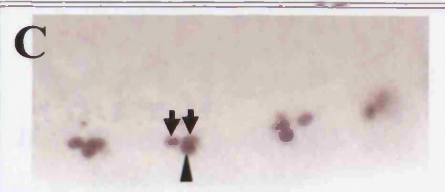
**Figure 5.20: The effect of *Dmeso17A-ΔWRPW* occurs during muscle differentiation.**

Wild-type and embryos over-expressing *Dmeso17A-ΔWRPW* using *twist/twist-GAL4* at 25°C were either stained with an anti-DMef2 antibody (A-B) or double stained with anti-Myosin and anti-DMef2 antibodies (C-F). (A-B) Stage 13. DMef2 expression is identical in the wild-type (A) and in embryos over-expressing *Dmeso17A-ΔWRPW* (B). (C-F) Stage 17. The overall DMef2 expression pattern looks essentially normal in embryos expressing *Dmeso17A-ΔWRPW* (compare C and D). However, there are defects such as the disorganisation of DMef2-expressing nuclei in the VO4 muscle (arrowheads in E and F).

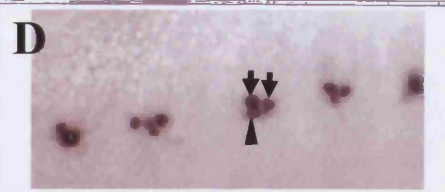
**Kruppel**

**Even-skipped**

**Wild-type**



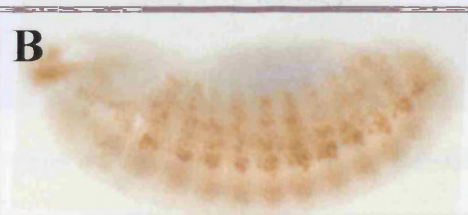
***UAS-Dmeso17A- $\Delta$ WRPW X***  
***twist/twist-GAL4***



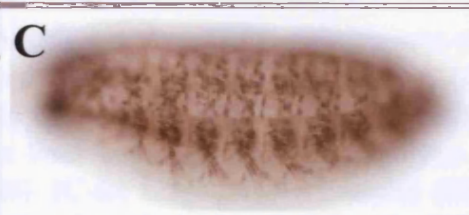
**Wild-type**

***UAS-Dmeso17A- $\Delta$ WRPW X***  
***twist/twist-GAL4***

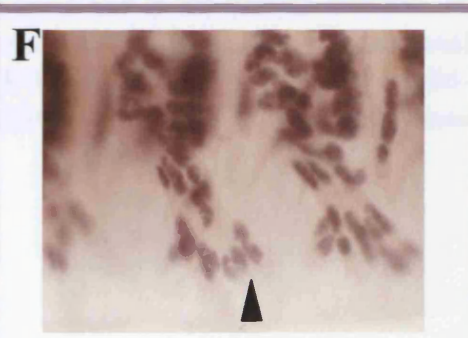
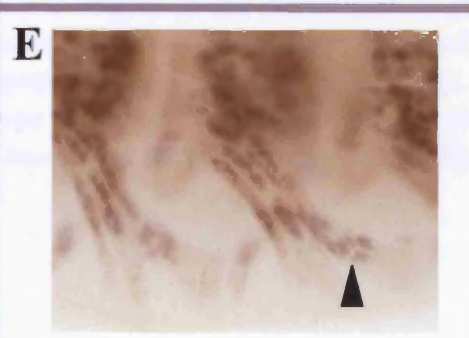
**DMEF2**

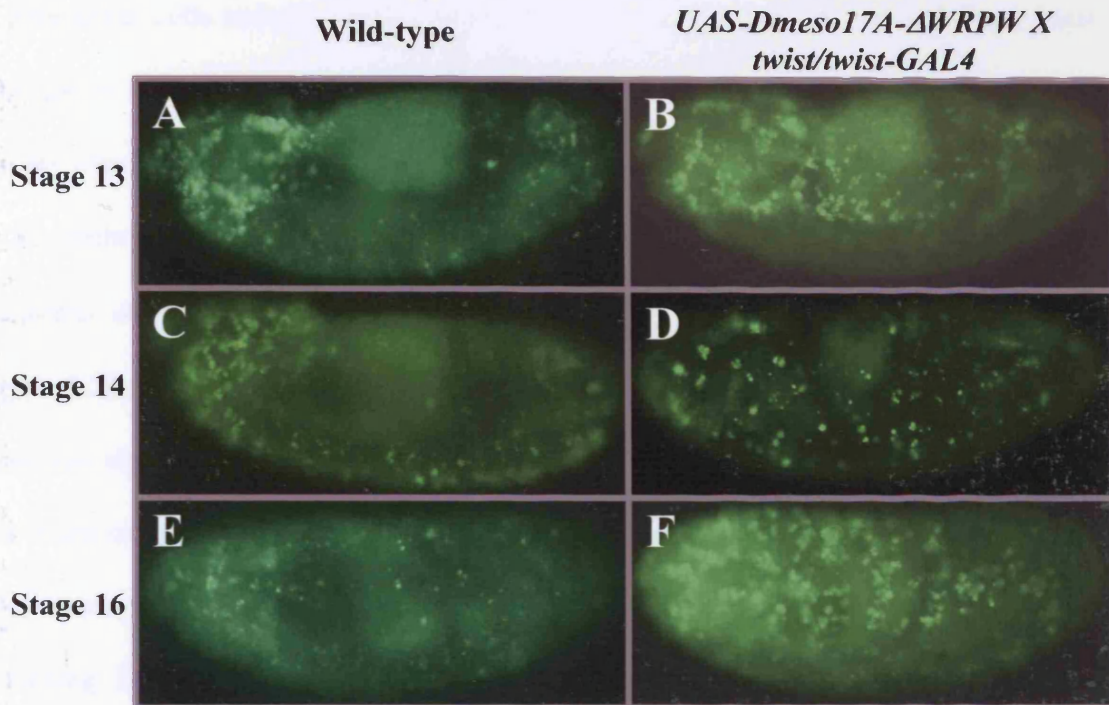


**MHC/  
DMEF2**



**MHC/  
DMEF2**





**Figure 5.21: *Dmeso17A-ΔWRPW* expression increases cell death during muscle differentiation.**

Acridine orange (AO) staining was carried out on wild-type (A, C, E) and embryos over-expressing *Dmeso17A-ΔWRPW* using *twist/twist-GAL4* at 25°C (B, D, F). (A-B) Stage 13. Only a few AO positive cells are detected in both wild-type (A) and embryos over-expressing *Dmeso17A-ΔWRPW* (B). (C-D) Stage 14. As muscles differentiate, cell death in the wild type (C) is largely in the dorsal part of the head and in the ventral midline. In embryos over-expressing *Dmeso17A-ΔWRPW* (D), some additional apoptotic cells are detected laterally. (E-F) Stage 16. Whereas in the wild-type (E) there are only a few AO positive cells, more are detected when *Dmeso17A-ΔWRPW* is expressed (F).

### 5.2.2.3 The effect of *Dmeso17A-ΔWRPW* expression on other mesodermal derivatives

Like for *Dmeso17A-RNAi*, *Dmeso17A-ΔWRPW* should only be effective in cells normally expressing *Dmeso17A*. I therefore tested the effect of *Dmeso17A-ΔWRPW* on the pericardial cells and the AMPs, which both express *Dmeso17A*. Nevertheless, I also investigated the effect on visceral musculature and on the cardioblasts. The assays I used are identical to those employed for *Dmeso17A-RNAi*.

In embryos expressing *Dmeso17A-ΔWRPW* using *Dmeso17A-GAL4* at 25°C, pericardial cell marker expression (*Zfh-1*, *Eve* and *Odd*) did not reveal any defects (Figure 5.22, compare A, C and E with B, D and F). Moreover, cell counting did not reveal any significant difference in the number of *Odd* and *Zfh-1*-expressing pericardial cells when compared to the wild type (Figure 5.23A and B). This was confirmed by a paired t-test (see legend of Figure 5.23). In addition, *Twist* staining on embryos expressing *Dmeso17A-ΔWRPW* using *twist/twist-GAL4* at 25°C did not show any difference in AMP number or position when compared to the wild type (Figure 5.24, compare A-B with C-D). Taken together these results suggest that the dominant negative effect is not strong enough to reduce *Dmeso17A* activity to a level where it would have an effect. Embryos expressing *Dmeso17A-ΔWRPW* at 25°C using *bap-GAL4* or *Dmef2-GAL4* display normal visceral musculature and cardioblast development. Visceral muscle precursors are present and organised as in the wild type (Figure 5.25, compare A with B). Midgut constrictions also are normal (Figure 5.25, compare C with D; Figure 5.26, compare A with B). Cardioblast development is not affected either in these embryos. *DMef2*,  $\beta$ 3-tubulin or myosin expression are not affected and always show two rows of cardioblasts (Figure 5.27, compare A, C and E with B, D

**Figure 5.22: *Dmeso17A-ΔWRPW* expression does not affect pericardial cell development.**

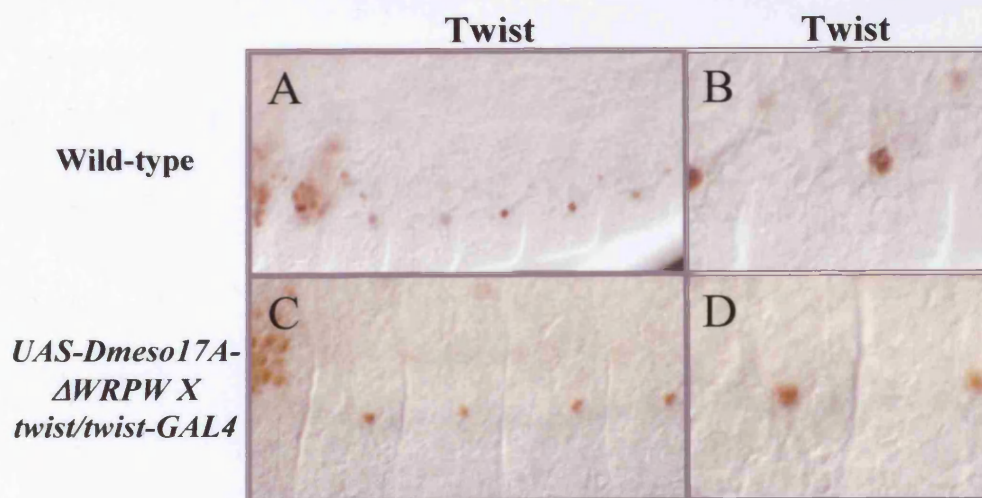
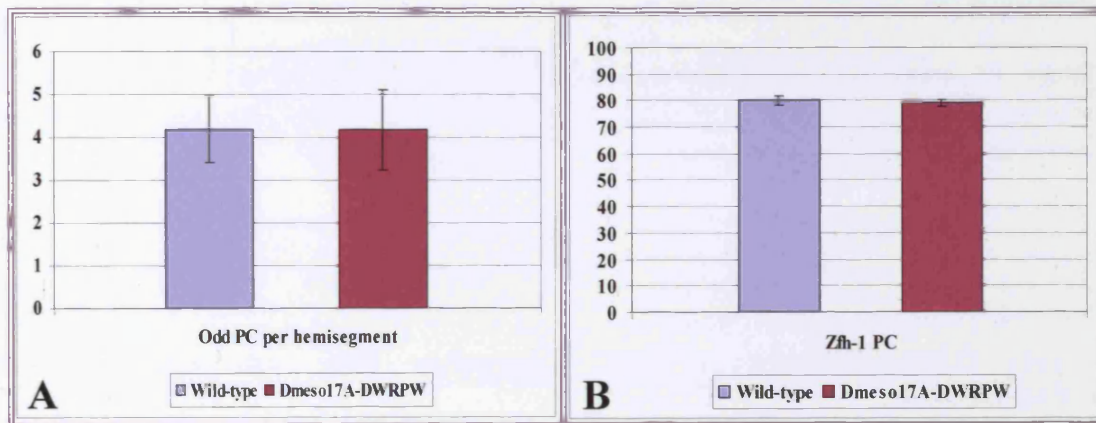
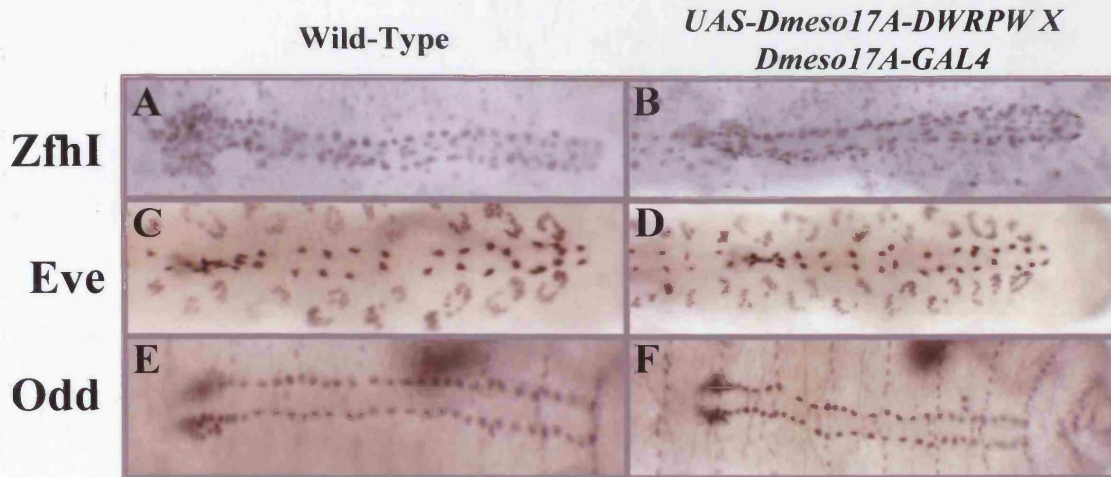
Stage 17 embryos, wild-type or expressing *Dmeso17A-ΔWRPW* using *Dmeso17A-GAL4* at 25°C, were stained with anti-Zfh-1 (A-B), anti-Eve (C-D) or anti-Odd (E-F) antibodies. The pattern of the cells expressing these markers in the wild type (A, C, E) and in *Dmeso17A-ΔWRPW*-expressing embryos (B, D, F) are comparable.

**Figure 5.23: *Dmeso17A-ΔWRPW* expression does not affect pericardial cell number.**

(A) The number of Odd-expressing cells per hemisegment was scored in both wild type and embryos over-expressing *Dmeso17A-ΔWRPW* at stage 14. 144 hemisegments were analysed in each case. Almost the same average number of cells per hemisegment (4.18 and 4.17) was found in the wild-type and in embryos over-expressing *Dmeso17A-ΔWRPW*. A paired t-test confirmed that there is no significant difference. The p value = 0.94 with a 95% confidence interval. (B) The number of Zfh-1-expressing cells was also scored in both wild type and embryos over-expressing *Dmeso17A-ΔWRPW* at stage 17. twenty embryos were analysed in each case. Again almost the same average number of cells (80 and 79) was found in the wild-type and in embryos over-expressing *Dmeso17A-ΔWRPW*. A paired t-test was carried out to and confirmed that there is no difference. The p value= 0.6 with a 95% confidence interval. Error bars indicate standard deviation.

**Figure 5.24: *Dmeso17A-ΔWRPW* expression does not affect the number of persistent Twist-expressing cells.**

Stage 14 embryos were stained with an anti-Twist antibody. Twist expression in the AMPs is identical in the wild-type (A-B) and in embryos expressing *Dmeso17A-ΔWRPW* using *twist/twist-GAL4* at 25°C (C-D).





**Figure 5.25: *Dmeso17A-ΔWRPW* expression does not affect visceral mesoderm development.**

Wild-type (A, C) and embryos over-expressing *Dmeso17A-RNAi* using the *bap-GAL4* driver at 25°C (B, D), were stained with an anti-FasIII antibody. Expression of *Dmeso17A-ΔWRPW* using *bap-GAL4* affects neither the organisation of the circular visceral muscle progenitors nor the midgut constrictions (compare A with B, and C with D).

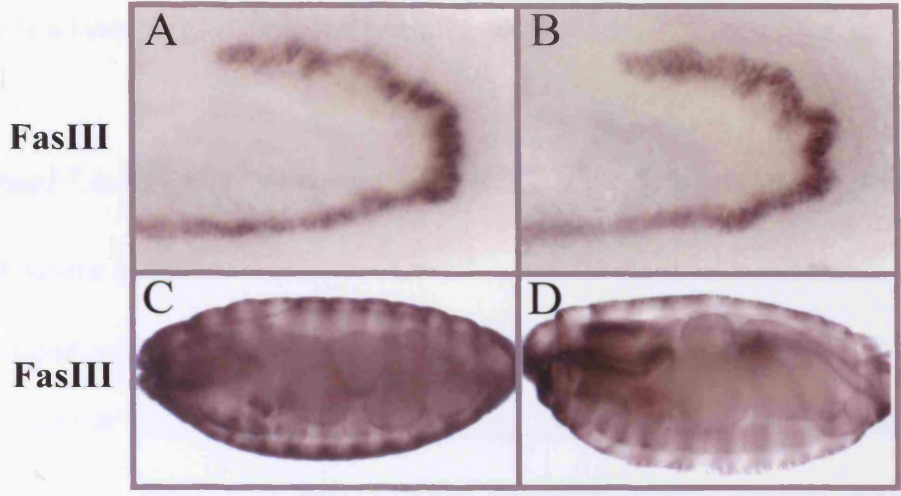
**Figure 5.26: *Dmeso17A-ΔWRPW* expression does not affect visceral muscle development.**

Stage 17 embryos were stained with an anti-Myosin antibody. In embryos over-expressing *Dmeso17A-ΔWRPW* using the *Dmef2-GAL4* driver (B), midgut constrictions occur as in the wild-type (A).

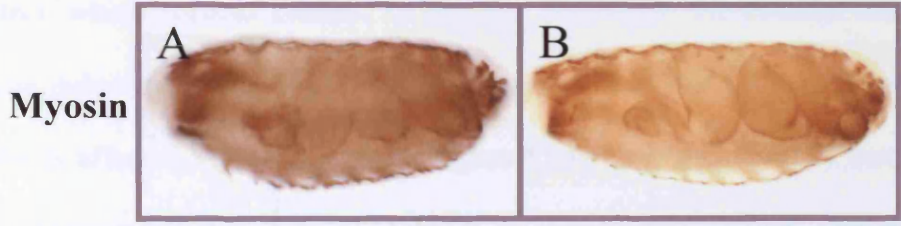
**Figure 5.27: *Dmeso17A-ΔWRPW* expression does not affect cardioblasts differentiation.**

Stage 17 embryos were stained with anti-DMef2 (A-B), anti-β3-tubulin (C-D) or anti-Myosin (E-F) antibodies. Expression of these three markers in the cardioblasts of *Dmeso17A-ΔWRPW*-expressing embryos using *Dmef2-GAL4* at 25°C (B, D, F) is comparable to that of the wild-type (A, C, E).

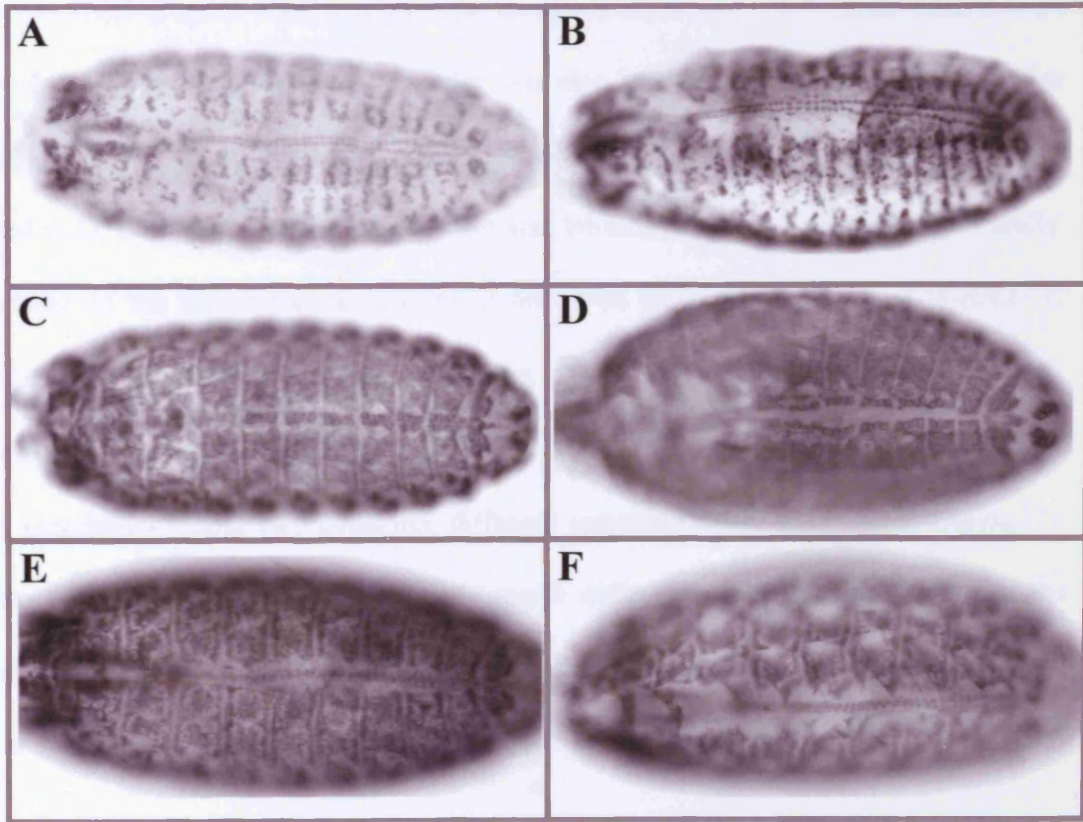
Wild-type      *UAS-Dmeso17A-ΔWRPW X Bap-GAL4*



Wild-type      *UAS-Dmeso17A-ΔWRPW X Dmef2-GAL4*



Wild-type      *UAS-Dmeso17A-ΔWRPW X Dmef2-GAL4*

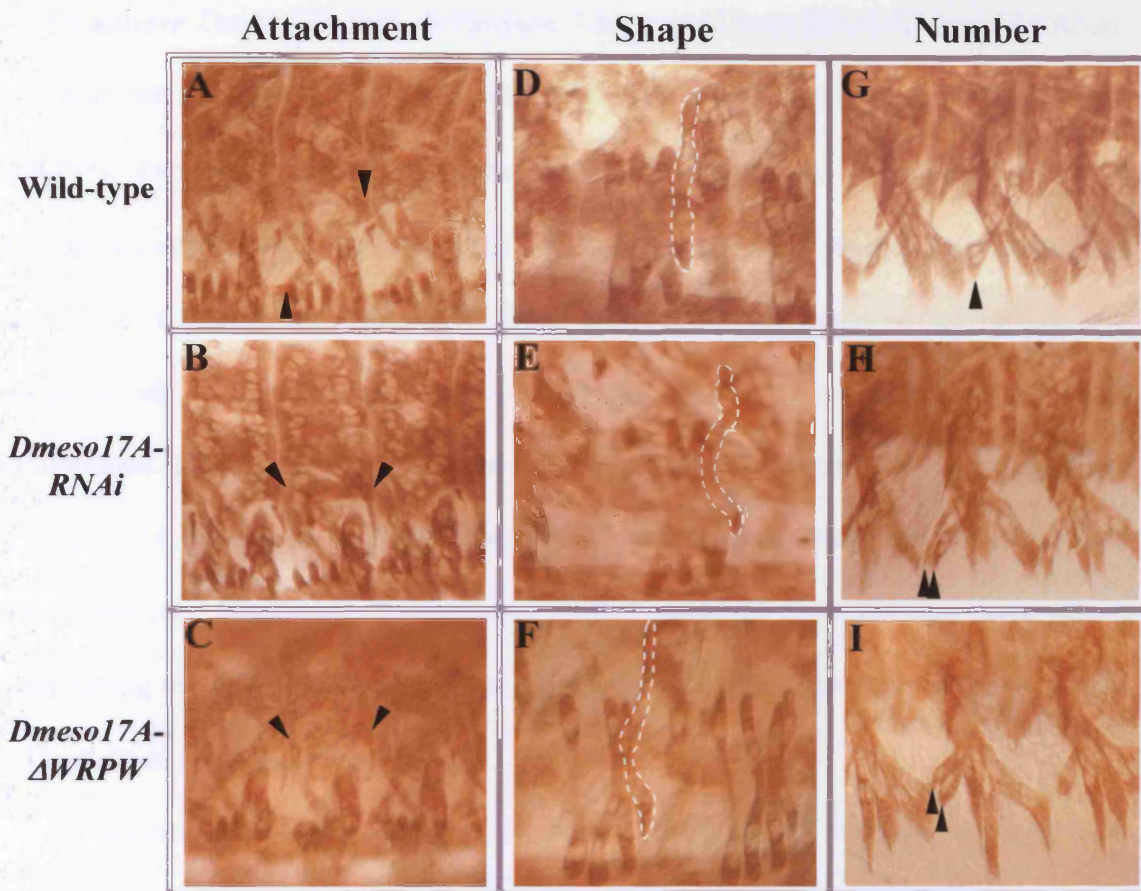


and F). These results confirm that, as expected, *Dmeso17A-ΔWRPW* is not effective in tissues or cells where *Dmeso17A* is not normally expressed.

### **5.2.3 *Dmeso17A-RNAi* vs *Dmeso17A-ΔWRPW*: different mechanisms of action but same effect**

As described in the previous sections, my results show that *Dmeso17A-RNAi* and *Dmeso17A-ΔWRPW* provide two mechanistically different ways of knocking down *Dmeso17A* function: *Dmeso17A-RNAi* induces degradation of *Dmeso17A* mRNA and therefore reduces *Dmeso17A* level, whereas *Dmeso17A-ΔWRPW* has a dominant negative effect, which reduces *Dmeso17A* activity. Strikingly, the detailed analysis of the phenotype induced by either of these transgenes showed that differentiation of the same muscles is affected in the same way. Figure 5.28 shows examples of similarities. In embryos expressing either *Dmeso17A-RNAi* or *Dmeso17A-ΔWRPW*, attachment of muscles can be affected. In particular, DA3 is often wrongly attached and is now parallel to DO2 (Figure 5.28, arrowheads, compare A, B and C). Similar effects were observed for DA1. The shape of muscles can also be affected in these embryos. For example, in both cases, LT4 can have a similar kinked shape (Figure 5.28, LT4 is outlined in D, E and F). VO4 or DO4-5 can also be misshapen in a similar way. Finally, duplication of the same muscles has been observed when either *Dmeso17A-RNAi* or *Dmeso17A-ΔWRPW* is expressed. This can affect VA3 (Figure 5.28 arrowheads, compare G, H and I) and DO1-2.

In conclusion, these two complete different approaches to knock down *Dmeso17A* function have exactly the same effect on muscle differentiation. This indicates that the phenotype observed is due to a *Dmeso17A* loss-of-function and therefore that normal level or activity of *Dmeso17A* is required for correct muscle development.



**Figure 5.28: *Dmeso17A-RNAi* and *Dmeso17A-ΔWRPW* induce the same effects.**

The muscle phenotypes of embryos expressing *Dmeso17A-RNAi* using *Dmeso17A-GAL4* or *Dmeso17A-ΔWRPW* using *twist/twist-GAL4* (both at 25°C) were compared. Examples are given showing that the same muscles are affected in the same way. (A-C) Not only is DA3 is incorrectly attached in embryos expressing either *Dmeso17A-RNAi* (B) or *Dmeso17A-ΔWRPW* (C) (compare with wild-type in A), but the attachment points are similar (arrowheads in B and C). (D-F) Compared to wild-type (D), LT4 has a similar kinked shape when either *Dmeso17A-RNAi* (E) or *Dmeso17A-ΔWRPW* (F) is expressed. (G-I) The same muscles are duplicated in embryos expressing *Dmeso17A-RNAi* or *Dmeso17A-ΔWRPW*. VA3 is given as an example (arrowheads; compare G, H and I).

## 5.3 Discussion

### 5.3.1 *Dmeso17A* loss-of-function results in aberrant somatic muscle differentiation

To achieve *Dmeso17A* loss-of-function, I have used both RNAi (*Dmeso17A-RNAi*) and a truncated form of *Dmeso17A*, which behaves as a dominant negative (*Dmeso17A-ΔWRPW*). Expression of either *Dmeso17A-RNAi* or *Dmeso17A-ΔWRPW* results in aberrant somatic muscle development with defects in size, shape, attachment and number of the muscles. Although RNAi and dominant negative effect are two mechanistically different approaches, they have the same effects on muscle development. These similarities and the fact that they both suppress the inhibitory effect of *Dmeso17A* suggest that the phenotype observed is specifically due to *Dmeso17A* loss-of-function. Moreover, Kr, Eve and DMef2 stainings revealed that these effects occur during the differentiation of muscle precursors. This is consistent with my results on the over-expression of *Dmeso17A*.

As shown previously, *Dmeso17A* is an inhibitor of muscle differentiation. Nevertheless, it is not obvious to know what would happen when an inhibitor function is removed. There are few examples in the literature. One of these is the phenotype of *zfh-1* mutant embryos. *Zfh-1* is a transcriptional repressor that may inhibit *Dmef2* expression (Postigo et al., 1999). In embryos lacking *zfh-1* function, the muscle pattern revealed a variety of errors with misshapen, mispositioned or missing muscles. A range of severity was also reported (Lai et al., 1993). This analysis of *Zfh-1* mutant phenotype was rather general and no detailed description was given. Nevertheless, it gives indications on the possible effects of the loss of an inhibitor of muscle differentiation and one can imagine different scenarios. Muscles might differentiate earlier than they normally do, leading to abnormal differentiation. Myoblasts might

differentiate at the right time, but produce an excessive amount of muscle specific proteins such as myosin or actin for example. This would lead to abnormal differentiation, for example muscles misshapen and/or incorrectly attached. Finally, founder cells might fuse with more FCMs than they normally do, and this excessive fusion could lead to the formation of bigger muscles. In embryos expressing *Dmeso17A-RNAi* or *Dmeso17A-ΔWRPW*, I found that muscle shape, size and attachment can be affected. This is consistent with a role of inhibitor of muscle differentiation for *Dmeso17A*.

I also tested the effect of *Dmeso17A-RNAi* or *Dmeso17A-ΔWRPW* on other mesodermal derivatives. Given that these approaches directly target *Dmeso17A* expression or activity, an effect was only expected where *Dmeso17A* is expressed. As anticipated, none of the tissues where *Dmeso17A* is not normally expressed was affected. However, among the cells normally expressing *Dmeso17A*, only the pericardial cells, when *Dmeso17A-RNAi* is expressed, showed defects in their organisation. Differentiation of the AMPs and the adepithelial cells was not affected. These results suggest that the level of *Dmeso17A* required for their development is lower than in somatic muscles. A stronger loss-of-function of *Dmeso17A* would therefore be necessary.

### 5.3.2 Conclusion

I have shown that *Dmeso17A-RNAi* and *Dmeso17A-ΔWRPW* can specifically knock-down *Dmeso17A* function. The reduction in *Dmeso17A* level or activity disrupts the differentiation of the muscles and the muscle defects observed are consistent with what one might expect from the loss-of-function of an inhibitor of differentiation.

Together these results suggest that the inhibitory function of *Dmeso17A* is required for proper muscle development.

Finally, I have shown that *Dmeso17A-RNAi* and *Dmeso17A-ΔWRPW* represent two useful tools to test genetic interactions between *Dmeso17A* and putative interactor(s) or target(s) such as *Dmef2*.

## CHAPTER 6: Genetic Interactions

### 6.1 Introduction

My data presented in Chapters 4 and 5 show that *Dmeso17A* is an inhibitor of muscle differentiation. The next step was to find interactor(s) and/or target(s) that could be used to dissect its mechanism of action. I therefore aimed to identify candidate genes that could interact with *Dmeso17A*, and then tested whether they did.

### 6.2 *Dmeso17A* and *Dmef2*

Being the key regulator of muscle differentiation, *Dmef2* should be part of the study of an inhibitor of differentiation such as *Dmeso17A*. Moreover, my results presented in Chapter 4 suggest that there might be a relationship between *Dmeso17A* and *Dmef2*. A clear indication of a possible link is that over-expression of *Dmeso17A* in the cardioblasts produces a phenotype very similar to that observed in *Dmef2* mutant embryos (Ranganayakulu et al., 1995; Damm et al., 1998). I therefore started my analysis of *Dmeso17A* mechanism of action by testing whether, it interacts with *Dmef2*.

Two approaches were taken to explore whether there are links between *Dmeso17A* and *Dmef2*. First, I carried out a detailed comparison of the phenotypes of embryos over-expressing *Dmeso17A* with that of *Dmef2* hypomorphic mutants. Second, I tested whether there is an *in vivo* genetic interaction between *Dmeso17A* and *Dmef2*. Details of these two approaches and the results obtained are described in the sections below.



### 6.2.1 *Dmeso17A* over-expression phenocopies *Dmef2* hypomorphic alleles.

In *Dmef2* null mutants, there is an almost complete lack of myosin expressing cells within the somatic mesoderm (Bour et al., 1995; Lilly et al., 1995; Ranganayakulu et al., 1995; Gunthorpe et al., 1999). Any detailed phenotypic comparison is therefore impossible. However, three *Dmef2* hypomorphic alleles have been described (Ranganayakulu et al., 1995; Gunthorpe et al, 1999). They can be placed in an allelic series based on their somatic muscle phenotype. In the strongest allele (*Dmef2*<sup>113</sup>), there is an almost complete lack of correctly formed muscle, in the intermediate (*Dmef2*<sup>424</sup>) more muscles are formed, although not all are properly shaped, and in the weakest allele (*Dmef2*<sup>65</sup>), only some muscles are missing. The differential effects of these alleles mimic in many instances the variations I observed when I over-expressed *Dmeso17A*. I therefore decided to carry a detailed comparison between the phenotypes of these three alleles and that induced by the over-expression of *Dmeso17A* driven by the *24B-GAL4* driver. The use of this driver seemed to be the most reasonable choice as it had already been used in several studies of *Dmef2*, including that of Gunthorpe et al. In this study, this driver was used to over-express a *UAS-Dmef2* transgene at different temperatures, to induce different levels of *Dmef2*, in order to rescue different aspects of the *Dmef2* null mutant phenotype (Gunthorpe et al, 1999).

I also used this property of the GAL4/UAS system that different severity of phenotype can be obtained at different temperatures, with greater effect seen at higher temperatures (Brand et al., 1994) (see Chapter 4, section 4.2.3). This was done in order to obtain a similar range of severity by over-expressing *Dmeso17A* as that observed in the different *Dmef2* alleles. For this reason, I raised the embryos over-expressing

*Dmeso17A* at either 18°C, 21°C or 25°C. Figure 6.1 shows some of the striking similarities observed during the comparison of the phenotypes.

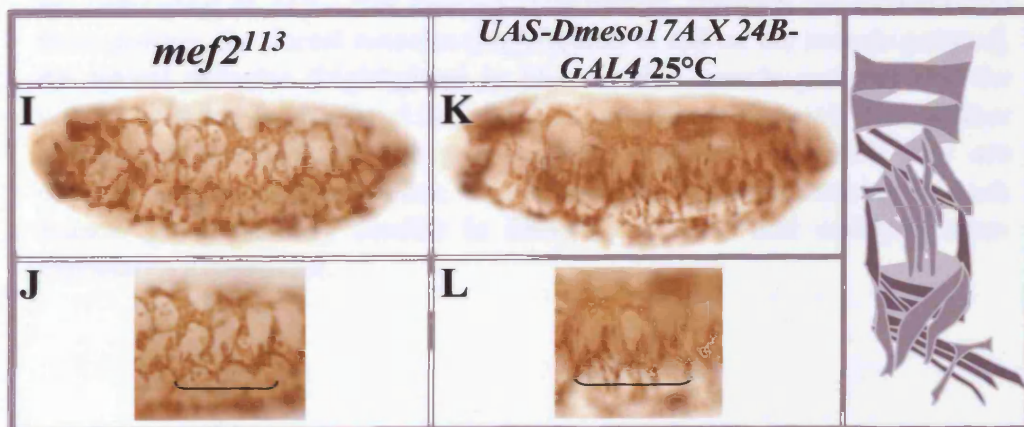
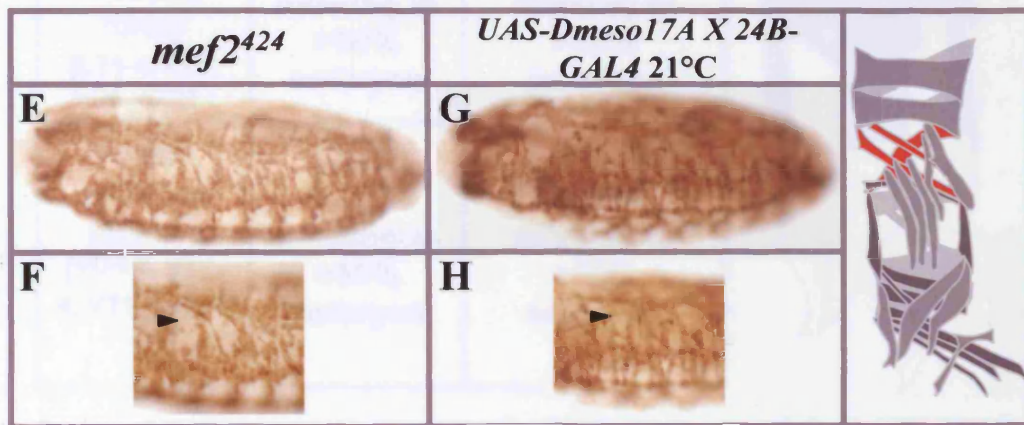
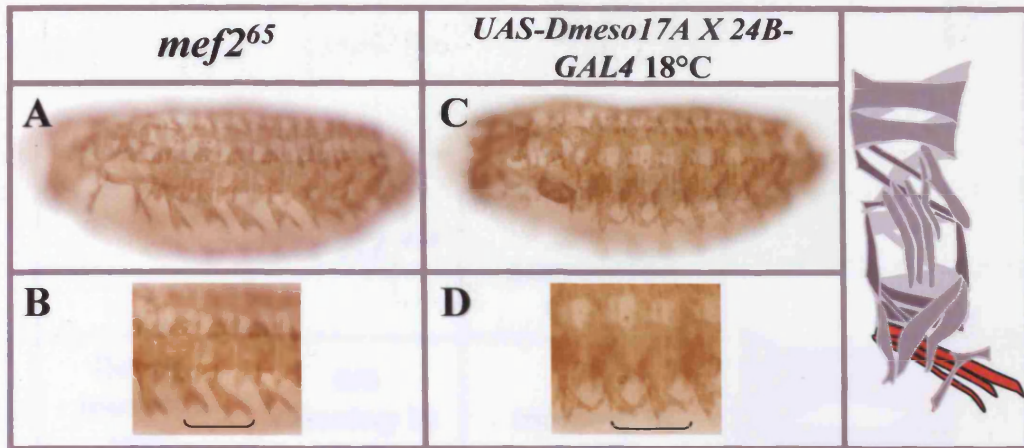
At 18°C, the *Dmeso17A* over-expression phenotype is very similar to that of *Dmef2*<sup>65</sup> embryos (Figure 6.1A-D). For example, VO muscles appear as one big muscle in about 40% of the embryos in both cases (Figure 6.1, brackets, compare A-B with C-D). Moreover, muscles such as VA3, LO1 or LT4 that are missing in more than 50% of *Dmef2*<sup>65</sup> embryos, are also missing or misshapen in a significant proportion of embryos over-expressing *Dmeso17A*. VA3 is missing in 35% of these embryos, LO1 in 40% and the LT muscles are misshapen in 53% of the embryos.

At 21°C, the phenotype of embryos over-expressing *Dmeso17A* is comparable to that of *Dmef2*<sup>424</sup> embryos (Figure 6.1E-H) with most muscles affected. For instance, VL muscles are misshapen in 40% of the embryos analysed in both cases. However, the most striking similarity is not so much related to the shape of the muscles, but more to the groups and the number of muscles that are absent in both cases. An example of this is given in Figure 6.1E-H where DO3-4 and DA3 are missing in both *Dmef2*<sup>424</sup> and *Dmeso17A*-over-expressing embryos (arrowheads, compare E-F with G-H). I have therefore compared the number of muscles missing in different muscle groups in these embryos (Figure 6.2). For the ease of comparison, I have divided the muscles into three groups: the 9 dorsal muscles (DO1-5, DA1-3 and DT1), the 7 lateral ones (LT1-4, LL1, LO1 and SBM) and the 14 ventral muscles (VO1-6, VL1-4, VT1 and VA1-3). This analysis revealed that the number of muscles missing in each group is very similar.

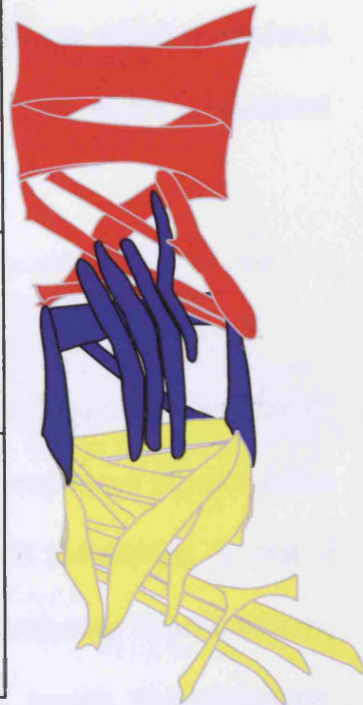
Finally, the phenotype produced by a strong decrease in *Dmef2* activity in the *Dmef2*<sup>113</sup> hypomorph is very similar to the effect of *Dmeso17A* over-expression at 25°C (Figure 6.1I-L). About 35% of *Dmeso17A*-over-expressing embryos have a phenotype similar to that observed in the *Dmef*<sup>d13</sup> allele. Very few muscles are formed correctly in

**Figure 6.1: *Dmeso17A* over-expression phenocopies *Dmef2* hypomorphic alleles.**

The phenotype of embryos over-expressing *Dmeso17A* driven by *24B-Gal4* at 18°C, 21°C or 25°C was compared to that of *Dmef2* hypomorphic mutants: *Dmef2*<sup>65</sup>, *Dmef2*<sup>424</sup> and *Dmef2*<sup>113</sup>. All embryos are stage 17 and stained with an antibody against muscle Myosin. A drawing of the wild-type muscle pattern is included for each part of the figure and the muscles described are in colour to facilitate their identification. **(A-D)** Comparison of the *Dmef2*<sup>65</sup> phenotype **(A-B)** with that produced by *Dmeso17A* over-expression at 18°C **(C-D)**. The two phenotypes are similar (compare A and C) and the same muscles are affected in the same way. For example, VO muscles (highlighted in red on the wild-type pattern) appear as one big muscle in both cases (brackets in C and D). **(E-H)** Comparison of the *Dmef2*<sup>424</sup> phenotype **(E-F)** with that produced by *Dmeso17A* over-expression at 21°C **(G-H)**. In both cases, most muscles are affected (compare E and G) and the same muscles or subsets of muscles are absent. For instance, in both *Dmef2*<sup>424</sup> and *Dmeso17A*-over-expressing embryos, DO3-4 and DA3 (highlighted in red in the wild-type pattern) are missing (arrowheads in F and H). **(I-L)** Comparison of the *Dmef2*<sup>113</sup> phenotype **(I-J)** with that produced by *Dmeso17A* over-expression at 25°C **(K-L)**. In both cases, very few muscles are formed correctly (compare I and K) and some muscles are affected in the same way with particular shapes (brackets in J and L).



	<i>Dmef2</i> <sup>424</sup>	<i>Dmeso17A</i> over- expression (21°C)
<b>Dorsal muscles</b> (red) (DO1-5, DA1-3, DT1)	<b>5/9</b> missing in >50% embryos	<b>4-5/9</b> missing in >40% embryos
<b>Lateral muscles</b> (blue) (LT1-4, LL1, LO1, SBM)	<b>2/7</b> missing in >50% embryos	<b>1/7</b> missing in >50% embryos
<b>Ventral muscles</b> (yellow) (VO1-6, VL1-4, VT1, VA1-3)	<b>5-7/14</b> missing in >50% embryos	<b>6-7/14</b> missing in >50% embryos



**Figure 6.2: Embryos over-expressing *Dmeso17A* at 21°C and *Dmef2*<sup>424</sup> mutants have similar phenotype.**

The number of muscles missing in different muscle groups was compared between *Dmef2*<sup>424</sup> mutants and embryos over-expressing *Dmeso17A* driven by *24B-GAL4* at 21°C. For ease of comparison, muscles are divided into three groups: the dorsal muscles (highlighted in red on the muscle pattern), the lateral muscles (highlighted in blue on the muscle pattern) and the ventral muscles (highlighted in yellow on the muscle pattern). The number of missing muscles and the proportion of embryos in which they are missing is given in each case. The number of muscles missing in each muscle group is very similar in *Dmef2*<sup>424</sup> mutants and embryos over-expressing *Dmeso17A*.

both cases but, most strikingly, some muscles are disrupted in the same way with very particular shapes (Figure 6.1, brackets, compare I-J with K-L).

In summary, an increase in *Dmeso17A* activity can phenocopy a decrease in *Dmef2* activity. There are striking similarities between the phenotypes produced by *Dmeso17A* over-expression and those of the *Dmef2* hypomorphic alleles. The same muscles or subsets of muscle are affected in the same way. These similarities strongly suggest that *Dmeso17A* is involved in the main pathway of muscle differentiation, which is regulated by *Dmef2*. They also indicate that both genes play antagonistic roles, which is consistent with a role of inhibitor of muscle differentiation for *Dmeso17A*.

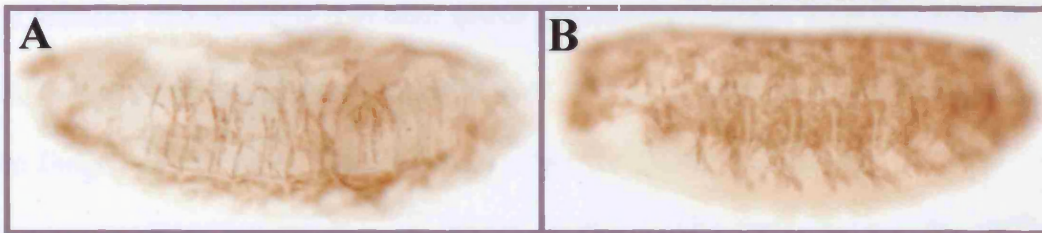
### 6.2.2 *Dmeso17A* genetically interacts with *Dmef2*

The results presented in the previous section suggest that *Dmeso17A* and *Dmef2* might interact. In this section, I tested this possibility. I over-expressed the two genes together to determine whether they genetically interact. The assumption is that if *Dmeso17A* over-expression inhibits muscle differentiation by reducing *Dmef2* activity, an increase of *Dmef2* activity in these embryos should rescue the phenotype. Homozygous flies for both *UAS-Dmeso17A* and *UAS-Dmef2* were crossed to a stock carrying *twist/twist-GAL4* at 18°C. As revealed by an antibody against muscle myosin, the phenotype is rescued towards wild type. The rescued embryos have many more correctly shaped muscles (Figure 6.3, compare A with B).

As shown in Figure 6.4 (right column), 40-45% of the embryos now have a phenotype close to wild-type, when only 25-30% did with *Dmeso17A* alone (Figure 6.4, compare A with D). Embryos with a moderate phenotype represent 25-30% of the cases, whereas in embryos over-expressing *Dmeso17A* alone only 15-20% have a moderate phenotype (Figure 6.4, compare B with E). Finally, the proportion of embryos severely

*UAS-Dmeso17A X twist/twist-GAL4*

*UAS-Dmeso17A; UAS-Dmef2 X  
twist/twist-GAL4*



**Figure 6.3: *Dmeso17A* genetically interacts with *Dmef2*.**

*Dmeso17A* and *Dmef2* were over-expressed together using *twist/twist-GAL4* at 18°C to test their genetic interaction. *Dmef2* rescues the *Dmeso17A* over-expression phenotype (A) towards wild-type (B).

affected is now reduced to 25-30%, whereas it represented more than 50% of the embryos over-expressing *Dmeso17A* alone (Figure 6.4, compare C with F). These results show that *Dmef2* can suppress the inhibitory effect of *Dmeso17A* over-expression and therefore that the two genes genetically interact.

This interaction of *Dmeso17A* with *Dmef2* is most clearly revealed by measuring the percentage of hatching and survival (Figure 6.5). 93.5% of the embryos over-expressing both *Dmeso17A* and *Dmef2* hatched, whereas 90% did with *Dmeso17A* alone. Most importantly, nearly 38% of the larvae are now able to survive until adulthood at 18°C, when only 18% survived with *Dmeso17A* over-expressed alone. These results clearly show a suppression of the *Dmeso17A* over-expression phenotype by *Dmef2*. It rescues the lethality and confirms that both genes genetically interact. Together with all my results, this implies that *Dmeso17A* inhibitory effect on muscle differentiation is centered on *Dmef2*. *Dmef2* might therefore be a target for *Dmeso17A* action.

In addition to these results, I over-expressed *Dmeso17A-RNAi* in the *Dmef2*<sup>65</sup> mutant background. The idea was that the reduction of *Dmeso17A* level might compensate the loss of *Dmef2* activity. However, as shown in Figure 6.6, the over-expression of *Dmeso17A-RNAi*, driven by *Dmeso17A-GAL4* at 25°C, did not rescue the *Dmef2*<sup>65</sup> phenotype (compare A-B with C-D). This suggests that the reduction of *Dmeso17A* level is not sufficient to balance the loss of *Dmef2* activity. This result will be discussed further in section 6.5.1.

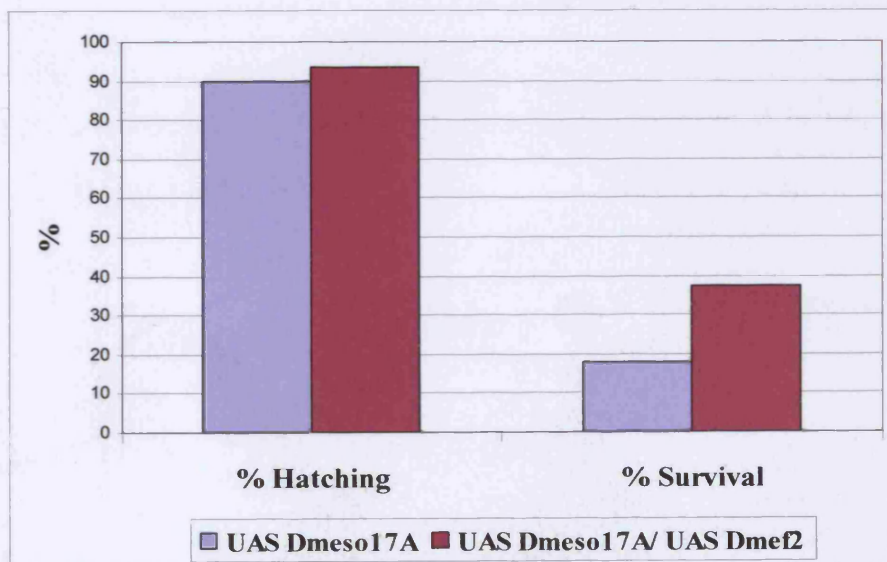
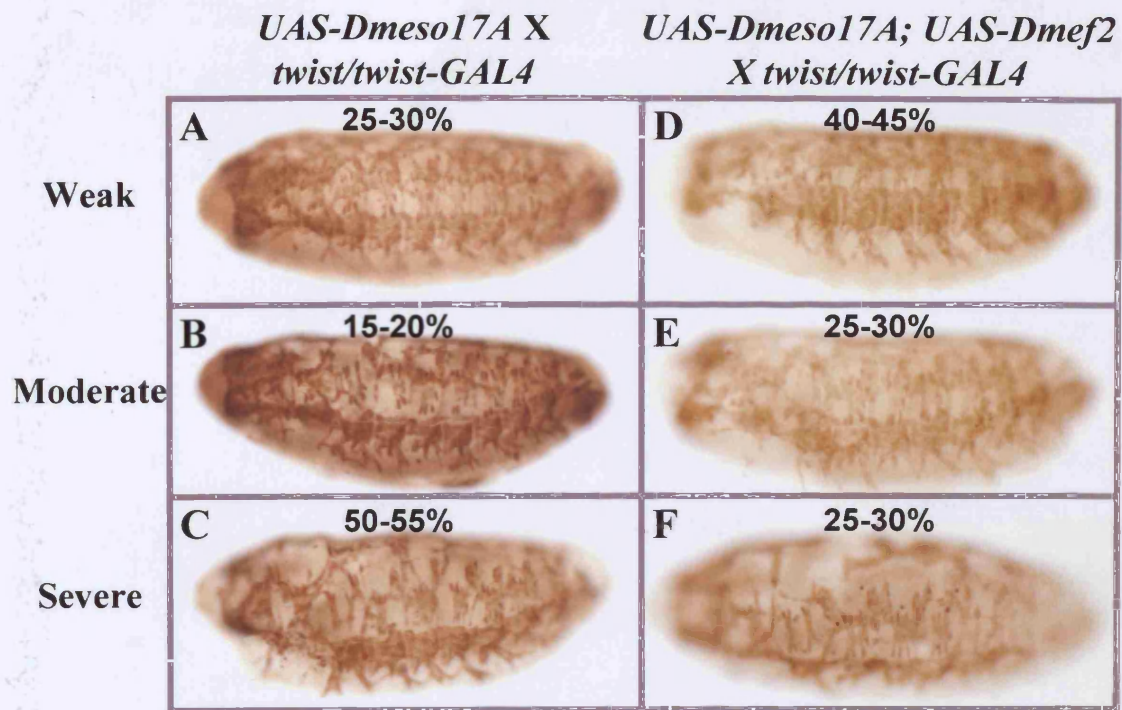


**Figure 6.4: *Dmef2* suppresses the inhibitory effect induced by *Dmeso17A* over-expression.**

*Dmeso17A* and *Dmef2* were over-expressed together using *twist/twist-GAL4* at 18°C to test their genetic interaction. (A-C) Variation of phenotype in *Dmeso17A* over-expressing embryos (categories are the same as in figure 4.2). (D-F) *Dmef2* suppresses the inhibitory effect of *Dmeso17A* over-expression. Embryos have more correctly shaped muscles. The proportion of embryos with weak (D) and moderate (E) phenotype has considerably increased, whereas the number of severely affected embryos (F) is reduced (compare with A, B and C respectively).

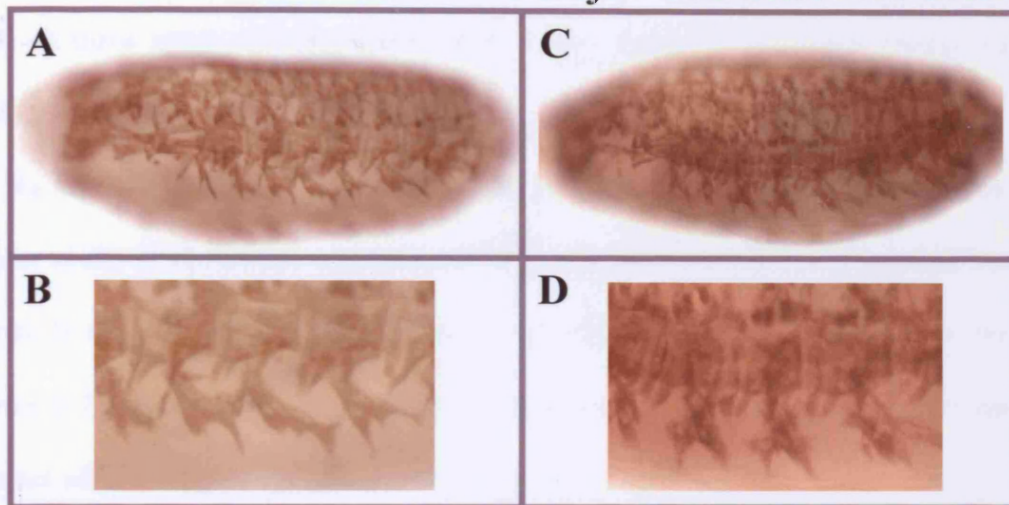
**Figure 6.5: *Dmef2* suppresses the lethality induced by *Dmeso17A* over-expression.**

The larval hatching and survival assay was carried out as described in Figure 4.4. The percentage of hatching of larvae over-expressing both *Dmeso17A* and *Dmef2* does not change substantially compared to that obtained with *Dmeso17A* alone. However, the percentage of survival is substantially increased. Mean percentages  $\pm$  S.D are: *Dmeso17A*, Hatching=90%  $\pm$  0.24, Survival=18%  $\pm$  0.31; *Dmeso17A+Dmef2*, Hatching=93.5%  $\pm$  0.094, Survival=37.6%  $\pm$  0.21.



*Dmef2*<sup>65</sup>

*UAS-Dmeso17A-RNAi*;  
*Dmef2*<sup>65</sup> X *Dmeso17A-GAL4*



**Figure 6.6:** *Dmeso17A-RNAi* does not rescue the *Dmef2*<sup>65</sup> mutant phenotype.

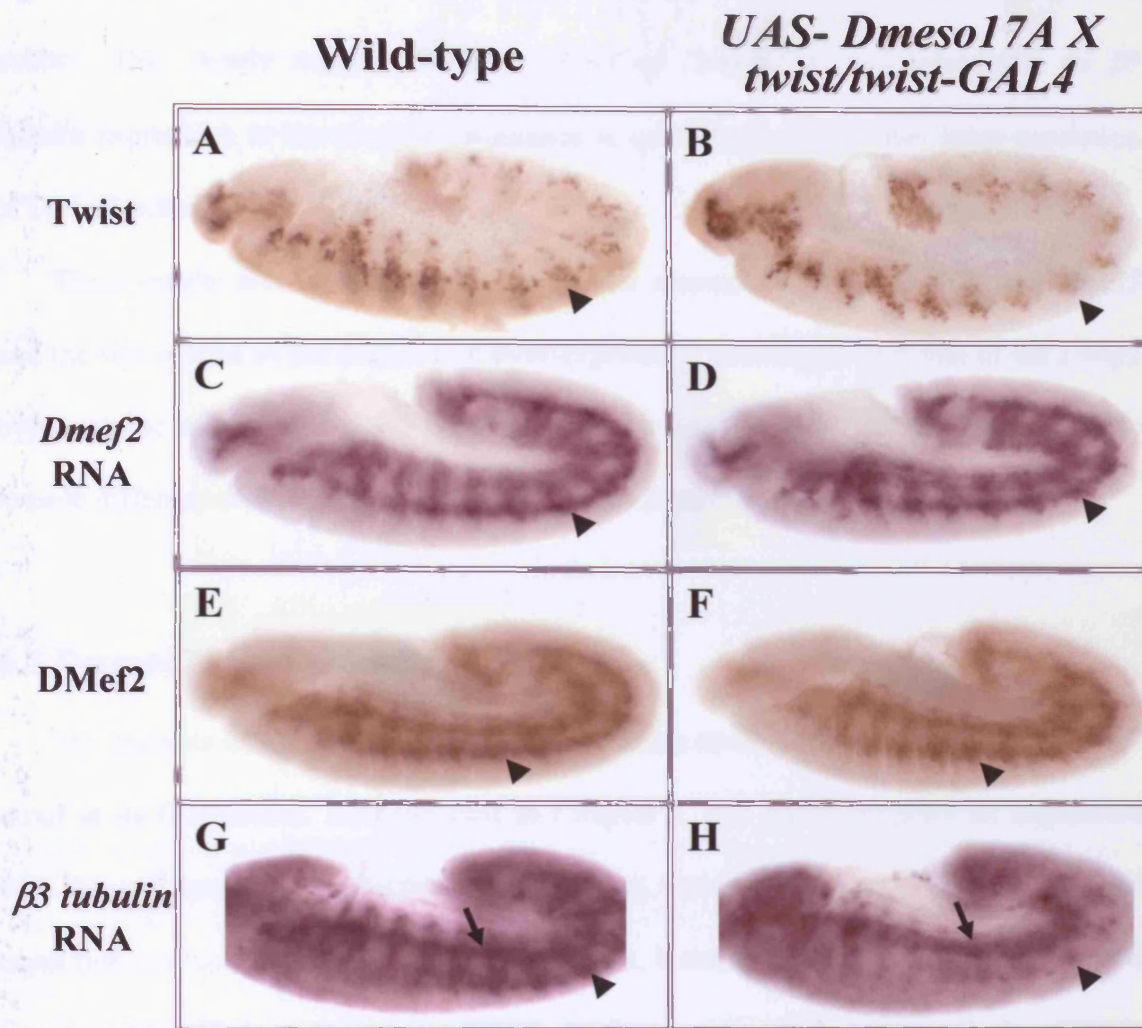
To investigate further the link between *Dmeso17A* and *Dmef2*, *Dmeso17A-RNAi* was over-expressed in a *Dmef2*<sup>65</sup> mutant background using *Dmeso17A-GAL4* at 25°C. *w*; *Dmef2*<sup>65</sup>/*CyO*,*lacZ*; *UAS-Dmeso17A-RNAi*/*UAS-Dmeso17A-RNAi* males were crossed with *w*; *Dmef2*<sup>65</sup>/*CyO*,*lacZ*; *Dmeso17A-GAL4*/*Dmeso17A-GAL4* virgin females. Progeny embryos were double stained with anti-Myosin and anti-βgalactosidase antibodies. Stage 17 embryos lacking *lacZ* expression (*w*; *Dmef2*<sup>65</sup>/*Dmef2*<sup>65</sup>; *Dmeso17A-GAL4*/*Dmeso17A-RNAi*) were selected and analysed. The *Dmef2*<sup>65</sup> mutant phenotype (A-B) is not rescued by *Dmeso17A-RNAi* (C-D).

### 6.2.3 *Dmeso17A* down-regulates DMef2 activity

The preceding sections show a close relationship between *Dmeso17A* and *Dmef2* and suggest the possibility that *Dmef2* might be a target for *Dmeso17A*. If that is the case, there are two possibilities. *Dmeso17A* could either affect *Dmef2* expression or activity. I tested these two possibilities in embryos over-expressing *Dmeso17A* using the *twist/twist-GAL4* driver at 25°C. To do so, I analysed the expression of Twist, *Dmef2* (RNA and protein) and *β3 tubulin* in these embryos. I examined stage 11 to 13 embryos when all three genes are expressed (Bate, 1993; Taylor et al., 1995; Buttgereit et al., 1996).

No effect was found on the expression of Twist, the upstream regulator of *Dmef2* (Taylor et al., 1995; Cripps and Olson, 1998), nor on *Dmef2* RNA (Figure 6.7, compare A with B and C with D). DMef2 protein expression is also comparable to wild type (Figure 6.7, compare E with F). These results show that *Dmeso17A* over-expression does not affect *Dmef2* expression.

However, as revealed by *β3 tubulin* expression, there was an effect on DMef2 activity (Figure 6.7 G-H). *β3 tubulin* is a direct target of DMef2 in the somatic mesoderm (Damm et al., 1998), its expression therefore reflects DMef2 activity. In embryos over-expressing *Dmeso17A*, whereas Twist and DMef2 expression are comparable to wild type, *β3 tubulin* expression is substantially reduced in somatic mesoderm (Figure 6.7 arrowheads, compare G with H). This result shows that *Dmeso17A* over-expression can down-regulate DMef2 activity. Variations, probably due to the use of the GAL4/UAS system, are observed in the extent to which *β3 tubulin* expression is affected. Nevertheless, the embryo shown in Figure 6.7H represents more than 45% of the cases. In addition, *β3 tubulin* expression in visceral mesoderm and the heart precursors is normal in embryos over-expressing *Dmeso17A* (Figure 6.7, arrows in



**Figure 6.7: *Dmeso17A* down-regulates DMef2 activity.**

Expression of Twist protein (A-B), *Dmef2* RNA and protein (C-F) or  $\beta 3$ -tubulin RNA (G-H) was assessed at stage 12 in both wild-type and embryos over-expressing *Dmeso17A* driven by *twist/twist-GAL4* at 25°C. (A-B) Embryos were stained with an anti-Twist antibody. Twist expression is comparable in the wild-type (A) and when *Dmeso17A* is over-expressed (B) (arrowheads). (C-F) Whole mount *in situ* hybridisation using a *Dmef2* RNA probe (C-D) and anti-DMef2 staining (E-F) were carried out to assess *Dmef2* expression. In both cases, expression in *Dmeso17A*-over-expressing embryos is comparable to wild-type (arrowheads) (compare C with D, and E with F). (G-H) Whole mount *in situ* hybridisation using a  $\beta 3$ -tubulin RNA probe. In the wild-type (G)  $\beta 3$ -tubulin is expressed in the somatic (arrowhead) and visceral (arrow) mesoderm. In embryos over-expressing *Dmeso17A* (H),  $\beta 3$ -tubulin expression is strongly reduced in the somatic mesoderm (arrowhead) where it is a DMef2 target, but is normal in the visceral mesoderm (arrow) where it is not.

G and H point at the visceral mesoderm). Expression of  $\beta 3$  tubulin in these tissues is not regulated by DMef2 (Damm et al., 1998), and therefore provides a convenient internal control. This clearly suggests that the effect of *Dmeso17A* over-expression on  $\beta 3$  tubulin expression in the somatic mesoderm is specifically due to the down-regulation of DMef2 activity.

These results are consistent with the genetic interaction of *Dmeso17A* with *Dmef2* and the similarities of the *Dmeso17A* over-expression phenotype with that of the *Dmef2* hypomorphic alleles. All these together, strongly suggest that *Dmeso17A* acts in the muscle differentiation pathway to down-regulate DMef2 activity.

### 6.3 *Dmeso17A* and *groucho*

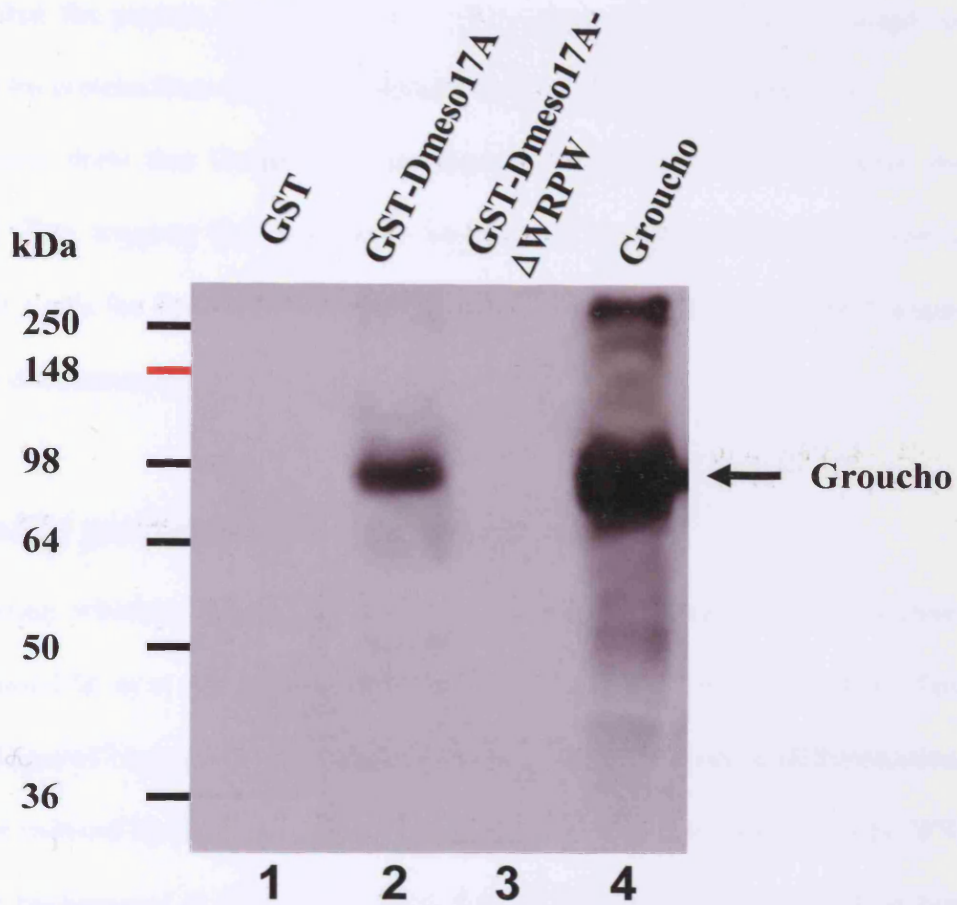
My analysis of the *Dmeso17A* protein sequence revealed the presence of a WRPW motif at its C-terminus. As discussed in Chapter 3, this motif suggests an interaction with the well-known co-repressor Groucho (Gro). Gro is the key member of a family of transcriptional co-repressors found in flies, mice, humans, frogs and worms (Fisher and Caudy, 1998; Chen and Courey, 2000). In *Drosophila*, it is expressed ubiquitously (Delidakis et al., 1991; Maier et al., 1993), and it is involved in diverse embryonic developmental processes such as segmentation, sex determination and terminal patterning (Fisher and Caudy, 1998, Parkhurst, 1998, Chen and Courey, 2000). Other studies have shown that *gro* function is critical for normal wing patterning (de Celis and Ruiz-Gomez, 1995; Heitzler et al., 1996). In vertebrates, the homologs of *Drosophila* Gro, the transducin-like Enhancer of split (TLE) proteins, contribute to regulation of neuronal development, skeletogenesis, hematopoiesis and might be implicated in myogenesis (reviewed in Gasperowicz and Otto, 2005).

Gro is a non-DNA binding protein and is recruited to DNA via protein-protein interactions with a large variety of transcriptional repressors. For example, Gro is required for repression by the members of the Hairy family of bHLH transcriptional repressors. Hairy, the main member of this family, regulates neurogenesis and segmentation (Rushlow et al., 1989) and recruits Gro via its C-terminal WRPW tetrapeptide motif (Paroush et al., 1994; Fisher et al., 1996). The WRPW motif has been shown to be necessary and sufficient to mediate protein-protein interaction with Gro (Paroush et al., 1994; Fisher et al., 1996). Once recruited to DNA, Gro can mediate repression by recruiting the class I histone deacetylase, HDAC1, which in *Drosophila* is encoded by the *rpd3* gene (Chen et al., 1999; for review see Courey and Songtao, 2001, Gasperowicz and Otto, 2005).

Although it does not possess a bHLH or a DNA binding domain, *Dmeso17A* could interact with Gro through its WRPW motif. I have explored the possibility of a link between *Dmeso17A* and Gro and the strategy adopted is divided in two parts. First, I have tested whether the two proteins could physically interact. A GST-pull-down assay was used for this. Second, using the GAL4/UAS system, I have tested whether *Dmeso17A* and *gro* genetically interact *in vivo*. To do so, I have over-expressed *Dmeso17A* in a *gro* mutant background. These results are described in the following sections.

### 6.3.1 *Dmeso17A* physically interacts with Gro

To test whether *Dmeso17A* and Gro could interact and if the WRPW motif is required for this interaction, I compared the ability of full length *Dmeso17A* and *Dmeso17A*- $\Delta$ WRPW to bind Gro *in vitro*. Full length and truncated forms of *Dmeso17A* were expressed in bacteria as glutathione S-transferase (GST) fusions,



**Figure 6.8: *Dmeso17A* binds to Gro *in vitro* and requires its WRPW motif for this interaction.**

Radiolabelled Gro was incubated with GST (Lane 1), GST-Dmeso17A (Lane 2) or GST-Dmeso17A- $\Delta$ WRPW (Lane 3), all bound to glutathione-sepharose beads. Retained Gro protein was visualised by SDS-PAGE and autoradiography. Whereas, full length Dmeso17A can bind Gro (Lane 2), the absence of the WRPW motif prevents this interaction (Lane 3). GST alone did not retain Gro (Lane 1). A sample of radiolabelled Gro was loaded as a control (Lane 4).



immobilised on glutathione sepharose beads and tested for their capacity to bind radiolabelled Gro protein. As shown in Figure 6.8, full length Dmeso17A can bind Gro (lane 2), whereas neither Dmeso17A- $\Delta$ WRPW (lane 3) nor the control (GST) (lane 1) do. To show that the protein binding to Dmeso17A corresponds to Gro, a sample of radiolabelled Gro protein from the TNT reaction was loaded as a control (lane 4).

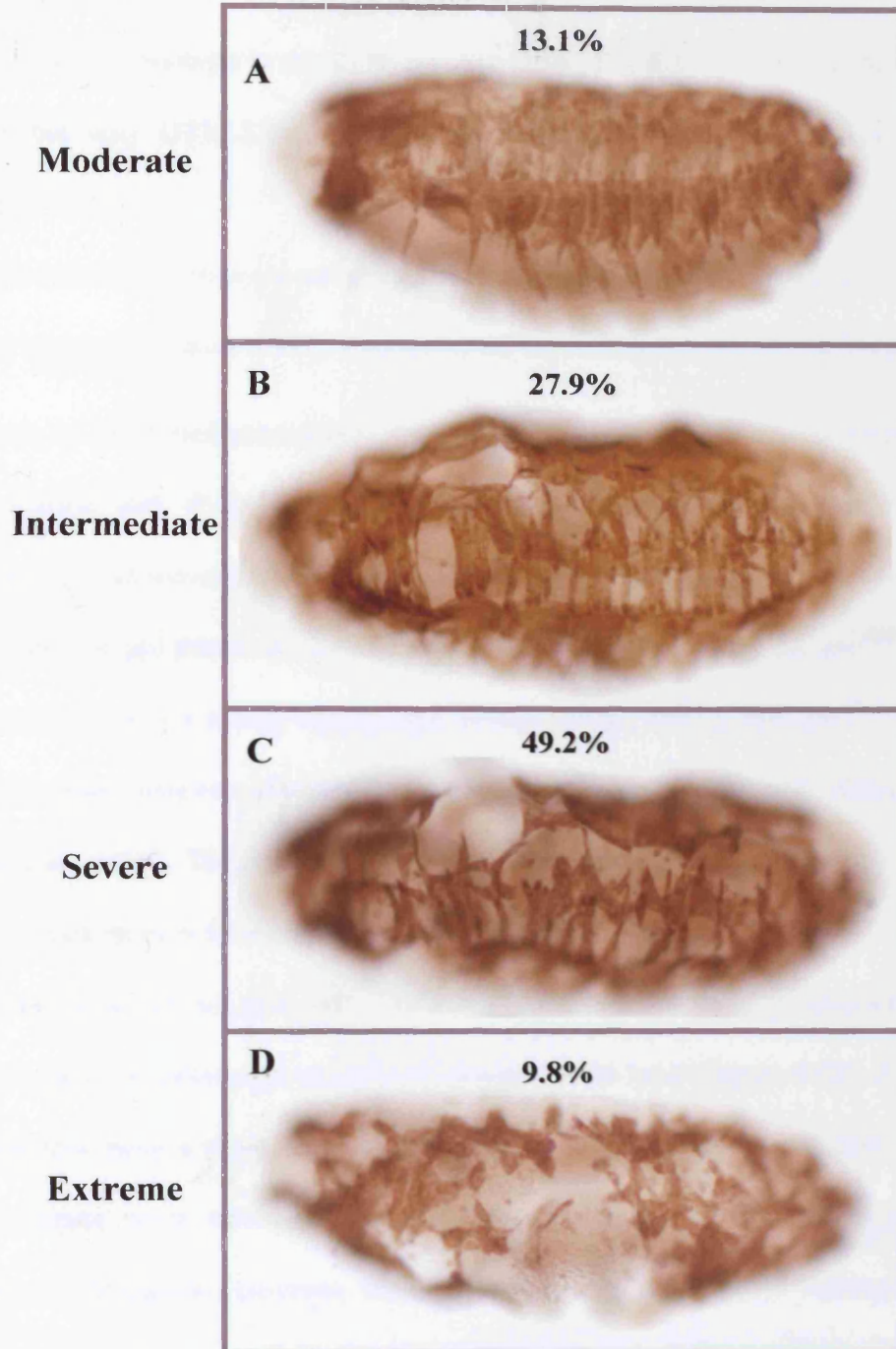
These results show that Dmeso17A can interact with Gro, and this requires the WRPW motif. This suggests that Gro might be required for Dmeso17A action and is consistent with a role for Dmeso17A in the inhibition of transcription of DMef2 targets during muscle differentiation.

### 6.3.2 *Dmeso17A* genetically interacts with *groucho*

To determine whether *Dmeso17A* and *gro* genetically interact *in vivo*, I over-expressed *Dmeso17A* in a *gro* mutant background using the *twist-GAL4* driver. This tests whether Dmeso17A requires *gro* function in order to inhibit muscle differentiation. The phenotype induced by the over-expression of *Dmeso17A* using *twist-GAL4* at 25°C in a wild type background is shown in Figure 6.9. As described in Chapter 4 section 4.2.1, when using *twist/twist-GAL4*, the over-expression of *Dmeso17A* using *twist-GAL4* gives a variable phenotype. Four categories of phenotype are observed, which I describe as moderate, intermediate, severe and extreme:

- 13.1% of the embryos have a moderate phenotype (Figure 6.9A). In these embryos, most muscles form correctly, with the exception of VO4-6 and VA3. Occasionally, there are defects in other muscles.
- When the phenotype is intermediate, in 27.9% of the cases, more muscles form correctly (Figure 6.9B). In most of these embryos, the dorsal muscles (DO1-5, DA1-

*UAS-Dmeso17A X twist-GAL4*



**Figure 6.9: Muscle phenotype variations in embryos over-expressing *Dmeso17A* driven by *twist-GAL4*.**

*Dmeso17A* was over-expressed using *twist-GAL4* at 25°C. A range of phenotype is observed: (A) moderate. Most muscles are present and correctly shaped. (B) Intermediate. More muscles are missing or misshapen. (C) Severe. The muscle pattern is considerably affected. (D) Extreme. No muscle is formed correctly. The proportion of each category is given.




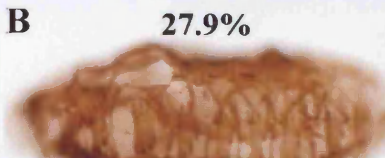

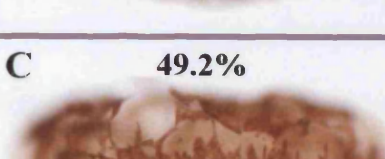
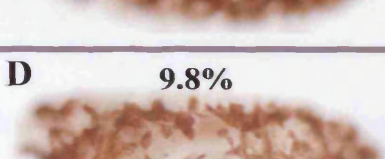
3) are affected and can be missing or misshapen. VO muscles are also misshapen most of the time.

- The severe phenotype is the most common (49.2% of the embryos). Some muscles form but only DT1, LTs, VLs and some dorsal muscles are clearly identifiable (Figure 6.9C).
- In the extreme phenotype category, although some myosin is expressed, no muscles form correctly (Figure 6.9D). This category represents 9.8% of the embryos analysed.

Thus, as described previously, the over-expression of *Dmeso17A* inhibits muscle differentiation and, if *gro* is required for *Dmeso17A* action, one might expect the absence of *gro* to prevent this effect and the muscle phenotype to be close to wild type.

To remove *gro* function, I used a combination of two *gro* alleles. *gro*<sup>E48</sup>, which is a point mutation and a strong hypomorph (Preiss et al., 1988), and *gro*<sup>BX22</sup>, which is a deficiency that removes several genes from the Enhancer of split (*E(spl)*) complex (Preiss et al., 1988). The reason for using a point mutation and a deficiency is to ensure that *gro* function only is removed.

In the absence of *gro*, the inhibitory effect of *Dmeso17A* over-expression is prevented and the phenotype is rescued towards wild type (Figure 6.10). 24.4% of the embryos now have a weak phenotype which is close to wild type (Figure 6.10E). No such embryos were observed when *Dmeso17A* is over-expressed in a wild-type background. Moreover, embryos with a moderate phenotype now represent 63.4% of the cases, in contrast to 13.1% in *Dmeso17A*-over-expressing embryos (Figure 6.10, compare A with F). Finally, the intermediate phenotype category of embryos is now reduced to 12.2% (Figure 6.10, compare B and G) and there are no embryos with severe and extreme phenotype.

	<i>UAS-Dmeso17A X twist-GAL4</i>	<i>UAS-Dmeso17A; gro<sup>E48</sup>/gro<sup>BX22</sup> X twist-GAL4</i>
Weak		<b>E</b> 24.4% 
Moderate	<b>A</b> 13.1% 	<b>F</b> 63.4% 
Intermediate	<b>B</b> 27.9% 	<b>G</b> 12.2% 
Severe	<b>C</b> 49.2% 	
Extreme	<b>D</b> 9.8% 	

**Figure 6.10: *Dmeso17A* genetically interacts with *gro*.**

In order to test a genetic interaction, *Dmeso17A* was over-expressed using *twist-GAL4* at 25°C in a *gro<sup>E48</sup>/gro<sup>BX22</sup>* mutant background. *w; UAS-Dmeso17A/UAS-Dmeso17A; gro<sup>BX22</sup>/TM3,GFP* males were crossed with *w; twist-GAL4/twist-GAL4; gro<sup>E48</sup>/TM3,GFP* virgin females. Progeny embryos were double stained with anti-Myosin and anti-GFP antibodies. Stage 17 embryos lacking GFP expression (*w; twist-GAL4/UAS-Dmeso17A; gro<sup>E48</sup>/gro<sup>BX22</sup>*) were selected and analysed. (A-D) Variation of phenotype in *Dmeso17A* over-expressing embryos (categories are the same as in figure 6.9). (E-G) The absence of zygotic *gro* suppresses the inhibitory effect of *Dmeso17A*. 24.4% of the embryos now have a weak phenotype (E) and the proportion of embryos with moderate phenotype (F) has considerably increased. Furthermore, the number of embryos with an intermediate phenotype is reduced (G), and there are no severely or extremely affected embryos (compare with A-D).

Unfortunately, I have not been able to apply the hatching and survival test to these embryos. As mentioned earlier, *gro* is implicated in a wide variety of developmental processes and although 96% of the embryos carrying the *gro*<sup>E48</sup>/*gro*<sup>BX22</sup> are able to hatch, they all die before pupation (Delidakis et al., 1991).

Nevertheless, together my results show that *Dmeso17A* and *gro* genetically and physically interact and that *Dmeso17A* requires *gro* function to inhibit muscle differentiation. This, together with the fact that *Dmeso17A* can down-regulate *DMef2* activity, suggest that *Dmeso17A* and *Gro* act in the same complex to inhibit the transcription of *DMef2*-regulated genes during muscle differentiation.

### 6.3.3 The loss of *gro* function affects muscle development

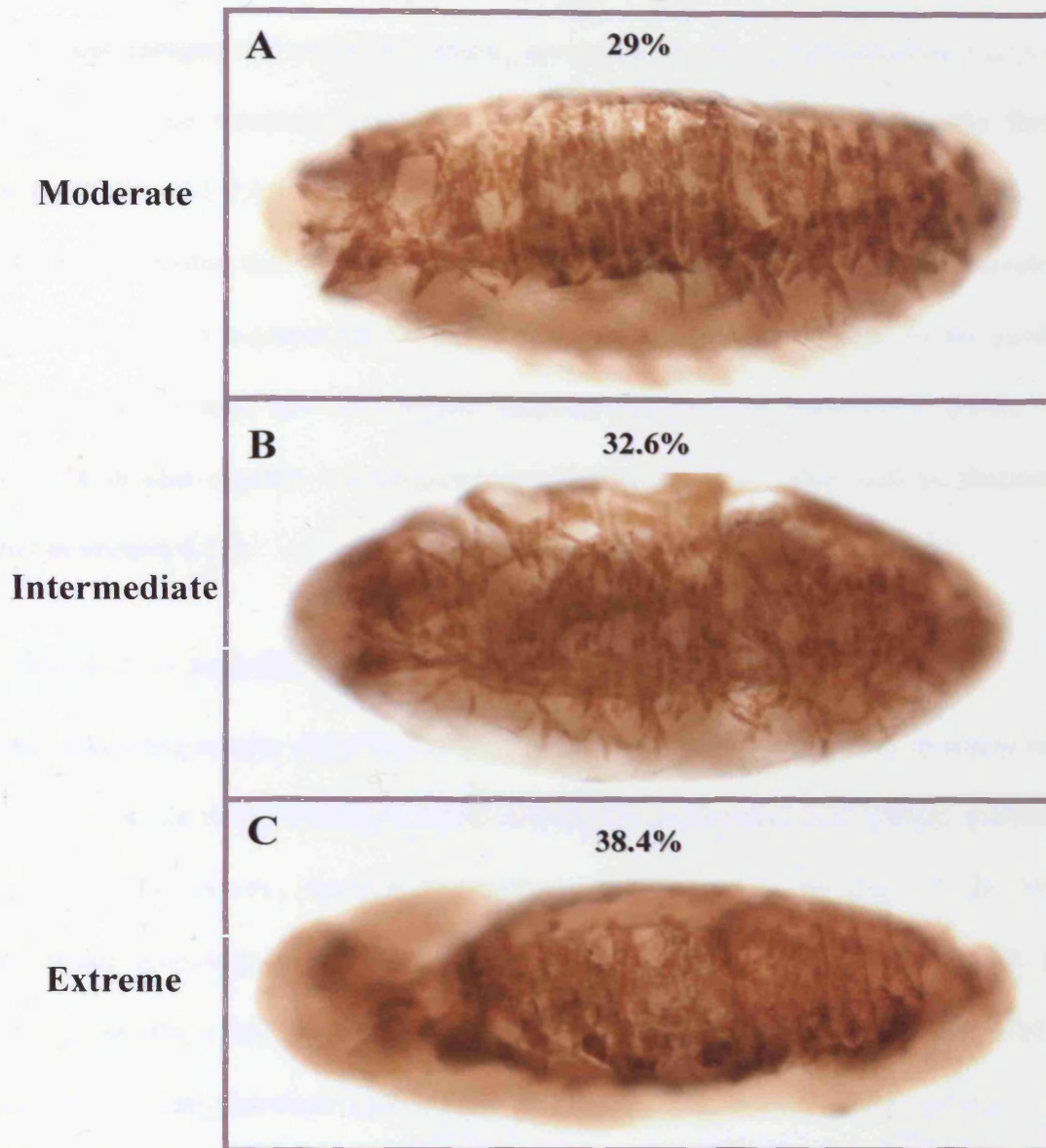
Although, in mammalian cell culture, there are indications that members of the TLE family might be implicated in myogenesis (Sasai et al., 1992; Gao et al., 2001; reviewed in Gasperowicz and Otto, 2005), there is no such evidence for *Gro* in *Drosophila* and no muscle phenotype has been recorded for *gro* mutant so far. However, my results indicate that *gro* plays a role in muscle development. It was therefore necessary to examine the muscle pattern in *gro* mutant embryos.

As shown in Figure 6.11, muscle myosin staining revealed that these mutants have a muscle phenotype. This phenotype is variable and the embryos can be classified into 3 categories according to the severity of the muscle defects.

The first category, which represents 29% of the embryos analysed, has a moderate phenotype (Figure 6.11A). Muscles form correctly with the exception of VL1-2, V5-6 and VA3. Occasionally, there are defects in other muscles.

The second category has an intermediate phenotype and represents 32.6% of the embryos analysed. In these embryos, the most dorsal muscles (DO1-2, DA1-2) and the

*gro*<sup>E48</sup>/*gro*<sup>BX22</sup>



**Figure 6.11: The *gro* mutant muscle phenotype.**

*w*; +/+; *gro*<sup>BX22</sup>/*TM3*,*GFP* males were crossed with *w*; +/+; *gro*<sup>E48</sup>/*TM3*,*GFP* virgin females. Progeny embryos were double stained with anti-Myosin and anti-GFP antibodies. Stage 17 embryos lacking GFP expression (*w*; +/+; *gro*<sup>E48</sup>/*gro*<sup>BX22</sup>) were selected and analysed. In the absence of zygotic *gro*, muscle development is affected and a range of phenotype is observed: (A) moderate. Only a few muscles are affected. (B) Intermediate. More muscles are missing or misshapen. (C) Extreme with no muscle formed correctly. The proportion of each category is given.

most ventral ones (VO4-6, VA1-3) are affected (Figure 6.11B). They are most of the time misshapen, but can also be missing. Defects in VL and LT muscles formation have also been observed.

The last category of embryos, which represents 38.4% of the embryos analysed, corresponds to an extreme phenotype. Myosin is expressed but no muscle forms correctly (Figure 6.11C).

This result shows that the absence of *gro* affects muscle development and therefore indicates that *gro* is required for the process. Moreover, it suggests that, in my genetic interaction experiment, not only is *gro* function required for *Dmeso17A* action, but *Dmeso17A* is also capable of compensating the loss of *gro*. This will be discussed further in section 6.5.2.

#### **6.4 *Dmeso17A* and HDAC**

My preceding results show that *Dmeso17A* physically and genetically interacts with *gro* and that it can down-regulate DMef2 activity. In mammalian cell culture, members of the Gro/TLE family, through interactions with HES1, a member of the HES (mammalian homologs of *Drosophila* Hairy and E(spl)) family, might inhibit the activity of MyoD, a key regulator of myogenesis (Weintraub et al., 1991, reviewed in Taylor, 2005), and therefore inhibit myogenesis (Sasai et al., 1992; reviewed in Gasperowicz and Otto, 2005). However, there is no record, *in vitro* or *in vivo*, of a direct link between Gro/TLE and Mef2 that would regulate myogenesis. Moreover, *Dmeso17A* does not possess a DNA binding domain or a Mef2 binding domain such as that described for the transcriptional co-regulator Cabin1 or classII HDACs (Miska et al., 1999; Lu et al., 2000; Han et al., 2003; Han et al., 2005; reviewed in Yang and Grégoire, 2005). Therefore there may be another protein that provides a link between

the Dmeso17A/Gro complex and DMef2. One possibility for such factors is members of classII HDACs, HDAC4 and HDAC5.

HDACs function as transcriptional repressors. They catalyse the deacetylation of histone and non histone proteins to create transcriptionally silent domains (Flores-Saaib and Courey, 2000; Thiagalingam et al., 2003). In vertebrates, classII HDACs interact with a wide variety of transcription factors and co-repressors (reviewed in Yang and Grégoire, 2005). In particular, HDAC4 and HDAC5 have been shown to directly bind to Mef2 and to repress its activity in cell cultures (Miska et al., 1999; Lemercier et al., 2000; Lu et al., 2000). Binding of these HDACs to Mef2 is mediated by a conserved 18 amino acids at their N-terminus (Miska et al., 1999; Lu et al., 2000; Han et al., 2005; reviewed in Yang and Grégoire, 2005). Another cell culture study showed that, once bound to Mef2, HDAC4 or 5 can promote its sumoylation and perhaps its phosphorylation, independently of their deacetylase activity. This results in the inhibition of Mef2 transcriptional activity (Grégoire and Yang, 2005). The activity of these HDACs is regulated by the phosphorylation of two serine residue by calcium/calmodulin-dependent protein Kinase (CaMK). When phosphorylated, these sites recruit the chaperone protein 14-3-3 and the complex HDAC/14-3-3 is exported out of the nucleus this results in the de-repression of Mef2-regulated genes (Grozinger et al., 2000; McKinsey et al., 2000 a and b; Wang et al., 2000). In addition to CaMK, a recent cell culture study revealed that HDAC5 phosphorylation and therefore activity can be regulated by a broad range of signalling pathways and transcriptional regulators. They suggest that HDAC5 (and other classII HDAC) is a point of convergence of diverse signalling cascades to regulate the expression of specific target genes (Chang et al., 2005).



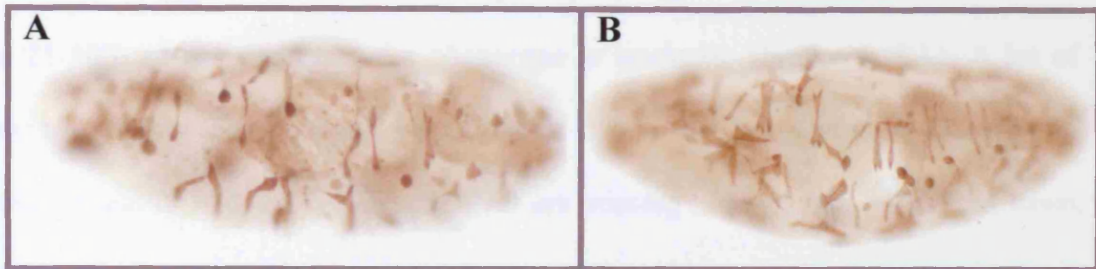
In *Drosophila*, there are only two classII HDACs, *dHDAC4* and *dHDAC6*. *dHDAC4* is involved in segmentation and is an ortholog of human HDAC4 with which it shares 36% amino acid identity overall and 64% in the catalytic domain (Zeremski et al., 2002). Most importantly, the Mef2 binding domain and the two serine residues, necessary for HDAC4 activity regulation, are conserved in *dHDAC4* (Zeremski et al., 2002, reviewed in Yang and Grégoire, 2005). This suggests that *dHDAC4* might act like its vertebrate orthologs to down-regulate DMef2 activity.

Moreover, in *Drosophila*, Gro can bind to the classI HDAC encoded by the *rpd3* gene. Rpd3 deacetylase activity is necessary for Gro mediated repression (Chen et al, 1999; for review see Courey and Songtao, 2001, Gasperowicz and Otto, 2005). No interaction between Gro/TLE proteins and classII HDACs has been reported in vertebrates or *Drosophila*. Nevertheless, the interaction of Gro with Rpd3, and the regulation of Mef2 activity by classII HDACs suggest that the link between the *Dmeso17A*/Gro complex and DMef2 could be an HDAC. Thus, I now wanted to test whether *Dmeso17A* interacts with HDAC.

#### **6.4.1 The HDAC over-expression phenotype resembles that of *Dmeso17A***

Besides the facts suggesting a link with *Dmeso17A*, preliminary experiments performed by another group suggested that over-expressing Human-HDAC5 disrupts myogenesis (Olson E.N., unpublished results). I therefore used the *UAS-hHDAC5* line available (a gift from Olson E.N.) to over-express this gene and compare the phenotype produced to that observed in *Dmeso17A* over-expression. This HDAC transgene contains a mutation in one of the phosphorylation sites necessary for HDAC5 nuclear export. It is therefore considered to be a constitutively active form of HDAC (for

*UAS-Dmeso17A X Dmef2-GAL4*      *UAS-hHDAC5 X Dmef2-GAL4*



**Figure 6.12: HDAC5 over-expression disrupts myogenesis.**

Flies homozygous for a *UAS-hHDAC5* construct were crossed to *Dmef2-GAL4* at 25°C to over-express *HDAC5* in the mesoderm. Stage 17 embryos were stained with an antibody anti-muscle Myosin. **(A)** Embryo over-expressing *Dmeso17A* using the same driver. **(B)** The effect of *hHDAC5* over-expression is similar to that produced by *Dmeso17A*.

HDAC5 phosphorylation and nuclear export see McKinsey et al., 2000 a and b). The GAL4 drivers I used in this experiment were *Dmef2-GAL4* and *twist-GAL4* at 18°C.

The expression of muscle myosin revealed that over-expression of *hHDAC5*, driven by *Dmef2-GAL4* at 25°C, results in myogenesis disruption that closely resembles the phenotype of *Dmeso17A* over-expression (Figure 6.12, compare A with B). However, the severity of the phenotype obtained using this driver is so extreme that the comparison is limited to the general aspect of the embryos. I therefore chose to use the *twist/twist-GAL4* driver, which with *Dmeso17A* gives a more moderate phenotype. Using this driver at 18°C, I obtained a variable phenotype with *hHDAC*, as was seen with *Dmeso17A*. Figure 6.13 shows the range of phenotypes obtained.



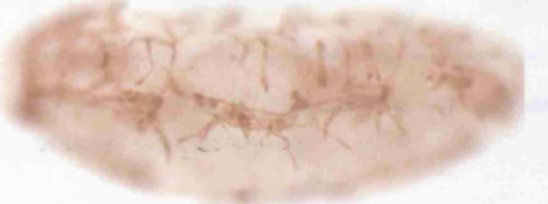
In 25-30% of the embryos, the phenotype is moderate (Figure 6.13A). A lot of muscles are missing or misshapen. For example, DT1 is misshapen in more than 80% of the embryos and DO3-5, LL1, LO1 and VA3 are missing in more than 70% of the cases.

In the most represented category (55-60% of the embryos), the phenotype is more severe (Figure 6.13B). DT1 is misshapen in more than 90% of the embryos, DA1-3, DO3-5, LL1, LO1, VA3 are missing in more than 50% of the case and ventrally 3 to 8 muscles are often present, but they are misshapen and hard to identify.

In the most severe category (10% of the embryos), only a few misshapen fibres can form (Figure 6.13C).




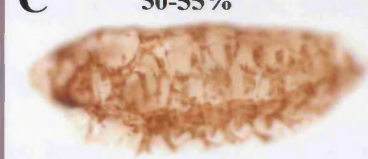
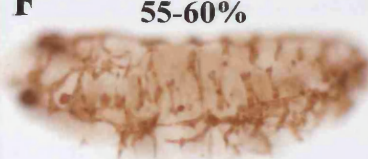


This phenotype is comparable to that obtained in embryos over-expressing *Dmeso17A* (Chapter 4 section 4.2.1). Figure 6.14 summarises the main similarities. Although the *hHDAC* phenotype is generally somewhat more severe than with *Dmeso17A*, similar variations in the phenotype are observed. The two most severe phenotype categories (Figure 6.14 C, F and D, G) represent the same proportion of embryos in both cases. The moderate phenotype category is present, but in a larger

***UAS-hHDAC-SA X twist/twist-GAL4***

<p><b>A</b></p> <p>25-30%</p> 	<p>DA2 missing in 40% of the embryos.</p> <p>DT1 misshapen in &gt;80%. DO3-5, LL1, LO1 and VA3 missing in &gt;70%.</p> <p>7-8 muscle present ventrally. VO4-6: often 1 or 2 present but always misshapen.</p>
<p><b>B</b></p> <p>55-60%</p> 	<p>DA1-2 missing in &gt;40% of the embryos.</p> <p>DT1 misshapen in &gt;90%. DA1-3, DO3-5, LL1, LO1 and VA3 are missing in &gt;50%.</p> <p>3-8 muscles present ventrally but misshapen.</p>
<p><b>C</b></p> <p>10%</p> 	<p>No muscle correctly formed</p>

**Figure 6.13: Muscle phenotype variations in embryos over-expressing *hHDAC5*.**

*hHDAC5* was over-expressed using *twist/twist-GAL4* at 18°C. Stage 17 embryos were stained with an antibody anti-muscle Myosin. A range of phenotype is observed: **(A)** Moderate. A lot of muscles are affected. **(B)** Severe. The number of muscles present and correctly shaped is considerably reduced. **(C)** Extreme. No muscles are formed correctly. The proportion of each category is given, as well as details of the muscle pattern defects.

	<i>UAS-Dmeso17A X</i> <i>twist/twist-GAL4</i>	<i>UAS-hHDAC-SA X</i> <i>twist/twist-GAL4</i>	
<b>Weak</b>	<b>A</b> 25-30% 		DT1 misshapen DO5 missing
<b>Moderate</b>	<b>B</b> 15-20% 	<b>E</b> 25-30% 	DT1 misshapen DO3, DO5, LL1 and VA3 missing
<b>Severe</b>	<b>C</b> 50-55% 	<b>F</b> 55-60% 	DT1, ventral muscles misshapen. DA1-3, DO3-5, LL1, LO1 and VA3 missing
<b>Extreme</b>	<b>D</b> 5-10% 	<b>G</b> 10% 	No muscle correctly formed

**Figure 6.14: Comparison of *Dmeso17A* and *hHDAC5* over-expression muscle phenotypes.**

*Dmeso17A* and *hHDAC5* were over-expressed using *twist/twist-GAL4* at 18°C. Stage 17 embryos were stained with an antibody anti-Myosin. (A-D) Variation of phenotype in *Dmeso17A* over-expressing embryos (categories are the same as in Figure 4.2). (E-G) Over-expression of *hHDAC5* produces a slightly more severe phenotype, but similar variations are observed. Embryos with a weak phenotype are absent. The proportion of moderately affected embryos (E) is more important than with *Dmeso17A* (compare with B). Severe (F) and extreme (G) phenotype categories represent the same proportion of embryos as in *Dmeso17A* over-expression (compare C with F and D with G). In both *Dmeso17A* and *hHDAC5* over-expressing embryos, particular muscles are affected in the same way. The main similarities are given in the right column.

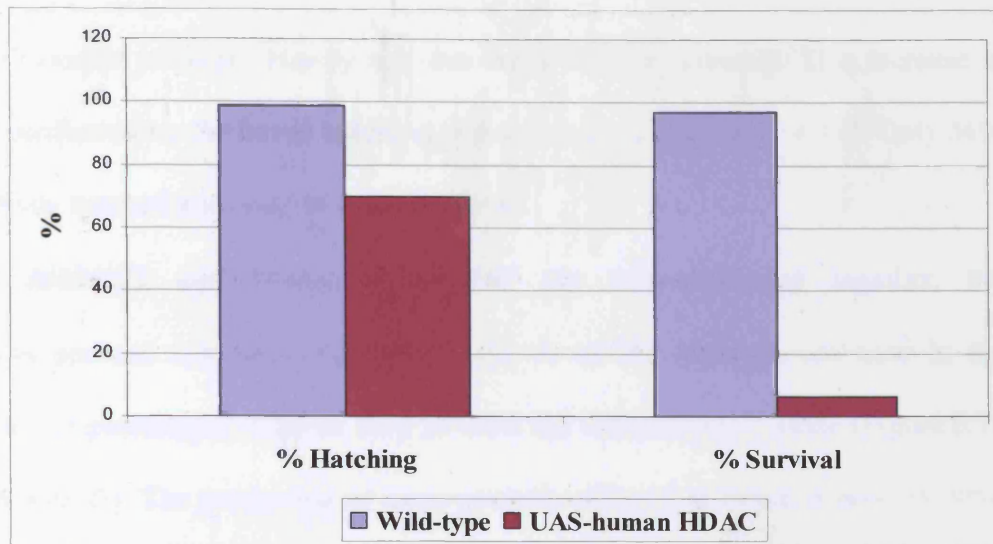
proportion in embryos over-expressing *hHDAC* (Figure 6.14, compare B and E). However, the weakest phenotype, is only observed in *Dmeso17A*-over-expressing embryos (Figure 6.14A). In addition to these comparable general muscle phenotypes, particular muscles are similarly affected in both *Dmeso17A* and *HDAC*-over-expressing embryos. For example, the most represented category of phenotype in both cases lack muscles such as DA1-3, DO3-5, LL1, LO1 and VA3. Also, DT1 and the ventral muscles are misshapen in most embryos (Figure 6.14, the main similarities for each category of phenotype are given in the right column).

The larval hatching and survival assay revealed that 70% of the embryos over-expressing *hHDAC* are able to hatch, but only 6.45 % survive (Figure 6.15). Analysis of the larvae under polarised light showed a pattern of muscle comparable to that in the embryo (Figure 6.16, compare A with B). Thus, as for *Dmeso17A* over-expression, embryos can hatch without a complete set of muscles, but in this case, the severity of the phenotype only allows a very small proportion to survive. Nevertheless, the similarities of the effects of *hHDAC5* and *Dmeso17A* over-expression suggest a possible interaction between the two genes

#### **6.4.2 *Dmeso17A* genetically interacts with *HDAC***

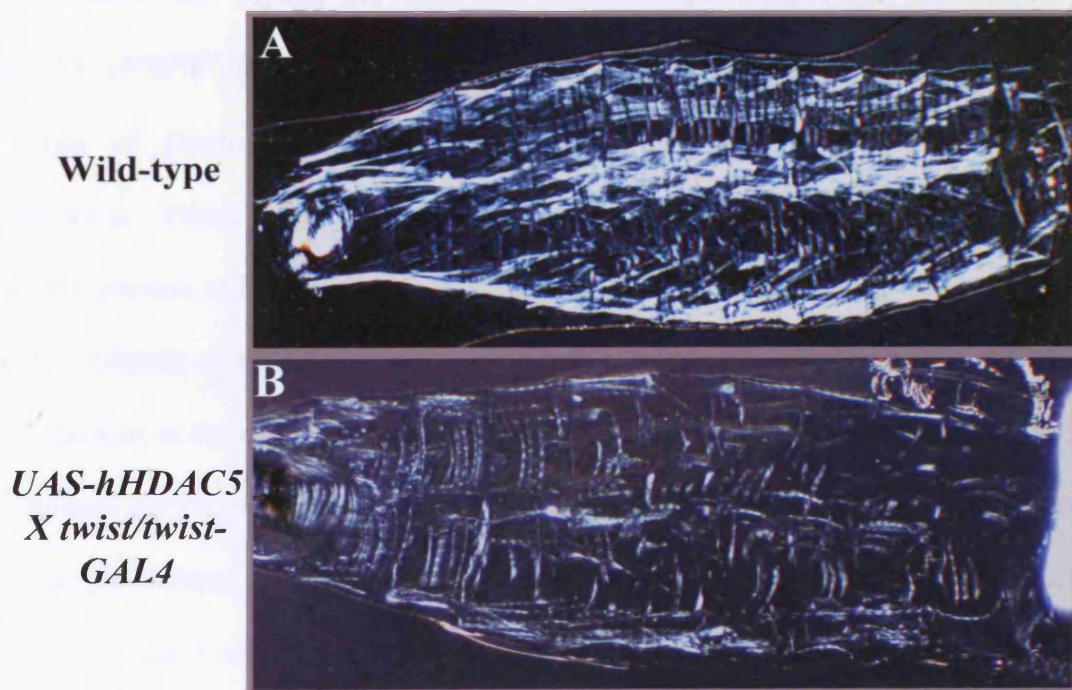
To test whether *Dmeso17A* and *hHDAC* can interact, I over-expressed both genes together and also used the dominant negative form of *Dmeso17A* (*Dmeso17A-ΔWRPW*) to try to rescue the phenotype induced by *hHDAC5* (Figure 6.17). *twist/twist-GAL4* was used as previously and crosses were kept at 18°C.

When both *Dmeso17A* and *hHDAC5* are over-expressed, muscle differentiation is more affected than with either alone. In more than 80% of the embryos, the number of myosin-expressing muscles is reduced compared to each gene over-expressed alone



**Figure 6.15: *hHDAC5* over-expression results in important larval lethality.**

A larval hatching and survival assay was carried out as described in Figure 4.4. The percentage of hatching of larvae over-expressing *hHDAC5*, although still high, is reduced compared to wild-type. The percentage of survival is dramatically reduced. Mean percentages  $\pm$  S.D are: wild-type, Hatching=99%  $\pm$  0.081, Survival=97%  $\pm$  0.16; *hHDAC5*, Hatching=70%  $\pm$  0.4, Survival=6.45%  $\pm$  0.32.



**Figure 6.16: *hHDAC5* over-expressing larvae can hatch with severe muscle defects.**

The muscle pattern of larvae over-expressing *hHDAC5* was analysed under polarised light. (A) Wild-type first instar larva with a normal pattern of muscle. (B) *hHDAC5* over-expressing larva. The muscle pattern is severely affected, as in Figure 6.13B, but that does not prevent hatching. The orientation is the same as in wild-type.

(Figure 6.17 central column). Hardly any muscle is formed correctly. This increase in severity is confirmed by the larval hatching and survival assay (Figure 6.18). Only 36% of the embryos hatched and none of them survived.

When *hHDAC5* and *Dmeso17A-ΔWRPW* are over-expressed together, the phenotype is rescued towards wild-type. 45-50 % of the embryos are now in the weakest class of phenotype, whereas only 25-30% are with *hHDAC5* alone (Figure 6.17, compare A with G). The proportion of more severely affected embryos is now 25-30%, whereas it is 55-60% when only *hHDAC5* is over-expressed (Figure 6.17, compare B and H). A dramatic phenotype is also observed in 20% of the embryos, but the effect is less extreme than with *hHDAC5* alone (Figure 6.17, compare C with I).

This rescue is confirmed by the larval hatching and survival assay (Figure 6.18). 85.6 % of the embryos are now able to hatch and 11.7% survived, whereas with *hHDAC5* alone the figures are 70% and 6.45% respectively. This indicates that *Dmeso17A-ΔWRPW* can suppress the lethality induced by *hHDAC5* and suggests that a diminution of *Dmeso17A* activity can prevent the *hHDAC5* effect on muscle differentiation. Taken together, these results show that *Dmeso17A* and *hHDAC5* genetically interact and supports the hypothesis in which HDAC could link *Dmeso17A* and *Gro* to *DMef2* to regulate muscle differentiation.

In addition to these results, Jun Han (a research assistant in the Taylor laboratory), has followed my experimental design, and tested whether *Dmeso17A-RNAi* could also rescue the phenotype induced by the over-expression of *hHDAC5*. Our analysis of her results shows that it can (Figures 6.19 and 6.20). Embryos expressing both *Dmeso17A-RNAi* and *hHDAC5* using *twist/twist-GAL4* at 18°C have more correctly shaped muscles compared to embryos over-expressing *hHDAC5* alone (Figure 6.19, compare A with B). Moreover, the hatching and survival test revealed that 39% of the embryos are now able

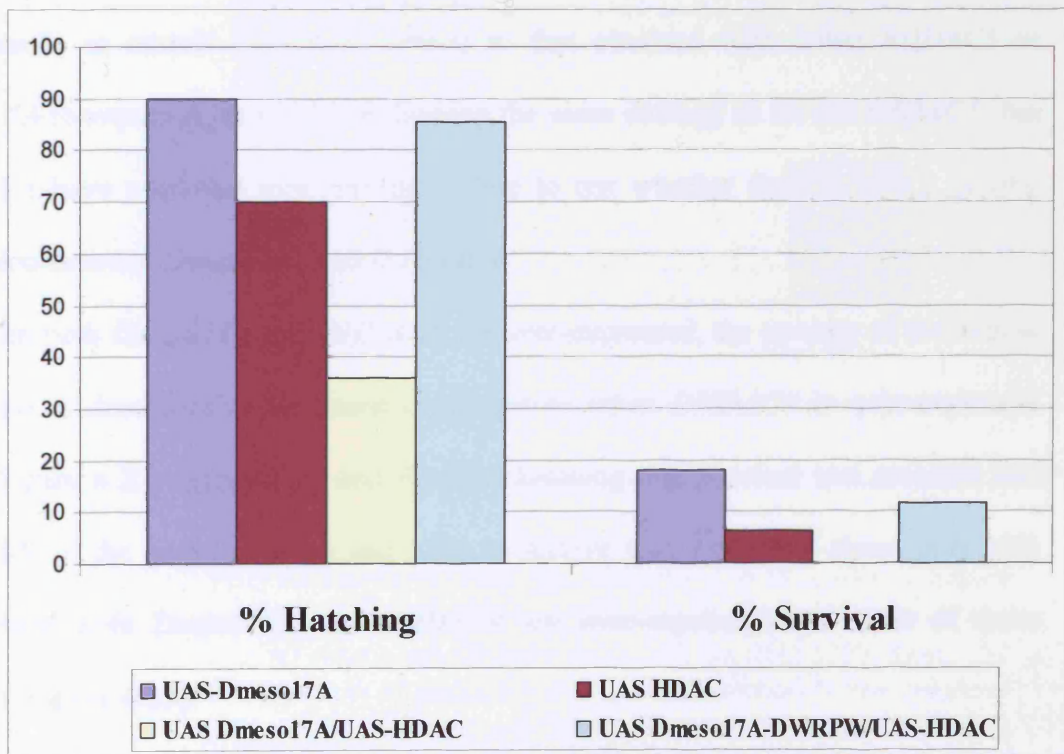
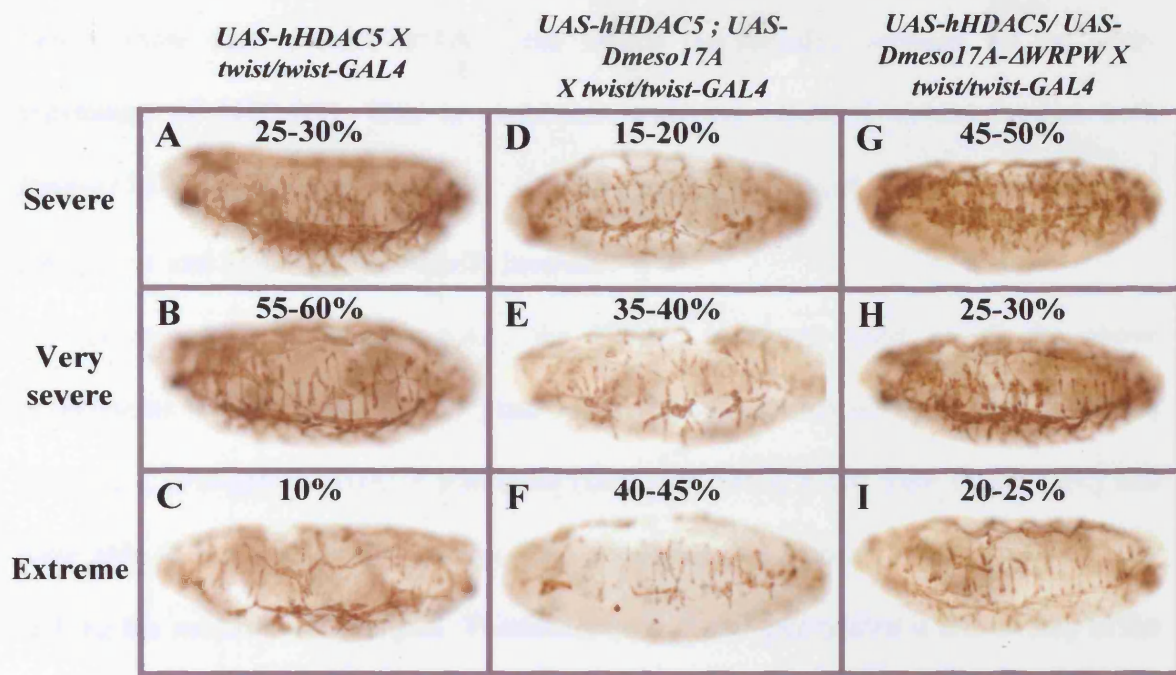


**Figure 6.17: *Dmeso17A* genetically interacts with *hHDAC5*.**

*hHDAC5* was over-expressed alone (A-C) or together with either *Dmeso17A* (D-F) or *Dmeso17A-ΔWRPW* (G-I). *twist/twist-GAL4* was used and crosses were kept at 18°C. Stage 17 embryos were stained with an antibody anti-muscle Myosin. (A-C) Variation of phenotype in *hHDAC5* over-expressing embryos (categories are the same as in Figure 6.13). (D-F) When both *hHDAC5* and *Dmeso17A* are over-expressed, the number of muscles present is dramatically reduced. Almost no muscles form correctly. (G-I) *Dmeso17A-ΔWRPW* suppresses the inhibitory effect of *hHDAC5*. The number of less severely affected embryos (G) has substantially increased, whereas the proportion of more severely affected ones (H) is reduced (compare with A and B respectively). A proportion of embryos have a more severe phenotype (I), but the effect is less severe than that with *hHDAC5* alone (C).

**Figure 6.18: The lethality in *hHDAC5* over-expressing larvae is suppressed by *Dmeso17A-ΔWRPW* and increased by *Dmeso17A*.**

The frequency of hatched and surviving larvae was scored as previously. Larvae over-expressing both *hHDAC5* and *Dmeso17A-ΔWRPW* have an increased hatching and survival. When *Dmeso17A* and *hHDAC5* are over-expressed together, both hatching and survival are reduced. The results are compared to those obtained with either *Dmeso17A* or *hHDAC5* alone. Mean percentages  $\pm$  S.D are: *Dmeso17A*, Hatching=90% $\pm$ 0.24, Survival=18%  $\pm$  0.31; *hHDAC5*, Hatching=70% $\pm$ 0.4, Survival=6.45%  $\pm$  0.32.; *Dmeso17A+hHDAC5*, Hatching=36%  $\pm$  0.37, Survival=0%; *Dmeso17A-ΔWRPW+hHDAC5*, Hatching=85.6% $\pm$ 0.66, Survival=11.7% $\pm$ 0.41.

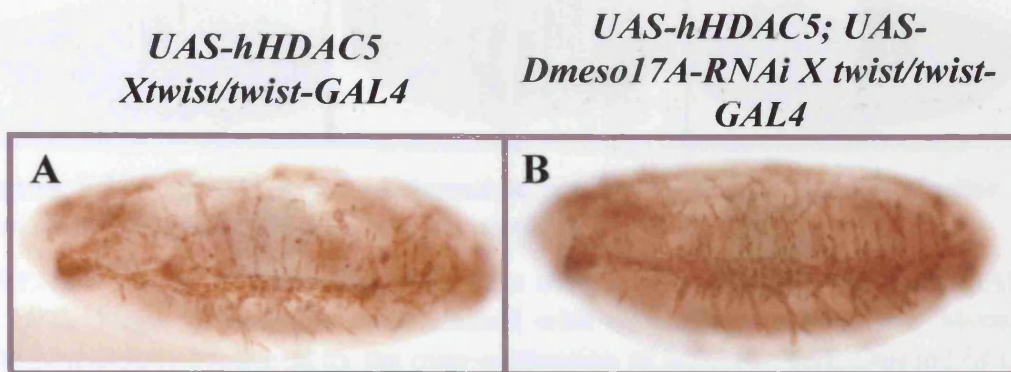


to survive to adulthood when only 2% did with HDAC5 alone (Figure 6.20). The percentage of hatching is almost identical in both cases (Figure 6.20). These results clearly show that *Dmeso17A-RNAi* can rescue the lethality induced by the over-expression of *hHDAC5*. This is consistent with the results I obtained when both *Dmeso17A-ΔWRPW* and *hHDAC5* are over-expressed together and confirms that *Dmeso17A* and *hHDAC5* genetically interact.

As described in section 6.4.1, the HDAC transgene used in all the above experiments is the human *HDAC5* gene. However, we recently obtained a stock of flies carrying a *Drosophila* HDAC4 transgene (*UAS-DHDAC4*, a gift from Olson E.N.) and were able to test it in similar assays. This transgene is a truncated form of DHDAC4, lacking the nuclear export signal. Therefore, even if phosphorylated it should stay in the nucleus and thus, like the *hHDAC5* transgene described above, it is considered as constitutively active.

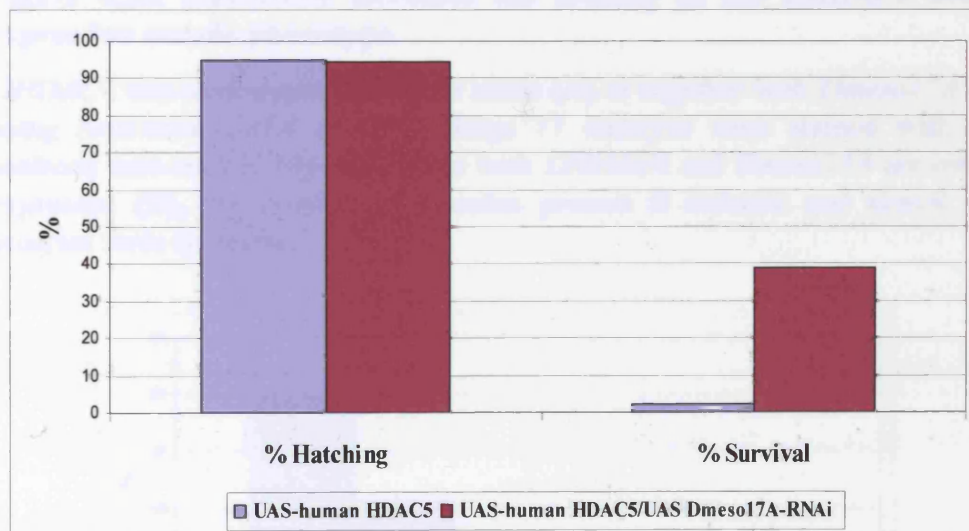
Figure 6.21 shows that over-expression of *DHDAC4* using *twist/twist-GAL4* at 18°C results in muscle disruption similar to that obtained with either *hHDAC5* or *Dmeso17A* (compare A, B and C). Following the same strategy as for the *hHDAC5*, Jun Han and I have used this new transgenic line to test whether there is also a genetic interaction between *Dmeso17A* and *D HDAC4*.

When both *Dmeso17A* and *DHDAC4* are over-expressed, the severity of the muscle phenotype is dramatically increased compared to when *DHDAC4* is over-expressed alone (Figure 6.22, compare A and B). The hatching and survival test revealed that while 20% of the embryos hatch and 1.5% to survive with *DHDAC4* alone, only 10% hatch when both *Dmeso17A* and *DHDAC4* are over-expressed and none of these survives (Figure 6.23).



**Figure 6.19: *Dmeso17A-RNAi* suppresses the inhibitory effect of *hHDAC5* over-expression on muscle development.**

*hHDAC5* and *Dmeso17A-RNAi* were over-expressed together using *twist/twist-GAL4* at 18°C. Stage 17 embryos were stained with an antibody anti-muscle Myosin. *Dmeso17A-RNAi* rescues the *hHDAC5* phenotype (A) towards wild-type (B). Embryos expressing both transgenes (B) have more correctly shaped muscles compared to when *hHDAC5* is expressed alone (A).



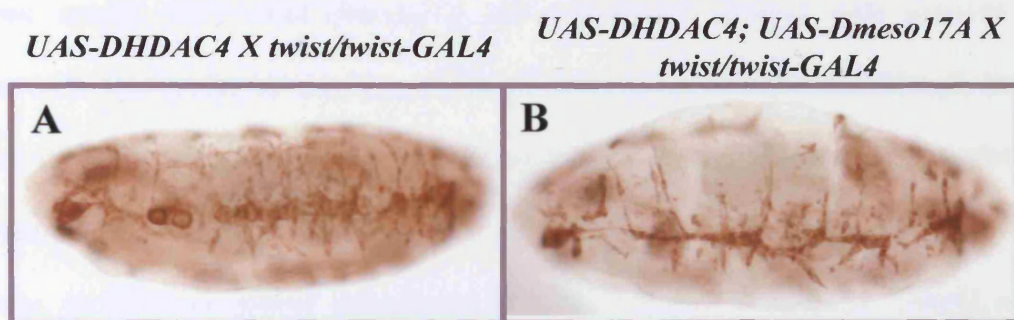
**Figure 6.20: *Dmeso17A-RNAi* suppresses the lethality induced by *hHDAC5* over-expression.**

A larval hatching and survival assay was carried out as described in Figure 4.4. The percentage of larvae hatching when both *Dmeso17A-RNAi* and *hHDAC5* are over-expressed almost does not change. However, the percentage of survival is substantially increased compared to that obtained with *hHDAC5* alone. Mean percentages  $\pm$  S.D are: *hHDAC5*, Hatching=95%  $\pm$  0.31, Survival=2%  $\pm$  0.15.; *hHDAC5+Dmeso17A-RNAi* Hatching=94.5%  $\pm$  0.82, Survival=39%  $\pm$  0.46.



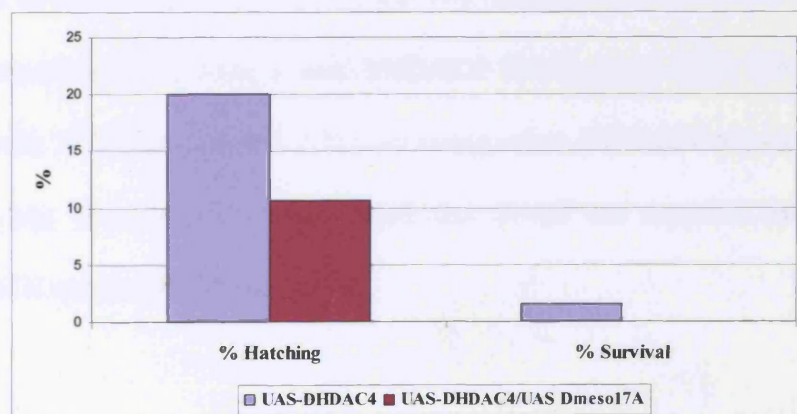
**Figure 6.21:** *DHDAC4* over-expression results in muscle defects similar to that obtained with *hHDAC5* and *Dmeso17A*.

*DHDAC4*, *Dmeso17A* and *hHDAC5* were over-expressed using *twist/twist-GAL4* at 18°C. Stage 17 embryos were stained with an antibody anti-muscle Myosin. The phenotypes produced by the over-expression of *hHDAC5* (A), *Dmeso17A* (B) or *DHDAC4* (C) are comparable.



**Figure 6.22:** *Dmeso17A* increases the severity of the *DHDAC4* over-expression muscle phenotype.

*DHDAC4* was over-expressed either alone (A) or together with *Dmeso17A* (B) using *twist/twist-GAL4* at 18°C. Stage 17 embryos were stained with an antibody anti-muscle Myosin. When both *DHDAC4* and *Dmeso17A* are over-expressed (B), the number of muscles present is reduced and almost no muscles form correctly.



**Figure 6.23:** *Dmeso17A* increases the lethality of *DHDAC4* over-expressing larvae.

The frequency of hatched and surviving larvae was scored as previously. When *Dmeso17A* and *DHDAC4* are over-expressed together, both hatching and survival are reduced, compared to with *DHDAC4* alone. Mean percentages  $\pm$  S.D are: *DHDAC4*, Hatching=20  $\pm$  0.05, Survival= 1.5  $\pm$  0.15; *DHDAC4*+*Dmeso17A*, Hatching= 10.6  $\pm$  0.59, Survival=0%.

Moreover, *Dmeso17A-RNAi* and *Dmeso17A-ΔWRPW* can rescue towards wild-type the phenotype produced by the over-expression of *DHDAC4* (Figure 6.24, compare A with B and C). This rescue is clearly demonstrated by the percentage of hatching and survival. 56% of the embryos over-expressing both *DHDAC4* and *Dmeso17A-RNAi* are able to hatch and 15.3% to survive, in contrast to 20% and 1.5% with *DHDAC4* alone. When *Dmeso17A-ΔWRPW* is used, hatching and survival increases to 43% and 14% respectively (Figure 6.26).

These results show that *Dmeso17A* can genetically interact with *DHDAC4*. Together with the results on the interactions of *Dmeso17A* with *gro* and *Dmef2*, they support a model in which *Dmeso17A*, together with *Gro* and *HDAC*, down-regulates *DMef2* activity.

Lastly, in order to further investigate the link between *Dmeso17A*, *Dmef2* and *HDAC*, we tested whether *Dmef2* and *DHDAC4* could genetically interact. To do so, we over-expressed both genes together. In embryos over-expressing both genes, more muscles are able to form compared to when only *DHDAC4* is over-expressed (Figure 6.25, compare A with B). Moreover, the percentage of hatching and survival showed a profound rescue of the lethality induced by the over-expression of *DHDAC4*. 94.5% of the embryos over-expressing *Dmef2* and *DHDAC4* hatched and 80% survived. This contrasts with only 20% hatching and 1.5% surviving when *DHDAC4* is over-expressed alone (Figure 6.26). These results clearly show that *Dmef2* can suppress the inhibitory effect of *DHDAC4* and reinforce my model.

**Figure 6.24: Comparison of *Dmeso17A-RNAi* and *Dmeso17A-ΔWRPW* in suppressing the inhibitory effect of *DHDAC4* over-expression on muscle development.**

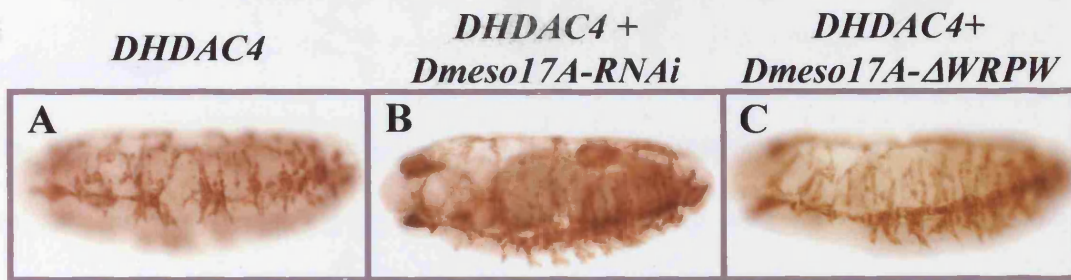
*DHDAC4* was over-expressed together with either *Dmeso17A-RNAi* (B) or *Dmeso17A-ΔWRPW* (C). *twist/twist-GAL4* was used and crosses were kept at 18°C. Stage 17 embryos were stained with an antibody anti-muscle Myosin. (A) Over-expression of *DHDAC4* disrupts muscle differentiation. *Dmeso17A-RNAi* (B) and *Dmeso17A-ΔWRPW* (C) suppress this effect.

**Figure 6.25: *DHDAC4* genetically interacts with *Dmef2*.**

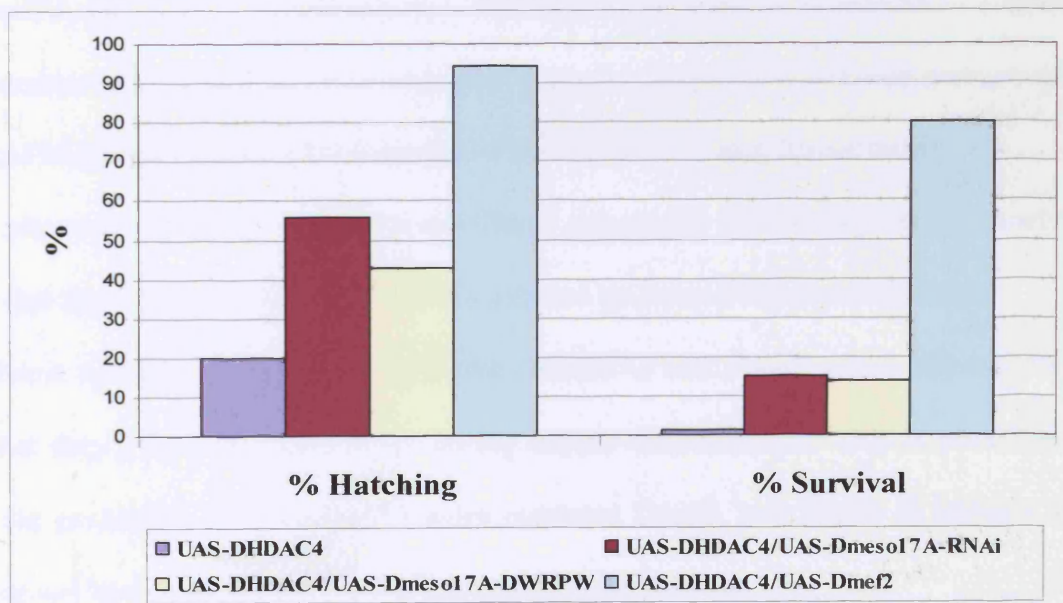
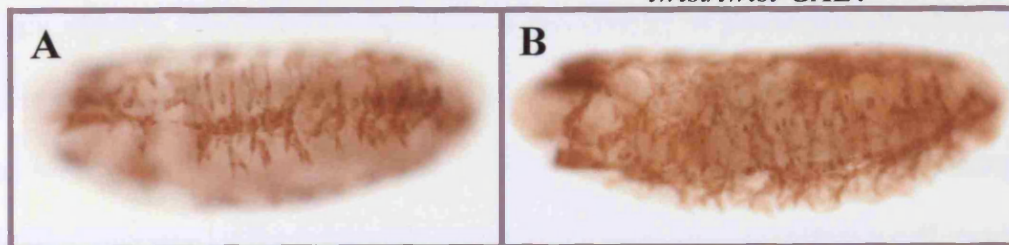
*DHDAC4* and *Dmef2* were over-expressed together using *twist/twist-GAL4* at 18°C. Stage 17 embryos were stained with an antibody anti-muscle Myosin. *Dmef2* rescues the *DHDAC4* phenotype (A) towards wild-type (B). Embryos expressing both transgenes (B) have more correctly shaped muscles compared to when *DHDAC4* is expressed alone (A).

**Figure 6.26: Comparison of *Dmeso17A-RNAi*, *Dmeso17A-ΔWRPW* and *Dmef2* in suppressing the lethality induced by *DHDAC4* over-expression.**

The frequency of hatched and surviving larvae was scored as previously. When *DHDAC4* is over expressed together with either *Dmeso17A-RNAi*, *Dmeso17A-ΔWRPW* or *Dmef2*, both hatching and survival are considerably increased compared to with *DHDAC4* alone. Mean percentages  $\pm$  S.D are: *DHDAC4*, Hatching= $20 \pm 0.05$ , Survival= $1.5 \pm 0.15$ ; *DHDAC4+Dmeso17A-RNAi*, Hatching= $56 \pm 0.31$ , Survival= $15.3 \pm 0.43$ ; *DHDAC4+Dmeso17A-ΔWRPW*, Hatching= $43 \pm 0.83$ , Survival= $14 \pm 0.67$ ; *DHDAC4+Dmef2*, Hatching= $94.5 \pm 0.21$ , Survival= $80 \pm 0.74$ .



**UAS-DHDAC4 X twist/twist-GAL4**                      **UAS-DHDAC4; UAS-Dmef2 X twist/twist-GAL4**





## 6.5 Discussion

### 6.5.1 *Dmeso17A* inhibits muscle differentiation by down-regulating DMef2 activity

My results, presented in Chapters 4 and 5, suggested that there could be a relationship between *Dmeso17A* and *Dmef2*. Whereas one can inhibit muscle differentiation, the other promotes it. If a link exists, the phenotype of *Dmeso17A* over-expression should closely resemble that of *Dmef2* loss-of-function. I therefore compared the phenotype of *Dmef2* hypomorphic alleles with that of embryos over-expressing *Dmeso17A*. Not only are there striking similarities in the way in which particular muscles are affected, but the same variations in the severity of phenotype are observed. The differential effects found between the *Dmef2* hypomorphic mutants can be attributed to different levels of DMef2 activity (Ranganayakulu et al., 1995; Gunthorpe et al., 1999). Moreover, it has been shown that different properties within a cell require different thresholds of DMef2 activity (Gunthorpe et al., 1999). The remarkable similarities I observed therefore strongly suggest that, in embryos over-expressing *Dmeso17A*, the level of DMef2 activity within particular muscles is reduced to a level comparable to that found in *Dmef2* mutants. They also suggest that different amounts of *Dmeso17A* activity result in the reduction of DMef2 activity to different levels.

I also tested whether *Dmeso17A* and *Dmef2* genetically interact. My results clearly show that *Dmef2* can suppress the lethality induced by *Dmeso17A* over-expression.

Taken together, these results show that *Dmeso17A* and *Dmef2* genetically interact and that they play antagonistic roles during muscle differentiation. This is consistent with the possibility that *Dmeso17A* down-regulates *Dmef2*, and begins to indicate a mechanism by which *Dmeso17A* inhibits muscle differentiation.

In order to explore further this interaction, I tested whether *Dmeso17A-RNAi* could rescue the phenotype of the *Dmef2*<sup>65</sup> hypomorphic allele. However, the phenotype remained unchanged. Assuming that *Dmeso17A* down-regulates *Dmef2*, this result could be explained as follows. In the hypomorphic mutant, DMef2 activity is lower than its normal level which leads to muscle defects. When *Dmeso17A-RNAi* is expressed in this mutant, DMef2 activity increases to a certain level. However, it may not reach the minimum threshold required for proper muscle differentiation. This suggests that a stronger loss-of-function or even a complete knock-out of *Dmeso17A* may be required to increase *Dmef2* activity to its wild-type level. However, as muscle differentiation starts, *Dmeso17A* disappears and therefore, *Dmeso17A-RNAi* is ineffective. This results in the decrease of DMef2 activity to its original “mutant level”. Therefore, during muscle differentiation, the level of mutant DMef2 activity is unchanged, even if *Dmeso17A-RNAi* is expressed. This therefore suggests that the loss-of *Dmeso17A* function may not rescue the *Dmef2* mutant phenotype.

The results discussed so far in this section indicate that there is a close relationship between *Dmeso17A* and *Dmef2* with *Dmeso17A* antagonising the function of *Dmef2*. To explore how it might do this, I asked whether *Dmef2* expression or activity is affected by *Dmeso17A*. In embryos over-expressing *Dmeso17A*, no effect was detected on *Dmef2* expression. However, there was an effect on its activity as revealed by the strong reduction of *β3-tubulin* expression in the somatic mesoderm, where it is a direct DMef2 target (Damm et al., 1998).

Taken together, all these results show that *Dmeso17A* acts in the main muscle differentiation pathway to down-regulate DMef2 activity.

### 6.5.2 *Dmeso17A* requires *groucho* to inhibit muscle differentiation

In the next steps of my study, I aimed to find interactor(s) to explore the mechanisms by which *Dmeso17A* down-regulates *DMef2* activity. This first led me to the co-repressor *Gro*.

*Gro* proteins cannot bind DNA, but they can repress transcription through physical interaction with transcription repressors such as *Hairy* (reviewed in Fisher and Caudy, 1998; Parkhurst, 1998; Gasperowicz and Otto, 2005). *Hairy* possesses a bHLH domain and a WRPW motif at its C-terminus. Once bound to DNA, it can recruit *Gro*, and the WRPW motif has been shown to be necessary and sufficient for this (Paroush et al., 1994; Fisher et al., 1996). *Dmeso17A* does not possess DNA binding or bHLH domains. Nevertheless, it possesses a WRPW motif at its C-terminus, that is required for its function. It was therefore still possible that *Dmeso17A* interacts with *Gro*, maybe functioning as an adaptor between *Gro* and transcriptional repressors.

I showed that *Dmeso17A* and the transcriptional co-repressor *Gro* interact both *in vitro* and *in vivo*. In a GST pull-down assay, *Dmeso17A* was able to bind *Gro*, whereas *Dmeso17A-ΔWRPW* was not. This demonstrates that *Dmeso17A* and *Gro* can physically interact and shows that the WRPW motif is required for this to happen. *In vivo*, the absence of *gro* could suppress the inhibitory effect of *Dmeso17A*. This shows that *Dmeso17A* requires *gro* for its function.

Taken together, these results suggest that *Dmeso17A* and *Gro* act in the same complex to inhibit muscle differentiation. *Gro* is a transcriptional co-repressor (reviewed in Fisher and Caudy, 1998; Parkhurst, 1998; Gasperowicz and Otto, 2005), and *Dmeso17A* can repress the expression of *β3-tubulin* by down-regulating *DMef2* activity. My results therefore suggest that the *Dmeso17A/Gro* complex inhibits

transcription during muscle differentiation and that its action could be centered on DMef2.

Moreover, these results implicate *gro* in *Drosophila* muscle differentiation for the first time. In mammalian cell culture, there are indications that the mammalian homologs of Gro, the proteins of the transducin-like Enhancer of split (TLE) family, might be implicated in myogenesis. This might be through interactions with members of the HES (mammalian homologs of *Drosophila* Hairy and E(spl)) family, HES-1 and HES-6. HES-1 can repress the activity of the bHLH transcription factor MyoD, and thus repress myogenesis (Sasai et al., 1992). HES-6, on the other hand, seems to promote myogenesis by downregulating MyoR (Gao et al., 2001), an antagonist of MyoD (Lu et al., 1999). Both HES-1 and HES-6 are known to interact with TLE1, and HES-6-mediated transcriptional repression requires its C-terminal WRPW motif (Grbavec and Stifani, 1996; Gao et al., 2001; reviewed in Gasperowicz and Otto, 2005). Nevertheless, despite these indications, there is no clear evidence (*in vitro* or *in vivo*) of a direct role for TLE/*gro* in mammalian or *Drosophila* muscle development.

My results provide *in vivo* evidence that *gro* plays a role in muscle differentiation in *Drosophila*. Study of *gro* and *Dmeso17A* function could therefore describe a novel mechanism of regulation of muscle differentiation.

To further investigate the role of *gro* in muscle development, I tested whether muscle formation in *gro* mutants is affected. Myosin staining revealed that muscle development is impaired in embryos lacking zygotic *gro*. This provides further *in vivo* evidence that *gro* plays a role in normal *Drosophila* muscle development. Moreover, the fact that *gro* mutants have a muscle phenotype reinforces my genetic interaction result with *Dmeso17A*. Indeed, the rescue described when *Dmeso17A* is over-expressed in *gro* mutants can now be interpreted from two points of view. First, as discussed above, the

*Dmeso17A* inhibitory effect is suppressed in *gro* mutant demonstrating that *Dmeso17A* requires *gro* for its action. Second, the *gro* mutant phenotype is rescued by the over-expression of *Dmeso17A*. As described in section 6.3.2, the *gro*<sup>E48</sup> allele I used is a point mutation and a hypomorph and thus the mutated protein produced may have some residual activity. One explanation for the rescue of the *gro* mutant phenotype could then be that the extra *Dmeso17A* interacts with the mutated Gro protein and enhances its activity, compensating the loss of *gro* function. Another interpretation could be that Gro, in addition of interacting with it, is an upstream regulator of *Dmeso17A*. In *gro* mutants, *Dmeso17A* over-expression could therefore compensate the reduction of *Dmeso17A* level.

### 6.5.3 *Dmeso17A* genetically interacts with HDACs

I have shown that *Dmeso17A* can interact with *Dmef2* and *gro*. However, there is no recorded interaction between *Dmef2* and *gro*, and *Dmeso17A* does not possess a DNA-binding or a *Dmef2*-binding domain. This therefore suggests that there is another factor linking the *Dmeso17A*/Gro complex to *Dmef2*. A possibility for such a factor is HDAC. In mammalian cell cultures, classII HDACs have been shown to bind to Mef2 and down-regulate its activity (Miska et al., 1999; Lemercier et al., 2000; Lu et al., 2000). Moreover, Gro, in *Drosophila*, interacts with the classI HDAC, Rpd3 to repress transcription (Chen et al, 1999; for review see Courey and Songtao, 2001, Gasperowicz and Otto, 2005).

I therefore explored whether *Dmeso17A* could also interact with HDAC. In all my experiments, two different lines of flies carrying classII HDAC transgenes have been used: *UAS-human HDAC5* and *UAS-Drosophila HDAC4*. Both gave similar results:

- The phenotype of embryos over-expressing *HDAC* is very similar to that obtained with *Dmeso17A*.
- The severity of this phenotype increases when both genes are over-expressed together.
- Most importantly, the lethality of embryos over-expressing *HDAC* is suppressed by *Dmeso17A-RNAi* and *Dmeso17A-ΔWRPW*.

These results indicate that *Dmeso17A* and *HDAC* genetically interact and that they work together in the same pathway to disrupt myogenesis.

The role(s) of HDACs has been extensively studied in mammalian cultured cells, and in particular their interaction with Mef2 (Miska et al, 1999; Sparrow et al, 1999; Lu et al, 2000, Youn et al, 2000; reviewed in McKinsey et al, 2001; Han et al, 2005; Yang and Grégoire, 2005). However, relatively little is known on the specific function of HDACs *in vivo*. Only HDAC4, 5 and 9 have been studied *in vivo* and have been implicated in cellular hypertrophy (Zhang et al., 2002; Chang et al., 2004; Vega et al., 2004). Mice lacking either HDAC5 or 9 are viable, but they have cardiac hypertrophy (Zhang et al., 2002; Chang et al., 2004). HDAC4 mutant mice display premature ossification due to chondrocyte hypertrophy (Vega et al., 2004). However, none of these studies implicated HDACs directly in muscle differentiation. The results I presented here provide *in vivo* evidence for how HDACs could function to inhibit myogenesis in *Drosophila*.

I also tested whether *HDAC* can genetically interact with *Dmef2*. In vertebrates, as mentioned previously, HDAC can bind to Mef2 and inhibit its activity (Miska et al., 1999; Lemercier et al., 2000; Lu et al., 2000). Nevertheless, there is no such evidence in *Drosophila*. My results show that *Dmef2* can suppress the lethality of embryos over-expressing *HDAC* and therefore that the two genes genetically interact. Together with

my preceding results, this supports a model in which Dmeso17A functions, together with Gro and HDAC, to downregulate DMef2 activity and repress muscle gene expression.

HDAC, Gro and Mef2 are highly conserved proteins. This allows an immediate parallel to be drawn between my study of *Dmeso17A* in *Drosophila* and muscle differentiation in vertebrates. Although no homologues have been found for Dmeso17A in vertebrates, its function in a transcription-repressing complex during muscle differentiation might be conserved. This is further supported by the fact that both human and *Drosophila* HDACs genetically interact with *Dmeso17A*. The possible significance of this for muscle diseases will be discussed in the concluding chapter.

## Chapter 7 Conclusions

It is apparent that inhibitory mechanisms are required during development to control when and where cells differentiate. Our knowledge of these mechanisms and the molecules implicated is however limited. In the particular case of muscle cell differentiation, some candidate negative regulators have been identified (reviewed in Taylor 2005; see Chapter 1, section 1.2), but their importance and *in vivo* mechanisms of action are not always clear. A more complete understanding of the molecular mechanisms regulating cell differentiation requires the identification and characterisation of restraining molecules.

The work presented in this dissertation focuses on muscle differentiation in *Drosophila* and shows that *Dmeso17A*, a novel gene isolated by Dr. Taylor (Taylor, 2000), encodes one such molecule. My approach to study *Dmeso17A* has been to first analyse its role during muscle differentiation and then to dissect its mechanism of action.

Using the GAL4/UAS system (Brand and Perrimon, 1993; Brand et al., 1994; see Chapter 2 section 3.3) to achieve gain and loss-of-function of *Dmeso17A*, I have shown that *Dmeso17A* is a novel inhibitor of muscle differentiation and that its inhibitory effect is required for proper muscle development. I then aimed to identify candidate genes that could interact with *Dmeso17A* to dissect how it is working. The results I obtained show that:

- 1 *Dmeso17A* genetically interacts with *Dmef2* and down-regulates its activity.
- 2 *Dmeso17A* genetically and physically interacts with *gro*.
- 3 *Dmeso17A* genetically interacts with *HDAC*.

These results taken together, allow me to draw a model for *Dmeso17A* mechanism of action. In this model, *Dmeso17A* first forms a complex with *Gro*. *Gro* is known to be recruited to its targets by DNA-binding factors, like *Hairy* (Paroush et al., 1994;



Jiménez et al., 1997) or by adaptor molecules such as Hairless, which lacks a DNA-binding domain and can be recruited to DNA by Su(H) (Barolo et al., 2002). As Dmeso17A appears to lack a DNA-binding domain, it is possible that it acts as an adaptor between Gro and a DNA-binding factor. The Dmeso17A/Gro complex then recruits HDAC which binds to DMef2. As mentioned in Chapter 6, section 6.4, HDACs are known to repress transcription by catalysing the deacetylation of histones (Flores-Saaib and Courey, 2000; Thiagalingam et al., 2003). However, recent studies showed that the activity of HDACs is not limited to histone deacetylation, but they can also directly modify transcription factors such as Mef2 to regulate their activity (Grégoire and Yang, 2005; Zhao et al., 2005). Zhao et al. showed that HDAC4 promotes the sumoylation of Mef2, thereby inhibiting its transcriptional activity. They also show that HDAC4 can directly interact with SIRT1, a classIII deacetylase, which can catalyse Mef2 deacetylation (Zhao et al., 2005). Therefore, in my model, it is possible that once recruited by the Dmeso17A/Gro complex, HDAC regulates DMef2 activity by acting on both its sumoylation and acetylation state. It is also possible that histone deacetylation by HDAC plays a role in the regulation of DMef2 activity. At the onset of muscle differentiation, Dmeso17A is down-regulated and the Dmeso17A/Gro HDAC complex is destabilised. Moreover, HDAC could be phosphorylated by CaMK (or other kinases), and exported out of the nucleus (see Chapter 6, section 6.4). DMef2 is then activated and can induce the expression of muscle differentiation genes.

More work needs to be done to explore different aspects of this model. For example, there is a need to understand how Gro and Dmeso17A are recruited to DNA and what is the role of Dmeso17A in this complex. HDAC can directly bind to Mef2 and inhibit its activity in cell culture. It would be interesting to know why Dmeso17A and Gro are needed. Does Dmeso17A stabilise the complex? Is it an adaptor between

Gro and a DNA binding factor, or does Dmeso17A also physically interact with HDACs to link it with Gro? One also cannot rule out the possibility that Dmeso17A directly interacts with DMef2. It would also be necessary to test whether the mechanism I describe for Dmeso17A action is specific to DMef2 or if it can also regulate other factors activity during muscle differentiation.

However, even though my model is not complete, it does provide information on an *in vivo* mechanism by which the activity of DMef2 can be regulated before the onset of muscle differentiation. My findings therefore bring a new insight in the understanding of the regulation of muscle progenitor differentiation. The mechanism of action of Dmeso17A could provide a possible explanation for how muscle progenitors are held in an undifferentiated state until cues trigger their differentiation. As discussed in the previous Chapter, the functional conservation of DMef2, Gro and HDAC suggest that even though Dmeso17A appears not to be conserved in higher organisms, its function could be. The mechanism I described here might therefore be conserved in the regulation of skeletal myogenesis in vertebrates and could be applied to explain how Mef2 is regulated *in vivo*. Moreover, one might imagine a similar mechanism for the regulation of MyoD or Myf5. Like *Dmef2* in *Drosophila*, these two MRFs are key regulators of skeletal muscle differentiation (Weintraub et al., 1991; Braun et al., 1992; Rudnicki et al., 1992; Rudnicki et al., 1993; reviewed in Taylor, 2005). They are expressed in undifferentiated myoblasts and yet, their target genes are only activated later during muscle differentiation (Kopan et al., 1994; Hirsinger et al., 2001). The regulation of MyoD activity has been extensively studied and involves deacetylases, such as Sir2 (the mouse homolog of SIRT1) which is a classIII HDAC, and HDAC1 (reviewed in Sartorelli and Caretti, 2005). My model might therefore be analogous to at

least some part of MyoD regulation to ensure that skeletal muscle differentiation is not prematurely activated.

Temporal control of cell differentiation is not only important for muscle development but is also crucial for the development of other tissues. For example, during osteoblast differentiation inhibition of Runx2 activity is necessary to prevent premature differentiation. Runx2 is a member of the runt family of transcription factors (Ducy et al., 1997) and is necessary and sufficient for osteoblast differentiation (Ducy et al., 1997; Komori et al., 1997; Otto et al., 1997). Like *Dmef2* and the MRFs during muscle differentiation, Runx2 is expressed long before osteoblasts start their differentiation (Ducy, 2000). A recent study showed that the transcriptional activity of Runx2 before the onset of osteoblast differentiation is directly regulated by Twist, which prevents Runx2 from binding DNA (Bialek et al., 2004). Interestingly, a previous study showed that Gro/TLE proteins can inhibit Runx2 dependent activation of the *osteoclastin* gene, which is characteristic of differentiating osteoblasts (Javed et al., 2000). Moreover, HDAC4 has been shown to directly interact with Runx2 and inhibits its activity, delaying chondrocyte hypertrophy, which is necessary for osteoblast differentiation (Vega et al., 2005).

Thus, the regulation of Runx2 during skeletogenesis can be placed in parallel with that of DMef2 in myogenesis: DMef2 and Runx2 are essential positive regulators of differentiation, they are expressed long before the onset of differentiation in their respective tissues and they appear to be regulated by the same molecules, i.e. Gro and HDACs. Moreover, as mentioned in Chapter 6, section 6.4, HDAC activity can be regulated by a variety of signalling pathways (Chang et al., 2005). This suggests that HDACs are involved in the regulation of gene expression during the differentiation of

various tissues. The mechanism I describe for *Dmeso17A* action may therefore be applicable to a more generalised method for cell differentiation regulation.

Finally, Understanding the genetic network governing how muscle progenitors differentiate is important for developing new approaches to tackling human muscle diseases. An interesting aspect of *Dmeso17A* resides in its expression in the AMPs. This is for two reasons. First, it suggests that *Dmeso17A* might be involved in the regulation of adult muscle differentiation and my preliminary results are consistent with this. As mentioned in chapter 1, section 1.4.4, the adult muscles in *Drosophila* are in many respects similar to vertebrates skeletal muscle. Findings on *Dmeso17A* function in the adult muscles, together with my results in larval somatic muscles, might therefore bring new insights in the mechanisms regulating skeletal muscle differentiation. Second, the AMPs are in some respects similar to the vertebrate satellite cells. Both remain quiescent, undifferentiated until triggered to proliferate and differentiate. The satellite cells play a crucial role in the regeneration of diseased or damaged skeletal muscles (Morgan and Partridge, 2003). Understanding how their differentiation is regulated could be crucial for the development of cell-based therapies. I have shown that persistent *Dmeso17A* expression in the thoracic AMPs can lead to defects in adult muscle formation, suggesting that it plays an important role in the control of the differentiation of these cells. Further analysis of *Dmeso17A* function in the AMPs could therefore be highly informative and may provide new directions for the study of the differentiation of satellite cells.

## References

- Abrams, J. M., White, K., Fessler, L. I. and Steller, H.** (1993). Programmed cell death during *Drosophila* embryogenesis. *Development* **117**, 29-43.
- Adams, M. D., Celniker, S. E., Holt, R. A., Evans, C. A., Gocayne, J. D., Amanatides, P. G., Scherer, S. E., Li, P. W., Hoskins, R. A., Galle, R. F. et al.** (2000). The genome sequence of *Drosophila melanogaster*. *Science* **287**, 2185-95.
- Agrawal, N., Dasaradhi, P. V., Mohmmmed, A., Malhotra, P., Bhatnagar, R. K. and Mukherjee, S. K.** (2003). RNA interference: biology, mechanism, and applications. *Microbiol Mol Biol Rev* **67**, 657-85.
- Alberga, A., Boulay, J. L., Kempe, E., Dennefeld, C. and Haenlin, M.** (1991). The snail gene required for mesoderm formation in *Drosophila* is expressed dynamically in derivatives of all three germ layers. *Development* **111**, 983-92.
- Anant, S., Roy, S. and VijayRaghavan, K.** (1998). Twist and Notch negatively regulate adult muscle differentiation in *Drosophila*. *Development* **125**, 1361-9.
- Arredondo, J. J., Ferreres, R. M., Maroto, M., Cripps, R. M., Marco, R., Bernstein, S. I. and Cervera, M.** (2001). Control of *Drosophila* paramyosin/miniparamyosin gene expression. Differential regulatory mechanisms for muscle-specific transcription. *J Biol Chem* **276**, 8278-87.
- Artero, R., Prokop, A., Paricio, N., Begemann, G., Pueyo, I., Mlodzik, M., Perez-Alonso, M. and Baylies, M. K.** (1998). The muscleblind gene participates in the organization of Z-bands and epidermal attachments of *Drosophila* muscles and is regulated by Dmef2. *Dev Biol* **195**, 131-43.
- Artero, R. D., Castanon, I. and Baylies, M. K.** (2001). The immunoglobulin-like protein Hibris functions as a dose-dependent regulator of myoblast fusion and is differentially controlled by Ras and Notch signaling. *Development* **128**, 4251-64.
- Azpiazu, N. and Frasch, M.** (1993). tinman and bagpipe: two homeo box genes that determine cell fates in the dorsal mesoderm of *Drosophila*. *Genes Dev* **7**, 1325-40.
- Azpiazu, N., Lawrence, P. A., Vincent, J. P. and Frasch, M.** (1996). Segmentation and specification of the *Drosophila* mesoderm. *Genes Dev* **10**, 3183-94.

- Barolo, S., Stone, T., Bang, A. G. and Posakony, J. W.** (2002). Default repression and Notch signaling: Hairless acts as an adaptor to recruit the corepressors Groucho and dCtBP to Suppressor of Hairless. *Genes Dev* **16**, 1964-76.
- Bate, M.** (1990). The embryonic development of larval muscles in *Drosophila*. *Development* **110**, 791-804.
- Bate, M. and Rushton, E.** (1993). Myogenesis and muscle patterning in *Drosophila*. *C R Acad Sci III* **316**, 1047-61.
- Bate, M., Rushton, E. and Currie, D. A.** (1991). Cells with persistent twist expression are the embryonic precursors of adult muscles in *Drosophila*. *Development* **113**, 79-89.
- Baylies, M. K. and Bate, M.** (1996). twist: a myogenic switch in *Drosophila*. *Science* **272**, 1481-4.
- Baylies, M. K., Bate, M. and Ruiz Gomez, M.** (1998). Myogenesis: a view from *Drosophila*. *Cell* **93**, 921-7.
- Benezra, R., Davis, R. L., Lockshon, D., Turner, D. L. and Weintraub, H.** (1990). The protein Id: a negative regulator of helix-loop-helix DNA binding proteins. *Cell* **61**, 49-59.
- Bialek, P., Kern, B., Yang, X., Schrock, M., Susic, D., Hong, N., Wu, H., Yu, K., Ornitz, D. M., Olson, E. N. et al.** (2004). A twist code determines the onset of osteoblast differentiation. *Dev Cell* **6**, 423-35.
- Black, B. L. and Olson, E. N.** (1998). Transcriptional control of muscle development by myocyte enhancer factor-2 (MEF2) proteins. *Annu Rev Cell Dev Biol* **14**, 167-96.
- Bodmer, R.** (1993). The gene tinman is required for specification of the heart and visceral muscles in *Drosophila*. *Development* **118**, 719-29.
- Borkowski, O. M., Brown, N. H. and Bate, M.** (1995). Anterior-posterior subdivision and the diversification of the mesoderm in *Drosophila*. *Development* **121**, 4183-93.
- Boulay, J. L., Dennefeld, C. and Alberga, A.** (1987). The *Drosophila* developmental gene snail encodes a protein with nucleic acid binding fingers. *Nature* **330**, 395-8.
- Bour, B. A., Chakravarti, M., West, J. M. and Abmayr, S. M.** (2000). *Drosophila* SNS, a member of the immunoglobulin superfamily that is essential for myoblast fusion. *Genes Dev* **14**, 1498-511.

- Bour, B. A., O'Brien, M. A., Lockwood, W. L., Goldstein, E. S., Bodmer, R., Taghert, P. H., Abmayr, S. M. and Nguyen, H. T.** (1995). Drosophila MEF2, a transcription factor that is essential for myogenesis. *Genes Dev* **9**, 730-41.
- Bourgouin, C., Lundgren, S. E. and Thomas, J. B.** (1992). Apterous is a Drosophila LIM domain gene required for the development of a subset of embryonic muscles. *Neuron* **9**, 549-61.
- Brand, A. H., Manoukian, A. S. and Perrimon, N.** (1994). Ectopic expression in Drosophila. *Methods Cell Biol* **44**, 635-54.
- Brand, A. H. and Perrimon, N.** (1993). Targeted gene expression as a means of altering cell fates and generating dominant phenotypes. *Development* **118**, 401-15.
- Braun, T., Rudnicki, M. A., Arnold, H. H. and Jaenisch, R.** (1992). Targeted inactivation of the muscle regulatory gene Myf-5 results in abnormal rib development and perinatal death. *Cell* **71**, 369-82.
- Breitbart, R. E., Liang, C. S., Smoot, L. B., Laheru, D. A., Mahdavi, V. and Nadal-Ginard, B.** (1993). A fourth human MEF2 transcription factor, hMEF2D, is an early marker of the myogenic lineage. *Development* **118**, 1095-106.
- Buckingham, M., Bajard, L., Chang, T., Daubas, P., Hadchouel, J., Meilhac, S., Montarras, D., Rocancourt, D. and Relaix, F.** (2003). The formation of skeletal muscle: from somite to limb. *J Anat* **202**, 59-68.
- Butler, M. J., Jacobsen, T. L., Cain, D. M., Jarman, M. G., Hubank, M., Whittle, J. R., Phillips, R. and Simcox, A.** (2003). Discovery of genes with highly restricted expression patterns in the Drosophila wing disc using DNA oligonucleotide microarrays. *Development* **130**, 659-70.
- Campos-Ortega, J. and Hartenstein, V.** (1997). *The embryonic development of Drosophila Melanogaster*. Springer-Verlag, Berlin/Heidelberg/New York.
- Carmena, A., Bate, M. and Jimenez, F.** (1995). Lethal of scute, a proneural gene, participates in the specification of muscle progenitors during Drosophila embryogenesis. *Genes Dev* **9**, 2373-83.
- Carmena, A., Murugasu-Oei, B., Menon, D., Jimenez, F. and Chia, W.** (1998). Inscuteable and numb mediate asymmetric muscle progenitor cell divisions during Drosophila myogenesis. *Genes Dev* **12**, 304-15.

- Castanon, I. and Baylies, M. K.** (2002). A Twist in fate: evolutionary comparison of Twist structure and function. *Gene* **287**, 11-22.
- Castanon, I., Von Stetina, S., Kass, J. and Baylies, M. K.** (2001). Dimerization partners determine the activity of the Twist bHLH protein during *Drosophila* mesoderm development. *Development* **128**, 3145-59.
- Chambers, A. E., Kotecha, S., Towers, N. and Mohun, T. J.** (1992). Muscle-specific expression of SRF-related genes in the early embryo of *Xenopus laevis*. *Embo J* **11**, 4981-91.
- Chang, S., Bezprozvannaya, S., Li, S. and Olson, E. N.** (2005). An expression screen reveals modulators of class II histone deacetylase phosphorylation. *Proc Natl Acad Sci U S A* **102**, 8120-5.
- Chang, S., McKinsey, T. A., Zhang, C. L., Richardson, J. A., Hill, J. A. and Olson, E. N.** (2004). Histone deacetylases 5 and 9 govern responsiveness of the heart to a subset of stress signals and play redundant roles in heart development. *Mol Cell Biol* **24**, 8467-76.
- Chen, E. H. and Olson, E. N.** (2001). Antisocial, an intracellular adaptor protein, is required for myoblast fusion in *Drosophila*. *Dev Cell* **1**, 705-15.
- Chen, E. H. and Olson, E. N.** (2004). Towards a molecular pathway for myoblast fusion in *Drosophila*. *Trends Cell Biol* **14**, 452-60.
- Chen, E. H., Pryce, B. A., Tzeng, J. A., Gonzalez, G. A. and Olson, E. N.** (2003). Control of myoblast fusion by a guanine nucleotide exchange factor, loner, and its effector ARF6. *Cell* **114**, 751-62.
- Chen, G. and Courey, A. J.** (2000). Groucho/TLE family proteins and transcriptional repression. *Gene* **249**, 1-16.
- Chen, G., Fernandez, J., Mische, S. and Courey, A. J.** (1999). A functional interaction between the histone deacetylase Rpd3 and the corepressor groucho in *Drosophila* development. *Genes Dev* **13**, 2218-30.
- Chen, Z. F. and Behringer, R. R.** (1995). twist is required in head mesenchyme for cranial neural tube morphogenesis. *Genes Dev* **9**, 686-99.
- Christ, B. and Ordahl, C. P.** (1995). Early stages of chick somite development. *Anat Embryol (Berl)* **191**, 381-96.



- Courey, A. J. and Jia, S.** (2001). Transcriptional repression: the long and the short of it. *Genes Dev* **15**, 2786-96.
- Cripps, R. M., Black, B. L., Zhao, B., Lien, C. L., Schulz, R. A. and Olson, E. N.** (1998). The myogenic regulatory gene Mef2 is a direct target for transcriptional activation by Twist during *Drosophila* myogenesis. *Genes Dev* **12**, 422-34.
- Cripps, R. M. and Olson, E. N.** (2002). Control of cardiac development by an evolutionarily conserved transcriptional network. *Dev Biol* **246**, 14-28.
- Cripps, R. M., Zhao, B. and Olson, E. N.** (1999). Transcription of the myogenic regulatory gene Mef2 in cardiac, somatic, and visceral muscle cell lineages is regulated by a Tinman-dependent core enhancer. *Dev Biol* **215**, 420-30.
- Cubas, P., Modolell, J. and Ruiz-Gomez, M.** (1994). The helix-loop-helix extramacrochaetae protein is required for proper specification of many cell types in the *Drosophila* embryo. *Development* **120**, 2555-66.
- Currie, D. A. and Bate, M.** (1991). The development of adult abdominal muscles in *Drosophila*: myoblasts express twist and are associated with nerves. *Development* **113**, 91-102.
- Curtis, N. J., Ringo, J. M. and Dowse, H. B.** (1999). Morphology of the pupal heart, adult heart, and associated tissues in the fruit fly, *Drosophila melanogaster*. *J Morphol* **240**, 225-35.
- Damm, C., Wolk, A., Buttgerit, D., Loher, K., Wagner, E., Lilly, B., Olson, E. N., Hasenpusch-Theil, K. and Renkawitz-Pohl, R.** (1998). Independent regulatory elements in the upstream region of the *Drosophila* beta 3 tubulin gene (beta Tub60D) guide expression in the dorsal vessel and the somatic muscles. *Dev Biol* **199**, 138-49.
- de Celis, J. F. and Ruiz-Gomez, M.** (1995). groucho and hedgehog regulate engrailed expression in the anterior compartment of the *Drosophila* wing. *Development* **121**, 3467-76.
- Delidakis, C., Preiss, A., Hartley, D. A. and Artavanis-Tsakonas, S.** (1991). Two genetically and molecularly distinct functions involved in early neurogenesis reside within the Enhancer of split locus of *Drosophila melanogaster*. *Genetics* **129**, 803-23.
- Doberstein, S. K., Fetter, R. D., Mehta, A. Y. and Goodman, C. S.** (1997). Genetic analysis of myoblast fusion: blown fuse is required for progression beyond the prefusion complex. *J Cell Biol* **136**, 1249-61.

- Dohrmann, C., Azpiazu, N. and Frasch, M.** (1990). A new *Drosophila* homeo box gene is expressed in mesodermal precursor cells of distinct muscles during embryogenesis. *Genes Dev* **4**, 2098-111.
- Drysdale, R.A., Rushton, E., Bate, M.** (1993). Genes required for embryonic muscle development in *Drosophila melanogaster*: A survey of the X chromosome. *Roux Arch. dev. Biol.* 1993 **202(5)**:276--295
- Ducy, P., Zhang, R., Geoffroy, V., Ridall, A. L. and Karsenty, G.** (1997). *Osf2/Cbfa1*: a transcriptional activator of osteoblast differentiation. *Cell* **89**, 747-54.
- Ducy, P.** (2000). *Cbfa1*: a molecular switch in osteoblast biology. *Dev Dyn* **219**, 461-71.
- Duffy, J. B.** (2002). GAL4 system in *Drosophila*: a fly geneticist's Swiss army knife. *Genesis* **34**, 1-15.
- Dutta, D., Anant, S., Ruiz-Gomez, M., Bate, M. and VijayRaghavan, K.** (2004). Founder myoblasts and fibre number during adult myogenesis in *Drosophila*. *Development* **131**, 3761-72.
- Dutta, D., Shaw, S., Maqbool, T., Pandya, H. and VijayRaghavan, K.** (2005). *Drosophila* Heartless Acts with Heartbroken/Dof in Muscle Founder Differentiation. *PLoS Biology* **3**.
- Dworak, H. A., Charles, M. A., Pellerano, L. B. and Sink, H.** (2001). Characterization of *Drosophila* *hibris*, a gene related to human *nephrin*. *Development* **128**, 4265-76.
- Edmondson, D. G., Lyons, G. E., Martin, J. F. and Olson, E. N.** (1994). *Mef2* gene expression marks the cardiac and skeletal muscle lineages during mouse embryogenesis. *Development* **120**, 1251-63.
- Englund, C., Loren, C. E., Grabbe, C., Varshney, G. K., Deleuil, F., Hallberg, B. and Palmer, R. H.** (2003). *Jeb* signals through the *Alk* receptor tyrosine kinase to drive visceral muscle fusion. *Nature* **425**, 512-6.
- Erickson, M. R., Galletta, B. J. and Abmayr, S. M.** (1997). *Drosophila* myoblast city encodes a conserved protein that is essential for myoblast fusion, dorsal closure, and cytoskeletal organization. *J Cell Biol* **138**, 589-603.
- Farrell, E. R., Fernandes, J. and Keshishian, H.** (1996). Muscle organizers in *Drosophila*: the role of persistent larval fibers in adult flight muscle development. *Dev Biol* **176**, 220-9.

- Fernandes, J., Bate, M. and Vijayraghavan, K.** (1991). Development of the indirect flight muscles of *Drosophila*. *Development* **113**, 67-77.
- Fisher, A. L. and Caudy, M.** (1998). Groucho proteins: transcriptional corepressors for specific subsets of DNA-binding transcription factors in vertebrates and invertebrates. *Genes Dev* **12**, 1931-40.
- Fisher, A. L., Ohsako, S. and Caudy, M.** (1996). The WRPW motif of the hairy-related basic helix-loop-helix repressor proteins acts as a 4-amino-acid transcription repression and protein-protein interaction domain. *Mol Cell Biol* **16**, 2670-7.
- Flores-Saaib, R. D. and Courey, A. J.** (2000). Analysis of Groucho-histone interactions suggests mechanistic similarities between Groucho- and Tup1-mediated repression. *Nucleic Acids Res* **28**, 4189-96.
- Fortini, M. E., Lai, Z. C. and Rubin, G. M.** (1991). The *Drosophila* *zfh-1* and *zfh-2* genes encode novel proteins containing both zinc-finger and homeodomain motifs. *Mech Dev* **34**, 113-22.
- Frasch, M.** (1995). Induction of visceral and cardiac mesoderm by ectodermal Dpp in the early *Drosophila* embryo. *Nature* **374**, 464-7.
- Frasch, M., Hoey, T., Rushlow, C., Doyle, H. and Levine, M.** (1987). Characterization and localization of the even-skipped protein of *Drosophila*. *Embo J* **6**, 749-59.
- Frommer, G., Vorbruggen, G., Pasca, G., Jackle, H. and Volk, T.** (1996). Epidermal *egr*-like zinc finger protein of *Drosophila* participates in myotube guidance. *Embo J* **15**, 1642-9.
- Gajewski, K., Zhang, Q., Choi, C. Y., Fossett, N., Dang, A., Kim, Y. H., Kim, Y. and Schulz, R. A.** (2001). Pannier is a transcriptional target and partner of Tinman during *Drosophila* cardiogenesis. *Dev Biol* **233**, 425-36.
- Gao, X., Chandra, T., Gratton, M. O., Quello, I., Prud'homme, J., Stifani, S. and St-Arnaud, R.** (2001). HES6 acts as a transcriptional repressor in myoblasts and can induce the myogenic differentiation program. *J Cell Biol* **154**, 1161-71.
- Gasperowicz, M. and Otto, F.** (2005). Mammalian Groucho homologs: redundancy or specificity? *J Cell Biochem* **95**, 670-87.

- Gaul, U., Seifert, E., Schuh, R. and Jackle, H. (1987).** Analysis of Kruppel protein distribution during early *Drosophila* development reveals posttranscriptional regulation. *Cell* **50**, 639-47.
- Gossett, L. A., Kelvin, D. J., Sternberg, E. A. and Olson, E. N. (1989).** A new myocyte-specific enhancer-binding factor that recognizes a conserved element associated with multiple muscle-specific genes. *Mol Cell Biol* **9**, 5022-33.
- Grbavec, D. and Stifani, S. (1996).** Molecular interaction between TLE1 and the carboxyl-terminal domain of HES-1 containing the WRPW motif. *Biochem Biophys Res Commun* **223**, 701-5.
- Gregoire, S. and Yang, X. J. (2005).** Association with class IIa histone deacetylases upregulates the sumoylation of MEF2 transcription factors. *Mol Cell Biol* **25**, 2273-87.
- Grozinger, C. M. and Schreiber, S. L. (2000).** Regulation of histone deacetylase 4 and 5 and transcriptional activity by 14-3-3-dependent cellular localization. *Proc Natl Acad Sci U S A* **97**, 7835-40.
- Gunthorpe, D., Beatty, K. E. and Taylor, M. V. (1999).** Different levels, but not different isoforms, of the *Drosophila* transcription factor DMEF2 affect distinct aspects of muscle differentiation. *Dev Biol* **215**, 130-45.
- Halfon, M. S., Carmena, A., Gisselbrecht, S., Sackerson, C. M., Jimenez, F., Baylies, M. K. and Michelson, A. M. (2000).** Ras pathway specificity is determined by the integration of multiple signal-activated and tissue-restricted transcription factors. *Cell* **103**, 63-74.
- Han, A., He, J., Wu, Y., Liu, J. O. and Chen, L. (2005).** Mechanism of recruitment of class II histone deacetylases by myocyte enhancer factor-2. *J Mol Biol* **345**, 91-102.
- Han, A., Pan, F., Stroud, J. C., Youn, H. D., Liu, J. O. and Chen, L. (2003).** Sequence-specific recruitment of transcriptional co-repressor Cabin1 by myocyte enhancer factor-2. *Nature* **422**, 730-4.
- Han, Z. and Olson, E. N. (2005).** Hand is a direct target of Tinman and GATA factors during *Drosophila* cardiogenesis and hematopoiesis. *Development* **132**, 3525-36.
- Hebrok, M., Wertz, K. and Fuchtbauer, E. M. (1994).** M-twist is an inhibitor of muscle differentiation. *Dev Biol* **165**, 537-44.

- Heitzler, P., Bourouis, M., Ruel, L., Carteret, C. and Simpson, P.** (1996). Genes of the Enhancer of split and achaete-scute complexes are required for a regulatory loop between Notch and Delta during lateral signalling in *Drosophila*. *Development* **122**, 161-71.
- Hirsinger, E., Malapert, P., Dubrulle, J., Delfini, M. C., Duprez, D., Henrique, D., Ish-Horowicz, D. and Pourquie, O.** (2001). Notch signalling acts in postmitotic avian myogenic cells to control MyoD activation. *Development* **128**, 107-16.
- Ip, Y. T. and Gridley, T.** (2002). Cell movements during gastrulation: snail dependent and independent pathways. *Curr Opin Genet Dev* **12**, 423-9.
- Ip, Y. T., Maggert, K. and Levine, M.** (1994). Uncoupling gastrulation and mesoderm differentiation in the *Drosophila* embryo. *Embo J* **13**, 5826-34.
- Ip, Y. T., Park, R. E., Kosman, D., Yazdanbakhsh, K. and Levine, M.** (1992). dorsal-twist interactions establish snail expression in the presumptive mesoderm of the *Drosophila* embryo. *Genes Dev* **6**, 1518-30.
- Ishibashi, M., Ang, S. L., Shiota, K., Nakanishi, S., Kageyama, R. and Guillemot, F.** (1995). Targeted disruption of mammalian hairy and Enhancer of split homolog-1 (HES-1) leads to up-regulation of neural helix-loop-helix factors, premature neurogenesis, and severe neural tube defects. *Genes Dev* **9**, 3136-48.
- Javed, A., Guo, B., Hiebert, S., Choi, J. Y., Green, J., Zhao, S. C., Osborne, M. A., Stifani, S., Stein, J. L., Lian, J. B. et al.** (2000). Groucho/TLE/R-esp proteins associate with the nuclear matrix and repress RUNX (CBF(alpha)/AML/PEBP2(alpha)) dependent activation of tissue-specific gene transcription. *J Cell Sci* **113** ( Pt 12), 2221-31.
- Jen, Y., Weintraub, H. and Benezra, R.** (1992). Overexpression of Id protein inhibits the muscle differentiation program: in vivo association of Id with E2A proteins. *Genes Dev* **6**, 1466-79.
- Jiang, J., Kosman, D., Ip, Y. T. and Levine, M.** (1991). The dorsal morphogen gradient regulates the mesoderm determinant twist in early *Drosophila* embryos. *Genes Dev* **5**, 1881-91.
- Jimenez, G., Paroush, Z. and Ish-Horowicz, D.** (1997). Groucho acts as a corepressor for a subset of negative regulators, including Hairy and Engrailed. *Genes Dev* **11**, 3072-82.

- Kaushal, S., Schneider, J. W., Nadal-Ginard, B. and Mahdavi, V.** (1994). Activation of the myogenic lineage by MEF2A, a factor that induces and cooperates with MyoD. *Science* **266**, 1236-40.
- Kelly, K. K., Meadows, S. M. and Cripps, R. M.** (2002). Drosophila MEF2 is a direct regulator of Actin57B transcription in cardiac, skeletal, and visceral muscle lineages. *Mech Dev* **110**, 39-50.
- Kennerdell, J. R. and Carthew, R. W.** (1998). Use of dsRNA-mediated genetic interference to demonstrate that frizzled and frizzled 2 act in the wingless pathway. *Cell* **95**, 1017-26.
- Kennerdell, J. R. and Carthew, R. W.** (2000). Heritable gene silencing in Drosophila using double-stranded RNA. *Nat Biotechnol* **18**, 896-8.
- Klapper, R., Heuser, S., Strasser, T. and Janning, W.** (2001). A new approach reveals syncytia within the visceral musculature of Drosophila melanogaster. *Development* **128**, 2517-24.
- Klapper, R., Stute, C., Schomaker, O., Strasser, T., Janning, W., Renkawitz-Pohl, R. and Holz, A.** (2002). The formation of syncytia within the visceral musculature of the Drosophila midgut is dependent on duf, sns and mbc. *Mech Dev* **110**, 85-96.
- Klinedinst, S. L. and Bodmer, R.** (2003). Gata factor Pannier is required to establish competence for heart progenitor formation. *Development* **130**, 3027-38.
- Knirr, S. and Frasch, M.** (2001). Molecular integration of inductive and mesoderm-intrinsic inputs governs even-skipped enhancer activity in a subset of pericardial and dorsal muscle progenitors. *Dev Biol* **238**, 13-26.
- Komori, T., Yagi, H., Nomura, S., Yamaguchi, A., Sasaki, K., Deguchi, K., Shimizu, Y., Bronson, R. T., Gao, Y. H., Inada, M. et al.** (1997). Targeted disruption of Cbfa1 results in a complete lack of bone formation owing to maturational arrest of osteoblasts. *Cell* **89**, 755-64.
- Kopan, R., Nye, J. S. and Weintraub, H.** (1994). The intracellular domain of mouse Notch: a constitutively activated repressor of myogenesis directed at the basic helix-loop-helix region of MyoD. *Development* **120**, 2385-96.
- Kremser, T., Hasenpusch-Theil, K., Wagner, E., Buttgereit, D. and Renkawitz-Pohl, R.** (1999). Expression of the beta3 tubulin gene (beta Tub60D) in the visceral mesoderm of

- Drosophila is dependent on a complex enhancer that binds Tinman and UBX. *Mol Gen Genet* **262**, 643-58.
- Lai, E. C., Burks, C. and Posakony, J. W.** (1998). The K box, a conserved 3' UTR sequence motif, negatively regulates accumulation of enhancer of split complex transcripts. *Development* **125**, 4077-88.
- Lai, E. C. and Posakony, J. W.** (1997). The Bearded box, a novel 3' UTR sequence motif, mediates negative post-transcriptional regulation of Bearded and Enhancer of split Complex gene expression. *Development* **124**, 4847-56.
- Lai, Z. C., Fortini, M. E. and Rubin, G. M.** (1991). The embryonic expression patterns of *zfh-1* and *zfh-2*, two Drosophila genes encoding novel zinc-finger homeodomain proteins. *Mech Dev* **34**, 123-34.
- Lai, Z. C., Rushton, E., Bate, M. and Rubin, G. M.** (1993). Loss of function of the Drosophila *zfh-1* gene results in abnormal development of mesodermally derived tissues. *Proc Natl Acad Sci U S A* **90**, 4122-6.
- Lang, D., Lu, M. M., Huang, L., Engleka, K. A., Zhang, M., Chu, E. Y., Lipner, S., Skoultschi, A., Millar, S. E. and Epstein, J. A.** (2005). Pax3 functions at a nodal point in melanocyte stem cell differentiation. *Nature* **433**, 884-7.
- Lawrence, P. A.** (1982). Cell lineage of the thoracic muscles of Drosophila. *Cell* **29**, 493-503.
- Lee, H., Habas, R. and Abate-Shen, C.** (2004). MSX1 cooperates with histone H1b for inhibition of transcription and myogenesis. *Science* **304**, 1675-8.
- Lee, H. H., Norris, A., Weiss, J. B. and Frasch, M.** (2003). Jelly belly protein activates the receptor tyrosine kinase Alk to specify visceral muscle pioneers. *Nature* **425**, 507-12.
- Leifer, D., Krainc, D., Yu, Y. T., McDermott, J., Breitbart, R. E., Heng, J., Neve, R. L., Kosofsky, B., Nadal-Ginard, B. and Lipton, S. A.** (1993). MEF2C, a MADS/MEF2-family transcription factor expressed in a laminar distribution in cerebral cortex. *Proc Natl Acad Sci U S A* **90**, 1546-50.
- Lemercier, C., Verdel, A., Galloo, B., Curtet, S., Brocard, M. P. and Khochbin, S.** (2000). mHDA1/HDAC5 histone deacetylase interacts with and represses MEF2A transcriptional activity. *J Biol Chem* **275**, 15594-9.

- Leptin, M.** (1991). twist and snail as positive and negative regulators during Drosophila mesoderm development. *Genes Dev* **5**, 1568-76.
- Leptin, M. and Grunewald, B.** (1990). Cell shape changes during gastrulation in Drosophila. *Development* **110**, 73-84.
- Lilly, B., Galewsky, S., Firulli, A. B., Schulz, R. A. and Olson, E. N.** (1994). D-MEF2: a MADS box transcription factor expressed in differentiating mesoderm and muscle cell lineages during Drosophila embryogenesis. *Proc Natl Acad Sci U S A* **91**, 5662-6.
- Lilly, B., Zhao, B., Ranganayakulu, G., Paterson, B. M., Schulz, R. A. and Olson, E. N.** (1995). Requirement of MADS domain transcription factor D-MEF2 for muscle formation in Drosophila. *Science* **267**, 688-93.
- Lin, M. H., Bour, B. A., Abmayr, S. M. and Storti, R. V.** (1997). Ectopic expression of MEF2 in the epidermis induces epidermal expression of muscle genes and abnormal muscle development in Drosophila. *Dev Biol* **182**, 240-55.
- Lin, M. H., Nguyen, H. T., Dybala, C. and Storti, R. V.** (1996). Myocyte-specific enhancer factor 2 acts cooperatively with a muscle activator region to regulate Drosophila tropomyosin gene muscle expression. *Proc Natl Acad Sci U S A* **93**, 4623-8.
- Lin, Q., Lu, J., Yanagisawa, H., Webb, R., Lyons, G. E., Richardson, J. A. and Olson, E. N.** (1998). Requirement of the MADS-box transcription factor MEF2C for vascular development. *Development* **125**, 4565-74.
- Lin, S. C., Lin, M. H., Horvath, P., Reddy, K. L. and Storti, R. V.** (1997). PDP1, a novel Drosophila PAR domain bZIP transcription factor expressed in developing mesoderm, endoderm and ectoderm, is a transcriptional regulator of somatic muscle genes. *Development* **124**, 4685-96.
- Lo, P. C. and Frasch, M.** (1998). bagpipe-Dependent expression of vimar, a novel Armadillo-repeats gene, in Drosophila visceral mesoderm. *Mech Dev* **72**, 65-75.
- Lu, J., McKinsey, T. A., Zhang, C. L. and Olson, E. N.** (2000). Regulation of skeletal myogenesis by association of the MEF2 transcription factor with class II histone deacetylases. *Mol Cell* **6**, 233-44.
- Lu, J., Webb, R., Richardson, J. A. and Olson, E. N.** (1999). MyoR: a muscle-restricted basic helix-loop-helix transcription factor that antagonizes the actions of MyoD. *Proc Natl Acad Sci U S A* **96**, 552-7.



- Maier, D., Marte, B. M., Schafer, W., Yu, Y. and Preiss, A.** (1993). *Drosophila* evolution challenges postulated redundancy in the E(spl) gene complex. *Proc Natl Acad Sci U S A* **90**, 5464-8.
- Martin, B. S., Ruiz-Gomez, M., Landgraf, M. and Bate, M.** (2001). A distinct set of founders and fusion-competent myoblasts make visceral muscles in the *Drosophila* embryo. *Development* **128**, 3331-8.
- Martin, J. F., Schwarz, J. J. and Olson, E. N.** (1993). Myocyte enhancer factor (MEF) 2C: a tissue-restricted member of the MEF-2 family of transcription factors. *Proc Natl Acad Sci U S A* **90**, 5282-6.
- McDermott, J. C., Cardoso, M. C., Yu, Y. T., Andres, V., Leifer, D., Krainc, D., Lipton, S. A. and Nadal-Ginard, B.** (1993). hMEF2C gene encodes skeletal muscle- and brain-specific transcription factors. *Mol Cell Biol* **13**, 2564-77.
- McKinsey, T. A., Zhang, C. L., Lu, J. and Olson, E. N.** <sup>a</sup> (2000). Signal-dependent nuclear export of a histone deacetylase regulates muscle differentiation. *Nature* **408**, 106-11.
- McKinsey, T. A., Zhang, C. L. and Olson, E. N.** <sup>b</sup> (2000). Activation of the myocyte enhancer factor-2 transcription factor by calcium/calmodulin-dependent protein kinase-stimulated binding of 14-3-3 to histone deacetylase 5. *Proc Natl Acad Sci U S A* **97**, 14400-5.
- McKinsey, T. A., Zhang, C. L. and Olson, E. N.** (2001). Control of muscle development by dueling HATs and HDACs. *Curr Opin Genet Dev* **11**, 497-504.
- Michelson, A. M.** (1994). Muscle pattern diversification in *Drosophila* is determined by the autonomous function of homeotic genes in the embryonic mesoderm. *Development* **120**, 755-68.
- Miller, A.** (1950). The internal anatomy and histology of the imago of *Drosophila melanogaster*. In *Biology of Drosophila*, (ed. M. Demerec), pp. 420-534: CSHL Press.
- Miska, E. A., Karlsson, C., Langley, E., Nielsen, S. J., Pines, J. and Kouzarides, T.** (1999). HDAC4 deacetylase associates with and represses the MEF2 transcription factor. *Embo J* **18**, 5099-107.

- Molkentin, J. D., Black, B. L., Martin, J. F. and Olson, E. N.** (1995). Cooperative activation of muscle gene expression by MEF2 and myogenic bHLH proteins. *Cell* **83**, 1125-36.
- Morgan, J. E. and Partridge, T. A.** (2003). Muscle satellite cells. *Int J Biochem Cell Biol* **35**, 1151-6.
- Morgan, T.H. et al.** (1915) *The Mechanism of Mendelian Heredity*. New York: Holt Rinehart & Winston. Reprinted. Johnson Reprint Corporation with an Introduction by Garland E. Allen, 1978.
- Morisaki, T., Sermsuvitayawong, K., Byun, S. H., Matsuda, Y., Hidaka, K., Morisaki, H. and Mukai, T.** (1997). Mouse Mef2b gene: unique member of MEF2 gene family. *J Biochem (Tokyo)* **122**, 939-46.
- Nongthomba, U. and Ramachandra, N. B.** (1999). A direct screen identifies new flight muscle mutants on the Drosophila second chromosome. *Genetics* **153**, 261-74.
- Nose, A., Mahajan, V. B. and Goodman, C. S.** (1992). Connectin: a homophilic cell adhesion molecule expressed on a subset of muscles and the motoneurons that innervate them in Drosophila. *Cell* **70**, 553-67.
- Olson, E. N.** (1992). Interplay between proliferation and differentiation within the myogenic lineage. *Dev Biol* **154**, 261-72.
- Otto, F., Thornell, A. P., Crompton, T., Denzel, A., Gilmour, K. C., Rosewell, I. R., Stamp, G. W., Beddington, R. S., Mundlos, S., Olsen, B. R. et al.** (1997). Cbfa1, a candidate gene for cleidocranial dysplasia syndrome, is essential for osteoblast differentiation and bone development. *Cell* **89**, 765-71.
- Pan, D. J., Huang, J. D. and Courey, A. J.** (1991). Functional analysis of the Drosophila twist promoter reveals a dorsal-binding ventral activator region. *Genes Dev* **5**, 1892-901.
- Parkhurst, S. M.** (1998). Groucho: making its Marx as a transcriptional co-repressor. *Trends Genet* **14**, 130-2.
- Paroush, Z., Finley, R. L., Jr., Kidd, T., Wainwright, S. M., Ingham, P. W., Brent, R. and Ish-Horowicz, D.** (1994). Groucho is required for Drosophila neurogenesis, segmentation, and sex determination and interacts directly with hairy-related bHLH proteins. *Cell* **79**, 805-15.

## References

---

- Patel, N. H., Snow, P. M. and Goodman, C. S. (1987).** Characterization and cloning of fasciclin III: a glycoprotein expressed on a subset of neurons and axon pathways in *Drosophila*. *Cell* **48**, 975-88.
- Payre, F. (2004).** Genetic control of epidermis differentiation in *Drosophila*. *Int J Dev Biol* **48**, 207-15.
- Pollock, R. and Treisman, R. (1991).** Human SRF-related proteins: DNA-binding properties and potential regulatory targets. *Genes Dev* **5**, 2327-41.
- Postigo, A. A. and Dean, D. C. (1997).** ZEB, a vertebrate homolog of *Drosophila* Zfh-1, is a negative regulator of muscle differentiation. *Embo J* **16**, 3935-43.
- Postigo, A. A., Ward, E., Skeath, J. B. and Dean, D. C. (1999).** zfh-1, the *Drosophila* homologue of ZEB, is a transcriptional repressor that regulates somatic myogenesis. *Mol Cell Biol* **19**, 7255-63.
- Preiss, A., Hartley, D. A. and Artavanis-Tsakonas, S. (1988).** The molecular genetics of Enhancer of split, a gene required for embryonic neural development in *Drosophila*. *Embo J* **7**, 3917-27.
- Prokop, A., Landgraf, M., Rushton, E., Broadie, K. and Bate, M. (1996).** Presynaptic development at the *Drosophila* neuromuscular junction: assembly and localization of presynaptic active zones. *Neuron* **17**, 617-26.
- Ranganayakulu, G., Schulz, R. A. and Olson, E. N. (1996).** Wingless signaling induces nautilus expression in the ventral mesoderm of the *Drosophila* embryo. *Dev Biol* **176**, 143-8.
- Ranganayakulu, G., Zhao, B., Dokidis, A., Molkentin, J. D., Olson, E. N. and Schulz, R. A. (1995).** A series of mutations in the D-MEF2 transcription factor reveal multiple functions in larval and adult myogenesis in *Drosophila*. *Dev Biol* **171**, 169-81.
- Rebeiz, M., Reeves, N. L. and Posakony, J. W. (2002).** SCORE: a computational approach to the identification of cis-regulatory modules and target genes in whole-genome sequence data. Site clustering over random expectation. *Proc Natl Acad Sci U S A* **99**, 9888-93.
- Reichhart, J. M., Ligoxygakis, P., Naitza, S., Woerfel, G., Imler, J. L. and Gubb, D. (2002).** Splice-activated UAS hairpin vector gives complete RNAi knockout of single or double target transcripts in *Drosophila melanogaster*. *Genesis* **34**, 160-4.

## References

---

- Reiter, L. T., Potocki, L., Chien, S., Gribskov, M. and Bier, E.** (2001). A systematic analysis of human disease-associated gene sequences in *Drosophila melanogaster*. *Genome Res* **11**, 1114-25.
- Reuter, R. and Scott, M. P.** (1990). Expression and function of the homoeotic genes Antennapedia and Sex combs reduced in the embryonic midgut of *Drosophila*. *Development* **109**, 289-303.
- Riechmann, V., Irion, U., Wilson, R., Grosskortenhaus, R. and Leptin, M.** (1997). Control of cell fates and segmentation in the *Drosophila* mesoderm. *Development* **124**, 2915-22.
- Roy, S. and VijayRaghavan, K.** (1998). Patterning muscles using organizers: larval muscle templates and adult myoblasts actively interact to pattern the dorsal longitudinal flight muscles of *Drosophila*. *J Cell Biol* **141**, 1135-45.
- Roy, S. and VijayRaghavan, K.** (1999). Muscle pattern diversification in *Drosophila*: the story of imaginal myogenesis. *Bioessays* **21**, 486-98.
- Rubin, G. M.** (2001). The draft sequences. Comparing species. *Nature* **409**, 820-1.
- Rudnicki, M. A., Braun, T., Hinuma, S. and Jaenisch, R.** (1992). Inactivation of MyoD in mice leads to up-regulation of the myogenic HLH gene Myf-5 and results in apparently normal muscle development. *Cell* **71**, 383-90.
- Rudnicki, M. A., Schnegelsberg, P. N., Stead, R. H., Braun, T., Arnold, H. H. and Jaenisch, R.** (1993). MyoD or Myf-5 is required for the formation of skeletal muscle. *Cell* **75**, 1351-9.
- Ruiz Gomez, M. and Bate, M.** (1997). Segregation of myogenic lineages in *Drosophila* requires numb. *Development* **124**, 4857-66.
- Ruiz-Gomez, M.** (1998). Muscle patterning and specification in *Drosophila*. *Int J Dev Biol* **42**, 283-90.
- Ruiz-Gomez, M., Coutts, N., Price, A., Taylor, M. V. and Bate, M.** (2000). *Drosophila* dumbfounded: a myoblast attractant essential for fusion. *Cell* **102**, 189-98.
- Ruiz-Gomez, M., Romani, S., Hartmann, C., Jackle, H. and Bate, M.** (1997). Specific muscle identities are regulated by Kruppel during *Drosophila* embryogenesis. *Development* **124**, 3407-14.

- Rushlow, C. A., Hogan, A., Pinchin, S. M., Howe, K. M., Lardelli, M. and Ish-Horowicz, D.** (1989). The Drosophila hairy protein acts in both segmentation and bristle patterning and shows homology to N-myc. *Embo J* **8**, 3095-103.
- Rushton, E., Drysdale, R., Abmayr, S. M., Michelson, A. M. and Bate, M.** (1995). Mutations in a novel gene, myoblast city, provide evidence in support of the founder cell hypothesis for Drosophila muscle development. *Development* **121**, 1979-88.
- Sartorelli, V. and Caretti, G.** (2005). Mechanisms underlying the transcriptional regulation of skeletal myogenesis. *Curr Opin Genet Dev* **15**, 528-35.
- Sasai, Y., Kageyama, R., Tagawa, Y., Shigemoto, R. and Nakanishi, S.** (1992). Two mammalian helix-loop-helix factors structurally related to Drosophila hairy and Enhancer of split. *Genes Dev* **6**, 2620-34.
- Schnorrer, F. and Dickson, B. J.** (2004). Muscle building; mechanisms of myotube guidance and attachment site selection. *Dev Cell* **7**, 9-20.
- Seale, P. and Rudnicki, M. A.** (2000). A new look at the origin, function, and "stem-cell" status of muscle satellite cells. *Dev Biol* **218**, 115-24.
- Sharma, Y., Cheung, U., Larsen, E. W. and Eberl, D. F.** (2002). PPTGAL, a convenient Gal4 P-element vector for testing expression of enhancer fragments in drosophila. *Genesis* **34**, 115-8.
- Shawber, C., Nofziger, D., Hsieh, J. J., Lindsell, C., Bogler, O., Hayward, D. and Weinmaster, G.** (1996). Notch signaling inhibits muscle cell differentiation through a CBF1-independent pathway. *Development* **122**, 3765-73.
- Simpson, P.** (1983). Maternal-Zygotic gene interactions during formation of the dorsoventral pattern in Drosophila embryos. *Genetics* **105**, 615-632.
- Sparrow, D. B., Miska, E. A., Langley, E., Reynaud-Deonauth, S., Kotecha, S., Towers, N., Spohr, G., Kouzarides, T. and Mohun, T. J.** (1999). MEF-2 function is modified by a novel co-repressor, MITR. *Embo J* **18**, 5085-98.
- Spicer, D. B., Rhee, J., Cheung, W. L. and Lassar, A. B.** (1996). Inhibition of myogenic bHLH and MEF2 transcription factors by the bHLH protein Twist. *Science* **272**, 1476-80.
- Staebling-Hampton, K., Hoffmann, F. M., Baylies, M. K., Rushton, E. and Bate, M.** (1994). dpp induces mesodermal gene expression in Drosophila. *Nature* **372**, 783-6.

- Stronach, B. E., Renfranz, P. J., Lilly, B. and Beckerle, M. C. (1999).** Muscle LIM proteins are associated with muscle sarcomeres and require dMEF2 for their expression during *Drosophila* myogenesis. *Mol Biol Cell* **10**, 2329-42.
- Strunkelnberg, M., Bonengel, B., Moda, L. M., Hertenstein, A., de Couet, H. G., Ramos, R. G. and Fischbach, K. F. (2001).** *rst* and its paralogue *kirre* act redundantly during embryonic muscle development in *Drosophila*. *Development* **128**, 4229-39.
- Stute, C., Schimmelpfeng, K., Renkawitz-Pohl, R., Palmer, R. H. and Holz, A. (2004).** Myoblast determination in the somatic and visceral mesoderm depends on Notch signalling as well as on milliways(*mili*(Alk)) as receptor for *Jeb* signalling. *Development* **131**, 743-54.
- Su, M. T., Fujioka, M., Goto, T. and Bodmer, R. (1999).** The *Drosophila* homeobox genes *zfh-1* and *even-skipped* are required for cardiac-specific differentiation of a numb-dependent lineage decision. *Development* **126**, 3241-51.
- Tapanes-Castillo, A. and Baylies, M. K. (2004).** Notch signaling patterns *Drosophila* mesodermal segments by regulating the bHLH transcription factor *twist*. *Development* **131**, 2359-72.
- Taylor, J. M., Dupont-Versteegden, E. E., Davies, J. D., Hassell, J. A., Houle, J. D., Gurley, C. M. and Peterson, C. A. (1997).** A role for the ETS domain transcription factor PEA3 in myogenic differentiation. *Mol Cell Biol* **17**, 5550-8.
- Taylor, M. V. (2000).** A novel *Drosophila*, *mef2*-regulated muscle gene isolated in a subtractive hybridization-based molecular screen using small amounts of zygotic mutant RNA. *Dev Biol* **220**, 37-52.
- Taylor, M. V. (2002).** Muscle differentiation: how two cells become one. *Curr Biol* **12**, R224-8.
- Taylor, M. V. (2003).** Muscle differentiation: signalling cell fusion. *Curr Biol* **13**, R964-6.
- Taylor, M. V. (2005).** Comparison of muscle development in *Drosophila* and vertebrates. In Sink H, ed. *Muscle development in Drosophila*. Landes Biosciences, 2005: Chapter 14.
- Taylor, M. V., Beatty, K. E., Hunter, H. K. and Baylies, M. K. (1995).** *Drosophila* MEF2 is regulated by *twist* and is expressed in both the primordia and differentiated cells of the embryonic somatic, visceral and heart musculature. *Mech Dev* **50**, 29-41.

- Thiagalingam, S., Cheng, K. H., Lee, H. J., Mineva, N., Thiagalingam, A. and Ponte, J. F.** (2003). Histone deacetylases: unique players in shaping the epigenetic histone code. *Ann N Y Acad Sci* **983**, 84-100.
- Thisse, B., el Messal, M. and Perrin-Schmitt, F.** (1987). The twist gene: isolation of a *Drosophila* zygotic gene necessary for the establishment of dorsoventral pattern. *Nucleic Acids Res* **15**, 3439-53.
- Thisse, B., Stoetzel, C., Gorostiza-Thisse, C. and Perrin-Schmitt, F.** (1988). Sequence of the twist gene and nuclear localization of its protein in endomesodermal cells of early *Drosophila* embryos. *Embo J* **7**, 2175-83.
- Thisse, C., Perrin-Schmitt, F., Stoetzel, C. and Thisse, B.** (1991). Sequence-specific transactivation of the *Drosophila* twist gene by the dorsal gene product. *Cell* **65**, 1191-201.
- Ticho, B. S., Stainier, D. Y., Fishman, M. C. and Breitbart, R. E.** (1996). Three zebrafish MEF2 genes delineate somitic and cardiac muscle development in wild-type and mutant embryos. *Mech Dev* **59**, 205-18.
- Vega, R. B., Matsuda, K., Oh, J., Barbosa, A. C., Yang, X., Meadows, E., McAnally, J., Pomajzl, C., Shelton, J. M., Richardson, J. A. et al.** (2004). Histone deacetylase 4 controls chondrocyte hypertrophy during skeletogenesis. *Cell* **119**, 555-66.
- Volk, T. and VijayRaghavan, K.** (1994). A central role for epidermal segment border cells in the induction of muscle patterning in the *Drosophila* embryo. *Development* **120**, 59-70.
- Wang, A. H., Kruhlak, M. J., Wu, J., Bertos, N. R., Vezmar, M., Posner, B. I., Bazett-Jones, D. P. and Yang, X. J.** (2000). Regulation of histone deacetylase 4 by binding of 14-3-3 proteins. *Mol Cell Biol* **20**, 6904-12.
- Ward, E. J. and Coulter, D. E.** (2000). odd-skipped is expressed in multiple tissues during *Drosophila* embryogenesis. *Mech Dev* **96**, 233-6.
- Ward, E. J. and Skeath, J. B.** (2000). Characterization of a novel subset of cardiac cells and their progenitors in the *Drosophila* embryo. *Development* **127**, 4959-69.
- Weintraub, H., Davis, R., Tapscott, S., Thayer, M., Krause, M., Benezra, R., Blackwell, T. K., Turner, D., Rupp, R., Hollenberg, S. et al.** (1991). The myoD gene family: nodal point during specification of the muscle cell lineage. *Science* **251**, 761-6.

- Weiss, J. B., Suyama, K. L., Lee, H. H. and Scott, M. P.** (2001). Jelly belly: a *Drosophila* LDL receptor repeat-containing signal required for mesoderm migration and differentiation. *Cell* **107**, 387-98.
- Wickens, M. and Stephenson, P.** (1984). Role of the conserved AAUAAA sequence: four AAUAAA point mutants prevent messenger RNA 3' end formation. *Science* **226**, 1045-51.
- Williams, J. A., Bell, J. B. and Carroll, S. B.** (1991). Control of *Drosophila* wing and haltere development by the nuclear vestigial gene product. *Genes Dev* **5**, 2481-95.
- Yang, D., Lu, H. and Erickson, J. W.** (2000). Evidence that processed small dsRNAs may mediate sequence-specific mRNA degradation during RNAi in *Drosophila* embryos. *Curr Biol* **10**, 1191-200.
- Yang, X. J. and Gregoire, S.** (2005). Class II histone deacetylases: from sequence to function, regulation, and clinical implication. *Mol Cell Biol* **25**, 2873-84.
- Yin, Z., Xu, X. L. and Frasch, M.** (1997). Regulation of the twist target gene tinman by modular cis-regulatory elements during early mesoderm development. *Development* **124**, 4971-82.
- Youn, H. D., Grozinger, C. M. and Liu, J. O.** (2000). Calcium regulates transcriptional repression of myocyte enhancer factor 2 by histone deacetylase 4. *J Biol Chem* **275**, 22563-7.
- Yu, Y. T., Breitbart, R. E., Smoot, L. B., Lee, Y., Mahdavi, V. and Nadal-Ginard, B.** (1992). Human myocyte-specific enhancer factor 2 comprises a group of tissue-restricted MADS box transcription factors. *Genes Dev* **6**, 1783-98.
- Zaffran, S. and Frasch, M.** (2002). The beta 3 tubulin gene is a direct target of bagpipe and biniou in the visceral mesoderm of *Drosophila*. *Mech Dev* **114**, 85-93.
- Zaffran, S. and Frasch, M.** (2002). Early signals in cardiac development. *Circ Res* **91**, 457-69.
- Zaffran, S., Kuchler, A., Lee, H. H. and Frasch, M.** (2001). biniou (FoxF), a central component in a regulatory network controlling visceral mesoderm development and midgut morphogenesis in *Drosophila*. *Genes Dev* **15**, 2900-15.
- Zeremski, M., Stricker, J. R., Fischer, D., Zusman, S. B. and Cohen, D.** (2003). Histone deacetylase dHDAC4 is involved in segmentation of the *Drosophila* embryo and is regulated by gap and pair-rule genes. *Genesis* **35**, 31-8.



## References

---

**Zhang, C. L., McKinsey, T. A., Chang, S., Antos, C. L., Hill, J. A. and Olson, E. N.** (2002). Class II histone deacetylases act as signal-responsive repressors of cardiac hypertrophy. *Cell* **110**, 479-88.

**Zhang, Y., Featherstone, D., Davis, W., Rushton, E. and Broadie, K.** (2000). Drosophila D-titin is required for myoblast fusion and skeletal muscle striation. *J Cell Sci* **113 ( Pt 17)**, 3103-15.

**Zhao, X., Sternsdorf, T., Bolger, T. A., Evans, R. M. and Yao, T. P.** (2005). Regulation of MEF2 by histone deacetylase 4- and SIRT1 deacetylase-mediated lysine modifications. *Mol Cell Biol* **25**, 8456-64.

## Appendix 1: UAS lines tested

Stock	Comments	Phenotype informations
<i>UAS-Dmeso17A (J7)</i>	<p>Full length <i>Dmeso17A</i> coding sequence under the control of UAS regulatory sequences.</p> <p>The stock is homozygous on the 2<sup>nd</sup> chromosome.</p>	<p>Disruption of somatic muscle differentiation. A range of effect is observed. Heart and visceral muscle development can be affected when using strong GAL4 driver such as <i>mef2-GAL4</i> (see text).</p>
<i>UAS-Dmeso17A (J13)</i>	<p>Full length <i>Dmeso17A</i> coding sequence under the control of UAS regulatory sequences.</p> <p>The stock is homozygous on the 3<sup>rd</sup> chromosome.</p>	<p>Phenotype very similar to that of the <i>J7</i> line</p>
<i>UAS-Dmeso17A (J8)</i>	<p>Full length <i>Dmeso17A</i> coding sequence under the control of UAS regulatory sequences.</p> <p>The stock is homozygous on the 2<sup>nd</sup> chromosome.</p>	<p>Phenotype very similar to that of the <i>J7</i> line but less severe</p>
<i>UAS-Dmeso17A-ΔWRPW (1a)</i>	<p><i>Dmeso17A</i> coding sequence lacking the last 9 base pairs under the control of UAS regulatory sequences.</p> <p>The stock is homozygous on the 2<sup>nd</sup> chromosome</p>	<p>The dominant negative effect leads to aberrant muscle differentiation. With defects in shape attachment and number of the muscles (see text).</p>
<i>UAS-Dmeso17A-ΔWRPW (1b)</i>	<p><i>Dmeso17A</i> coding sequence lacking the last 9 base pairs under the control of UAS regulatory sequences.</p> <p>The stock is homozygous on the 3<sup>rd</sup> chromosome</p>	<p>Phenotype very similar to that of the <i>1a</i> line.</p>

Stock	Comments	Phenotype informations
<i>UAS-Dmeso17A-ΔWRPW (10-orangeC)</i>	<i>Dmeso17A</i> coding sequence lacking the last 9 base pairs under the control of UAS regulatory sequences. The stock is homozygous on the 2 <sup>nd</sup> chromosome	Phenotype very similar to that of the <i>1a</i> line. Dorsal muscles look very dense.
<i>UAS-Dmeso17A-RNAi (L1.4.2)</i>	Full length <i>Dmeso17A</i> coding sequence cloned sense and antisense under the control of UAS regulatory sequences. The stock is homozygous on the 3 <sup>rd</sup> chromosome	Reduction of <i>Dmeso17A</i> level disrupts muscle differentiation. Defects are observed in muscle shape, size, attachment, number and in nuclei organisation.
<i>UAS-Dmeso17A-RNAi (L4.2)</i>	Full length <i>Dmeso17A</i> coding sequence cloned sense and antisense under the control of UAS regulatory sequences. The stock is homozygous on the 2 <sup>nd</sup> chromosome	Phenotype very similar to that of the <i>L1.4.2</i> line.
<i>UAS-Dmeso17A-RNAi (L3.1)</i>	Full length <i>Dmeso17A</i> coding sequence cloned sense and antisense under the control of UAS regulatory sequences. The stock is homozygous on the X chromosome	Phenotype less severe than that of the <i>L1.4.2</i> line although the same defects are observed.

